Stem Cells International

Mesenchymal Stem Cell Biodistribution, Migration, and Homing *In Vivo*

Guest Editors: Weian Zhao, Donald G. Phinney, Dominique Bonnet, Massimo Dominici, and Mauro Krampera

Mesenchymal Stem Cell Biodistribution, Migration, and Homing *In Vivo*

Stem Cells International

Mesenchymal Stem Cell Biodistribution, Migration, and Homing *In Vivo*

Guest Editors: Weian Zhao, Donald G. Phinney, Dominique Bonnet, Massimo Dominici, and Mauro Krampera

Editorial Board

Contents

Hindawi Publishing Corporation
Stem Cells International
Volume 2014, Article ID 292109, 2 pages
http://dx.doi.org/10.1155/2014/292109

Editorial

Mesenchymal Stem Cell Biodistribution, Migration, and Homing *In Vivo*

Weian Zhao,[1] Donald G. Phinney,[2] Dominique Bonnet,[3] Massimo Dominici,[4] and Mauro Krampera[5]

[1] *Sue and Bill Gross Stem Cell Research Center, Chao Family Comprehensive Cancer Center, Department of Biomedical Engineering and Department of Pharmaceutical Sciences, University of California, Irvine, USA*
[2] *Department of Molecular Therapeutics, The Scripps Research Institute, Jupiter, FL, USA*
[3] *Haematopoietic Stem Cell Laboratory Cancer Research UK, London Research Institute, Lincoln's Inn Fields Laboratories, London, UK*
[4] *Laboratory of Cell Biology and Advanced Cancer Therapies, Department of Medical and Surgical Sciences for Children & Adults, University Hospital of Modena and Reggio Emilia, Modena, Italy*
[5] *Section of Hematology, Stem Cell Research Laboratory and Cell Factory, Department of Medicine, University of Verona, Policlinico G.B. Rossi, P.le L.A., Italy*

Correspondence should be addressed to Weian Zhao; weianz@uci.edu

Received 6 February 2014; Accepted 6 February 2014; Published 11 March 2014

Mesenchymal stem cells (MSCs) were originally defined by their capacity to differentiate into various connective tissue lineages as well as support hematopoiesis *in vitro* via the production of various cytokines, chemokines, and adhesion molecules [1, 2]. During the past decade, MSCs have been shown to exhibit angiogenic, trophic, anti-inflammatory, and immunomodulatory activity using a variety of experimental paradigms [3–6]. Together with their easy availability and amenability to large-scale expansion *ex vivo*, these properties have propelled MSC-based therapies to the forefront of regenerative medicine and immune regulatory cell therapy. Currently, MSCs from a variety of tissue sources are being evaluated in over 200 clinical trials for the treatment of a diverse array of disease indications. Completed Phase I and II clinical trials have reported statistically significant benefits in patients with steroid-resistant graft versus host disease [7], severe systemic lupus erythematosus [8], complex perianal fistulas [9], and ischemic cardiomyopathy [10]. However, not all trials have met their primary endpoint of efficacy and while many factors contribute to suboptimal patient outcomes, key among them are the molecular mechanisms that govern MSC engraftment, homing, and biodistribution *in vivo*. Indeed, despite rapid progress in describing the therapeutic potency of MSCs in experimental animal models of disease, progress in understanding their biodistribution and mechanism of action *in vivo* has been slow to develop. For example, robust methodologies to track the fate of MSCs *in vivo* are critical toward establishing their tissue tropism, duration of engraftment, and rates of clearance. In addition, the identification of endogenous factors that function as chemoattractants and repellents also plays critical roles in directing transplanted cells to sites of tissue injury. Moreover, a clearer understanding of the signaling axes that regulate MSC trafficking *in vivo* would provide a means to direct cells to specific tissue and organs, thereby increasing overall efficacy of MSC-based therapies. The latter may also provide a means to mobilize endogenous MSCs and enhance their regenerative and immune regulatory properties. Finally, cellular crosstalk and cell-to-cell interactions also likely affect the biodistribution and survival of exogenously administered MSCs, but scant information exists regarding these processes *in vivo*. In fact, it is a subject of debate whether MSCs localize to tissue due to passive entrapment in small vessels, particularly in lung, or if cells employ active mechanisms similar to leukocytes to home to specific tissues. Therefore, continued study into the mechanism that regulates trafficking

of endogenous and transplanted MSCs will shed novel insight into basic MSC biology and lead to the development of more potent cell-based therapies.

We hope that the readers of this special issue will find it highly informative. The papers contained within it address many of the aforementioned issues including methods to track MSCs *in vivo*, mechanisms that mediate MSC migration and homing including within the CNS, and novel delivery methods to target cells to specific organs. This piece of information will serve as a useful resource with respect to current limitations in the field and provide insights as to how to improve current methods to achieve more beneficial outcomes for MSC-based therapies.

Weian Zhao
Donald G. Phinney
Dominique Bonnet
Massimo Dominici
Mauro Krampera

References

[1] D. J. Prockop, "Marrow stromal cells as stem cells for non-hematopoietic tissues," *Science*, vol. 276, no. 5309, pp. 71–74, 1997.

[2] T. M. Dexter, L. H. Coutinho, E. Spooncer et al., "Stromal cells in haemopoiesis," *Ciba Foundation Symposium*, vol. 148, pp. 76–86, 1990.

[3] S. Tomita, D. A. G. Mickle, R. D. Weisel et al., "Improved heart function with myogenesis and angiogenesis after autologous porcine bone marrow stromal cell transplantation," *Journal of Thoracic and Cardiovascular Surgery*, vol. 123, no. 6, pp. 1132–1140, 2002.

[4] L. A. Ortiz, M. Duteil, C. Fattman et al., "Interleukin 1 receptor antagonist mediates the antiinflammatory and antifibrotic effect of mesenchymal stem cells during lung injury," *Proceedings of the National Academy of Sciences of the United States of America*, vol. 104, no. 26, pp. 11002–11007, 2007.

[5] A. Uccelli, L. Moretta, and V. Pistoia, "Mesenchymal stem cells in health and disease," *Nature Reviews Immunology*, vol. 8, no. 9, pp. 726–736, 2008.

[6] A. I. Caplan and D. Correa, "The MSC: an injury drugstore," *Cell Stem Cell*, vol. 9, no. 1, pp. 11–15, 2011.

[7] K. le Blanc, F. Frassoni, L. Ball et al., "Mesenchymal stem cells for treatment of steroid-resistant, severe, acute graft-versus-host disease: a phase II study," *The Lancet*, vol. 371, no. 9624, pp. 1579–1586, 2008.

[8] D. Wang, H. Zhang, J. Liang et al., "Allogeneic mesenchymal stem cell transplantation in severe refractory systemic lupus erythematosus: 4 years experience," *Cell Transplantation*, 2013.

[9] W. Y. Lee, K. J. Park, Y. B. Cho et al., "Autologous adipose tissue-derived stem cells treatment demonstrated favorable and sustainable therapeutic effect for Crohn's fistula," *Stem Cells*, vol. 31, no. 11, pp. 2575–2581, 2013.

[10] J. M. Hare, J. E. Fishman, G. Gerstenblith et al., "Comparison of allogeneic vs. autologous bone marrow-derived mesenchymal stem cells delivered by transendocardial injection in patients with ischemic cardiomyopathy: the POSEIDON randomized trial," *The Journal of the American Medical Association*, vol. 308, pp. 2369–2379, 2012.

Hindawi Publishing Corporation
Stem Cells International
Volume 2014, Article ID 939275, 13 pages
http://dx.doi.org/10.1155/2014/939275

Research Article

Long-Term Quantitative Biodistribution and Side Effects of Human Mesenchymal Stem Cells (hMSCs) Engraftment in NOD/SCID Mice following Irradiation

Sabine François,[1,2] Benoit Usunier,[1] Luc Douay,[2] Marc Benderitter,[1] and Alain Chapel[1]

[1] *PRP-HOM, SRBE, Laboratory of Radiopathology and Experimental Therapy, Radiological Protection and Human Health Division, Institute of Radiological Protection and Nuclear Safety, 92260 Fontenay-aux-Roses, France*
[2] *UMRS 938 Department of Hematology, Saint Antoine Hospital APHP and UPMC University, 75012 Paris, France*

Correspondence should be addressed to Sabine François; sabine.francois@irba.fr and Alain Chapel; alain.chapel@irsn.fr

Received 2 May 2013; Revised 21 November 2013; Accepted 22 November 2013; Published 11 February 2014

Academic Editor: Mauro Krampera

There is little information on the fate of infused mesenchymal stem cells (MSCs) and long-term side effects after irradiation exposure. We addressed these questions using human MSCs (hMSCs) intravenously infused to nonobese diabetic/severe combined immunodeficient (NOD/SCID) mice submitted to total body irradiation (TBI) or local irradiation (abdominal or leg irradiation). The animals were sacrificed 3 to 120 days after irradiation and the quantitative and spatial distribution of hMSCs were studied by polymerase chain reaction (PCR). Following their infusion into nonirradiated animals, hMSCs homed to various tissues. Engraftment depended on the dose of irradiation and the area exposed. Total body irradiation induced an increased hMSC engraftment level compared to nonirradiated mice, while local irradiations increased hMSC engraftment locally in the area of irradiation. Long-term engraftment of systemically administered hMSCs in NOD/SCID mice increased significantly in response to tissue injuries produced by local or total body irradiation until 2 weeks then slowly decreased depending on organs and the configuration of irradiation. In all cases, no tissue abnormality or abnormal hMSCs proliferation was observed at 120 days after irradiation. This work supports the safe and efficient use of MSCs by injection as an alternative approach in the short- and long-term treatment of severe complications after radiotherapy for patients refractory to conventional treatments.

1. Introduction

Multipotent stromal cells, also named mesenchymal stromal cells or mesenchymal stem cells (MSCs), have been identified in the bone marrow as multipotent progenitor cells that differentiate into osteocytes, chondrocytes, adipocytes, and stromal cells [1, 2]. In human, the use of MSCs is being tested for tissue remodelling including cardiovascular repair, treatment of lung fibrosis, spinal cord injury, and bone and cartilage repair; for review see [3, 4]. Regarding radio-induced lesion studies showed engraftment of MSCs at the site of injury [5–7] and repair to damaged tissues [8–11] but no one evaluated the long-term MSC engraftment. MSCs biodistribution has been studied in animal [12]; however, only one report described human MSC (hMSC) engraftment in human. The amount of MSCs detected in most tissues is exceedingly low and transitory. A low level of MSCs donor DNA was identified in bone marrow in some patients [13, 14]. Von Bahr et al. examined autopsies and tissue samples of patients treated with MSC infusions to assess MSC engraftment and examine the risk of tumour and/or ectopic tissue formation. Among the fifteen patients available for PCR analysis, long-term engraftment of MSCs appeared to be low due to rejection by the recipient immune system or an inability of MSCs to survive and engraft after intravenous infusion. MSC injections did not induce side effects [15]. Finally, in spite of successful clinical trials using MSCs, there is few data concerning the long-term engraftment and side effects after MSC systemic injections; transplanted stem cells must not form teratomas or undergo transformation and they must not promote tumour recurrence.

Clinical trials using MSCs in accidental irradiation [16], late severe damage of irradiation [17, 18], or radiotherapy

[19, 20] of breast cancer allowed for tissue regeneration when other therapies failed [21]. There is more to consider than radiation induced DNA damage and long-term inhibition of growth of exposed cells mediated by P53 and other pathways. P53 activation stops cell growth long enough to repair the DNA damage. MSC therapy allows cells to continue to repair the tissue over the short term [22]. The long-term consequences of this "repair" are not known. Allowing the cells to progress through cell cycle with a damaged DNA template will result in severe long-term consequences including cancer induction. In this report we have investigated the long-term effect of hMSCs injected just after irradiation. We describe a xenogeneic experimental transplant model that we built to evaluate the full long-term potential of hMSC engraftment after intravenous injection and to examine the risk of tumour in irradiated tissues and ectopic tissue formation. We have tested at long-term period after irradiation (120 days) whether MSCs engraftment depends of the configuration irradiation and could induce any abnormalities, neoplastic tissue, or uncontrolled cell proliferation.

We used NOD/SCID mice to evaluate the engraftment of hMSCs in irradiated tissues. Our results showed that local irradiation increased engraftment with a direct correlation with the dose of irradiation and modified the biodistribution of hMSCs in tissues. We observed a long-term engraftment in some organs and no side effects of hMSCs over a long-time period in irradiated tissues. We believe that these observations are relevant to several clinical situations such as total body irradiation given as a pretransplant conditioning regimen, radiotherapy for the treatment of cancer, and accidental irradiation, in promoting the use of MSC infusion as part of the therapeutic scheme for the treatment of radiation side effects after radiotherapy in the short and long term.

2. Materials and Methods

Isolation, Purification, and Expansion of hMSCs. Bone marrow cells were obtained from iliac crest aspirates from healthy volunteers after informed consent and were used in accordance with the procedures approved by the Human Experimentation and Ethic Committees of Hospital St Antoine as previously described [6, 7].

hMSC Infusion into NOD/SCID Mouse Model. All experiments and procedures were carried out in accordance with the Guide for the Care and Use of Laboratory Animals as published by the US National Institutes of Health (NIH Publications Numbers 85-23, revised 1996), with European Directives (86/609/CEE), in compliance with the French Ministry of Agriculture Regulations for Animal Experimentation (Act reference 87-847, October 19, 1987, modified May 2001), and approved by the Local Ethical Committee (P04-07). NOD-LtSz-scid/scid (NOD/SCID) mice from breeding pairs originally purchased from Jackson Laboratory (Bar Harbor, ME, USA) were bred in our pathogen-free unit and maintained in sterile microisolator cages. A total of 134 eight-week-old male mice, divided in 4 groups, were used for this study. Group 1 was not irradiated before receiving 2.5 millions of hMSC intravenously (10 mice). Group 2 received local irradiation to the right posterior leg from 15 to 25 Gray (28 mice). Group 3 received local irradiation to the abdomen at a dose of 8.5 Gray (36 mice). Group 4 received TBI at a sublethal dose of 3.5 Gray (50 mice). Irradiations were performed as previously described [6]. Groups 2, 3, and 4 received intravenous hMSC infusion, 24 hours after irradiation. Animals were sacrificed from 3 to 120 days after irradiation and the quantitative and spatial distribution of the hMSC was studied through PCR and immunohistological analyses. Peripheral blood, bone marrow (femur), heart, lungs, liver, kidneys, spleen, stomach, gut, brain, right leg, quadriceps muscles, tibias, and skin were collected. Second-passage hMSCs were collected for infusion; the rates of viability to blue trypan were of 98%.

Detection and Quantitative Analysis of Engrafted hMSCs, DNA Extraction, and PCR Analysis. Human cells (hMSCs) in mouse tissues were detected as previously described by François et al. The biological samples were submitted to DNA extraction and PCR analysis to detect the presence of human cells in mouse recipients. Genomic DNA for PCR analysis was prepared from tissues using the QIAamp DNA Mini Kit, Qiagen. Amplification of human beta-globin gene was used to quantify the amount of human DNA in each sample of mouse tissue after DNA extraction. Endogenous mouse RAPSYN gene (Receptor-Associated Protein at the Synapse) was also amplified, as an internal control. Absolute standard curves were generated for the human beta-globin and mouse RAPSYN genes. Evaluation of human specificity of human beta-globin amplification was demonstrated using tenfold dilution between 100 ng and 0.05 ng of hMSC DNA with mouse DNA, without cross-reactivity, to quantify human cells in mouse tissue. One hundred nanograms of purified DNA from various tissues was amplified using TaqMan universal PCR master mix (Applied Biosytems). The primers and probe for human beta-globin were forward primer 5′GTGCACCTGACTCCTGAGGAGA3′ and reverse primer 5′CCTTGATACCAACCTGCCCAGG3′; the probe labelled with fluorescent reporter and quencher was 5′FAM-AAGGTGAACGTGGATGAAGTTGGTGG-TAMRA-3′. The primers and probe for mouse RAPSYN gene were forward primer 5′ACCCACCCATCCTGCAAAT3′ and reverse primer 5′ACCTGTCCGTGCTGCAGAA3′; the probe labelled with fluorescent reporter and quencher was 5′FAM-CGGTGCCAGTGATGAGGTTGGTC-TAMRA-3′.

2.1. Immunohistochemistry. To assess the tissue architectural changes induced by exposure to ionizing radiation, we performed a histological study of all organs collected and analyzed by PCR.

Before each sampling, the NOD/SCID mice were anesthetized by an intraperitoneal injection of 350 of Imlagen/Rompun solution (350 μL). Blood is collected directly by intracardiac punction and the animals were perfused with saline solution to remove blood from the organs. Each organ is divided into two parts: one that will be incubated 12 hours in a solution of 4% paraformaldehyde (for histological study)

and the other part will be stored in 1 mL of RNAlater buffer at −20°C (for PCR analysis).

One half of each tissue was used for PCR and immunohistology. For histological study, samples were fixed for 12 hours in 4% paraformaldehyde.

Following paraformaldehyde fixation, the organs were rinsed with distilled water and dehydrated. Tissues were sectioned at 5 μm on a rotary microtome (LEICA). For immunohistochemical staining of the paraffin embedded samples, microtomed sections were deparaffinized in xylene and rehydrated though ethanol baths and PBS 1x. The sections were dip into PBS-triton (0.1x) in order to increase tissue permeability. After being rinsed with distilled water, the sections were digested with 2% trypsin for 30 minutes resulting in the endogenous biotin being blocked. The polyclonal anti-beta-2-microglobulin antibody (product NCL-B2Mp, Novocastra) was added at a dilution of 1 : 50. Negative controls were incubated with rabbit IgG diluted to 1 : 100. Detection of bound primary antibody was carried out with biotinylated secondary antibody. The biotinylated anti-rabbit IgG secondary antibody was diluted to 1 : 200 in PBS 1x and incubated for 8 minutes. The immunoreactivity was performed using alkaline phosphatase reaction with a FARED substrate detection kit for 30 minutes. For antibody detection we used the Ventana kit, followed by counterstaining with hemalun for 4 minutes. This procedure was performed using NexES special staining automation system to ensure reproducibility. On successive sections we carried out a hematoxylin-eosin-saffron (HES) staining of paraffined slides that was performed on all tissues collected at 3 and 15 days after TBI. For a global vision of morphology and tissue damage, the observation of HES-stained section (5 μm) of splenic biopsies has been realized by using normal brightfield microscopy. Every 25 μm, one section is colored by HES staining. In general, 5 or 7 sections of tissue were analyzed for each animal. Each section was observed by microscopy in its entirety with objective ×20. The cell depletion is determined by the decrease of blue purple chromatin intensity. Color intensity could be quantified by Histolab software. All spleens (10 per group) were collected and analyzed by microscopy. All HES-stained sections have been performed at the same time to avoid seeing the differences in color intensity. The chromatin intensity is measured with 5 random areas per tissue section.

3. Results

hMSCs implanted in mouse tissues were detected by PCR of the for human β-gene globin. Human DNA accounted for engraftment. Results are expressed as the number of mice (or percentage) with an hMSC implantation in an organ (PCR positive for the gene for human β-globin) in comparison to the total number of mice injected with hMSCs. Day 0 the hMSC biodistribution kinetics corresponds to the day of irradiation. hMSCs were intravenously injected 24 hours after irradiation. The control (named sham) consists in nonirradiated mice injected with $5 \cdot 10^6$ hMSCs.

Table 1: hMSC engraftment in nonirradiated mice 3 days after injection.

Organs	Number of positive mice for 10 mice
Brain	10/10 (100%)
Heart	5/10 (50%)
Lung	10/10 (100%)
Liver	10/10 (100%)
Spleen	10/10 (100%)
Abdominal area	
Kidney	10/10 (100%)
Muscle	0/10 (0%)
Stomach	9/10 (90%)
Duodenum	2/10 (20%)
Jejunum	10/10 (100%)
Ileum	1/10 (10%)
Cecum	1/10 (10%)
Proximal colon	1/10 (10%)
Distal colon	1/10 (10%)
Posterior leg	
Skin	1/10 (10%)
Muscle	4/10 (40%)
Bone	3/10 (30%)
Bone marrow	10/10 (100%)
Blood	3/10 (30%)
Number of positive organs	102/190
Frequency	54%

Human DNA accounted for engraftment. hMSCs implanted in mouse tissues were detected by PCR of the gene for human β-globin. The rate of implantation of human cells was determined on a series of non-irradiated mice grafted with hMSC injection at $5{\cdot}10^6$ cells per mouse. The percentages represent the ratio of positive mice for the presence of human β-globin on the total number of mice analyzed.

Infused hMSCs Are Present for a Short-Time Period in Nonirradiated NOD/SCID Mice Tissues (Table 1). A preliminary experiment was conducted to determine in which organs hMSCs home in nonirradiated animals. The rate of implantation of human cells was determined on a series of nonirradiated mice injected with $5 \cdot 10^6$ hMSCs (sham animals). The percentages represent the ratio of positive mice for one organ for the presence of human β-globin over the total number of mice analyzed. Human DNA (PCR analysis) accounted for engraftment of hMSCs following their infusion into nonirradiated animals in various tissues. The qualitative study of MSC engraftment in sham mice is shown in Table 1. Three days after injection, without irradiation, hMSCs isolated from human bone marrow migrated to murine bone marrow (10 mice PCR positive for the gene for human β-globin on 10 mice, 100%). Without irradiation, lung, brain, liver, and spleen appeared to be a preferential site of migration for the injected human cells. Human cells were detected only in 20% of animals whose peripheral blood was analyzed.

Table 2: hMSC biodistribution in function of the irradiation dose 6 weeks after local irradiation of the right posterior leg at 15 to 25 Gy.

Organs (positive per mice)	Dose of irradiation		
	15 Gy	20 Gy	25 Gy
Brain	0/8 (0%)	4/10 (40%)	8/8 (100%)
Heart	6/8 (75%)	0/6 (0%)	8/8 (100%)
Lung	2/6 (33%)	4/10 (40%)	8/8 (100%)
Liver	0/8 (0%)	6/8 (75%)	8/8 (100%)
Spleen	0/8 (0%)	5/10 (50%)	8/8 (100%)
Abdominal area			
Kidney	2/6 (33%)	6/10 (60%)	8/8 (100%)
Muscle	2/8 (25%)	0/6 (0%)	6/8 (75%)
Stomach	0/8 (0%)	6/10 (60%)	8/8 (100%)
Duodenum	0/8 (0%)	10/10 (100%)	8/8 (100%)
Jejunum	0/6 (0%)	0/10 (0%)	6/8 (75%)
Ileum	0/8 (0%)	4/10 (40%)	6/8 (75%)
Cecum	0/8 (0%)	4/10 (40%)	6/8 (75%)
Proximal colon	0/8 (0%)	4/10 (40%)	6/8 (75%)
Colon distal	0/8 (0%)	4/10 (40%)	6/8 (75%)
Posterior leg			
Skin	0/8 (0%)	4/10 (40%	6/8 (75%)
Muscle	0/8 (0%)	1/8 (12.5%)	8/8 (100%)
Bone	1/8 (12.5%)	3/8 (38%)	8/8 (100%)
Bone marrow	2/6 (33%)	5/10 (50%)	6/8 (75%)
Number of positive organs	15/136	70/166	128/144
Frequency	11%	42%	89%

Results are expressed as the number of mice (or percentage) with hMSC implantation in an organ (PCR positive for the gene for human β-globin) in comparison to the total number of mice injected with hMSCs. Day 0 of the kinetics of hMSC biodistribution corresponds to the day of irradiation. hMSCs were intravenously injected 24 hours after irradiation. hMSCs appear to migrate preferentially in the organs of the irradiated area; their implantation rate seems to be dose-dependent in these organs. hMSCs were not found in blood; $n = 10$ (data are not shown).

hMSC Engraftment Is Related to the Irradiation Dose (Table 2). The biodistribution was investigated in function of the dose of irradiation 6 weeks after a local irradiation of the right posterior leg at 15 to 25 Gy.

hMSCs appeared to migrate preferentially in the organs of the irradiated area; their implantation rate seemed to be dose-dependent in these organs. For example, in bone, the percentage of hMSC engraftment varied from 12.5% at 15 Gy to 38% at 20 Gy and finally 100% of injected mice at 25 Gy.

These human cells also migrated in organs outside of the irradiated area such as kidneys. The site and frequency of implantation seem to be dose-dependent.

Configurations of Irradiation Modify Long-Term Biodistribution of hMSCs in Organs (Table 3, Figure 1). Table 3 summarizes the levels of hMSC engraftment after abdominal irradiation. Mice received localized irradiation to the abdomen. Sixty days after abdominal irradiation, very few mice were positive for human DNA. Biodistribution of human cells is maximum at 15 days. hMSC engraftment was detectable from 3 days after irradiation to at least 60 days. hMSC engraftment varies from 12% of organs at day 3 (D3), 54% on D15, 51% on D30, to 17% at day 60. The homing of human cells appeared to increase up to day 15 or day 30 depending on organs and then decreased with time. After abdominal irradiation, hMSCs appeared to preferentially migrate into the lungs, liver, kidneys, and spleen. For these organs, more than 50% of the animals were positive for the presence of the human gene at 2 and 4 weeks after irradiation. Injected human cells also colonized the abdominal muscles, the heart, liver, stomach, jejunum, quadriceps, bone (femur), and bone marrow but more moderately. For these organs, 35 to 50% of animals were positive for the presence of hMSCs. However very few hMSCs were engrafted in other parts of the intestine and the skin; for these organs less than 20% of the animals were positive for the presence of hMSCs.

Abdominal irradiation as compared to total body irradiation (TBI) modifies hMSC engraftment in the exposed area, that is, biodistribution. Abdominal irradiation increases hMSC engraftments from 3 to 60 days in stomach, duodenum, jejunum, and ileum and decreases engraftment in cecum and colon. Conversely, neither localized irradiation nor TBI modified hMSC engraftment in lung.

hMSC Implantation Increases during the First Two Weeks after Total Body Irradiation (TBI) and Persists for a Long-Time Period in Lung and Liver (Table 4, Figure 1). hMSC implantation (human DNA) was detectable in lung 24 hours after intravenous injection of human cells in lung.

Day 3 after-TBI, hMSCs were localized in heart, lung, liver, muscle (abdominal), stomach, and intestine (duodenum and jejunum, distal colon). They were not detectable

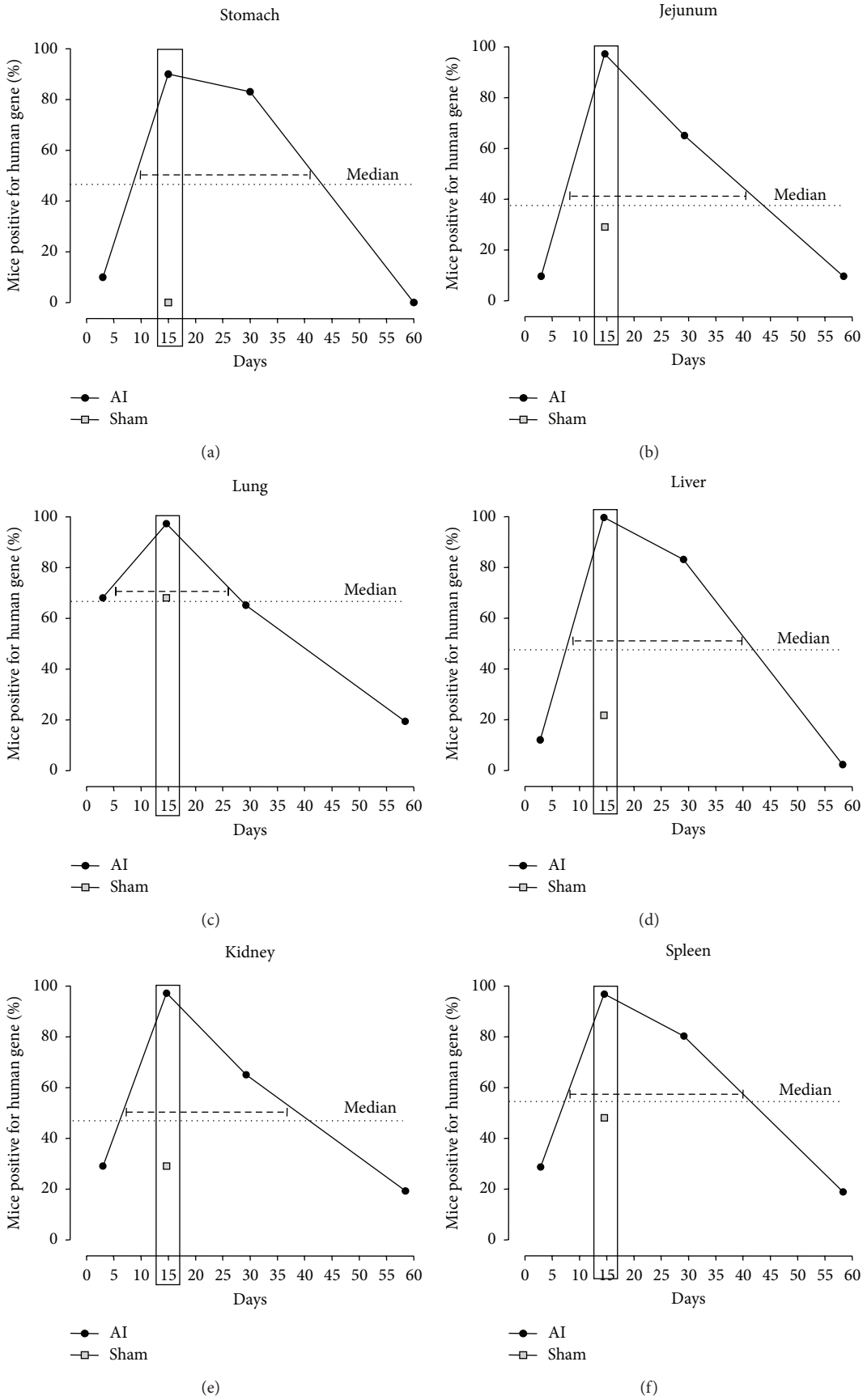

Figure 1: Continued.

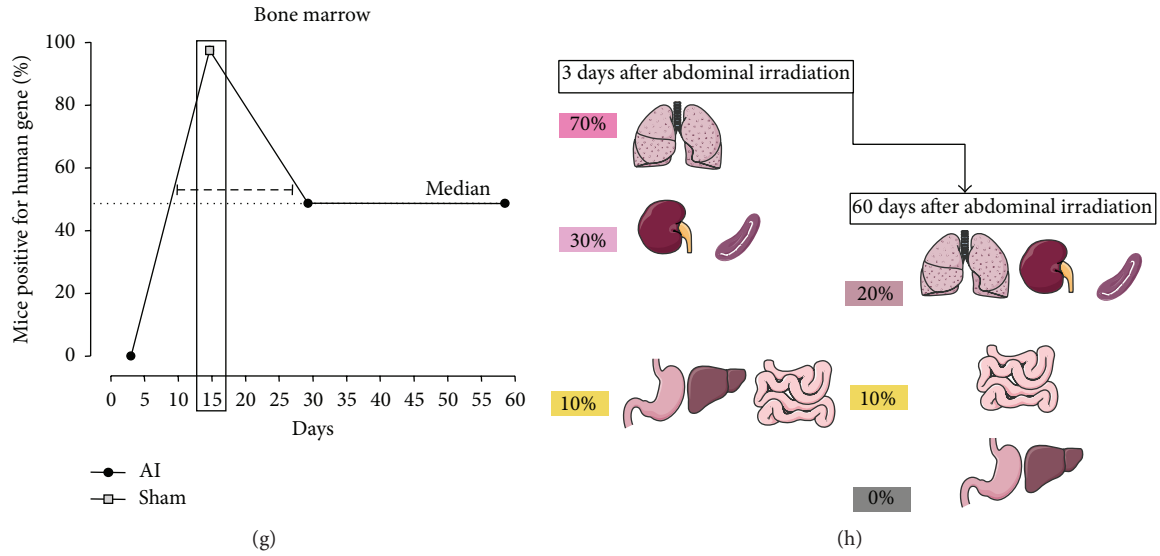

Figure 1: Kinetics of implantation of hMSCs during 60 days after abdominal irradiation. The percentage of positive mice for the human β-globin gene detected by PCR (AI) has been calculated after abdominal irradiation (AI). The human gene has been detected in (a) stomach, (b) jejunum, (c) lungs, (d) liver, (e) kidney, (f) spleen, and (g) bone marrow. The tissues were collected at 3, 15, 30, and 60 days after acute AI. The percentages represent the ratio (number of positive mice for the human beta-globin presence divided by total number of animals tested). At each analysis time, each group consisted of 10 animals. The control (named sham) consists in nonirradiated mice injected with $5 \cdot 10^6$ hMSCs. The dotted line represents the median of the positive animal percentage during the 60 days after radiation exposure. (h) Illustration of anatomical variations in the presence of MSC after acute abdominal radiation.

in the bone marrow until day 7. hMSCs isolated from bone marrow did not seem to preferentially colonize their tissue of origin in xenogeneic mouse model.

Day 7 after-TBI, hMSCs appeared to preferentially colonize the lung (100%), spleen, stomach, and heart (75%). hMSCs were still present in muscle (50%) and distal colon (25%). HMSCs started to engraft in bone (25%) and bone marrow (12.5%).

Day 15 was the short-term point at which biodistribution of hMSCs was the largest (Figure 2). The number of tissues in which the gene for human β-globin is present increased during the first two weeks, from 14% on day 3, 28% on day 7, to 47% on day 15. 100% of livers, 75% brain, and 50% of kidneys (see localization in Figures 2(c), 2(d), 2(e), and 2(f)) were positive for human DNA by PCR. hMSCs were implanted in all organs with the exception of the distal colon and ileum. An hMSC circulation was observed in peripheral blood (as illustrated in Figures 2(c), 2(d), and 2(e)) which corresponded to the time when the engraftment was maximum in tissues. The presence of hMSCs in peripheral blood may be due to the dissemination of cells in a large variety of tissues. At 15 days, implantation of hMSCs into muscle was detected in 88% of quadriceps. In the intestine, engraftment was observed in duodenum (33%), jejunum (25%), and proximal colon (38%). The duodenum and proximal colon were the part of the intestine most colonized by hMSCs. Very few skins and bone (femurs) analyzed were positive by PCR, 38% and 12.5% at 15 days, respectively. To localize human cells in engrafted tissues, we performed immunologic experiment using a human beta-2-microglobulin specific antibody. 14 days after hMSC graft, we observed by microscopy that human cells were integrated into functional tissue structures such as vascular endothelial system (VES) of different organs (especially in liver (Figure 3(c)), brain (Figure 3(d)), and kidney (Figures 3(f) and 3 (g))) and tissue functional units such as the glomerulus (Figure 3(e)).

Compared to nonirradiated mice, we observed that preferential colonization sites of hMSCs appeared to be modified by radiation exposure. Figure 4 indicates the quantitative engraftment 15 days after irradiation. TBI before hMSC infusion increased the levels of engraftment in brain, hearth, liver (Figure 4(a)) but not all in jejunum compared to nonirradiated mice (sham, Figure 4(b)). Irradiation at local site (abdomen) increased hMSCs implantation not only at the site of local irradiation (Figure 4(b)), but also in distant organs outside the local irradiation field (brain, heart, Figure 4(a)). This suggests mobilization induced by cytokines and potentially specific homing induced by chemokines, all released by inflammation.

At 30 days after-TBI, hMSCs were detected in all types of tissues except the duodenum, ileum, and the skin. Nevertheless, the hMSC biodistribution was more important at D15 (47%) than D30 (34%). After D30, the biodistribution of hMSCs injected was reduced. The number of positive blood analyzed by PCR increased at D30 (57%), suggesting a recirculation of human cells after implantation in the organs. In the intestine, hMSCs were present, in 25% of jejunum, 25% of ileum, 38% of cecum, 43% of proximal colons, and 20% of distal colons analyzed. hMSCs were not detected in the ileum and duodenums analyzed. Over a longer-time period, the duodenum was not the most colonized part of the intestine by MSCs. Although the intestine is a tissue with a rapid renewal,

Table 3: Levels of hMSC engraftment at 4 different time points after abdominal irradiation at 8.5 Gray.

Organs (positive per mice)	Days after irradiation			
	3 days	15 days	30 days	60 days
Brain	4/10 (40%)	10/10 (100%)	2/6 (33%)	1/10 (10%)
Heart	2/10 (20%)	5/10 (50%)	4/6 (67%)	4/10 (40%)
Lung	7/10 (70%)	10/10 (100%)	4/6 (67%)	2/10 (20%)
Liver	1/10 (10%)	10/10 (100%)	5/6 (83%)	0/10 (0%)
Spleen	3/10 (30%)	10/10 (100%)	5/6 (83%)	2/10 (20%)
Abdominal area				
Kidney	3/10 (30%)	10/10 (100%)	4/6 (67%)	2/10 (20%)
Muscle	1/10 (10%)	2/10 (20%)	6/6 (100%)	1/6 (17%)
Stomach	1/10 (10%)	9/10 (90%)	5/6 (83%)	0/8 (0%)
Duodenum	0/10 (0%)	2/10 (20%)	2/6 (33%)	1/10 (10%)
Jejunum	1/10 (10%)	10/10 (100%)	4/6 (67%)	1/10 (10%)
Ileum	1/10 (10%)	1/10 (10%)	2/6 (33%)	1/10 (10%)
Cecum	0/10 (0%)	1/10 (10%)	1/6 (17%)	1/10 (10%)
Proximal colon	0/10 (0%)	1/10 (10%)	2/6 (33%)	3/10 (30%)
Distal colon	0/10 (0%)	1/10 (10%)	2/6 (33%)	2/10 (20%)
Posterior leg (right)				
Skin	0/10 (0%)	1/10 (10%)	0/6 (0%)	0/10 (0%)
Muscle	1/10 (10%)	4/10 (40%)	2/6 (33%)	1/8 (12.5%)
Bone	1/10 (10%)	3/10 (30%)	5/6 (83%)	5/10 (50%)
Bone marrow	0/10 (0%)	10/10 (100%)	3/6 (50%)	4/8 (50%)
Blood	0/10 (0%)	3/10 (30%)	0/6 (0%)	0/10 (0%)
Number of positive organs	23/190	102/190	58/114	31/186
Frequency	12%	54%	51%	17%

The biodistribution of human cells is maximum at 15 days. hMSC engraftment is detectable from 3 days after irradiation to at least 60 days. hMSC engraftment varies from 12% of organs at day 3, 54% on D15, 51% on D30, to 17% at day 60. The homing of human cells appeared to increase up to day 15 and then decreased with time.

MSCs appeared to have incorporated all other sections of the intestine several months after-injection.

The time in which the implantation of hMSCs was optimum varied from one organ to another (Figure 1). The movement of hMSCs in the peripheral blood was maximum at day 30. For stomach, duodenum, and spleen, the highest hMSC implantation was observed at day 7. For bone marrow, muscle, brain, kidneys, liver, lungs, heart, jejunum, and cecum, after TBI, the maximum of hMSC engraftment in mice corresponds to day 15. For bone and skin, the maximum engraftment of hMSCs appeared later at days 60 and 90, respectively. The implantation of human cells appeared to decrease with time between D30 and D90.

hMSCs were detectable at least up to 120 days after injection of human cells in a number of organs. In the long term after TBI, hMSCs preferentially stayed in lung (100%), heart (67%), kidney (67%), muscle (33%), cecum and distal colon (33%), and stomach and bone marrow (17%).

hMSCs Do Not Induce Tissue Abnormality in Irradiated Tissues after Long-Term Injection (Table 5). The trichromatic staining HES was performed on tissue taken between day 3 and day 120 after-irradiation. Histological study on D15 has highlighted that irradiation induced cell depletion in spleen (Figures 1(a) and 1(b)). 120 days after total body irradiation, histological observation of all tissues was done. No abnormality was observed in mice injected with hMSCs. hMSCs did not seem to have anarchical proliferation or any other side effect on tissue structure after long-term engraftment in irradiated mice (see Table 5). After hMSC injections, transplanted stem cells not form teratomas or undergo transformation and did not promote tumour growth. Histological analysis of various radiation-induced tissue damage was performed on all organs collected (heart, lung, liver, kidney, spleen, stomach, whole intestine, muscle and skin of the posterior femur of right leg, and the brain). Long-term histological analysis performed on different parts of the intestine (duodenum, jejunum, ileum, cecum, proximal, and distal colon) from day 3 to day 120 after irradiation revealed that the gut tissue retained its integrity in the early time after total body irradiation. No tumours were found in tissues (defined by neoplastic tissue or uncontrolled cell proliferation). Tissue samples showed no disruption, as defined by tissue discontinuity (e.g., rupture in intestinal epithelial barrier). We did not observe any abnormalities (e.g., inflammatory foci or abnormal cell proliferation). In addition, the size of the intestinal villi had not changed. No tissue damage or structural changes were observed in other

Table 4: Kinetics of hMSC biodistribution after total body irradiation (TBI) at 3.5 Gray.

Organs (positive per mice)	Days after irradiation						
	3 days	7 days	15 days	30 days	60 days	90 days	120 days
Brain	0/10 (0%)	0/10 (0%)	6/8 (75%)	2/6 (33%)	4/8 (50%)	0/8 (0%)	0/6 (0%)
Heart	8/10 (80%)	6/8 (75%)	7/8 (88%)	6/8 (75%)	0/8 (0%)	4/8 (50%)	4/6 (67%)
Lung	4/10 (40%)	10/10 (100%)	8/8 (100%)	6/8 (75%)	0/8 (0%)	3/8 (38%)	6/6 (100%)
Liver	2/10 (20%)	0/10 (0%)	8/8 (100%)	4/7 (57%)	4/8 (50%)	0/8 (0%)	0/6 (0%)
Spleen	0/10 (0%)	6/8 (75%)	5/8 (63%)	4/7 (57%)	4/8 (50%)	2/6 (33%)	0/6 (0%)
Kidney	0/10 (0%)	0/10 (0%)	4/8 (50%)	3/7 (43%)	0/8 (0%)	0/8 (0%)	2/6 (33%)
Abdominal area							
Muscle	2/10 (20%)	5/10 (50%)	2/6 (33%)	0/8 (0%)	0/6 (0%)	4/8 (50%)	2/6 (33%)
Stomach	4/10 (40%)	6/8 (75%)	4/7 (57%)	4/6 (67%)	0/8 (0%)	3/8 (38%)	1/6 (17%)
Duodenum	2/10 (20%)	5/10 (50%)	2/6 (33%)	0/7 (0%)	0/8 (0%)	0/8 (0%)	0/6 (0%)
Jejunum	2/10 (20%)	0/10 (0%)	2/8 (25%)	2/8 (25%)	0/8 (0%)	2/8 (25%)	0/6 (0%)
Ileum	0/10 (0%)	0/10 (0%)	0/8 (0%)	0/8 (0%)	0/8 (0%)	0/8 (0%)	0/6 (0%)
Cecum	0/10 (0%)	0/10 (0%)	3/8 (38%)	3/8 (38%)	0/8 (0%)	2/8 (25%)	2/6 (33%)
Proximal colon	0/10 (0%)	0/10 (0%)	3/8 (38%)	3/7 (43%)	0/8 (0%)	2/8 (25%)	0/6 (0%)
Distal colon	2/10 (20%)	2/8 (25%)	0/8 (0%)	1/5 (20%)	0/8 (0%)	0/8 (0%)	2/6 (33%)
Posterior leg (right)							
Skin	0/10 (0%)	0/10 (0%)	3/8 (38%)	0/6 (0%)	0/8 (0%)	3/8 (38%)	0/6 (0%)
Muscle	0/10 (0%)	5/10 (50%)	7/8 (88%)	2/8 (25%)	4/8 (50%)	0/8 (0%)	0/6 (0%)
Bone	0/10 (0%)	2/8 (25%)	1/8 (12.5%)	0/8 (0%)	4/8 (50%)	2/8 (25%)	0/6 (0%)
Bone marrow	0/10 (0%)	1/8 (12.5%)	5/8 (63%)	3/8 (38%)	0/8 (0%)	0/8 (0%)	1/6 (17%)
Blood	0/10 (0%)	0/10 (0%)	1/8 (12.5%)	4/7 (57%)	0/8 (0%)	0/8 (0%)	0/6 (0%)
Number of positive organs	26/190	48/178	71/151	47/137	40/150	27/150	20/114
Frequency	14%	28%	47%	34%	27%	18%	18%

The time at which the implantation of hMSCs is optimum varies from one organ to another. hMSCs were detectable at least up to 120 days after injection of human cells in a number of organs. Abdominal irradiation as compared to TBI modifies hMSC engraftment in the exposed area. Abdominal irradiation increased hMSC engraftment from 3 to 60 days in the stomach, duodenum, jejunum, and ileum and decreased engraftment in cecum and colon.

organs, 120 days after TBI. Similar results were observed after local irradiation (data is not shown).

4. Discussion

We addressed the question of the potential therapeutic impact of MSC infusion and their potential side effects on tissues in the context of irradiation damage. We investigated the short- and long-term biodistribution of MSCs when infused intravenously (IV) to various tissues in relation to the dose after irradiation. To answer this question, we built a preclinical model in which hMSCs were infused to NOD/SCID mice, without previous irradiation, and following irradiation. Irradiation consisted of local irradiation exposure to the leg (15 to 25 Gray) or abdomen (8.5 Gray) or total body irradiation (3.5 Gray). These configurations induced damage to the exposed tissues as previously reported [6, 7]. Abdominal irradiation induced transient gut damage [9–11] and leg irradiation induced strong ulceration of the skin and muscles [8]. To assess the impact of localized irradiation which induced local damage, one group was subjected to irradiation of the right posterior leg and another group was subjected to irradiation of the abdomen.

In the described experiments following irradiation and hMSC infusion, most of the implanted human cells were found in weakly damaged areas and the frequency of engraftment of hMSCs was proportional to the dose of irradiation. This dose-dependent localization of hMSCs throughout the body after a localized irradiation suggested both unrestricted colonization of hMSCs and the existence of a global body's reaction following radiation exposure with an increased engraftment related to the dose of irradiation.

MSC migration reported here is in agreement with previous reports in radiation-induced multiorgan failure, ischemic brain injury, myocardial infarction, and acute renal failure [12]. In a different set of experiments that we conducted in a nonhuman primate model submitted to mixed gamma-neutron irradiation and infused with green fluorescent protein (GFP) labelled nonhuman primate MSCs, we observed that MSCs engrafted preferentially in regenerating tissues [5]. In NOD/SCID mice, as previously observed, two weeks after combined irradiation, hMSCs migrated to damage area [6, 7]. These results suggest that MSCs may participate in the preservation of the targeted tissues without side effects on irradiated tissues. We have previously published that MSC engraftment in irradiated tissues improves their functional recovery [7–11].

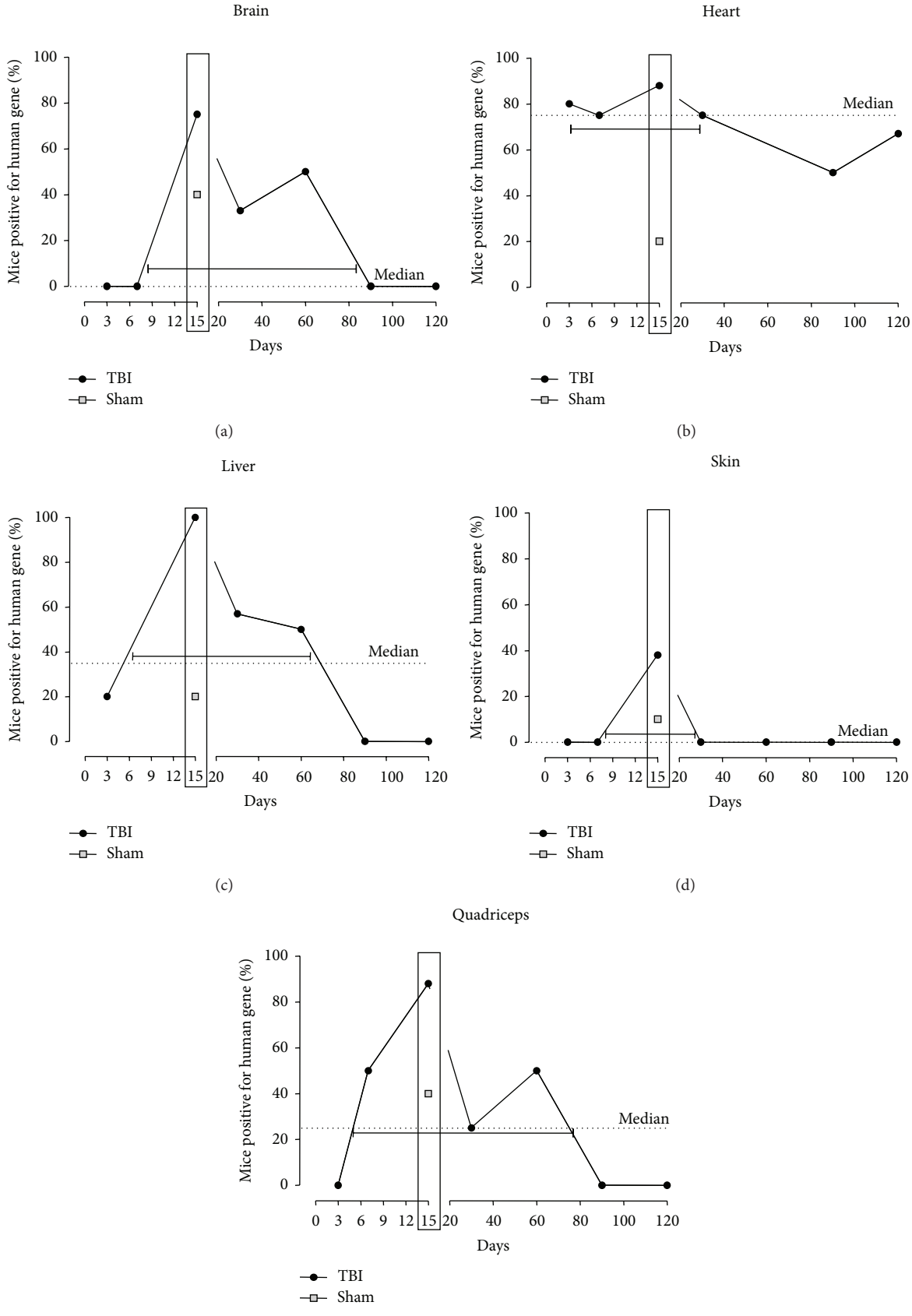

Figure 2: Continued.

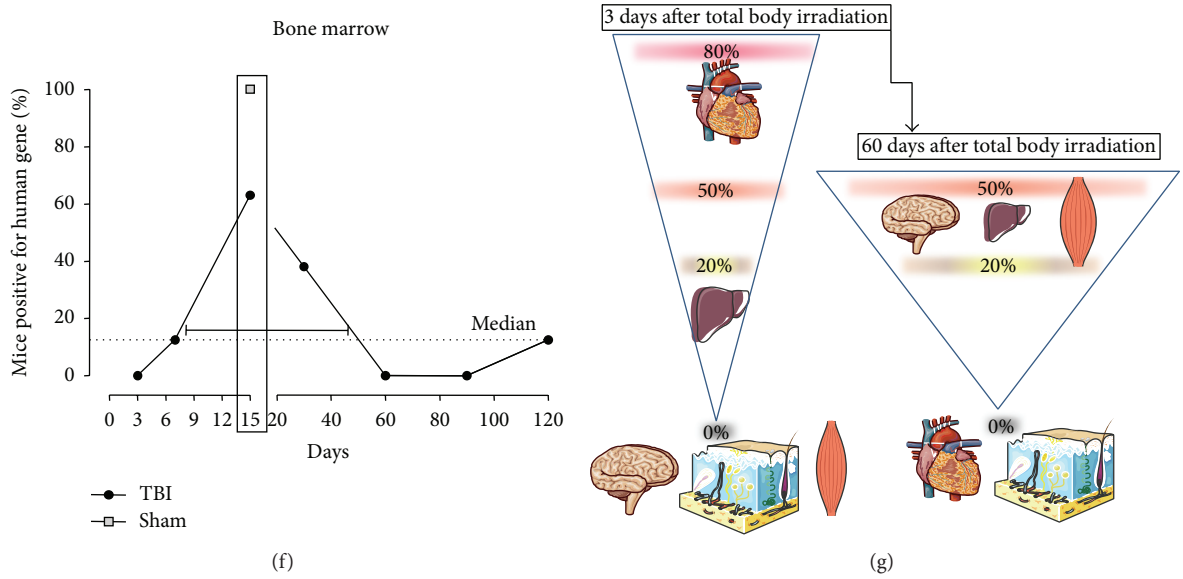

Figure 2: Kinetics of implantation of hMSCs during 120 days after total body irradiation. The percentage of positive mice for the human β-globin gene detected by PCR has been calculated after a sublethal total body irradiation (TBI). The human gene has been detected in (a) brain, (b) heart, (c) liver, (d) skin, (e) quadriceps, and (f) bone marrow. The tissues were collected at 3, 7, 15, 30, 60, and 120 days after TBI. The percentages represent the ratio (number of positive mice for the human beta-globin presence divided by total number of animals tested). At each analysis time, each group consisted of 10 animals. The control (named sham) consists in nonirradiated mice injected with hMSCs. The dotted line represents the median of the positive animal percentage during the 60 days after radiation exposure. (g) Illustration of anatomical variations in the presence of MSC after sublethal TBI.

Table 5: Histological analysis of tissue at 120 days after total body irradiation at 3.5 Gray in hMSC injected mice.

Organs	Positive organs				Negative organs			
	Number of mice	Tumour	Tissue		Number of mice	Tumour	Tissue	
			Disruption	Abnormality			Disruption	Abnormality
Brain	1	Neg.	Neg.	Neg.	9	Neg.	Neg.	Neg.
Heart	4	Neg.	Neg.	Neg.	6	Neg.	Neg.	Neg.
Lung	2	Neg.	Neg.	Neg.	8	Neg.	Neg.	Neg.
Liver	0	ND	ND	ND	10	Neg.	Neg.	Neg.
Spleen	2	Neg.	Neg.	Neg.	8	Neg.	Neg.	Neg.
Kidney	2	Neg.	Neg.	Neg.	8	Neg.	Neg.	Neg.
Abdominal area								
Muscle	1	Neg.	Neg.	Neg.	5	Neg.	Neg.	Neg.
Stomach	0	ND	ND	ND	8	Neg.	Neg.	Neg.
Duodenum	1	Neg.	Neg.	Neg.	9	Neg.	Neg.	Neg.
Jejunum	1	Neg.	Neg.	Neg.	9	Neg.	Neg.	Neg.
Ileum	1	Neg.	Neg.	Neg.	9	Neg.	Neg.	Neg.
Cecum	1	Neg.	Neg.	Neg.	9	Neg.	Neg.	Neg.
Colon proximal	3	Neg.	Neg.	Neg.	7	Neg.	Neg.	Neg.
Colon distal	2	Neg.	Neg.	Neg.	8	Neg.	Neg.	Neg.
Posterior leg (right)								
Skin	0	ND	ND	ND	10	Neg.	Neg.	Neg.
Muscle	1	Neg.	Neg.	Neg.	7	Neg.	Neg.	Neg.
Bone	5	Neg.	Neg.	Neg.	5	Neg.	Neg.	Neg.
Bone marrow	4	Neg.	Neg.	Neg.	5	Neg.	Neg.	Neg.

Histological analysis of various radiation-induced tissue damage was performed on all organs collected (heart, lung, liver, kidney, spleen, stomach, intestine in its entirety, muscle and skin of the posterior femur of left leg, and the brain). No tissue damage or structural changes were observed in the studied organs.

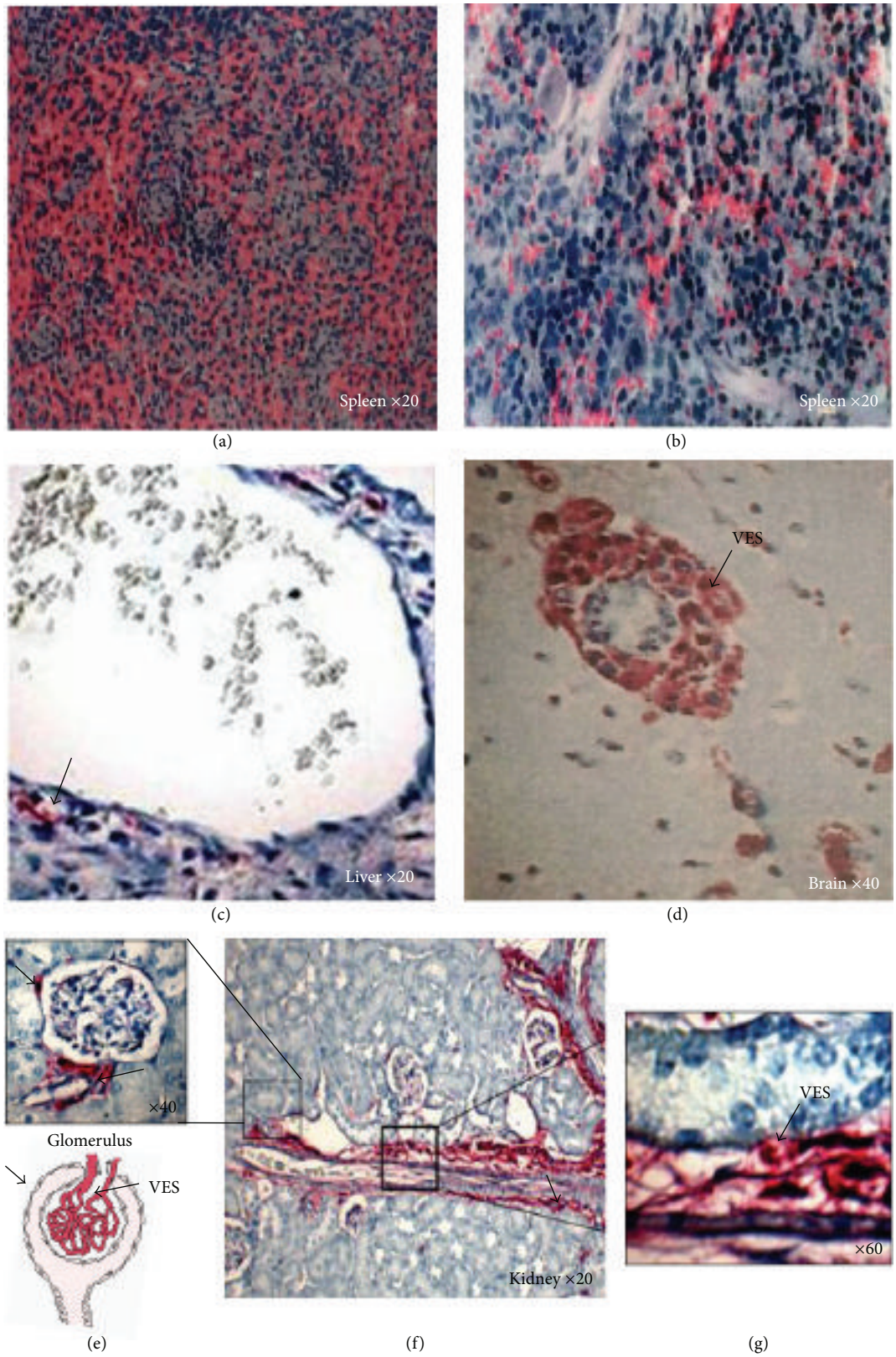

Figure 3: Histological examination of radiation exposed tissues by HES staining and human beta-2-microglobulin immunostaining in spleen and kidney. (a) illustrates a spleen of nonirradiated mice (control), (b) shows cell depletion 15 days after total body irradiation. The human cells expressing the human beta-2-microglobulin are stained in red. hMSCs migrated around the vascular axis (f), in functional structure such as glomerulus (e). Into glomerulus human cells have integrated both unitary structures: the glomerulus (e) and vascular endothelial system of this organ (g).

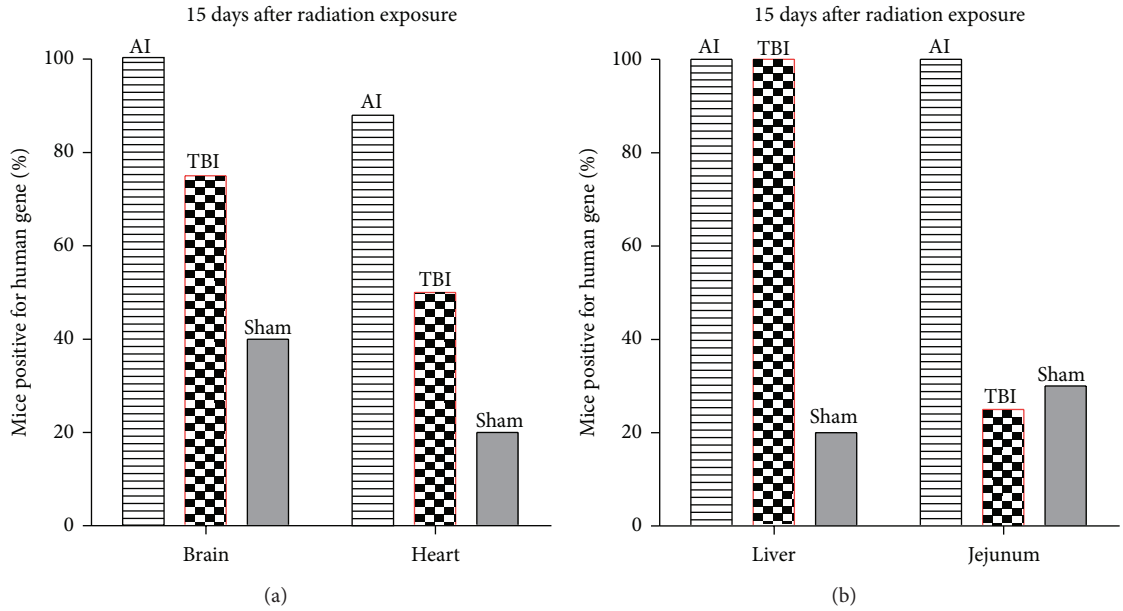

Figure 4: Radiation exposure promotes optimal chemotaxis of MSC. The percentage was calculated 15 days after radiation exposure and compared according to the irradiation configuration (abdominal irradiation (AI), represented in gray strips; total body irradiation (TBI) in red; and sham control group in gray). The histogram (a) represents the presence of the human beta-globin gene in organs outside the abdominal area such as the brain and heart. The histogram (b) represents the presence of the human gene in abdominal pelvic organs such as the liver and jejunum. Each group consisted in 10 animals. 15 days after AI, 100% of brain and 83% of hearts have human DNA. AI resulted in a mobilization of injected human stem cells on all the body via the vasculature system promoting communication into and between organs.

To our knowledge, no study reports the circulation of hMSCs in peripheral blood. We detected the circulation of hMSCs in peripheral blood and their passage through endothelial walls from days 15 to 30 after irradiation. The *in vivo* homing potential of hMSCs circulating in the bloodstream to the sites of injury/inflammation can be regulated by adhesion of hMSCs to the endothelium. Crossing of the endothelial barrier is another critical step in tissue migration of circulating cells [23].

Radiotherapy is used to treat 50% of cancer; 5% to 10% of patients develop late complications that alter quality of life [17]. Conventional therapies are palliative, poorly tolerated, costly, and lacking efficacy. The benefit of cell therapy by injection of mesenchymal stem cells for treatment of pelvic diseases has been documented [17]. A proof of concept was performed on 4 patients accidentally overirradiated after radiotherapy treatment for prostate cancer who suffered from chronic and fistulising colitis [18]. MSC injections might provide an efficient, safe, and well-tolerated alternative approach in the treatment of severe complications after pelvic radiotherapy for patients refractory to conventional therapy. Nevertheless understanding mechanisms in which adult somatic stem cells modulate tumour growth and long-term effect of MSCs after irradiation is essential to safely develop cell therapy as a therapeutic tool to treat radiation damage. We report no long-term side effects of hMSCs in irradiated tissues. Since the first reported trial in 1995, cultured MSCs have been used in 125 registered clinical trials (registered at http://www.clinicaltrial.gov/) without any reported side effect for cell therapy treatment. Clinical data support the long-term safety of MSCs. Furthermore the followup of patients after cell therapy treatment after-radiotherapy for breast [24], bladder, or prostate cancers [25] has never revealed side effects over a long-time period. A methodical review of clinical trials examined the safety of MSCs using MEDLINE, EMBASE, and the Cochrane Central Register of Controlled Trials (to June 2011). Systematic analysis examination for adverse events related to the use of MSCs did not identify any significant safety signals other than transient fever. This report further supports the safety of cell therapy to treat the consequence of radiation exposure in healthy tissues [26].

5. Conclusion

This work, along with our previously published studies on MSCs, supports the larger use of hMSC infusion to repair damaged tissues in patients following accidental irradiation and to treat side effects of radiotherapy in patient refractory to conventional treatments.

Conflict of Interests

The authors declare that there is no conflict of interests regarding the publication of this paper.

Authors' Contribution

Sabine Francois, Benoit Usunier, and Alain Chapel participated in research design, conducted experiments, performed

data analysis, and wrote the paper. Luc Douay and Marc Benderitter wrote the paper.

Acknowledgments

The authors thank Bruno L'homme and Magali Leroy for their helpful contributions.

References

[1] D. J. Prockop, "Marrow stromal cells as stem cells for nonhematopoietic tissues," *Science*, vol. 276, no. 5309, pp. 71–74, 1997.

[2] M. F. Pittenger, A. M. Mackay, S. C. Beck et al., "Multilineage potential of adult human mesenchymal stem cells," *Science*, vol. 284, no. 5411, pp. 143–147, 1999.

[3] J. Doorn, G. Moll, K. Le Blanc, C. van Blitterswijk, and J. de Boer, "Therapeutic applications of mesenchymal stromal cells: paracrine effects and potential improvements," *Tissue Engineering B*, vol. 18, no. 2, pp. 101–115, 2012.

[4] G. Ren, X. Chen, F. Dong et al., "Concise review: mesenchymal stem cells and translational medicine: emerging issues," *Stem Cells Translational Medicine*, vol. 1, no. 1, pp. 51–58, 2012.

[5] A. Chapel, J. M. Bertho, M. Bensidhoum et al., "Mesenchymal stem cells home to injured tissues when co-infused with hematopoietic cells to treat a radiation-induced multi-organ failure syndrome," *Journal of Gene Medicine*, vol. 5, no. 12, pp. 1028–1038, 2003.

[6] S. François, M. Bensidhoum, M. Mouiseddine et al., "Local irradiation not only induces homing of human mesenchymal stem cells at exposed sites but promotes their widespread engraftment to multiple organs: a study of their quantitative distribution after irradiation damage," *Stem Cells*, vol. 24, no. 4, pp. 1020–1029, 2006.

[7] M. Mouiseddine, S. François, A. Semont et al., "Human mesenchymal stem cells home specifically to radiation-injured tissues in a non-obese diabetes/severe combined immunodeficiency mouse model," *The British Journal of Radiology*, vol. 80, no. 1, pp. S49–S55, 2007.

[8] S. François, M. Mouiseddine, N. Mathieu et al., "Human mesenchymal stem cells favour healing of the cutaneous radiation syndrome in a xenogenic transplant model," *Annals of Hematology*, vol. 86, no. 1, pp. 1–8, 2007.

[9] A. Sémont, S. François, M. Mouiseddine et al., "Mesenchymal stem cells increase self-renewal of small intestinal epithelium and accelerate structural recovery after radiation injury," *Advances in Experimental Medicine and Biology*, vol. 585, pp. 19–30, 2006.

[10] A. Sémont, M. Mouiseddine, A. François et al., "Mesenchymal stem cells improve small intestinal integrity through regulation of endogenous epithelial cell homeostasis," *Cell Death and Differentiation*, vol. 17, no. 6, pp. 952–961, 2010.

[11] M. Mouiseddine, S. François, M. Souidi, and A. Chapel, "Intravenous human mesenchymal stem cells transplantation in NOD/SCID mice preserve liver integrity of irradiation damage," *Methods in Molecular Biology*, vol. 826, pp. 179–188, 2012.

[12] D. M. Patel, J. Shah, and A. S. Srivastava, "Therapeutic potential of mesenchymal stem cells in regenerative medicine," *Stem Cells International*, vol. 2013, Article ID 496218, 15 pages, 2013.

[13] O. N. Koç, J. Day, M. Nieder, S. L. Gerson, H. M. Lazarus, and W. Krivit, "Allogeneic mesenchymal stem cell infusion for treatment of metachromatic leukodystrophy (MLD) and Hurler syndrome (MPS-IH)," *Bone Marrow Transplantation*, vol. 30, no. 4, pp. 215–222, 2002.

[14] L. Fouillard, M. Bensidhoum, D. Bories et al., "Engraftment of allogeneic mesenchymal stem cells in the bone marrow of a patient with severe idiopathic aplastic anemia improves stroma," *Leukemia*, vol. 17, no. 2, pp. 474–476, 2003.

[15] L. von Bahr, I. Batsis, G. Moll et al., "Analysis of tissues following mesenchymal stromal cell therapy in humans indicates limited long-term engraftment and no ectopic tissue formation," *Stem Cells*, vol. 30, no. 7, pp. 1575–1578, 2012.

[16] J. J. Lataillade, C. Doucet, E. Bey et al., "New approach to radiation burn treatment by dosimetry-guided surgery combined with autologous mesenchymal stem cell therapy," *Regenerative Medicine*, vol. 2, no. 5, pp. 785–794, 2007.

[17] J. Voswinkel, S. Francois, J. M. Simon et al., "Use of mesenchymal stem cells (MSC) in chronic inflammatory fistulizing and fibrotic diseases: a comprehensive review," *Clinical Reviews in Allergy and Immunology*, vol. 45, no. 2, pp. 180–192, 2013.

[18] J. Voswinkel, S. Francois, N. C. Gorin, and A. Chapel, "Gastrointestinal autoimmunity: preclinical experiences and successful therapy of fistulizing bowel diseases and gut Graft versus host disease by mesenchymal stromal cells," *Immunologic Research*, vol. 56, no. 2-3, pp. 241–248, 2013.

[19] F. Caviggioli, L. Maione, D. Forcellini, F. Klinger, and M. Klinger, "Autologous fat graft in postmastectomy pain syndrome," *Plastic and Reconstructive Surgery*, vol. 128, no. 2, pp. 349–352, 2011.

[20] G. Rigotti, A. Marchi, M. Galiè et al., "Clinical treatment of radiotherapy tissue damage by lipoaspirate transplant: a healing process mediated by adipose-derived adult stem cells," *Plastic and Reconstructive Surgery*, vol. 119, no. 5, pp. 1409–1422, 2007.

[21] M. Benderitter, P. Gourmelon, E. Bey et al., "New emerging concepts in the medical management of local radiation injury," *Health Physics*, vol. 98, no. 6, pp. 851–857, 2010.

[22] A. Chapel, "Mesenchymal stromal cell therapy to repair radiation-induced intestinal damage: implications for treatment of abdominopelvic malignancy," *Cytotherapy*, vol. 14, no. 10, pp. 1157–1158, 2012.

[23] H. Motaln, C. Schichor, and T. T. Lah, "Human mesenchymal stem cells and their use in cell-based therapies," *Cancer*, vol. 116, no. 11, pp. 2519–2530, 2010.

[24] G. Rigotti, A. Marchi, P. R. Micciolo, and P. G. Baroni, "On the safety of autologous fat grafting for breast reconstruction," *Plastic and Reconstructive Surgery*, vol. 130, no. 1, pp. 206e–207e, 2012.

[25] A. Chapel, S. Francois, L. Douay, M. Benderitter, and J. Voswinkel, "New insights for pelvic radiation disease treatment: multipotent stromal cell is a promise mainstay treatment for the restoration of abdominopelvic severe chronic damages induced by radiotherapy," *World Journal of Stem Cells*, vol. 5, no. 4, pp. 106–111, 2013.

[26] M. M. Lalu, L. McIntyre, C. Pugliese et al., "Safety of cell therapy with mesenchymal stromal cells (SafeCell): a systematic review and meta-analysis of clinical trials," *PLoS ONE*, vol. 7, no. 10, Article ID e47559, 2012.

Hindawi Publishing Corporation
Stem Cells International
Volume 2013, Article ID 678063, 5 pages
http://dx.doi.org/10.1155/2013/678063

Review Article

Biodistribution of Mesenchymal Stem/Stromal Cells in a Preclinical Setting

Luc Sensebé[1,2] and Sandrine Fleury-Cappellesso[1,2]

[1] *UMR5273 CNRS, UPS, EFS—INSERM U1031, STROMALab, Toulouse, France*
[2] *EFS Pyrénées-Méditerranée, Toulouse, France*

Correspondence should be addressed to Luc Sensebé; luc.sensebe@efs.sante.fr

Received 14 May 2013; Accepted 8 July 2013

Academic Editor: Mauro Krampera

Due to their multi/pluripotency and immunosuppressive properties, mesenchymal stem/stromal cells (MSCs) are important tools for treatment of immune disorders and tissue repair. The increasing uses of MSCs lead to the development of production processes that need to be in accordance with good manufacturing practices (GMP). In Europe, MSCs are somatic cell-therapy products, referred to as advanced-therapy medicinal products (ATMPs), and in the United States MSCs must comply with current good tissue practice requirements. The safety and efficacy of MSCs must be ensured, whatever the cell source, and studies of dose and biodistribution are important aspects of safety testing. Preclinical data on biodistribution and pharmacodynamics are mandatory for approval. It is important to demonstrate that MSCs do not have unwanted homing that could drive to inappropriate differentiation in some organ or to support cancer development as suggested in some experiments. All these aspects should be addressed in a risk-based approach according to recently published guidelines by EMA. In the present article, we summarize the main approaches for labeling and tracking of infused MSCs, report on current animal models, and give an overview of available results on biodistribution.

1. Introduction

One of the most promising tools in cellular therapy and regenerative medicine is the use of mesenchymal stem/stromal cells (MSCs) because of their dual differentiation potential and immune regulatory properties. First described by Alexander Friedenstein, in the 1960s/70s [1], as mesodermic-derived nonhematopoietic bone marrow (BM) cells adhering to plastic that developed into colonies with a fibroblastic appearance, MSCs were called stem cells of skeletal tissues (e.g., bone, cartilage) [2]. The first clinical use was their combination with biomaterials to repair long bone fractures [3]. Later, emerging cells of the MSC type were found to originate from the neural crest and not the mesoderm [4], and cells with some features of BM-MSCs were found in almost all tissues of the fetus, neonate, and adult [5].

An international expert panel [6] described the common minimal criteria for cells in the MSC category: cells adhering to plastic; able to form colony-forming unit fibroblasts (CFU-Fs); positive for membrane markers CD90, CD73, and CD105 but negative for the hematopoietic molecules CD45, CD34, and HLA-DR; and able to differentiate via osteoblastic, chondrocytic, and adipocytic pathways. These main characteristics apply to cultured BM-MSCs, but some differences appear depending on the tissue of origin (e.g., adipose tissue-derived MSC expression of CD34 and CD54 [7]). As well, MSCs from different tissues are not equivalent in phenotype and function [8].

The MSC field has moved rapidly with the demonstration that *ex vivo*-expanded MSCs show immuno suppressive properties that were exploited in a wide range of phase 2 clinical trials from treatment of drug-resistant graft-versus-host disease [9] to organ transplantation [10]. Finally, MSCs have trophic effects mediated by numerous growth factors and the cytokines they produce [11].

Cells referred to as MSCs originating from various tissues are now widely used in clinical trials. In Europe, MSCs are somatic cell-therapy products, referred to as advanced-therapy medicinal products (ATMPs) and are under European Regulation No. 1394/2007. In the United States, like

the production of any other cellular and tissue-based product, MSCs must comply with Current Good Tissue Practice requirements, under the US Code of Federal Regulations. The safety and efficacy of MSCs must be ensured, whatever the cell source, and studies of dose and biodistribution are important aspects of safety testing. Moreover, before approval, regulatory authorities require preclinical data on bio-distribution and pharmacodynamics; in the European Union, these data should be generated according to the European Pharmacopoeia. In fact, biodistribution of MSCs is one of the main preclinical data required for safety; it is important to demonstrate that MSCs do not have unwanted homing that could drive to inappropriate differentiation in some organ [12] or support cancer development as suggested in some experiments [13, 14]. All these aspects should be addressed in a risk-based approach. Guideline on the risk-based approach was recently published by the Committee for Advanced Therapies (CAT) of EMA (Guideline on the risk-based approach according to annex I, part IV of directive 2001/83/EC for ATMPs: EMA/CAT/CPWP/686637/2011). The guideline defines risks, for example, unwanted targeting of cells/organs, unwanted tissue formation, and tumor formation; risk factors, as qualitative or quantitative characteristics that contribute to a specific risk following administration of ATMPs. All available information on risks and risk factors should be integrated for building risk profiling, and bio-distribution is one of the main preclinical data giving information in different risks and risk factors. To reach this target, biodistribution has to be conducted according to the European Pharmacopoeia and according to the Good Laboratory Practices.

After injection of MSCs, whatever the route, the study of biodistribution is challenging; different aspects must be analyzed, the main ones being methods for cell labeling or staining and tracking, animal models, and relevance for human use.

2. Labeling and Tracking of MSCs

As for other living cells, MSCs can be labeled or stained by numerous methods. They can be easily labeled with an intracellular dye such as 5-carboxyfluorescein diacetate succinimidyl ester or a synthetic nucleoside such as 5-bromo-2′-deoxyuridine (BrdU) during culture. BrdU is incorporated into the newly synthesized DNA of replicating cells, substituting for thymidine during DNA replication. During the labeling phase, this method requires dividing cells, which could result in nonhomogeneous labeling, with an inconsistent percentage of residual unlabeled MSCs. After infusion, labeled MSCs can be detected in tissues with BrdU-specific antibodies [15]. For these two labeling molecules, cell division results in sequential halving of incorporated molecules that could decrease the quantity per cell to below the detection threshold. It should be stressed that these methods are more useful for studying distribution or local spreading after intraorgan injection. Another easy method of cell labeling in MSCs is transfection of cells with a gene coding a fluorescent protein (e.g., green fluorescent protein [GFP]) [16]. Two problems can be encountered: autofluorescence of some tissues and nonspecific expression due to reuptake of protein by other cells such as macrophages. Finally, all these methods do not allow for *in vivo* followup of the biodistribution of MSCs; after animals are killed, specific staining and histological analyses of different tissues are required. For *in vivo* followup, several labeling techniques are useful: labeling with a radioactive tracer molecule such as technetium-99 m, ^{111}indium-oxine [17] or fludeoxyglucose (18FDG), with positron emission tomography (PET) [18]; transfection of MSCs with luciferase and external camera-based acquisition of bioluminescence after injection of a substrate (luciferin) [19]; or incorporation of iron magnetic nanoparticles in MSCs and *in vivo* MRI [20, 21].

The use of different molecules for labeling may have consequences on MSC functions particularly in differentiation or immunosuppression. With iron nanoparticles, studies have shown contradictory results: Chang et al. [20] reported impaired *in vitro* osteogenic and chondrogenic differentiations after labeling of human MSCs with amine-surface-modified superparamagnetic iron oxide nanoparticles; on the contrary, Schmidtke-Schrezenmeier et al. [21] found that labeling MSCs with iron oxide-poly(L-lactide) nanoparticles did not affect a large set of functions of labelled MSCs: viability, phenotype, proliferation, differentiation, or immunosuppression. These conflicting results could be related to differences in iron particles used, number of particles per cell, or the production processes and age of cells.

Finally, in xenogeneic models, without previous labeling, human MSCs can be tracked by the use of quantitative PCR (qPCR) of human Alu sequences [22] or histology after labeling of human specific antigens. The human Alu sequences are highly repeated, species-specific, and 300 bp sequences. Because of their high repetition and species specificity, Alu sequences are a marker of choice to detect invasion of a few human cells in a mouse organ. The presence and quantification of the Alu marker is evaluated by qPCR amplification with DNA extracted from multiple tissue samples from mice as templates and from healthy noninduced mice as a negative control. A standard curve indicating the quantity of human DNA versus mouse DNA can be established with known amounts of DNA extracted from the different mouse tissues and human MSCs. This standard curve allows for estimating the number of cells per weight unit of tissue as 230 human cells/g of tissue (LS, personal data); with an improved technique, the threshold could reach 100 human cells/organ [23].

3. Animal Models

As for other preclinical data, the choice of animal model is critical. For studying biodistribution, a first step could be the use of MSCs from the same animal species. However, regulatory authorities require data for human MSCs. To prevent rejection of human MSCs, which could interfere with the biodistribution and maintenance within different tissues, the most popular models are injection in immunocompromised rodents, such as nude mice, or to prevent any rejection, NOD/SCID mice. Owing to the incomplete disappearance of immunity in nude and even NOD/SCID mice, the best model seems to be NOD-Rag mice [24]. The main

problem with mouse models is the dose of intravenous-infused MSCs, generally between 0.5 to 2 million, to prevent death by lung embolization. These doses, corresponding to 100 to 200 million of MSCs/kg, deviate greatly from the clinically relevant doses for humans. In a European program of the 7th Framework Program of the European Commission (REBORNE: FP7-HEALTH-241879), we studied biodistribution of MSCs from two different tissues: bone marrow and adipose tissue. Studies were conducted in SCID mice after IV infusion or after subcutaneous implantation of MSCs loaded in a ceramic scaffold. Whatever the sources of MSCs, using qPCR for human Alu sequences, there was never any unwanted homing of MSCs after IV infusion. At day 7, on the contrary of AT-MSC, we did not find any BM-MSCs in lungs; at day 91, only with some AT MSCs there was remaining human DNA in lungs. Following subcutaneous implantation of MSCs + scaffold, there were never any recirculation and homing in other organs. Moreover, histological analysis of different organs did not show any tumor formation. These data demonstrated the safety of using BM and AT MSCs, and based on these results and other preclinical data, the French, German, Spanish, and Italian regulatory authorities delivered authorization for starting clinical studies in bone repair.

Use of other models, such as nonhuman primates, seems more relevant but is difficult for ethical reasons, and when testing human MSCs, use of immuneosuppressive drugs is mandatory.

Regarding intended clinical uses, models should be relevant for the route of MSC infusion—intravenous, intra-arterial, or local injection or implantation—and for the treated condition. MSCs preferentially home to injured tissues such as radiation-injured tissues [25]. The bio-distribution and pharmacodynamics must be studied in both normal and animal models of diseases.

Finally, because MSCs from different tissues are not equivalent [8] and culture processes differ, MSCs from different types of preparation should be tested.

4. Biodistribution of MSCs

4.1. In Animal Models. Detection of the human Alu sequence revealed that human BM-MSCs intravenously injected in mice are rapidly trapped in lungs. After this first embolization, MSCs may be recirculated, as demonstrated 15 min postinfusion by culture of peripheral blood mononuclear cells showing CFU-Fs of human origin [23]. During a short followup, infused human MSCs home to different organs, mainly liver, but this secondary recirculation seems to concern only a small amount of infused MSCs. In this model, at 48 and 96 hr postinfusion, only 0.04% and 0.01% of injected human MSCs were recovered in 6 tissues (liver, spleen, pancreas, brain, kidney, heart, and bone marrow). On studying human BM-MSC distribution in mice for a longer time (7 days and 3 months), human cells were found only at 7 days in spleen (LS, personal data). Labeling techniques appear to be important: labeling with technetium-99 m and intravenous infusion of human BM-MSCs revealed a long-term persistence of human cells up to 4 to 13 months in bone, bone marrow, spleen, muscle, and cartilage [26].

BM-MSCs intravenously infused, as human AT-MSCs, adipose tissue are trapped first in lung. Human adipose tissue MSCs transfected with luciferase in nude mice showed that human cells were cleared at 1 week from the lung, and then persisted for 31 weeks in liver [19]. On detecting the Alu sequence of human adipose tissue MSCs in NOD/SCID mice, 7 days postinfusion, human cells were located in spleen but mainly remained within lungs and persisted there for 3 months without any other secondary localization (LS, personal data). Recently, after intravenous infusion of human adipose tissue MSCs, human cells were rapidly cleared and mostly found at days 11 and 28 in lungs and gastrointestinal tract. As well, results were highly variable: only 17% to 25% of mice were positive [22]. Regarding specific regulatory requirements, intravenously infused human MSCs were not found in testis or ovary [22, 27].

Findings were similar for human BM-MSCs intraarterially infused in mice and for intravenously infused cells [23] but differed by animal model used for the disease. For example, in rat with cerebral ischemia, injection of human BM-MSCs resulted in transient localization of human cells in the brain [28].

Results could differ when using animal MSCs in the same species for an abnormality. After intravenous infusion of ^{111}indium-oxine-labeled rat MSCs, Yoon et al. observed brain uptake in rats with brain trauma [29]. In an irradiated primate model, intravenous infusion of primate GFP-labeled BM-MSCs and hematopoietic stem cells resulted in localization in bone marrow, skin, gut, and muscle from 12 to 82 days afterinfusion, with no cells in lungs [27].

Finally, in models with local injection, for example, intraarticular [22] and intramuscular [30], cells remained for a long time at the injection site. After intramuscular injection, no human DNA was detected in any evaluated tissues outside muscle [30]. In contrast, after intraarticular injection at different times (from day 11 to 186), human Alu sequences were found in heart, spleen, intestine, brain, testis, or liver of 10% to 20% of analyzed mice [22]. When cells are implanted with biomaterial or a scaffold, locally tracking and demonstrating persistence of human cells can be difficult [31], but BM-MSCs or AT-MSCs do not spread (LS, personal data).

4.2. In Humans. Few data are available on the bio-distribution of MSCs in humans. The results can be somewhat similar to these found in rodent models in terms of lung trapping, with differences in recirculation that could be related to the disease or species. Gholamrezanezhad et al. [17] used radiolabeled (^{111}In-oxine) BM-MSCs intravenously infused in patients with advanced cirrhosis and found that after initial lung accumulation, BM-MSCs relocalized in liver and spleen: radioactivity decreased from 33.5% to 2% in lung and increased from 2% to 42% in spleen. In 3 patients receiving allogeneic BM-MSCs for treatment of corticoid-resistant graft-versus-host disease (GVHD) after hematopoietic stem cell transplantation, postmortem analysis of one patient revealed donor DNA targeting GVHD in a lymph node and in the gastrointestinal tract, but donor DNA was never found in lung, liver, or spleen [32].

5. Conclusions and Perspectives

Studies of MSC biodistribution are mandatory for safety reasons, regulatory requirements, and for risk-based approach of ATMPs uses. Labeling of MSCs is easy, but the limitations of each technique and the desired followup should be considered. Classical techniques (e.g., GFP labeling) do not allow for *in vivo* followup. A labeling system allowing for external followup (e.g., luciferase, iron particles, or radioactivity) may decrease detection sensitivity. Detection of human Alu sequences by qPCR appears to be simple and sensitive and can be used when continuous external followup is not required. In preclinical settings, the main animal models used are immunocompromised mice (nude, NOD/SCID, or NOG-Rag). Although easy to use and informative, such models have limitations: they are xenogeneic, human MSCs are larger than mouse MSCs, and the physiologic features differ between rodents and humans. Whatever the model, MSCs seem to be initially trapped in lungs. After this lung embolization, MSCs are recirculated, but the number of recirculating cells seems low, and secondary homing occurs at the liver, spleen, and inflammatory or injured sites.

Two main recommendations are (1) use of the most sensitive technique for labeling and/or tracking and (2) a relevant animal model in terms of immune rejection potential and the intended disease to treat. Finally, animal models are required, informative but not enough, and more data in humans are needed. It could be discussed with regulatory authorities performing some phase 1 studies for validating tracking systems and biodistribution in human. Moreover, registries reporting all available data in human will be of major importance.

Acknowledgments

This work was supported by Grants from the 7th Framework Program of the European Commission: CASCADE (FP7-HEALTH-233236) and REBORNE (FP7-HEALTH-241879), by Grant from Agence Nationale pour la Recherche: SAFE (ANR-2011-RPIB-01201) and the Infrastructure Program ECELLFRANCE (ANR-11-INSB-005), and by grant from région Midi-Pyrénées (NOMASEC), Oncodesign company (Dijon, France) for study in SCID mouse.

References

[1] A. J. Friedenstein, J. F. Gorskaja, and N. N. Kulagina, "Fibroblast precursors in normal and irradiated mouse hematopoietic organs," *Experimental Hematology*, vol. 4, no. 5, pp. 267–274, 1976.

[2] A. I. Caplan, "The mesengenic process," *Clinics in Plastic Surgery*, vol. 21, no. 3, pp. 429–435, 1994.

[3] R. Quarto, M. Mastrogiacomo, R. Cancedda et al., "Repair of large bone defects with the use of autologous bone marrow stromal cells," *New England Journal of Medicine*, vol. 344, no. 5, pp. 385–386, 2001.

[4] Y. Takashima, T. Era, K. Nakao et al., "Neuroepithelial cells supply an initial transient wave of MSC differentiation," *Cell*, vol. 129, no. 7, pp. 1377–1388, 2007.

[5] M. Crisan, S. Yap, L. Casteilla et al., "A perivascular origin for mesenchymal stem cells in multiple human organs," *Cell Stem Cell*, vol. 3, no. 3, pp. 301–313, 2008.

[6] M. Dominici, K. le Blanc, I. Mueller et al., "Minimal criteria for defining multipotent mesenchymal stromal cells. The International Society for Cellular Therapy position statement," *Cytotherapy*, vol. 8, no. 4, pp. 315–317, 2006.

[7] D. A. de Ugarte, K. Morizono, A. Elbarbary et al., "Comparison of multi-lineage cells from human adipose tissue and bone marrow," *Cells Tissues Organs*, vol. 174, no. 3, pp. 101–109, 2003.

[8] D. G. Phinney and L. Sensebé, "Mesenchymal stromal cells: misconceptions and evolving concepts," *Cytotherapy*, vol. 15, pp. 140–145, 2013.

[9] K. le Blanc, I. Rasmusson, B. Sundberg et al., "Treatment of severe acute graft-versus-host disease with third party haploidentical mesenchymal stem cells," *The Lancet*, vol. 363, no. 9419, pp. 1439–1441, 2004.

[10] J. Tan, W. Wu, X. Xu et al., "Induction therapy with autologous mesenchymal stem cells in living-related kidney transplants: a randomized controlled trial," *Journal of the American Medical Association*, vol. 307, no. 11, pp. 1169–1177, 2012.

[11] D. G. Phinney and D. J. Prockop, "Concise review: mesenchymal stem/multipotent stromal cells: the state of transdifferentiation and modes of tissue repair—current views," *Stem Cells*, vol. 25, no. 11, pp. 2896–2902, 2007.

[12] M. Breitbach, T. Bostani, W. Roell et al., "Potential risks of bone marrow cell transplantation into infarcted hearts," *Blood*, vol. 110, no. 4, pp. 1362–1369, 2007.

[13] F. Djouad, P. Plence, C. Bony et al., "Immunosuppressive effect of mesenchymal stem cells favors tumor growth in allogeneic animals," *Blood*, vol. 102, no. 10, pp. 3837–3844, 2003.

[14] J. Houghton, H. Li, X. Fan et al., "Mutations in bone marrow-derived stromal stem cells unmask latent malignancy," *Stem Cells and Development*, vol. 19, no. 8, pp. 1153–1166, 2010.

[15] G. Bouchez, L. Sensebé, P. Vourc'h et al., "Partial recovery of dopaminergic pathway after graft of adult mesenchymal stem cells in a rat model of Parkinson's disease," *Neurochemistry International*, vol. 52, no. 7, pp. 1332–1342, 2008.

[16] M. Bensidhoum, A. Chapel, S. Francois et al., "Homing of in vitro expanded Stro-1^- or Stro-1^+ human mesenchymal stem cells into the NOD/SCID mouse and their role in supporting human CD34 cell engraftment," *Blood*, vol. 103, no. 9, pp. 3313–3319, 2004.

[17] A. Gholamrezanezhad, S. Mirpour, M. Bagheri et al., "In vivo tracking of ^{111}In-oxine labeled mesenchymal stem cells following infusion in patients with advanced cirrhosis," *Nuclear Medicine and Biology*, vol. 38, no. 7, pp. 961–967, 2011.

[18] E. Wolfs, T. Struys, T. Notelaers et al., "^{18}F-FDG labeling of mesenchymal stem cells and multipotent adult progenitor cells for PET imaging: effects on ultrastrucute and differentiation capacity.," *Journal of Nuclear Medicine*, vol. 54, pp. 447–454, 2013.

[19] M. Vilalta, I. R. Dégano, J. Bagó et al., "Biodistribution, long-term survival, and safety of human adipose tissue-derived mesenchymal stem cells transplanted in nude mice by high sensitivity non-invasive bioluminescence imaging," *Stem Cells and Development*, vol. 17, no. 5, pp. 993–1004, 2008.

[20] Y.-K. Chang, Y.-P. Liu, J. H. Ho, S.-C. Hsu, and O. K. Lee, "Amine-surface-modified superparamagnetic iron oxide nanoparticles interfere with differentiation of human mesenchymal stem cells," *Journal of Orthopaedic Research*, vol. 30, pp. 1499–1506, 2012.

[21] G. Schmidtke-Schrezenmeier, M. Urban, A. Musyanovych et al., "Labeling of mesenchymal stromal cells with iron oxide-poly(l-lactide) nanoparticles for magnetic resonance imaging: uptake, persistence, effects on cellular function and magnetic resonance imaging properties," *Cytotherapy*, vol. 13, no. 8, pp. 962–975, 2011.

[22] K. Toupet, M. Maumus, J.-A. Peyrafitte et al., "Long-term detection of human adipose derived mesenchymal stem cells after intra-articular injection," *Arthritis & Rheumatism*, vol. 65, no. 7, pp. 1786–1794, 2013.

[23] R. H. Lee, A. A. Pulin, M. J. Seo et al., "Intravenous hMSCs improve myocardial infarction in mice because cells embolized in lung are activated to secrete the anti-inflammatory protein TSG-6," *Cell Stem Cell*, vol. 5, no. 1, pp. 54–63, 2009.

[24] M. G. Manz and J. P. di Santo, "Renaissance for mouse models of human hematopoiesis and immunobiology," *Nature Immunology*, vol. 10, no. 10, pp. 1039–1042, 2009.

[25] M. Mouiseddine, S. François, A. Semont et al., "Human mesenchymal stem cells home specifically to radiation-injured tissues in a non-obese diabetes/severe combined immunodeficiency mouse model," *British Journal of Radiology*, vol. 80, no. 1, pp. S49–S55, 2007.

[26] C. Allers, W. D. Sierralta, S. Neubauer, F. Rivera, J. J. Minguell, and P. A. Conget, "Dynamic of distribution of human bone marrow-derived mesenchymal stem cells after transplantation into adult unconditioned mice," *Transplantation*, vol. 78, no. 4, pp. 503–508, 2004.

[27] A. Chapel, J. M. Bertho, M. Bensidhoum et al., "Mesenchymal stem cells home to injured tissues when co-infused with hematopoietic cells to treat a radiation-induced multi-organ failure syndrome," *Journal of Gene Medicine*, vol. 5, no. 12, pp. 1028–1038, 2003.

[28] B. Mitkari, E. Kerkelä, J. Nystedt et al., "Intra-arterial infusion of human bone marrow-derived mesenchymal stem cells results in transient localization in the brain after cerebral ischemia in rats," *Experimental Neurology*, vol. 239, pp. 158–162, 2013.

[29] J.-K. Yoon, B.-N. Park, W.-Y. Shim, J. Y. Shin, G. Lee, and Y. H. Ahn, "In vivo tracking of ^{111}In-labeled bone marrow mesenchymal stem cells in acute brain trauma model," *Nuclear Medicine and Biology*, vol. 37, no. 3, pp. 381–388, 2010.

[30] Y. Ramot, M. Meiron, A. Toren, M. Steiner, and A. Nyska, "Safety and biodistribution profile of Placental-derived mesenchymal stromal cells (PLX-PAD) following intramuscular delivery," *Toxicologic Pathology*, vol. 37, no. 5, pp. 606–616, 2009.

[31] A. Bouacida, P. Rosset, V. Trichet et al., "Pericyte-like progenitors show high immaturity and engraftment potential as compared with mesenchymal stem cells," *PLoS One*, vol. 7, no. 11, Article ID e48648, 2012.

[32] O. Ringdén, M. Uzunel, I. Rasmusson et al., "Mesenchymal stem cells for treatment of therapy-resistant graft-versus-host disease," *Transplantation*, vol. 81, no. 10, pp. 1390–1397, 2006.

Hindawi Publishing Corporation
Stem Cells International
Volume 2013, Article ID 130763, 8 pages
http://dx.doi.org/10.1155/2013/130763

Review Article

Mesenchymal Stem Cells Migration Homing and Tracking

Abhishek Sohni and Catherine M. Verfaillie

Stem Cell Biology and Embryology, Department of Development and Regeneration, KU Leuven, 3000 Leuven, Belgium

Correspondence should be addressed to Abhishek Sohni; abhishek.sohni@med.kuleuven.be and
Catherine M. Verfaillie; catherine.verfaillie@med.kuleuven.be

Received 27 March 2013; Accepted 8 July 2013

Academic Editor: Mauro Krampera

In this review, we discuss the migration and homing ability of mesenchymal stem cells (MSCs) and MSC-like cells and factors influencing this. We also discuss studies related to the mechanism of migration and homing and the approaches undertaken to enhance it. Finally, we describe the different methods available and frequently used to track and identify the injected cells *in vivo*.

1. Potential of MSC and MSC-Like Cells for Cell-Based Therapies

For stem cells to be used in the clinical setting, they should be safe, that is, do not form tumors, and be readily harvested and/or expanded. Although embryonic stem cells (ESCs) are pluripotent and could be used to replace any tissue, they can form teratomas. Hence, their potential use in cell-based therapies will require that no undifferentiated ESCs persist in the graft. In addition, culture methods for human ESCs are still quite demanding; hence, scaleup is not yet straightforward.

The best-studied transplanted stem cell is the hematopoietic stem cell (HSC) that can be harvested from different sources (bone marrow, blood, and umbilical cord blood) in sufficient numbers for transplantation. HSCs have then also been used for cell-based therapies especially in an allogeneic setting for more than a quarter of a century.

Other adult stem cell populations that are being evaluated clinically are MSCs and multipotent adult progenitor cells (MAPCs; trade name MultiStem) both derived from human postnatal tissue.

MSCs were first described in the 1970s by Friedenstein et al. who described a population of cells derived from bone marrow that had the appearance of fibroblasts and could generate aside from fibroblasts, also adipocytes, chondrocytes, and osteocytes [1, 2]. These cells grew out as colonies and were therefore termed "colony forming units" or CFUs. Later on, Caplan and others termed these cells "mesenchymal stem cells" (MSCs) [3, 4]. MSCs are classically isolated from bone marrow however; they can be found in multiple tissues, such as adipose tissue, fetal lung, placenta, Wharton's jelly, and UCB, among others [5–8]. MSCs are characterized as adherent cells with the ability to differentiate into fibroblasts, adipocytes, chondrocytes, osteocytes, and smooth muscle cells apart from supportive hematopoietic "stromal" cells [1, 3, 4, 9] and with a characteristic cell surface antigen profile.

Many MSCs or MSC-like cells with varying differentiation potential have been described and reviewed elsewhere [10]. Although the cell surface repertoire and the gene expression pattern vary among these cells, this is likely a reflection of the tissue of origin or the culture conditions used for maintenance of these cells [11, 12]. A standardized phenotype was proposed for MSCs by the International Society for Cellular Therapies. A typical human (h)MSC should express CD105, CD90, and CD73 but not CD79a, CD45, CD34, CD19, CD14, CD11b, and HLA-DR on its surface [3, 4, 13]. Most hMSCs or hMSC-like adult progenitors give rise to mesoderm derivatives such as fat, bone, and cartilage [9]. Apart from the mesenchymal lineages, MSCs and MSC-like cells such as hMAPC have been reported to also be able to give rise to skeletal myocytes, cardiomyocytes smooth muscle cells, and endothelial cells [11, 14–16] (also reviewed in [10]). Although some studies have suggested that MSCs can give rise to neurons and endodermal progeny [17–19], it remains unclear whether such progeny has all properties of primary neuroectodermal and endodermal cells.

Apart from being able to differentiate to multiple cell types *in vitro* (and *in vivo*), MSCs and MSC-like adult stem cells have extensive immunomodulatory and immunological tolerance inducing characteristics [20–26]. hMSCs that characteristically lack expression of MHC-II, CD40, CD80 and CD86 but express MHC-I present themselves as nonimmunogenic. Although the presence of MHC-I may activate T-cells, due to lack of costimulatory molecules, MSCs fail to elicit an immune response [27]. MSCs also efficiently suppress an immune response by modulating T-cell activation and proliferation [28, 29], either by a direct cell-cell interaction [30] or mediated via soluble factors [28, 31] and this is independent of MHC matching. This immunomodulating effect of MSCs is being explored as adjuvants during allogenic transplantation to prevent graft-versus-host disease (GVHD) [32, 33] and during organ transplantation to prevent immune rejection [29, 34–36]. In addition, the immunomodulatory characteristics of MSCs are being evaluated in the setting of autoimmune diseases, such as Crohn's Disease, among others [37, 38].

MSCs also produce innumerable growth factors and cytokines, which make them suitable for inducing endogenous repair. For instance, MSCs express bone morphogenic protein(s) (BMPs) which is effective in enhancing cartilage, bone, and tendon repair [39]. Likewise, MSCs produce factors that enhance revascularisation, even if their nature is not understood, and are therefore being evaluated in therapies for ischemic disorders, such as stroke, myocardial infarct, or peripheral arterial disorders. Yet another field of therapeutic applications is grafting MSCs that have been genetically modified to overexpress a protein in diseased tissues due to the genetic mutation of the given factor.

2. Homing of MSCs

The lingering problem in the field of cell-based therapies is the delivery of the cells to the site of injury, a process termed "homing." As discussed above, the therapeutic efficacy of MSCs is greatly dependent on their ability to produce juxtacrine or paracrine factors that enhance regeneration from endogenous (stem) cells. For juxtacrine effects to be possible, migration of MSCs to the diseased organ/tissue is required. Migration and homing to the tissue of injury is influenced by multiple factors including age and passage number of the cells, culture conditions, and the delivery method, among others. We here provide a review of the literature demonstrating the effect of various factors on migration and homing of MSCs.

2.1. Age, Passage Number, and Dosage of MSCs. It has been shown that with higher passage number, the engraftment efficiency of MSCs decreased. Rombouts et al. had performed a time course experiment, where they showed that freshly isolated MSCs had a better efficiency of homing compared to cultured cells [40]. Moreover, they showed that culture of MSCs for 24 hr decreased the homing efficiency to 10% from 55–65% and to near 0% when cultured for 48 hr. It is well documented that with age, the ability of an organism to repair and heal goes down which is in part due to decreased potency of resident stem/progenitor cell. Thus, it is possible that *in vitro* multiplication also causes "aging" and hence decreases potency. However, another possibility is that for other stem cells like HSCs, culture alters the expression and function of cell surface ligands required for homing; it will be discussed below.

2.2. Source and Culture Conditions of MSCs. As alluded earlier, MSCs can and have been isolated from multiple different tissues [41] with differences in the phenotype of the cells isolated [42]. These differences are likely in part due to differences in the native microenvironment from where they are isolated [43]. This presents a challenge for the use of MSCs for therapeutic purposes. In order to define an MSC, the Mesenchymal and Tissue Stem Cell Committee of the International Society for Cellular Therapy (ISCT) proposed certain standards to be considered while using human MSCs therapeutically [44]. Apart from the source of the MSCs, culture methods greatly influence MSC characteristics, including their homing potential. As mentioned earlier, freshly isolated MSCs home better than their cultured counterparts [40]. The CXCR4 chemokine receptor that recognizes CXCL12 (also termed SDF-1α) is highly expressed on bone marrow MSCs, but is lost upon culturing [45, 46]. However, when MSCs are cultured with cytokines (such as HGF, SCF, IL-3, and IL-6) [47], and under hypoxic conditions, CXCR4 expression can be reestablished [48]. Similarly, matrix metalloproteases (MMPs), known to be important in migration of cells, have been demonstrated to play a role in MSC migration [49–51]. Expression of MMPs in MSCs is influenced by factors such as hypoxia [50] and increased culture confluence [49]. Moreover, inflammatory cytokines TGF-β1, IL-1β, and TNF-α also enhance migration by upregulation of MMPs (MMPs) [51] affecting homing of MSCs. Hence, culture conditions to which MSCs are exposed play a vital role in their homing ability.

2.3. Delivery Method. The efficacy, bioavailability, and functionality of a pharmacological drug are dependent on the method via which it is being administered. In order to enhance efficacy and availability, the method of administration of MSCs should hence facilitate homing of MSCs to the desired tissue. Intravenous infusion is one of the major routes of administration of MSC [52–55]. When MSCs are infused systemically, they are trapped into capillary beds of various tissues, especially the lungs [52, 56–58]. Therefore, intra-arterial injection of MSCs has been assessed. Delivery of MSCs via the internal carotid artery significantly improved their migration and homing in the injured brain compared with injection via the femoral vein [59]. Similarly, in humans with subacute spinal cord injury (SCI), delivery of MSCs via the vertebralis artery leads to a greater functional improvement than when cells were administered via the intravenous route [60]. However, delivery of cells in an artery may lead to "microvascular occlusions" [59]. While to treat myocardial infraction (MI), delivery of bone marrow cells or MSCs directly in the heart or close to the site of injury

enhances the number of cells found in the peri-infarct region [61]. Similarly, direct injection of adipose-derived MSC in damaged skeletal muscle leads to an increase in mass and functional capacity [62].

2.4. Host Receptability-Injury versus Noninjured. MSCs have the luxury of being tolerated by the host immune system due to low immunogenicity as discussed earlier. Their bioavailability and efficacy are dependent on the host pathological condition. During an injury, host cells release different chemo-attractants that have a positive influence on homing of MSCs. This possibly explains the observation that MSCs home better when injected 24 hrs after injury than after 14 days in a myocardial injury model [63]. Many such chemoattractants and the associated receptors on MSCs have been identified. Moreover, MSCs are being genetically engineered to overexpress such receptors to enhance their homing to the damaged tissue [61, 63–66]. Moreover, strategies to precondition the host for better distribution and to prevent injected cells from being entrapped in small vessels especially of the lungs have proven beneficial. One such approach was the pretreatment of host with vasodilator such as sodium nitroprusside (SNP) which resulted in increased MSC passage through the lung microvasculature compared to untreated hosts [58].

3. Mechanism of Homing

Most insights in the mechanisms underlying migration and homing are from studies that evaluated leukocyte migration [67] into inflamed tissues, HSCs [68] the and metastatic cancer cells [69]. A significant body of the literature also exists related to mechanism of MSCs migration towards the target tissue and the role of cell surface receptors and molecules in aiding this migration. The role of activated endothelial cells in migration of MSCs is also being extensively studied. We here describe the factors that aid MSCs in migration and homing to tissue of interest.

3.1. Expression of Receptors and Adhesion Molecules. Similar to leucocytes, MSCs express many receptors and cell adhesion molecules that aid in migration and homing to target tissues. However, the precise mechanisms by which MSCs are recruited are not yet fully understood.

Homing is in a significant part dependent on the chemokine receptor, CXCR4, and its binding partner that was previously characterized in HSC homing, that is, stromal-derived factor-1 CXCL12 [61, 64, 70–72]. Wynn et al. demonstrated that CXCR4 is resent on a subpopulation of MSCs, which aid in CXCL12-dependent migration and homing [45]. Aside from CXCR4, freshly isolated BM MSCs and cultured MSCs also express CCR1, CCR4, CCR7, CCR10, CCR9, CXCR5, and CXCR6 [72, 73] which are also involved in MSC migration

Integrins are another family of cell surface molecules involved in migration of variety of cells and are expressed on adipose-derived MSC-like cells [74]. Neutralizing antibodies against integrins, more specifically the integrin-beta1 integrin, but not integrin-alpha4, inhibit, MSC homing to infracted myocardium [75]. However, other studies have shown that integrin-alpha4 plays a role in MSC migration [76]. Interestingly, integrin ligands such as VCAM and ICAM are also expressed on MSCs [77].

3.2. Interaction with Endothelial Cells. Migration and homing requires that cells can attach to and migrate between endothelial cells (ECs) to enter the target tissue. While it well established that leukocytes attach to ECs, roll over the ECs, and then transmigrate between ECs, how MSCs interact with ECs is not well understood. MSCs express molecules as a number of adhesion molecules, including selectins and integrins, involved in these steps. Rüster et al. using a parallel plate flow chamber, demonstrated that MSCs like HSCs bind to ECs derived from human umbilical cord vein (HUVECs) [76]. The binding was enhanced when ECs were activated by TNF-α [76]. The cells migrate by extending podia followed by rolling and adhesion on the EC. They further demonstrated that the binding and rolling of MSCs were mediated by the P-selectin adhesion molecule, whereas migration involved the binding of VLA-4 (or integrin-beta1 & integrin-alpha4 dimer) on MSC with VCAM-1 found on ECs [76]. Steingen et al. found a similar mechanism by which VLA-4/VCAM-1 is required for transendothelial migration. In addition, migration was dependent on the phenotype of the vascular bed [78] and also involved proteolytic enzymes [78]. This is consistent with the studies from De Becker et al. and others demonstrating a role of the MMP class of proteolytic enzymes in MSC homing and migration [49, 51]. MMP-2 belongs to the gelatinase class of proteolytic enzymes that cleave gelatin and collagen-IV, the two major constituents of basement membrane.

4. Approaches to Improve Homing

For MSCs to home and target a specific tissue, they require the right combination of signaling molecules from the injured tissue and the corresponding receptors on MSC. The expression of chemokine receptors on MSCs is influenced by many factors. Although freshly isolated MSCs home better, only limited numbers of cells can be isolated. Therefore, approaches to expand MSCs while retaining expression of receptors needed for efficient homing are being developed. For instance, pretreatment of cultured MSCs with cytokines (such as IL-6, HGF, etc.) increased expression of chemokine receptors (CXCR4) and improved their migration both *in vivo* [47] and *in vitro* [79]. Likewise, IL-1β pre-treatment enhanced the efficacy by MSCs homing in a colitis model [80].

Other approaches include changing culture conditions and coculture of MSC. Hung et al. demonstrated that short-term exposure of MSCs to hypoxia leads to increased expression of chemokine receptors (CX3CR1 and CXCR4) that may aid engraftment *in vivo* [81]. A similar increase in chemokine receptor (CXCR4) apart from cell proliferation-associated cyclin (cyclin D1, D3) expression was observed when humans umbilical cord MSCs were cocultured with

Sertoli cells [82]. Yet another approach is the use of genetically engineered MSCs that overexpress chemokine receptors such as CXCR4 and integrin-alpha4 to influence their homing ability. Kumar et al. transduced MSCs with an adenovirus encoding integrin-alpha4, which enhanced their ability to home to bone [83]. A similar approach was taken to overexpress CXCR4 in MSCs to enhance their homing ability and to improve recovery after myocardial infraction [84]. Compared with untransduced MSCs, CXCR4 overexpressing MSCs resulted in a decrease in anterior wall thinning, and left ventricular chamber dimensions were better maintained and remodeling was observed [84]. Although these genetically modified MSCs may not yet be available for therapeutic use in humans, pre-treatment approach may well be applicable.

5. Tracking Mesenchymal Stem Cells *In Vivo*

As homing of MSCs is inefficient and many MSCs are trapped in the lung following systemic administration, it is imperative that we can trace the fate of the injected cells. One classical method to label cells is with retroviral vectors to express fluorescent proteins, which has been helpful in gaining insights in MSC homing and engraftment [85]. However, the visualization of cells that homed in different organs requires sacrificing of the animal, as the tissue penetrability of fluorescence is limited. Hence, more advanced techniques to track the injected cells *in vivo*, such as bioluminescence imaging (BLI), single-photon emission CT (SPECT), positron emission tomography (PET), multiple photon microscopy, and magnetic resonance imaging (MRI), are being employed. The noninvasive cellular imaging allows for tracking the injected cells in multiple tissues and over time.

To trace cells by MRI requires labeling of the cells with contrast reagents in order for the cells to be visualized. Cells can be labeled with contrast agents: either positive contrast agents used in T_1-weighted MRI such as lanthanide chelates [86] or Mn-containing compounds [87, 88]; or negative contrast agents, such as superparamagnetic iron oxide (SPIO) [89–92], ultra-small superparamagnetic iron oxide (USPIO) particles [90, 92, 93], or micron-sized iron oxide particles [94, 95], that are highly sensitive and have a dominant effect on the T_2/T_2^* relaxation times, causing negative contrast enhancement in the regions of interest. For use with stem cells, the role of these agents on cell potency and function needs to be evaluated. Crabbe et al. evaluated the effect of different MRI contrast reagents on the cellular function of embryonic and postnatal stem cells including MSC in an ischemic stroke model [96]. Differences were observed in terms of size, densities, and number of inclusions among the different reagents tested. Moreover, the labeling did not interfere with the migratory capacities of these cells *in vivo* [96]. One drawback of MRI-based cell tracking is that whole body scans are difficult to achieve, and, hence, determination of where the labeled cells traffic to other than the tissue that is damaged, is difficult. A second drawback is that the iron oxide particles are retained in a tissue even if the grafted (stem) cell dies, hence, leading to false positive signals. Yet another problem as shown by Vandeputte et al. is that a pronounced hypointense signal intensity on 3D T_2^*w MR images can be seen spontaneously, corresponding to damaged blood vessels and inflammatory cells, thus, warranting caution [97].

PET imaging relies on the activation of a tracer dye by a protein such as herpes simplex virus type 1 thymidine kinase (HSV1-tk) or varicella zoster virus thymidine kinase (VZV-tk), expressed by genetically engineering into the injected cells [98, 99]. Two main tracer classes used as probes for HSV1-tk substrate are pyrimidine nucleoside derivatives and acycloguanosine derivatives [100]. PET/SPECT visualizes the emission from a tracer dye that can be toxic and interferes with cellular function. Alternatively, cells can be directly labeled with tracer dyes such as ^{18}F-FDG. Wolfs et al. demonstrated that ^{18}F-FDG, a positron emitting glucose analogue, can be easily taken up by MSC and MSC-like cells without interfering with cellular functions [101]. Further, the presence of this analogue did not significantly affect the viability, proliferation, differentiation, and migratory capacities of these cells [101]. However, this only allows following the cells for a short period of time, as the tracer decays over 109 minutes [102].

BLI requires the expression of a bioluminescence protein that can be visualized and is hindered less by tissue mass unlike fluorescent proteins. With the availability of instrumentation for visualization, the BLI method has been quite useful in tracing cells in mouse models. Bioluminescence can be obtained using proteins from the luciferase family (firefly or *Renilla*), which again needs to be genetically engineered in the injected MSCs [103, 104]. In a study evaluating the immunogenicity of such xenoproteins in genetically engineered MSCs, Bergwerf et al. found no immunological response when such MSCs were injected in the brain. In contrast, they found reporter gene-specific immune-reactive T-cell responses when they were injected in the muscle [105].

Kraitchman et al., using dual labeled cells (tracer and contrast reagent), were able to follow the cells for up to a week in an MI mouse model [106]. Their tracing showed that the cells initially home to the lungs followed by redistribution to nontarget organs within 48 hrs. MSCs were also found at the site of infarct up to one week after injection [106]. However, the cells were unable to be located using MRI, rather, they were traceable using high sensitive SPECT [106].

Many such reagents and cell tracing methodologies have been developed and evaluated for stem and progenitor cells. The efficacy, toxicity and resolution are the main factors that determine the choice of imaging technique.

6. Conclusion

Postnatal MSC or MSC-like cells are currently the primary source of stem cells that have found clinical relevance. Embryo-derived stem cells such as ESC although have a greater differentiation potential, they suffer from their ability to induce teratomas *in vivo*; hence, it has been difficult to translate their clinical use. As alluded here, a great deal of work has been done to harness the potential of these adult stem cells for the treatment of patients. MSC and the likes are already undergoing clinical trials for use in patients

especially for their immunomodulatory features. However, their heterogeneity and off-target homing especially lodging in the lungs impede the clinical use of MSC and MSC-like cells. Owing to this, a large number of cells are required to obtain desired effect at the target organ(s). Different methods as discussed above, such as targeted delivery, cytokine pretreatment, and assisted homing, are being used to circumvent such impedances.

References

[1] A. J. Friedenstein, R. K. Chailakhyan, and N. V. Latsinik, "Stromal cells responsible for transferring the microenvironment of the hemopoietic tissues. Cloning in vitro and retransplantation in vivo," *Transplantation*, vol. 17, no. 4, pp. 331–340, 1974.

[2] A. J. Friedenstein, U. F. Deriglasova, and N. N. Kulagina, "Precursors for fibroblasts in different populations of hematopoietic cells as detected by the in vitro colony assay method," *Experimental Hematology*, vol. 2, no. 2, pp. 83–92, 1974.

[3] A. I. Caplan, "Mesenchymal stem cells," *Journal of Orthopaedic Research*, vol. 9, no. 5, pp. 641–650, 1991.

[4] D. J. Prockop, "Marrow stromal cells as stem cells for nonhematopoietic tissues," *Science*, vol. 276, no. 5309, pp. 71–74, 1997.

[5] A. Erices, P. Conget, and J. J. Minguell, "Mesenchymal progenitor cells in human umbilical cord blood," *British Journal of Haematology*, vol. 109, no. 1, pp. 235–242, 2000.

[6] D. A. De Ugarte, K. Morizono, A. Elbarbary et al., "Comparison of multi-lineage cells from human adipose tissue and bone marrow," *Cells Tissues Organs*, vol. 174, no. 3, pp. 101–109, 2003.

[7] R. Anzalone, M. L. Iacono, S. Corrao et al., "New emerging potentials for human wharton's jelly mesenchymal stem cells: immunological features and hepatocyte-like differentiative capacity," *Stem Cells and Development*, vol. 19, no. 4, pp. 423–438, 2010.

[8] S. Kern, H. Eichler, J. Stoeve, H. Klüter, and K. Bieback, "Comparative analysis of mesenchymal stem cells from bone marrow, umbilical cord blood, or adipose tissue," *Stem Cells*, vol. 24, no. 5, pp. 1294–1301, 2006.

[9] M. F. Pittenger, "Multilineage potential of adult human mesenchymal stem cells," *Science*, vol. 284, no. 5411, pp. 143–147, 1999.

[10] A. Sohni and C. M. Verfaillie, "Multipotent adult progenitor cells," *Best Practice and Research*, vol. 24, no. 1, pp. 3–11, 2011.

[11] V. D. Roobrouck, C. C. Carlos Clavel, S. A. Jacobs et al., "Differentiation potential of human postnatal mesenchymal stem cells, mesoangioblasts, and multipotent adult progenitor cells reflected in their transcriptome and partially influenced by the culture conditions," *Stem Cells*, vol. 29, no. 5, pp. 871–882, 2011.

[12] V. D. Roobrouck, K. Vanuytsel, and C. M. Verfaillie, "Concise review: culture mediated changes in fate and/or potency of stem cells," *Stem Cells*, vol. 29, no. 4, pp. 583–589, 2011.

[13] B. Sacchetti, A. Funari, S. Michienzi et al., "Self-renewing osteoprogenitors in bone marrow sinusoids can organize a hematopoietic microenvironment," *Cell*, vol. 131, no. 2, pp. 324–336, 2007.

[14] X. L. Aranguren, A. Luttun, C. Clavel et al., "In vitro and in vivo arterial differentiation of human multipotent adult progenitor cells," *Blood*, vol. 109, no. 6, pp. 2634–2642, 2007.

[15] M. Kucia, M. Halasa, M. Wysoczynski et al., "Morphological and molecular characterization of novel population of $CXCR4^+$ $SSEA\text{-}4^+$ $Oct\text{-}4^+$ very small embryonic-like cells purified from human cord blood—preliminary report," *Leukemia*, vol. 21, no. 2, pp. 297–303, 2007.

[16] G. Kogler, S. Sensken, J. A. Airey et al., "A new human somatic stem cell from placental cord blood with intrinsic pluripotent differentiation potential," *The Journal of Experimental Medicine*, vol. 200, no. 2, pp. 123–135, 2004.

[17] D. Woodbury, E. J. Schwarz, D. J. Prockop et al., "Adult rat and human bone marrow stromal cells differentiate into neurons," *Journal of Neuroscience Research*, vol. 61, no. 4, pp. 364–370, 2000.

[18] Y. Sato, H. Araki, J. Kato et al., "Human mesenchymal stem cells xenografted directly to rat liver are differentiated into human hepatocytes without fusion," *Blood*, vol. 106, no. 2, pp. 756–763, 2005.

[19] K. Timper, D. Seboek, M. Eberhardt et al., "Human adipose tissue-derived mesenchymal stem cells differentiate into insulin, somatostatin, and glucagon expressing cells," *Biochemical and Biophysical Research Communications*, vol. 341, no. 4, pp. 1135–1140, 2006.

[20] M. Kovacsovics-Bankowski, P. R. Streeter, K. A. Mauch et al., "Clinical scale expanded adult pluripotent stem cells prevent graft-versus-host disease," *Cellular Immunology*, vol. 255, no. 1-2, pp. 55–60, 2009.

[21] W. Van't Hof, N. Mal, Y. Huang et al., "Direct delivery of syngeneic and allogeneic large-scale expanded multipotent adult progenitor cells improves cardiac function after myocardial infarct," *Cytotherapy*, vol. 9, no. 5, pp. 477–487, 2007.

[22] S. Beyth, Z. Borovsky, D. Mevorach et al., "Human mesenchymal stem cells alter antigen-presenting cell maturation and induce T-cell unresponsiveness," *Blood*, vol. 105, no. 5, pp. 2214–2219, 2005.

[23] R. Ramasamy, C. K. Tong, H. F. Seow, S. Vidyadaran, and F. Dazzi, "The immunosuppressive effects of human bone marrow-derived mesenchymal stem cells target T cell proliferation but not its effector function," *Cellular Immunology*, vol. 251, no. 2, pp. 131–136, 2008.

[24] F. Dazzi and F. M. Marelli-Berg, "Mesenchymal stem cells for graft-versus-host disease: close encounters with T cells," *European Journal of Immunology*, vol. 38, no. 6, pp. 1479–1482, 2008.

[25] X. Jiang, Y. Zhang, B. Liu et al., "Human mesenchymal stem cells inhibit differentiation and function of monocyte-derived dendritic cells," *Blood*, vol. 105, no. 10, pp. 4120–4126, 2005.

[26] A. Corcione, F. Benvenuto, E. Ferretti et al., "Human mesenchymal stem cells modulate B-cell functions," *Blood*, vol. 107, no. 1, pp. 367–372, 2006.

[27] W. T. Tse, J. D. Pendleton, W. M. Beyer, M. C. Egalka, and E. C. Guinan, "Suppression of allogeneic T-cell proliferation by human marrow stromal cells: implications in transplantation," *Transplantation*, vol. 75, no. 3, pp. 389–397, 2003.

[28] M. D. Nicola, C. Carlo-Stella, M. Magni et al., "Human bone marrow stromal cells suppress T-lymphocyte proliferation induced by cellular or nonspecific mitogenic stimuli," *Blood*, vol. 99, no. 10, pp. 3838–3843, 2002.

[29] A. Bartholomew, C. Sturgeon, M. Siatskas et al., "Mesenchymal stem cells suppress lymphocyte proliferation in vitro and prolong skin graft survival in vivo," *Experimental Hematology*, vol. 30, no. 1, pp. 42–48, 2002.

[30] M. Krampera, S. Glennie, J. Dyson et al., "Bone marrow mesenchymal stem cells inhibit the response of naive and memory antigen-specific T cells to their cognate peptide," *Blood*, vol. 101, no. 9, pp. 3722–3729, 2003.

[31] K. Le Blanc, L. Tammik, B. Sundberg, S. E. Haynesworth, and O. Ringdén, "Mesenchymal stem cells inhibit and stimulate mixed lymphocyte cultures and mitogenic responses independently of the major histocompatibility complex," *Scandinavian Journal of Immunology*, vol. 57, no. 1, pp. 11–20, 2003.

[32] H. M. Lazarus, O. N. Koc, S. M. Devine et al., "Cotransplantation of HLA-identical sibling culture-expanded mesenchymal stem cells and hematopoietic stem cells in hematologic malignancy patients," *Biology of Blood and Marrow Transplantation*, vol. 11, no. 5, pp. 389–398, 2005.

[33] K. Le Blanc, I. Rasmusson, B. Sundberg et al., "Treatment of severe acute graft-versus-host disease with third party haploidentical mesenchymal stem cells," *The Lancet*, vol. 363, no. 9419, pp. 1439–1441, 2004.

[34] C. Wan, R. Cheng, H. Wang, and T. Liu, "Immunomodulatory effects of mesenchymal stem cells derived from adipose tissues in a rat orthotopic liver transplantation model," *Hepatobiliary and Pancreatic Diseases International*, vol. 7, no. 1, pp. 29–33, 2008.

[35] M. J. Crop, C. C. Baan, S. S. Korevaar et al., "Donor-derived mesenchymal stem cells suppress alloreactivity of kidney transplant patients," *Transplantation*, vol. 87, no. 6, pp. 896–906, 2009.

[36] S. Inoue, F. C. Popp, G. E. Koehl et al., "Immunomodulatory effects of mesenchymal stem cells in a rat organ transplant model," *Transplantation*, vol. 81, no. 11, pp. 1589–1595, 2006.

[37] K. Le Blanc, F. Frassoni, L. Ball et al., "Mesenchymal stem cells for treatment of steroid-resistant, severe, acute graft-versus-host disease: a phase II study," *The Lancet*, vol. 371, no. 9624, pp. 1579–1586, 2008.

[38] R. E. Newman, D. Yoo, M. A. LeRoux, and A. Danilkovitch-Miagkova, "Treatment of inflammatory diseases with mesenchymal stem cells," *Inflammation and Allergy*, vol. 8, no. 2, pp. 110–123, 2009.

[39] A. J. Nixon, L. R. Goodrich, M. S. Scimeca et al., "Gene therapy in musculoskeletal repair," *Annals of the New York Academy of Sciences*, vol. 1117, pp. 310–327, 2007.

[40] W. J. C. Rombouts and R. E. Ploemacher, "Primary murine MSC show highly efficient homing to the bone marrow but lose homing ability following culture," *Leukemia*, vol. 17, no. 1, pp. 160–170, 2003.

[41] M. Crisan, S. Yap, L. Casteilla et al., "A perivascular origin for mesenchymal stem cells in multiple human organs," *Cell Stem Cell*, vol. 3, no. 3, pp. 301–313, 2008.

[42] P. Bianco, P. G. Robey, and P. J. Simmons, "Mesenchymal stem cells: revisiting history, concepts, and assays," *Cell Stem Cell*, vol. 2, no. 4, pp. 313–319, 2008.

[43] L. D. Meirelles, P. C. Chagastelles, and N. B. Nardi, "Mesenchymal stem cells reside in virtually all post-natal organs and tissues," *Journal of Cell Science*, vol. 119, part 11, pp. 2204–2213, 2006.

[44] M. Dominici, K. le Blanc, I. Mueller et al., "Minimal criteria for defining multipotent mesenchymal stromal cells. The International Society for Cellular Therapy position statement," *Cytotherapy*, vol. 8, no. 4, pp. 315–317, 2006.

[45] R. F. Wynn, C. A. Hart, C. Corradi-Perini et al., "A small proportion of mesenchymal stem cells strongly expresses functionally active CXCR4 receptor capable of promoting migration to bone marrow," *Blood*, vol. 104, no. 9, pp. 2643–2645, 2004.

[46] D. G. Phinney and D. J. Prockop, "Concise review: mesenchymal stem/multipotent stromal cells: the state of transdifferentiation and modes of tissue repair—current views," *Stem Cells*, vol. 25, no. 11, pp. 2896–2902, 2007.

[47] M. Shi, J. Li, L. Liao et al., "Regulation of CXCR4 expression in human mesenchymal stem cells by cytokine treatment: role in homing efficiency in NOD/SCID mice," *Haematologica*, vol. 92, no. 7, pp. 897–904, 2007.

[48] T. Schioppa, B. Uranchimeg, A. Saccani et al., "Regulation of the chemokine receptor CXCR4 by hypoxia," *Journal of Experimental Medicine*, vol. 198, no. 9, pp. 1391–1402, 2003.

[49] A. De Becker, P. Van Hummelen, M. Bakkus et al., "Migration of culture-expanded human mesenchymal stem cells through bone marrow endothelium is regulated by matrix metalloproteinase-2 and tissue inhibitor of metalloproteinase-3," *Haematologica*, vol. 92, no. 4, pp. 440–449, 2007.

[50] B. Annabi, Y. Lee, S. Turcotte et al., "Hypoxia promotes murine bone-marrow-derived stromal cell migration and tube formation," *Stem Cells*, vol. 21, no. 3, pp. 337–347, 2003.

[51] C. Ries, V. Egea, M. Karow, H. Kolb, M. Jochum, and P. Neth, "MMP-2, MT1-MMP, and TIMP-2 are essential for the invasive capacity of human mesenchymal stem cells: differential regulation by inflammatory cytokines," *Blood*, vol. 109, no. 9, pp. 4055–4063, 2007.

[52] R. F. Pereira, M. D. O'Hara, A. V. Laptev et al., "Marrow stromal cells as a source of progenitor cells for nonhematopoietic tissues in transgenic mice with a phenotype of osteogenesis imperfecta," *Proceedings of the National Academy of Sciences of the United States of America*, vol. 95, no. 3, pp. 1142–1147, 1998.

[53] E. M. Horwitz, D. J. Prockop, L. A. Fitzpatrick et al., "Transplantability and therapeutic effects of bone marrow-derived mesenchymal cells in children with osteogenesis imperfecta," *Nature Medicine*, vol. 5, no. 3, pp. 309–313, 1999.

[54] Y. Akiyama, C. Radtke, O. Honmou, and J. D. Kocsis, "Remyelination of the spinal cord following intravenous delivery of bone marrow cells," *Glia*, vol. 39, no. 3, pp. 229–236, 2002.

[55] T. Nomura, O. Honmou, K. Harada, K. Houkin, H. Hamada, and J. D. Kocsis, "I.v. infusion of brain-derived neurotrophic factor gene-modified human mesenchymal stem cells protects against injury in a cerebral ischemia model in adult rat," *Neuroscience*, vol. 136, no. 1, pp. 161–169, 2005.

[56] R. H. Lee, A. A. Pulin, M. J. Seo et al., "IIntravenous hMSCs improve myocardial infarction in mice because cells embolized in lung are activated to secrete the anti-inflammatory protein TSG-6," *Cell Stem Cell*, vol. 5, no. 1, pp. 54–63, 2009.

[57] J. Gao, J. E. Dennis, R. F. Muzic, M. Lundberg, and A. I. Caplan, "The dynamic in vivo distribution of bone marrow-derived mesenchymal stem cells after infusion," *Cells Tissues Organs*, vol. 169, no. 1, pp. 12–20, 2001.

[58] S. Schrepfer, T. Deuse, H. Reichenspurner, M. P. Fischbein, R. C. Robbins, and M. P. Pelletier, "Stem cell transplantation: the Lung barrier," *Transplantation Proceedings*, vol. 39, no. 2, pp. 573–576, 2007.

[59] P. Walczak, J. Zhang, A. A. Gilad et al., "Dual-modality monitoring of targeted intraarterial delivery of mesenchymal stem cells after transient ischemia," *Stroke*, vol. 39, no. 5, pp. 1569–1574, 2008.

[60] E. Syková, P. Jendelová, L. Urdzíková, P. Lesný, and A. Hejčl, "Bone marrow stem cells and polymer hydrogels—two strategies for spinal cord injury repair," *Cellular and Molecular Neurobiology*, vol. 26, no. 7-8, pp. 1113–1129, 2006.

[61] D. Zhang, G. Fan, X. Zhou et al., "Over-expression of CXCR4 on mesenchymal stem cells augments myoangiogenesis in the infarcted myocardium," *Journal of Molecular and Cellular Cardiology*, vol. 44, no. 2, pp. 281–292, 2008.

[62] F. Bacou, R. Boubaker El Andalousi, P. Daussin et al., "Transplantation of adipose tissue-derived stromal cells increases mass and functional capacity of damaged skeletal muscle," *Cell Transplantation*, vol. 13, no. 2, pp. 103–111, 2004.

[63] S. Schenk, N. Mal, A. Finan et al., "Monocyte chemotactic protein-3 is a myocardial mesenchymal stem cell homing factor," *Stem Cells*, vol. 25, no. 1, pp. 245–251, 2007.

[64] Y. Zhuang, X. Chen, M. Xu, L. Zhang, and F. Xiang, "Chemokine stromal cell-derived factor 1/CXCL12 increases homing of mesenchymal stem cells to injured myocardium and neovascularization following myocardial infarction," *Chinese Medical Journal*, vol. 122, no. 2, pp. 183–187, 2009.

[65] J. Tang, J. Wang, J. Yang et al., "Mesenchymal stem cells overexpressing SDF-1 promote angiogenesis and improve heart function in experimental myocardial infarction in rats," *European Journal of Cardio-Thoracic Surgery*, vol. 36, no. 4, pp. 644–650, 2009.

[66] S. K. Ghadge, S. Mühlstedt, C. Özcelik, and M. Bader, "SDF-1α as a therapeutic stem cell homing factor in myocardial infarction," *Pharmacology and Therapeutics*, vol. 129, no. 1, pp. 97–108, 2011.

[67] B. Moser and P. Loetscher, "Lymphocyte traffic control by chemokines," *Nature Immunology*, vol. 2, no. 2, pp. 123–128, 2001.

[68] A. Peled, I. Petit, O. Kollet et al., "Dependence of human stem cell engraftment and repopulation of NOD/SCID mice on CXCR4," *Science*, vol. 283, no. 5403, pp. 845–848, 1999.

[69] A. Müller, B. Homey, H. Soto et al., "Involvement of chemokine receptors in breast cancer metastasis," *Nature*, vol. 410, no. 6824, pp. 50–56, 2001.

[70] C. H. Ryu, S. A. Park, S. M. Kim et al., "Migration of human umbilical cord blood mesenchymal stem cells mediated by stromal cell-derived factor-1/CXCR4 axis via Akt, ERK, and p38 signal transduction pathways," *Biochemical and Biophysical Research Communications*, vol. 398, no. 1, pp. 105–110, 2010.

[71] A. Kortesidis, A. Zannettino, S. Isenmann, S. Shi, T. Lapidot, and S. Gronthos, "Stromal-derived factor-1 promotes the growth, survival, and development of human bone marrow stromal stem cells," *Blood*, vol. 105, no. 10, pp. 3793–3801, 2005.

[72] M. Honczarenko, Y. Le, M. Swierkowski, I. Ghiran, A. M. Glodek, and L. E. Silberstein, "Human bone marrow stromal cells express a distinct set of biologically functional chemokine receptors," *Stem Cells*, vol. 24, no. 4, pp. 1030–1041, 2006.

[73] I. Von Lüttichau, M. Notohamiprodjo, A. Wechselberger et al., "Human adult CD34$^-$ progenitor cells functionally express the chemokine receptors CCR1, CCR4, CCR7, CXCR5, and CCR10 but not CXCR4," *Stem Cells and Development*, vol. 14, no. 3, pp. 329–336, 2005.

[74] D. A. De Ugarte, Z. Alfonso, P. A. Zuk et al., "Differential expression of stem cell mobilization-associated molecules on multi-lineage cells from adipose tissue and bone marrow," *Immunology Letters*, vol. 89, no. 2-3, pp. 267–270, 2003.

[75] J. E. Ip, Y. Wu, J. Huang, L. Zhang, R. E. Pratt, and V. J. Dzau, "Mesenchymal stem cells use integrin β1 not CXC chemokine receptor 4 for myocardial migration and engraftment," *Molecular Biology of the Cell*, vol. 18, no. 8, pp. 2873–2882, 2007.

[76] B. Rüster, S. Göttig, R. J. Ludwig et al., "Mesenchymal stem cells display coordinated rolling and adhesion behavior on endothelial cells," *Blood*, vol. 108, no. 12, pp. 3938–3944, 2006.

[77] M. Krampera, G. Pizzolo, G. Aprili, and M. Franchini, "Mesenchymal stem cells for bone, cartilage, tendon and skeletal muscle repair," *Bone*, vol. 39, no. 4, pp. 678–683, 2006.

[78] C. Steingen, F. Brenig, L. Baumgartner, J. Schmidt, A. Schmidt, and W. Bloch, "Characterization of key mechanisms in transmigration and invasion of mesenchymal stem cells," *Journal of Molecular and Cellular Cardiology*, vol. 44, no. 6, pp. 1072–1084, 2008.

[79] A. L. Ponte, E. Marais, N. Gallay et al., "The in vitro migration capacity of human bone marrow mesenchymal stem cells: comparison of chemokine and growth factor chemotactic activities," *Stem Cells*, vol. 25, no. 7, pp. 1737–1745, 2007.

[80] H. Fan, G. Zhao, L. Liu et al., "Pre-treatment with IL-1beta enhances the efficacy of MSC transplantation in DSS-induced colitis," *Cellular & Molecular Immunology*, vol. 9, no. 6, pp. 473–481, 2012.

[81] S. Hung, R. R. Pochampally, S. Hsu et al., "Short-term exposure of multipotent stromal cells to low oxygen increases their expression of CX3CR1 and CXCR4 and their engraftment in vivo," *PLoS ONE*, vol. 2, no. 5, article e416, 2007.

[82] F. Zhang, Y. Hong, W. Liang et al., "Co-culture with Sertoli cells promotes proliferation and migration of umbilical cord mesenchymal stem cells," *Biochemical and Biophysical Research Communications*, vol. 427, no. 1, pp. 86–90, 2012.

[83] S. Kumar and S. Ponnazhagan, "Bone homing of mesenchymal stem cells by ectopic α4 integrin expression," *The FASEB Journal*, vol. 21, no. 14, pp. 3917–3927, 2007.

[84] Z. Cheng, L. Ou, X. Zhou et al., "Targeted migration of mesenchymal stem cells modified with CXCR4 gene to infarcted myocardium improves cardiac performance," *Molecular Therapy*, vol. 16, no. 3, pp. 571–579, 2008.

[85] F. Belema-Bedada, S. Uchida, A. Martire, S. Kostin, and T. Braun, "Efficient homing of multipotent adult mesenchymal stem cells depends on FROUNT-mediated clustering of CCR2," *Cell Stem Cell*, vol. 2, no. 6, pp. 566–575, 2008.

[86] S. G. Crich, L. Biancone, V. Cantaluppi et al., "Improved route for the visualization of stem cells labeled with a Gd-/Eu-chelate as dual (MRI and fluorescence) agent," *Magnetic Resonance in Medicine*, vol. 51, no. 5, pp. 938–944, 2004.

[87] M. Widerøe, Ø. Olsen, T. B. Pedersen et al., "Manganese-enhanced magnetic resonance imaging of hypoxic-ischemic brain injury in the neonatal rat," *NeuroImage*, vol. 45, no. 3, pp. 880–890, 2009.

[88] M. Yamada and P. Yang, "In vitro labeling of human embryonic stem cells for magnetic resonance imaging," *Journal of Visualized Experiments*, no. 18, article e827, 2008.

[89] C. Vandeputte, D. Thomas, T. Dresselaers et al., "Characterization of the inflammatory response in a photothrombotic stroke model by MRI: implications for stem cell transplantation," *Molecular Imaging and Biology*, vol. 13, no. 4, pp. 663–671, 2011.

[90] C. Berger, M. Rausch, P. Schmidt, and M. Rudin, "Feasibility and limits of magnetically labeling primary cultured rat T cells with ferumoxides coupled with commonly used transfection agents," *Molecular Imaging*, vol. 5, no. 2, pp. 93–104, 2006.

[91] J. W. M. Bulte and D. L. Kraitchman, "Iron oxide MR contrast agents for molecular and cellular imaging," *NMR in Biomedicine*, vol. 17, no. 7, pp. 484–499, 2004.

[92] E. Küstermann, U. Himmelreich, K. Kandal et al., "Efficient stem cell labeling for MRI studies," *Contrast Media and Molecular Imaging*, vol. 3, no. 1, pp. 27–37, 2008.

[93] M. Hoehn, E. Küstermann, J. Blunk et al., "Monitoring of implanted stem cell migration in vivo: a highly resolved in vivo magnetic resonance imaging investigation of experimental stroke in rat," *Proceedings of the National Academy of Sciences of the United States of America*, vol. 99, no. 25, pp. 16267–16272, 2002.

[94] E. M. Shapiro, O. Gonzalez-Perez, J. Manuel García-Verdugo, A. Alvarez-Buylla, and A. P. Koretsky, "Magnetic resonance imaging of the migration of neuronal precursors generated in the adult rodent brain," *NeuroImage*, vol. 32, no. 3, pp. 1150–1157, 2006.

[95] J. P. Sumner, E. M. Shapiro, D. Maric, R. Conroy, and A. P. Koretsky, "In vivo labeling of adult neural progenitors for MRI with micron sized particles of iron oxide: quantification of labeled cell phenotype," *NeuroImage*, vol. 44, no. 3, pp. 671–678, 2009.

[96] A. Crabbe, C. Vandeputte, T. Dresselaers et al., "Effects of MRI contrast agents on the stem cell phenotype," *Cell Transplantation*, vol. 19, no. 8, pp. 919–936, 2010.

[97] C. Vandeputte, J. Taymans, C. Casteels et al., "Automated quantitative gait analysis in animal models of movement disorders," *BMC Neuroscience*, vol. 11, article 92, 2010.

[98] C. M. Deroose, S. K. Chitneni, R. Gijsbers et al., "Preliminary validation of varicella zoster virus thymidine kinase as a novel reporter gene for PET," *Nuclear Medicine and Biology*, vol. 39, no. 8, pp. 1266–1274, 2012.

[99] S. S. Gambhir, J. R. Barrio, M. E. Phelps et al., "Imaging adenoviral-directed reporter gene expression in living animals with positron emission tomography," *Proceedings of the National Academy of Sciences of the United States of America*, vol. 96, no. 5, pp. 2333–2338, 1999.

[100] H. Hong, Y. Yang, and W. Cai, "Imaging gene expression in live cells and tissues," *Cold Spring Harbor Protocols*, vol. 6, no. 4, 2011.

[101] E. Wolfs, T. Struys, T. Notelaers et al., " ^{18}F-FDG labeling of mesenchymal stem cells and multipotent adult progenitor cells for PET imaging: effects on ultrastructure and differentiation capacity," *Journal of Nuclear Medicine*, vol. 54, no. 3, pp. 447–454, 2013.

[102] C. Caracó, L. Aloj, L. Chen, J. Y. Chou, and W. C. Eckelman, "Cellular release of [^{18}F]2-fluoro-2-deoxyglucose as a function of the glucose-6-phosphatase enzyme system," *The Journal of Biological Chemistry*, vol. 275, no. 24, pp. 18489–18494, 2000.

[103] J. Tolar, A. J. Nauta, M. J. Osborn et al., "Sarcoma derived from cultured mesenchymal stem cells," *Stem Cells*, vol. 25, no. 2, pp. 371–379, 2007.

[104] N. de Vocht, D. Lin, J. Praet et al., "Quantitative and phenotypic analysis of mesenchymal stromal cell graft survival and recognition by microglia and astrocytes in mouse brain," *Immunobiology*, vol. 218, no. 5, pp. 696–705, 2013.

[105] I. Bergwerf, N. De Vocht, B. Tambuyzer et al., "Reporter gene-expressing bone marrow-derived stromal cells are immune-tolerated following implantation in the central nervous system of syngeneic immunocompetent mice," *BMC Biotechnology*, vol. 9, article 1, 2009.

[106] D. L. Kraitchman, M. Tatsumi, W. D. Gilson et al., "Dynamic imaging of allogeneic mesenchymal stem cells trafficking to myocardial infarction," *Circulation*, vol. 112, no. 10, pp. 1451–1461, 2005.

Hindawi Publishing Corporation
Stem Cells International
Volume 2013, Article ID 983059, 18 pages
http://dx.doi.org/10.1155/2013/983059

Review Article

Cellular Kinetics of Perivascular MSC Precursors

William C. W. Chen,[1,2] Tea Soon Park,[3] Iain R. Murray,[4,5] Ludovic Zimmerlin,[3] Lorenza Lazzari,[6] Johnny Huard,[1,7] and Bruno Péault[4,5,8]

[1] *Stem Cell Research Center, Department of Orthopaedic Surgery, School of Medicine, University of Pittsburgh, Pittsburgh, PA 15219, USA*
[2] *Department of Bioengineering, University of Pittsburgh, Pittsburgh, PA 15260, USA*
[3] *Institute for Cell Engineering and Department of Pediatric Oncology, School of Medicine, Johns Hopkins University, Baltimore, MD 21205, USA*
[4] *Centre for Regenerative Medicine, University of Edinburgh, Edinburgh, EH16 4TJ, UK*
[5] *Orthopaedic Hospital Research Center and David Geffen School of Medicine at UCLA, University of California at Los Angeles, 615 Charles E. Young Drive South, Los Angeles, CA 90095-7358, USA*
[6] *Cell Factory, Fondazione Ospedale Maggiore Policlinico, 20122 Milan, Italy*
[7] *McGowan Institute for Regenerative Medicine, Pittsburgh, PA 15219, USA*
[8] *Centre for Cardiovascular Science, University of Edinburgh, Queen's Medical Research Institute, 47 Little France Crescent, Edinburgh EH16 4TJ, UK*

Correspondence should be addressed to Bruno Péault; bpeault@mednet.ucla.edu

Received 14 May 2013; Accepted 13 July 2013

Academic Editor: Donald G. Phinney

Mesenchymal stem/stromal cells (MSCs) and MSC-like multipotent stem/progenitor cells have been widely investigated for regenerative medicine and deemed promising in clinical applications. In order to further improve MSC-based stem cell therapeutics, it is important to understand the cellular kinetics and functional roles of MSCs in the dynamic regenerative processes. However, due to the heterogeneous nature of typical MSC cultures, their native identity and anatomical localization in the body have remained unclear, making it difficult to decipher the existence of distinct cell subsets within the MSC entity. Recent studies have shown that several blood-vessel-derived precursor cell populations, purified by flow cytometry from multiple human organs, give rise to *bona fide* MSCs, suggesting that the vasculature serves as a systemic reservoir of MSC-like stem/progenitor cells. Using individually purified MSC-like precursor cell subsets, we and other researchers have been able to investigate the differential phenotypes and regenerative capacities of these contributing cellular constituents in the MSC pool. In this review, we will discuss the identification and characterization of perivascular MSC precursors, including pericytes and adventitial cells, and focus on their cellular kinetics: cell adhesion, migration, engraftment, homing, and intercellular cross-talk during tissue repair and regeneration.

1. Introduction

The availability of mesenchymal stem/stromal cells (MSCs) and MSC-like multipotent stem/progenitor cells marked a major milestone in stem cell therapies [1, 2]. For more than a decade, MSC has been a highly promising stem cell source and extensively investigated for its therapeutic potentials [3, 4]. Unlike embryonic stem cells (ESCs) or induced pluripotent stem cells (iPSCs), MSCs are inherently more relevant to clinical applications due to the lack of ethical and safety issues, despite lower developmental versatility [5]. MSCs and similar mesodermal stem/progenitor cells have been shown to repair and/or regenerate a wide variety of damaged/defective organs, including bone, cartilage, muscle, heart, and skin [6–10]. MSCs have also been reported to support hematopoiesis and suppress immune reaction after cell/organ transplantation [11–14].

Nevertheless, owing to the nature of MSC isolation by plastic adherence in tissue culture, the native identity and anatomical localization of MSCs have remained unclear for

years [15]. Recently, several studies have indicated that MSCs represent a heterogeneous entity in culture, and a number of multipotent precursor cells potentially contributing to the MSC pool have been identified *in vivo* [16, 17]. Increasing evidence further suggests that MSCs and some tissue-specific progenitor cells are anatomically and functionally associated with vascular/perivascular niches in various tissues [18–21]. Following the hypothesis that blood vessels throughout the body serve as a systemic reservoir of multipotent stem/progenitor cells, we and other researchers have identified, purified, and characterized distinct populations of MSC-like multilineage precursors from the vasculature of multiple human organs [17, 22]. These human blood vessel-derived precursor cell subsets, including pericytes (PCs) [23], adventitial cells (ACs) [24], and myogenic endothelial cells (MECs) [25], can be isolated via fluorescence-activated cell sorting (FACS) based on their unique expression of cell surface antigens. Purified PCs, ACs, and MECs not only exhibit typical mesodermal multipotency in culture but also demonstrate robust regenerative capacities in animal disease models. Consequently these precursor cell subsets, particularly PCs and ACs that can be universally derived from definitive structures of blood vessel walls, represent active contributors to the MSC entity [17].

In this review, we will discuss the identification and characterization of perivascular MSC precursors (i.e., PCs and ACs) from multiple organs and focus on their cellular kinetics during regenerative events, including cell adhesion, migration, engraftment, homing, and intercellular cross-talk.

2. Native Distribution of MSCs and MSC-Like Multipotent Stem/Progenitor Cells

MSCs and MSC-like stem/progenitor cells have been found in nearly all organs in the human body. Despite slight differences in phenotypes and cellular functions, MSCs and MSC-like cells from various ontogenies share basic features in general, including selective plastic adherence, expression of typical MSC surface markers, and mesenchymal multipotency such as osteogenesis, chondrogenesis, and adipogenesis. Some of the most common MSCs and MSC-like multilineage cells are briefly introduced here.

2.1. Bone Marrow-Derived MSCs (BM-MSCs). Bone marrow (BM) harbors multiple types of stem/progenitor cells, including hematopoietic stem cells (HSCs), endothelial progenitor cells (EPCs), and BM-MSCs [26, 27]. As a standard MSC population, BM-MSCs are defined as nonhematopoietic, plastic adherent progenitor cells that self-renew, differentiate into typical mesodermal cell lineages including osteogenic, chondrogenic, and adipogenic lineages, and express CD73, CD90, and CD105 but are negative for CD11b, CD14, CD19, CD34, CD45, CD79α, and HLA-DR1 [28]. Estimated by the colony forming unit fibroblasts assay (CFU-F) *in vitro,* BM-MSCs typically exist at a very low frequency within the BM mononucleated cell population (0.01%–0.1% of total BM cells) but can be efficiently expanded in culture, making them one of the most investigated autologous stem/progenitor cell populations. Interestingly, multipotent BM-MSC clones retain approximately twofold higher CD146 expression level than unipotent clones [29].

2.2. Adipose-Derived Stem/Stromal Cells (ASCs). The stromal vascular fraction (SVF) of adipose can be isolated via enzymatic digestion of intact fat tissue or lipoaspirate, followed by the depletion of mature adipocytes through centrifugation. The SVF embodies a broad and heterogeneous cellular compartment, including vascular cells (endothelial and perivascular populations), hematopoietic cells (resident and circulating cells), and stromal fibroblasts. In 1976, human adipogenic progenitors (aka preadipocytes) were successfully isolated by two independent groups from the adipose SVF by selective adherence to culture plastics [30, 31]. The adherent fraction of the adipose SVF was later identified as a source of mesenchymogenic progenitors [32], termed adipose-derived stem/stromal cells (ASC) [33]. ASCs are defined *in vitro* using the same criteria as *bona fide* BM-MSCs [34], including their selective plastic adherence, mesenchymal differentiation capacities and immunophenotypes [32], although ASCs only resemble BM-MSCs at subsequent passages in culture [35]. Unlike BM-MSCs, early-passage ASCs temporarily retain expression of mucosialin (CD34) [35], a well-established marker for stem/progenitor cells in both hematopoietic [36] and endothelial [37] cell lineages. On another note, the temporary retention of CD34 expression in primary ASCs led to confusion regarding their origin *in situ*. This misperception was accentuated in light of the recent characterization of CD34-negative PCs as a source of MSCs in a variety of mesodermal tissues, including fat [23]. While the adipogenic activity is mainly exhibited by the prevalent CD34+/CD31− subset of the adipose SVF [38], the CD34-negative fraction can also generate ASCs *in vitro* [24, 39, 40]. Immunohistochemical studies have confined these mesenchymogenic subpopulations to the adipose microvasculature where they coexist, respectively, in the media and adventitia in an annular fashion [24, 39, 41, 42]. Both PCs and an outer supra-adventitial layer of CD34-positive cells (adventitial cells/supra-adventitial stromal cells, ACs) possess high adipogenic potential *in vitro* [39, 43] and may contribute together to replenish the pool of adipocytes essential to sustain the high fat turnover *in vivo* [44].

2.3. Umbilical Cord-Derived Mesenchymal Stem/Stromal Cells (UC-MSCs). Stem/progenitor cells isolated from disposable perinatal tissues, including amnion/amniotic fluid, umbilical cord blood, placental tissue, umbilical cord blood vessels, and the Wharton's jelly, have been deemed promising for clinical applications because of the minimal safety and ethical concerns [45, 46]. MSCs and MSC-like cells have been isolated from different compartments of the umbilical cord, including umbilical vein subendothelial zone, umbilical cord blood, and specifically, Wharton's jelly [45, 47]. Wharton's jelly is the parenchyma within the umbilical cord, a mucoid connective tissue surrounding umbilical cord arteries and vein [45]. The Wharton's jelly can be further divided into three anatomical regions where MSCs can be derived from the perivascular

zone, the intervascular zone, and the subamnion [47]. Similar to BM-MSCs, MSCs derived from Wharton's jelly exhibit plastic adherence, mesenchymal multipotency, and expression of CD10, CD13, CD29, CD44, CD73, CD90, CD105, and HLA-class I but are negative for CD11b, CD14, CD19, CD31, CD34, CD45, CD56, CD79, and HLA class II [45–47].

3. Blood Vessels as a Source of MSC Precursors

The similarities between MSCs derived from many different tissues aroused the idea that a common reservoir of MSCs may exist in the body. The blood vessel, which typically consists of three structural layers: *tunica intima*, *tunica media*, and *tunica adventitia* [48], is distributed throughout nearly all human organs and therefore represents a favorable candidate. Early evidence supporting the hypothesis that the vascular wall serves as a systemic source of stem cells came from a study of the emerging hematopoietic system in the embryo and fetus, where hematopoietic cells emerged in close vicinity to vascular endothelial cells (ECs) in both intra- and extraembryonic blood-forming tissues [22]. Recently, several studies have indicated the possibility that blood vessels in different organs contain multilineage precursors that possess MSC-like features and contribute to tissue repair/regeneration [49, 50]. New evidence further pointed out that tissue-specific multipotent stem/progenitor cells, including osteogenic, neural, odontoblastic, and adipogenic progenitors, may originate from and/or associate with vascular/perivascular niches *in vivo* [18–21].

Microvascular pericytes (PCs), a set of perivascular mural cells surrounding *the intima* of microvessels and capillaries, are traditionally regarded as a structural component of blood vessels, regulating vascular contractility, stability, and integrity [51, 52]. Intimate interactions between PCs and ECs tightly regulate vascular growth, maturation, and remodeling [51, 53–55]. Recently, PCs have been implicated in a number of pathological conditions, making them potential targets for therapeutic interventions [55, 56]. On the other hand, the *tunica adventitia*, the outermost layer of large blood vessels, has long been considered as a structural bystander, consisting of loosely structured collagen-rich extracellular matrix (ECM), which embeds stromal cells/fibroblasts, the *vasa vasorum*, and perivascular nerves [57]. The importance of the *tunica adventitia* was recently reevaluated due to a number of studies reporting its active role in vascular remodeling, immune response mediation, cell trafficking, and atherosclerosis [57–59]. In a vascular remodeling setting following an injury, it has been shown that adventitial cells (ACs) start a process of proliferation, migration into the tunicae media and intima, and differentiation into smooth muscle cells [60–62]. Recently, we and several other groups reported new strategies for the identification and purification of the elusive PCs and ACs [23, 24, 39, 63–65]. Using immunohistochemistry and flow cytometry, we identified human PCs and ACs *in situ* and purified these cells to homogeneity based on their unique expressions of cell surface antigens. Details of the isolation and characterization of PCs and ACs will be described in the following sections.

Unlike the *tunicae media* and *adventitia*, the subendothelial zone of *tunica intima* has previously been suggested as one of the sources of EPCs [66, 67]. Apart from PCs and ACs, some of us have also reported a rare but distinct subset of blood-vessel-derived stem cells, that is, myogenic endothelial cells (MECs), residing within the intima of microvasculature in human skeletal muscle [25]. MECs, presumably the human counterpart of murine muscle derived stem cells (MDSCs), not only express the myogenic cell marker, CD56, but also display endothelial cell markers, CD34 and CD144. Following purification by FACS, MECs (CD34+/CD56+/CD144+/CD45−) can be clonally expanded and exhibited osteo-, chondro-, adipo-, and myogenic differentiation capacities *in vitro* [25]. Furthermore, MECs exhibited superior cardiac repair capacity in ischemic hearts and myogenic regeneration in injured skeletal muscle than conventional CD56+ myoblasts and ECs [25, 68, 69]. Nevertheless, despite their MSC-like features and tissue reparative/regenerative capability, whether MECs contribute significantly to the MSC entity remains to be clarified due to their restricted presence in skeletal muscle.

4. Identification and Purification of Perivascular MSC Precursors

4.1. Placenta. While placenta and umbilical cord are often discarded at birth, these extraembryonic tissues contain large numbers of stem/progenitor cells, making them attractive sources of donor cells for regenerative medicine. We and others have isolated multipotent PCs (CD146+/CD34−/CD45−/CD56−) from these tissues and utilized them toward multiple tissue repair/regeneration, including skeletal muscle [70], lung [71], dermal [72], and nervous tissues [73].

Placenta is a highly vascularized extraembryonic tissue, which serves as fetomaternal interface to sustain proper oxygen transportation, waste disposal, and nutrient delivery. The placental vasculature has been thoroughly characterized throughout fetal development previously and consists of all sizes/types of blood vessels and both pericytes/perivascular cells and ECs at all stages [74, 75]. Placenta PCs are critical to maintain blood vessel homeostasis and promote angiogenesis [76, 77]. PC abnormity in placenta capillaries leads to defects in sinusoidal integrity, a phenotype often observed during pregnancy complications due to diabetes, postmaturity, or preeclampsia [78]. In addition to their supportive role in the fetal vasculature, placental PCs have also been identified as a source of MSCs [23, 70, 79]. Our previous studies have discriminated mesenchymogenic placental PCs based on the expression of the cell adhesion molecule CD146 and lack of EC markers: CD34, CD144, and vWF [23, 70]. Similarly, Castrechini et al. described a perivascular population residing in human fetal and term placenta, which coexpressed MSC/PC markers (Stro-1, 3G5, CD105, CD106, CD146, CD49a, α-SMA) but not hematovascular markers (CD117, CD34, vWF) and were competent for trilineage mesenchymal differentiation [79]. In our hands, human fetal and term chorionic villi

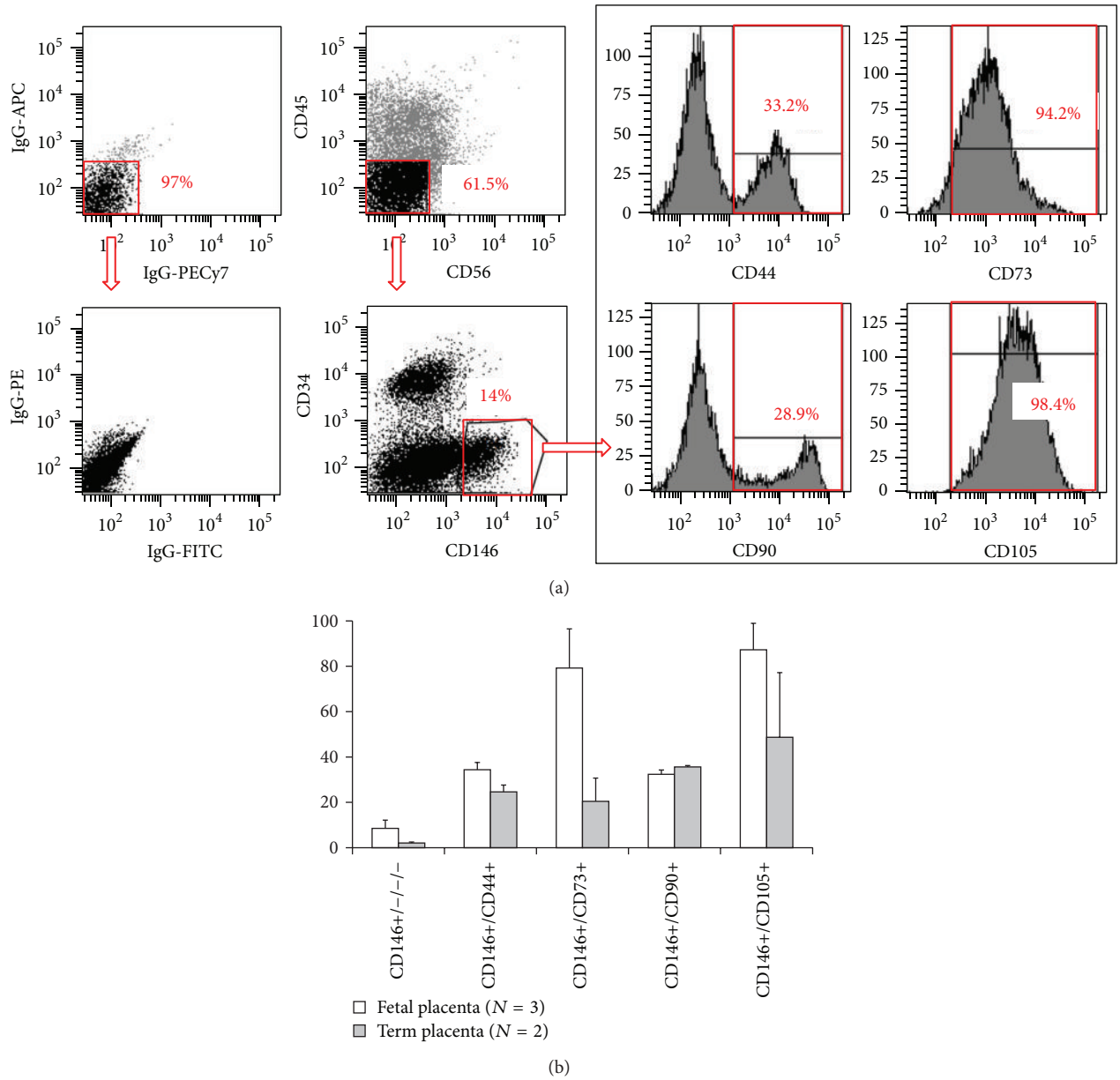

Figure 1: Flow cytometry analysis of mesenchymal stem cell marker expression in freshly isolated fetal and term placental pericytes. (a) Representative flow cytometry analysis of human placenta that was mechanically dissociated and enzymatically digested and subsequently stained for CD45, CD56, CD34, and CD146 along with CD44, CD73, CD90, or CD105. Matching isotype controls were shown in the left column. (b) Human fetal placenta ($N = 3$, average 20 weeks of gestation) and term placenta ($N = 2$, average 39 weeks of gestation) were used to isolate subsets of pericytes using surface expression of CD146+/CD34−/CD45−/CD56− (CD146+/−/−/−) and colabeled with one of the mesenchymal stem cell markers (CD146+/CD44+, CD146+/CD73+, CD146+/CD90+, CD146+/CD105+) as shown in (a). Values are mean ± standard error.

of placentas included 8.5 ± 3.66% ($N = 3$, 19 to 21 weeks of gestation) and 2.1 ± 0.43% ($N = 2$, 39 weeks of gestation) of PCs (CD146+/CD34−/CD45−/CD56−), respectively (Figure 1).

The native expression of CD146 by mesenchymogenic PCs in many tissues including bone marrow, fetal and term placentas has been reported [23, 70]. Using FACS, we purified PCs from mechanically and enzymatically dissociated placental chorionic villi [23, 70]. Freshly isolated placenta PCs natively expressed MSC markers (CD44, CD73, CD90, and CD105) at varying levels (30 to 87% of fetal and 20 to 48% of term placental CD146+/CD34−/CD45−/CD56− PCs) (Figure 1). We have previously demonstrated that when placed onto ECM-coated plates, dissected fetal placental villi release a population of vascular cells, which possess high migratory activity and robust capacity to regenerate skeletal muscle fibers in dystrophic mice [70]. The cells migrating out of placental villi included predominantly CD146+ cells

which coexpressed PC (NG2 and PDGFRβ) and MSC (CD44, CD73, CD90, and CD105) surface antigens and were deprived of EC antigens (CD31, CD34, CD144, and vWF) [70]. Maier et al. employed a similar approach to isolate PCs from the cellular outgrowth of human term placenta explants [80]. Consistently with fetal placenta, term placenta PCs expressed high levels of PC/MSC markers (CD146, PDGFRβ, NG2, CD90, and calponin), including 65 transcripts that are highly expressed in undifferentiated MSCs, and lacked endothelial/hematopoietic cell marker expression (CD31, CD34, and CD45) [80].

4.2. Umbilical Cord. Human umbilical cord (HUC) has been known as an abundant source of ECs as well as MSCs derived from the Wharton's jelly. Recently some of us demonstrated that human full-term UCs and, at a higher frequency, fetal (preterm) UCs contain perivascular cells that exhibit features of MSCs. These perivascular smooth muscle-like cells present in the HUC co-expressed CD146 and alpha-smooth muscle actin (αSMA) but did not express the established EC markers: CD144, CD34, CD31, and Ulex europaeus agglutinin (UEA-1) receptor. Using FACS, Montemurro et al. isolated a population of PCs (CD146+/NG2+/PDGFRβ+) from umbilical cords of preterm newborns [71]. These HUC-derived perivascular cells (HUCPCs) can be maintained in long-term culture, exhibiting classical spindle-shape PC morphology. When characterized by flow cytometry during subsequent passages, they maintained the expression of CD44, CD90, CD73, CD105, HLA class I, CD146, NG2, αSMA, and PDGFRβ as well as retained their multipotency to differentiate towards different cell types, including osteogenic, adipogenic, and myogenic cell lineages [71].

4.3. Skeletal Muscle. Skeletal muscle has been shown to harbor several adult stem/progenitor cell populations in mammals including humans, in addition to the typical muscle stem cells, that is, satellite cells [81–83]. Many studies have demonstrated that muscle derived stem/progenitor cells are capable of differentiating into a variety of cell lineages *in vitro* and *in vivo*, including blood cells and fat [25, 81, 84–86]. Using similar immunohistochemical and flow cytometry strategies, we first identified microvascular PCs *in situ* within human skeletal muscle and subsequently purified them from mechanically and enzymatically dissociated muscle biopsies via FACS [23]. Similar to PCs sorted from other tissues, muscle PCs (CD146+/CD34−/CD45−/CD56−) expressed typical PC markers: CD146, NG2, PDGFR-β, alkaline phosphatase (ALP), and α-smooth muscle actin (α-SMA), with the absence of EC markers: CD31, CD34, CD144, and vWF as well as the hematopoietic cell marker CD45 and myogenic cell marker CD56. Muscle PCs can be efficiently expanded in culture, at the clonal level, while maintaining robust mesodermal developmental potentials. Freshly isolated and long-term cultured muscle PCs both displayed robust myogenic capacity *in vitro* and *in vivo*. Moreover, muscle PCs natively and in culture expressed classic MSC markers: CD44, CD73, CD90, and CD105, indicating their developmental status as MSC ancestors [23].

4.4. Adipose. Vasculogenic CD34+/CD31− cell populations have been described in the adventitial *vasa vasorum* of large blood vessels such as the vena saphena [65] and the thoracic aorta [67], but microvascular CD34+ ACs seem to be a specific feature of the adipose and subcutaneous tissue [87]. Apart from CD34 expression and their adjacent anatomical localization within the blood vessel wall, ACs can be discriminated from adipose PCs due to the lack of native expression of PC markers (αSMA, CD146, NG2, PDGFRβ) [24, 39, 42]. The high prevalence (~50%) of CD34+/CD146− progenitor cells in the nonhematopoietic adipose SVF [39, 88, 89] and their limited clonogenicity and heterogeneous proliferative capacity [24] do not preclude the possibility that distinct CD34+ stem/progenitor cells exist within adult adipose tissue. Using a peroxisome proliferator-activated receptor gamma (PPARγ) reporter mouse model, Tang et al. demonstrated that adipogenic progenitors emerge from CD34+ cells which later adopt a perivascular niche and express PC markers (αSMA, NG2, PDGFRβ) [21]. Similarly, human adipose CD34+/CD146− ACs can acquire PC markers (αSMA, CD146, NG2, PDGFRβ) *in vitro*, following treatment with angiotensin II or angiopoietin-2 [24].

While developmentally mesenchymogenic PCs may arise from transient CD34+ cell population(s), the persistence of such CD34+ precursors in the adult and their ontological relationship to the bulk of CD34+ ACs in human fat will require further investigation. Indeed, rare CD34+ mesenchymogenic cells have been reported in fetal [24, 90, 91] and adult [92, 93] bone marrow, as well as in fetal muscle and fetal lung [24]. A multipotent CD34+ cell population residing in the wall of dorsal aorta, the mesoangioblast, has been proposed to be an ancestor of adult mesenchymogenic PCs in the mouse [49, 81]. Some groups have reported the direct derivation of CD34+ primitive MSCs from human embryonic stem cells (hESC) [94, 95], while Vodyanik et al. described the emergence of a multipotent MSC precursor, the mesenchymoangioblast, from hESC-derived CD34+ cells in a stepwise differentiation system [96]. Furthermore, Dar et al. recently reported successful derivation of CD105+/CD90+/CD73+/CD31− multipotent mesodermal precursors from embryoid bodies of either human ESCs or iPSCs that exhibit clonogenicity, mesenchymal differentiation potentials, and *bona fide* pericyte features, including angiogenic/vasculogenic capacity and expression of CD146, NG2, and PDGFRβ but not αSMA, CD56, CD34, or EC markers [97]. These hPSC-derived PCs significantly facilitated vascular and muscle regeneration when transplanted into the ischemic limb of immunodeficient mice, with the presence of hPSC-PCs in both recovered vasculature and myofibers, indicating robust vasculogenic and myogenic capacities *in vivo* similar to their adult counterparts [97]. Yet, the reciprocity of all these fetal populations to all or part of adult MSC precursors remains to be clarified.

A rare CD34+/CD146+/CD31−/CD45− population of adipose PCs has also been characterized in the SVF [39, 98–103] and may represent a developmental intermediate between PCs and some or all ACs [102]. This elusive CD34+ PC population is not easily detected within the vascular wall by immunohistochemistry [24, 42] and requires

stringent rare-event strategies for its detection and isolation by flow cytometry [100, 103]. Traktuev et al. suggested the existence of CD34+ cells exhibiting a native pericytic phenotype [98]. They demonstrated that primary cultures of AC-like CD34+CD144−CD45− SVF cells can express PC markers (NG2, PDGFRα, PDGFRβ) without requirement of blood vessel remodeling growth factors in contrast to CD34+CD146− cells [24]. Though these disparities may be related to culture conditions, SVF isolation techniques, and cell sorting strategies, the intricacy and anatomical proximity of these distinct subpopulations highlight the necessity to use multidimensional strategies for their isolation via exclusion of hematopoietic (CD45) and endothelial (CD31, CD144) lineages and combinatory positive selection of pericytic (i.e., CD146, NG2, PDGFRβ), adventitial (CD34), or MSC (CD44, CD73, CD90, CD105) cell subsets. A number of studies have employed preliminary sorting strategies relying on single markers, such as CD146 [104, 105] or CD34 [40, 106, 107], which may be inadequate in regard to the overlapping phenotypes of the vascular/perivascular cell subsets populating the adipose tissue.

Recently, using a combination of above-mentioned positive and negative selection antigens, we performed advanced flow cytometry analyses and FACS in the adipose SVF in order to identify and simultaneously purify these MSC precursor subpopulations [23, 24, 39, 101]. Both CD146+/CD34−/CD45− PCs and CD34+/CD31−/CD45−/CD146− ACs purified from adipose SVF have been shown to express MSC markers *in vivo* and in culture [23, 24, 101]. Furthermore, our quantitative multiparameter studies showed that only a third of adipose PCs (CD146+/CD34−/CD31−/Lineage−/CD45−) natively coexpress the MSC markers CD73, CD90, and CD105, which reveals the cellular heterogeneity of the pericyte compartment [101]. In contrast, both CD146+ (putative PC-AC intermediates) and CD146− (ACs) subsets of CD34+/CD31−/Lineage−/CD45− SVF cells homogenously co-express MSC markers [101]. On the other hand, among these MSC-like perivascular cells, two subpopulations in the adipose SVF can be discerned on the basis of CD34 expression and further distinguished by their proliferation pattern: a low proliferative CD34− subset and a high proliferative CD34+ subset. While CD34− is a typical phenotype of multipotent mesenchymogenic PCs in adipose and most other tissues [23], the CD34+ phenotype may represent transit-amplifying intermediates between stem-like adipose PCs and highly prevalent ACs *in vivo* but require prudent interpretations in culture due to its instability.

5. Adhesion and Migration of Perivascular MSC Precursors

In view of future stem cell-based approaches and therapies, it is crucial to identify predictive parameters that allow the researchers and clinicians to foresee the *in vivo* action of stem/progenitor cells. Since cell adhesion and migration capacities are tightly correlated with *in vivo* cell trafficking and homing, these parameters represent potential predictors for the clinical outcome of stem cell-treated patients and require further investigation [108–110]. Herein we discuss recent progresses in the understanding of perivascular MSC precursors in regard to cell adhesion, migration, and response to hypoxia.

5.1. Cell Adhesion. Anatomically, PCs closely surround ECs populating the vascular intima with specific adhesion and migration properties that allow them to regulate the blood vessel stability/integrity as well as the proliferation and motility of adjacent ECs [51]. Up to 1000 contacts can be secured by peg-sockets to a juxtaposing EC via cytoplasmic fingers inserted into endothelial invaginations [111]. Pericytic elongated terminal arms include adhesion plaques that strongly embed into the basement membrane and EC body to secure their location [111]. Different molecules and pathways have been involved in mural cell motility and adhesion. Notably, ephB/ephrin-B interactions mediate human MSC/PC adhesion, migration, and differentiation [112, 113]. The eph/ephrin family of tyrosine kinase receptors has been identified as an important factor contributing to bone homeostasis and regulating MSC adhesion. Inhibition of ephrin-B signaling prevents MSC attachment and spreading by activation of Src-, PI3 Kinase-, and JNK-dependent signaling pathways [112]. Ephrin-B2-deficient mural cells display major defects in spreading, focal-adhesion formation, and polarized migration as well as exhibiting increased motility [113]. Our group investigated adhesion molecules and proteins involved in PC migratory capacity. We demonstrated that CD146+/NG2+/PDGFRβ+/CD144− PCs exhibited more robust adherence to extracellular matrix substrates (e.g., collagen type-I, gelatin, and fibronectin) and greater migratory capacity than the CD146− population. Enhanced adherence and migratory capacities may result from high expression levels of alpha and beta subunits of integrin and matrix metalloproteinase (MMP)-2, respectively [70]. On the other hand, PCs express intercellular adhesion molecule 1 (ICAM-1) and upregulate its expression in response to tumor necrosis factor (TNF) and pattern-recognition receptor (PRR) ligands. ICAM-1 also regulates interactions of neutrophils and monocytes with PCs *in vitro* [114]. Moreover, it has been suggested that arteriolar and capillary PCs can detect inflammatory stimuli and increase their adhesive interactions with innate leukocytes, implicating their role in the regulation of inflammatory responses [114, 115].

5.2. Cell Migration. PC recruitment and migration occur frequently in response to pathophysiological events such as wound healing, inflammation, or angiogenesis. During vascular development, ECs release PDGF-BB to recruit PCs and stabilize the newly formed blood vessels [116, 117]. Increase of PC density by activation of PDGF-BB/ PDGFRβ signaling pathways has also been detected during wound healing and tumor vascular remodeling [56, 111, 118]. Inversely, disruption of PDGF-BB/PDGFRβ pathways may occur during pathologic conditions (e.g., diabetic retinopathy), resulting in PC apoptosis and augmented permeability of the vascular wall [111, 119]. Upon inflammatory events, PCs control the pattern and efficiency of leukocyte interstitial migration *in vivo* [114,

120]. A recent study highlighted the constitutive expression of chemoattractants by NG2+ PCs: CSC-chemokine ligand-1 (CXCL1) and -8 (CXCL8), macrophage migration inhibitory factor (MIF), CC-chemokine ligand 2 (CCL2), and interleukin-6 (IL-6). PCs further upregulated the expression of these chemo-attractants following stimulation by PRR ligands [114, 115]. Therefore, PCs not only chemotactically migrate to the site of angiogenesis, injury, or inflammation but also actively recruit other proinflammatory participants, including myeloid leukocytes, neutrophils, and macrophages.

Using an *in vitro* model of tissue damage, some of us previously mimicked the ability of HUCPCs to migrate towards the injury site *in vivo* and predicted their capacity to secrete cytokines and trophic factors [71]. Envisioning a possible clinical application of stem cells in the context of extremely immature newborns with an acute lung injury, where alveolar type II cells crucial for producing surfactant and regulating alveolar fluid levels and host defense are damaged, HUC can be readily considered as a convenient source of stem cells. Consequently, a coculture model of pulmonary tissue damage was set up, where an alveolar type II cell line was damaged with bleomycin, an anticancer drug with known pulmonary toxicity [71]. Dye-labeled HUCPCs in coculture were mobilized and migrated towards the damaged alveolar type II cells. HUCPCs showed a great ability to secrete angiogenic/antiapoptotic cytokines and trophic factors compared to the control, in particular high level of keratinocyte growth factor (KGF) [71]. KGF appears to play a crucial role mediating tissue improvement in a range of experimental lung injuries, presumably due to its versatile effects including cellular repair, cytoprotection, and alveolar fluid clearance modulation and immunomodulation [121, 122]. Similarly, skeletal muscle-derived PCs secrete high levels (superior to those of BM-MSCs) of KGF and vascular endothelial growth factor (VEGF) as well as heparin binding-epidermal growth factor (HB-EGF) and basic-fibroblast growth factor (bFGF), which are all considered playing critical roles during wound healing [123, 124].

The abundance of mesenchymogenic progenitors in the SVF of adipose tissue (5,000 CFU-F per gram) [125] provides a great advantage for the development of clinical applications without any *in vitro* expansion requirements [126, 127]. ASC-based therapeutic strategies have been proposed for either regenerative or targeted therapies and often rely on native tropism of ASCs for wound healing, inflammation, or cancer. Although investigations of cell adhesion and migration in purified ACs are currently ongoing, much can be learned from the unfractionated ASCs which have been shown to home to sites of injury and promote tissue repair following systemic injections in animal models of myocardial infarction [128, 129], liver injury [130, 131], olfactory dysfunction [132], hypoxia-ischemia induced brain damage [133], allergic rhinitis [134], inflammatory neuropathy [135], sciatic crush [136], cranial injury [137], and muscular dystrophy [138, 139]. The migratory activity of early-passage ASCs can be modulated by a set of chemokines and growth factors, including PDGF-AB, TGF-β1, and TNFα [140]. These soluble factors can stimulate ASCs via activation of an array of migration-associated receptors such as C-C chemokine receptor types 1 and 7 (CCR1, CCR7), C-X-C chemokine receptor types 4, 5, and 6 (CXCR4, CXCR5, CXCR6), EGF receptor, fibroblast growth factor receptor 1, TGF-β receptor 2, TNF receptor superfamily member 1A, and PDGF receptors α and β [140–142].

ASCs have been proposed to affect various neighboring cells within the subcutaneous tissue via paracrine signals during active remodeling processes such as wound healing [143–145]. In a recent study, ASC-conditioned medium promoted *in vitro* migration of vascular ECs, fibroblasts, and keratinocytes [146]. These data support the impact of ASCs on the proliferation and recruitment of these distinct cell subsets during wound healing via secretion of high levels of promigratory cytokines, including angiopoietin-like-1, EGF, FGF, HGF, TGFβ, SDF-1, and VEGF [145–149].

Similarly to BM-MSCs [150, 151], ASCs have been associated with enhanced migratory activities during tumorigenesis. ASC tropism towards various tumors such as glioma [152, 153], colon cancer [154], and prostate cancer [155] has been exploited to develop targeted therapies. On the other hand, ASCs can modulate the migration of cancer cells, promoting metastasis of breast cancer cells [156, 157] via CCR5/CCL5 signaling in animal models despite the inhibition of breast cancer metastasis in a different model [158]. An antimetastatic result was also observed with pancreas cancer cells [159].

5.3. Cellular Response to Hypoxia. Hypoxia has been shown to promote proliferation and migration of both PCs and MSCs [160, 161]. A recent study highlighted the involvement of the ERK signaling pathway during the modulation of mitogenic and chemotactic responses of human muscle PCs to a low oxygen concentration (6% O_2). This activation of ERK signaling and associated integrins occurred without any detectable alteration on the cell phenotypes or differentiation potentials [160, 162]. A number of growth factors, including PDGF, EGF, and FGF, can activate the Ras-Raf-MEK1/2-ERK signaling axis [163], which controls the adhesion dynamics and cell migratory properties via formation of protrusions within cell membrane and enhancement of the focal adhesion turnover [164]. Culture of MSCs in hypoxic conditions also resulted in higher survival and migration in a hind-limb ischemia model, presumably through Akt signaling [165]. The activation of the Akt pathway has been linked to the cell migratory ability and can be mediated by hepatocyte growth factor (HGF). MSCs under hypoxia exhibited higher expression of cMet, a critical HGF receptor [165, 166], and two receptors of the chemokine stromal-derived factor-1 (SDF-1), CXCR4 and CXCR7, whose expression can also be mediated by hypoxia via the hypoxia-inducible factor-1 alpha (HIF-1α) and Akt phosphorylation [167]. Additionally, even under a 2.5% O_2 hypoxia, the paracrine function of PCs remained highly active when compared to 21% O_2 normoxic culture, with increased expression of VEGF-A, PDGF-B, and TGFβ1 and decreased expression of angiopoietin-1, bFGF, EGF, HGF, and MCP-1, and similar levels of leukemia inhibitory factor (LIF), cyclooxygenase-2 (COX-2/PTGS-2, prostaglandin endoperoxide synthase-2), heme oxygenase-1

(HMOX-1), IL-6, HIF-1α, and MMP-2 [168]. Understanding cellular responses of perivascular MSC precursors and MSCs to hypoxia would help researchers and clinicians to develop better approaches to improve the efficacy of MSC-based cell therapy, including genetic modification, cellular preconditioning, and pharmacological adjunct therapy [9].

6. Migratory and Homing Characteristics of Perivascular MSC Precursors during Tissue Repair/Regeneration

Perivascular MSC precursors have recently been demonstrated as efficient regenerative/supportive units for tissue repair and regeneration. In particular, human muscle PCs and saphenous vein-derived ACs exhibited superior angiogenic, paracrine, and cardioprotective capacities and augmented functional recovery in murine myocardial infarction and hind-limb ischemia models when compared to myoblasts or unfractionated MSCs [65, 168, 169]. Additionally, muscle and placental PCs were shown to repair/regenerate injured and dystrophic muscles in animal disease models as well as contribute to the muscle stem cell (satellite cell) pool [23, 64, 70, 170]. Some of us also showed that HUCPCs prevented/rescued the oxygen-induced arrest in alveolar growth and restored lung function and architecture, primarily through their paracrine function [171]. Interestingly, CD146+ PCs extracted from adipose tissue were shown to support the long-term persistence of human hematopoietic stem/progenitor cells in coculture [172]. Moreover, purified human PCs and ACs exhibited bone formation or healing when implanted into animal models of ectopic bone formation or critical-sized calvarial bone injury, respectively [88, 89, 173]. In this section, we will discuss the current understanding of the cell engraftment, migration, and homing of transplanted perivascular MSC precursors during some of these regenerative events.

6.1. Cardiac Repair. When intramyocardially transplanted into a mouse model of acute myocardial infarction (AMI), purified human muscle PCs contributed to cardiac functional and anatomic recovery after infarction, presumably through multiple cardioprotective and regenerative mechanisms: reversal of ventricular remodeling, reduction of cardiac fibrosis, diminution of chronic inflammation, promotion of host angiogenesis, and small-scale myocardial regenerative events [168]. The engraftment ratio of intramyocardially injected GFP-labeled PCs was approximately 9% at the first week, decreasing to roughly 3% at 8 weeks after infarction. Above all, a fraction of donor PCs was identified in perivascular positions, juxtaposing host CD31+ ECs (Figure 2). In contrast to the engraftment ratio, the vessel-homing ratio of transplanted PCs slightly increased over time, implicating the potential benefit of niche-homing for long-term donor cell survival. Moreover, cellular interactions between donor PCs and host ECs were demonstrated by the expression of human-specific ephrin type-B receptor 2 (EphB2) in some GFP+ PCs adjacent to ECs as well as the formation of connexin 43 gap junctions with ECs [168]. Additionally, immune cells

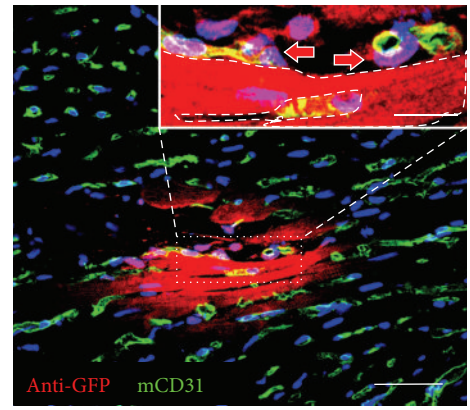

Figure 2: Human pericytes home to perivascular locations. Confocal microscopy showed that GFP+ human pericytes (red), identified by anti-GFP immunostaining, can be located at the interstitial space where host CD31+ capillaries (green) reside (main, scale bar = 50 μm). Some GFP+ donor cells (inset, red arrows) are in close contact with mouse CD31+ endothelial cells (green). Dash line in the inset picture delineates a putative GFP+ cardiomyocyte (inset, scale bar = 10 μm).

in the ischemic tissue release chemokines such as interleukins and monocyte chemoattractant protein-1 (MCP-1), which are involved in the homing of MSCs to the ischemic heart [174]. Moreover, the paracrine anti-inflammatory function of human MSCs was also demonstrated by the high expression of anti-inflammatory protein TSG-6 from MSCs embolized in lung, which led to decreased inflammatory responses, reduced infarct size, and improved cardiac function [175].

Similarly, Katare et al. reported that transplantation of human saphenous vein-derived ACs (hSV-ACs), a putative PC progenitor population, promoted functional improvement in a mouse model of MI, primarily through angiocrine activities and neovascularization via both donor and recipient cells as well as other cardioprotective mechanisms including improved myocardial blood flow, attenuated vascular permeability, and reduction of myocardial remodeling, cardiomyocyte apoptosis, and interstitial fibrosis [169]. hSV-ACs produced and released microRNA-132 (miR-132) as a paracrine agent, which exerts proangiogenic, prosurvival, and antifibrotic activities and likely plays a key role as an activator of cardiac healing. While retaining their original antigenic and perivascular phenotype, homing of hSV-ACs to perivascular locations was confirmed by Dil-labeled hSV-ACs juxtaposing isolectin-positive capillary ECs [169].

6.2. Muscle Regeneration. As mentioned previously, we have demonstrated that intramuscular injection of freshly sorted or cultured PCs derived from human adipose or skeletal muscle regenerated human myofibers efficiently in the mouse dystrophic or injured muscle [23]. In another study, we showed that intramuscular implantation of dissected human placental villi resulted in crude outgrowth of human cells in dystrophic mice [70]. Ample amount of cells of human origin released from placental villi fragments participated in host muscle regeneration, revealed by the

detection of human dystrophin-positive (hDys3t) and/or human spectrin-positive myofibers. Many of these human myofibers coexpressed human lamin A/C, indicating their sole human origin and not intermediate products of cell fusion. Surprisingly, human myofibers were located not only close to the implantation area (500 μm to 2 mm) but also in far more distant regions (up to 2 cm), suggesting active migration of outgrown human myogenic precursors over long distances. Similarly, freshly isolated placental PCs possessed high migratory activity and actively contributed to host skeletal muscle regeneration [70].

6.3. Pulmonary Repair. As mentioned previously, PCs isolated from umbilical cords migrated efficiently *in vitro* toward alveolar type II cells damaged by bleomycin, with an elevated secretion of KGF and VEGF [71]. Using a preclinical animal model of oxygen-arrested lung growth (exposure to 95% oxygen, i.e., hyperoxia), which mimics bronchopulmonary dysplasia (BPD), Pierro et al. tested the *in vivo* therapeutic potential of HUCPCs [171]. To examine suitable approaches for future clinical applications, two different administration strategies, prophylactic or therapeutic, as well as two different therapeutic modalities, direct cell transplantation or HUCPC-conditioned medium injection, were investigated. Intratracheal transplantation of HUCPCs prevented/rescued oxygen-induced arrested alveolar growth and restored normal alveolar architecture. However, immunofluorescence and qPCR revealed very few donor cells localized within the lung. This low cell engraftment suggested that cell replacement is not the primary mechanism of the observed therapeutic effects. Indeed similar therapeutic benefits can be achieved by daily intraperitoneal administration of conditioned medium, resulting in improved alveolar architecture and lung function. In both administration strategies, long-term efficacy and safety were demonstrated till 6 months with an improved exercise capacity and normal alveolar architecture. No suspicious tumor formation was noted by total body CT scans. In conclusion, the therapeutic potential of HUCPCs for pulmonary repair can be exploited by either direct cell therapy or the production of trophic factors, expanding new clinical perspectives for HUCPCs and other perivascular MSC precursors.

6.4. Skeletal Regeneration. To investigate their skeletal regenerative capacity, human PCs and ACs purified from lipoaspirate SVF have been seeded onto osteoinductive scaffolds and implanted into animal models of ectopic bone formation or critical-sized calvarial bone injury, respectively [88, 89, 176]. Significantly greater osteogenesis or bone healing by PCs and ACs in murine muscle pockets or calvarial defects than control SVF cells was observed, respectively. Additionally, the high osteogenic capability of human ACs and PCs can be further enhanced by Nel-like molecule-1 (NELL-1), an osteoinductive growth factor that is a direct transcriptional target of Runx2 [89, 173, 176, 177]. On the other hand, the role of the SDF-1/CXCR4 pathway in MSCs/PCs recruitment during the injury response has been established in a murine model of femoral bone graft, where SDF-1 deficient mice were unable to recruit MSCs at bone fracture sites and consequently limited their participation to local bone repair [178]. The role of the SDF-1/CXCR4 axis in PC recruitment has also been revealed during tumorigenesis [179]. Overexpression of PDGF-BB increased malignant PC growth via activation of the SDF-1/CXCR4 axis and induced expression of SDF-1 in ECs. The upregulation of SDF-1 was directly mediated by inhibition of the Akt/mTOR pathway or HIF-1α. Accordingly, both donor and host stem cell homing can be further enhanced by MSCs genetically modified to overexpress SDF-1 [180].

7. Angiogenic Capacities of Perivascular MSC Precursors and Cellular Interactions with ECs

7.1. Pericyte-EC Cellular Interactions: A Perivascular Niche for MSC Precursors. PCs are ubiquitously present in microvasculature where they extend primary cytoplasmic processes along the abluminal surface of the endothelial tube. They are enveloped in a basement membrane that is continuous with the EC basement membrane to which both cells contribute [181, 182]. The majority of the PC-EC interface is separated by basement membrane, with the two cell types contacting each other at discrete points through peg-socket type interactions, occluding contacts, gap junctions, and adhesion plaques [183, 184]. The intimate anatomical relationship between ECs and PCs suggests close interactions involving not only direct contact but also paracrine or juxtacrine signaling. EC-to-PC ratios in normal tissues vary between 1 : 1 to 10 : 1 and may be up to 100 : 1 (in skeletal muscle), while PC coverage of the endothelial abluminal surface ranges between 10% and 70% [185, 186]. PC density and coverage appear to correlate with endothelial barrier properties (i.e., brain > lungs > muscle) [111], EC turnover (large turnover leading to less coverage) [184], and orthostatic blood pressure (larger coverage in lower body parts) [185], in keeping with a role of PCs in regulating capillary barriers, endothelial proliferation, and capillary diameter [111]. Genetically modified mouse models have demonstrated that these two vascular cell types are interdependent: primary defects in one cell type have obligated consequences for the other. There is growing evidence to suggest that ECs can manipulate the migratory and angiogenic properties of PCs, while *in vitro* data highlighting EC influence on mesenchymal differentiation potential of PCs points to a possible role of ECs as gatekeepers within the context of an adult stem cell niche.

7.2. EC Interactions Regulate Pericyte Recruitment and Angiogenesis. The formation of new capillaries during angiogenesis requires a series of well-orchestrated cellular events allowing ECs and PCs to migrate into the perivascular space. In vessel sprouting, angiogenic factors (e.g., VEGF) stimulate ECs, which in turn secrete proteases that degrade basement membrane and allow EC invasion. An endothelial column, guided by a migrating EC at the very tip, then moves toward a VEGF gradient [183]. Studies of the *corpus luteum* indicate that PCs are also capable of guiding sprouting processes by migrating

Table 1: The influence of ECs on the multipotency of tissue-specific MSCs.

Niche Component	Model	Stem cell surrogate	Niche surrogate	Lineage assessed	Effect on differentiation	Context	Proposed mechanism	Investigator
Endothelial cell	3D	ASC	HUVEC	Osteogenesis	↓	Paracrine	↑Wnt	Rajashekhar et al. [203]
Endothelial cell	3D	ASC	HUVEC	Osteogenesis	↓	Juxtacrine	↑Wnt	Rajashekhar et al. [203]
Endothelial cell	2D	BMSC	HUVEC	Osteogenesis	↑	Paracrine	(Dkk1-Wnt, FGF, PDGF, BMP, TGFβ, Notch)	Saleh et al. [204]
Endothelial cell	2D	BMSC	HUVEC	Adipogenesis	—	Paracrine	—	Saleh et al. [205]
Endothelial cell	2D	BMSC	HUVEC	Osteogenesis	↑	Juxtacrine	—	Xue et al. [206]
Endothelial cell	2D	BMSC	HDMEC	Osteogenesis	↑	Juxtacrine	BMP-2	Kaigler et al. [207]
Endothelial cell	2D	BMSC	HDMEC	osteogenesis	—	Paracrine	—	Kaigler et al. [207]
Endothelial cell	2D	BMSC	HDMEC	Osteogenesis	↑	Juxtacrine	N-cadherin	Li et al. [208]
Endothelial cell	2D	BMSC	HDMEC	Osteogenesis	↑	Paracrine	VEGF	Grellier et al. [209]
Endothelial cell	2D	BMSC	HDMEC	Osteogenesis	↓	Paracrine	Osterix/OSX	Meury et al. [210]
Endothelial cell	2D	BMSC	HUVEC	Osteogenesis	↑	Juxtacrine	Cx43/gap junctions	Villars et al. [211]
Endothelial cell	2D	BMSC	HUVEC	Osteogenesis	↑	Juxtacrine	—	Villars et al. [212]
Endothelial cell	2D	HOP	HUVEC	Osteogenesis	↑	Juxtacrine	—	Guillotin et al. [213]
Endothelial cell	2D	HOP	EPC, HSVEC	Osteogenesis	↑	Juxtacrine	Cx43/gap junctions	Guillotin et al. [213]

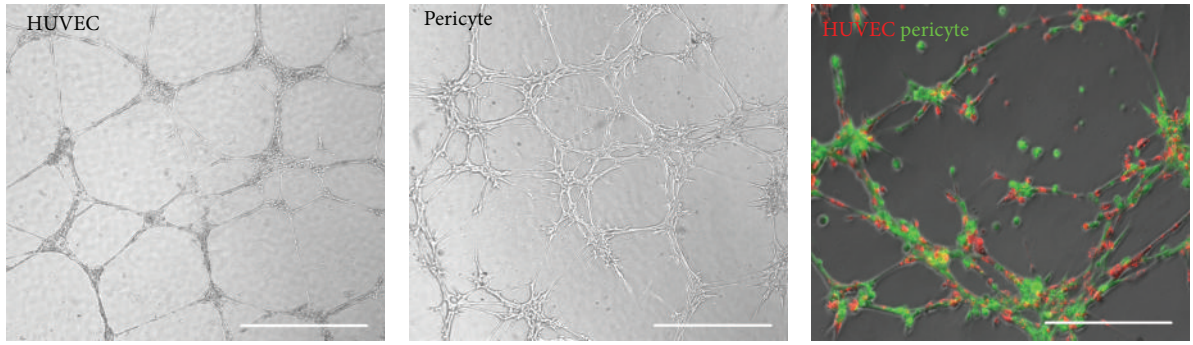

(a) (b) (c)

Figure 3: Human pericytes support formation of microvascular structures. (a) HUVECs seeded onto Matrigel-coated wells formed typical capillary-like structures after 24 hours (scale bar = 1 mm). (b) Human muscle pericytes formed morphologically similar network structures within 6–8 hours (scale bar = 1 mm). (c) Cocultured dye-labeled HUVECs (red) and pericytes (green) at 1 : 1 ratio on Matrigel showed coformation of capillary-like networks within 6–8 hours (scale bars = 500 μm).

ahead of ECs and expressing VEGF [187–189]. Emerging endothelial tubes then secrete growth factors, partly to attract PCs that envelop the vessel wall, and promote vessel maturation. Key pathways implicated in PC-EC signaling include PDGF/PDGFRβ, angiopoietins and Tie receptors, sphingosine-1-phosphate signaling, TGF-β signaling, Notch and Wnt [116, 186, 190, 191]. It is believed that PCs, because of their vessel-embracing position, are able to transfer angiogenic signals along the vessel length by contacting numerous ECs. The recruitment and contribution of PCs to developing endothelial tubes and angiogenic process can be observed *in vitro* through Matrigel culture. Human muscle PCs alone can form network structures in Matrigel culture that were morphologically similar to networks formed by ECs but at an accelerated fashion (Figures 3(a) and 3(b)). Coculture of dye-labeled PCs and ECs at 1 : 1 ratio in Matrigel showed network formation by both cell types, facilitated by the presence of PCs (Figure 3(c)). Blocki et al. further demonstrated that while the capacity to colocalize and/or coform network structures with endothelial tubules on Matrigel is not restricted to PCs, only PCs (CD146+/CD34−) effectively stabilize endothelial networks and improve endothelial sprout integrity [192]. Nevertheless, it is noteworthy that the EC-to-PC ratio may play an important role in the formation of vascular networks and PC functionality *in vitro*.

7.3. ECs: The Gatekeepers of Pericyte Mesenchymal Activation? A growing number of studies demonstrate that tissue resident stem cells reside in vascular niches, including neural, hematopoietic, and MSCs [19, 193–195]. Adult stem cell niche components provide signals that control the balance between quiescence, self-renewal, and differentiation [194]. A significant obstacle in identification of the perivascular origin of

MSCs was the reluctance of PCs to express mesenchymal phenotypes in their native microenvironment [196]. Although it is feasible that PCs acquire MSC potentials upon exiting the microvasculature, it is intuitive that MSC features are expressed by PCs *in situ* but environmentally downregulated. Studies using unfractionated SVF have demonstrated poor and unreliable tissue formation [197] or lower regeneration efficacy relative to prospectively isolated and purified MSCs [197], lending further support to a hypothesis that certain cellular component(s) of SVF have an inhibitory/adverse effect on differentiating MSCs. As such, the influence of ECs on the multipotency of tissue-specific MSCs is now under investigation even though preliminary results to date have been divergent (Table 1). Osteogenic and adipogenic differentiation is not seen within the perivasculature of healthy tissues where the PC-EC relationship is undisturbed. However, disturbed PC-EC interactions have been observed in conditions associated with pathological mineralization and adipogenesis, for example, heterotopic ossification and atherosclerosis [198, 199]. In addition, the ECM proteins, also present within a perivascular niche, have been shown to modify growth and differentiation of MSCs, with collagen type I-, fibronectin-, and vitronectin-treated plates enhancing mineralization *in vitro* [200]. The secretome and proteome of human MSCs have now been extensively documented [201] with studies identifying numerous transcription factors and multiple extracellular and intracellular signaling pathways that regulate adipogenesis and osteogenesis. Interestingly, inducers of differentiation along one lineage often inhibit differentiation along another. For example, the transcription factor PPARγ is a prime inducer of adipogenesis that inhibits osteogenesis, highlighting the mutual exclusivity of these lineages [202]. It is therefore likely that signaling mechanisms responsible for the mesenchymal fate of PCs will be multifactorial and distinct for different lineages.

8. Conclusion

In this review, we described the identification and characterization of perivascular MSC precursors with regard to their adhesion, migration, engraftment/homing, and intercellular cross-talk in culture and in experimental animal models. Although PCs and ACs both exhibit multilineage mesenchymogenic capacities and are derived from adjacent perivascular structural layers, further investigations are required to clarify their developmental relationship as well as the involvement of an ontogenic intermediate. Through the understanding of their unique cellular kinetics and regenerative potential, we will be able to define the pathophysiological role and therapeutic value of the individual blood-vessel-derived MSC precursor population under a particular pathological circumstance. Ultimately, through the purification and/or recombination of these distinct subsets of MSC precursors, it is feasible to further enhance stem cell therapy by eliminating cells with none or limited regenerative potentials in a specific disorder, creating a customized therapeutic modality for the personalized medicine.

Authors' Contribution

Iain R. Murray and Ludovic Zimmerlin contributed equally to this work.

References

[1] S. P. Bruder, D. Gazit, L. Passi-Even, I. Bab, and A. I. Caplan, "Osteochondral differentiation and the emergence of stage-specific osteogenic cell-surface molecules by bone marrow cells in diffusion chambers," *Bone and Mineral*, vol. 11, no. 2, pp. 141–151, 1990.

[2] P. A. Zuk, M. Zhu, H. Mizuno et al., "Multilineage cells from human adipose tissue: implications for cell-based therapies," *Tissue Engineering*, vol. 7, no. 2, pp. 211–228, 2001.

[3] A. I. Caplan and J. E. Dennis, "Mesenchymal stem cells as trophic mediators," *Journal of Cellular Biochemistry*, vol. 98, no. 5, pp. 1076–1084, 2006.

[4] J. García-Castro, C. Trigueros, J. Madrenas, J. A. Pérez-Simón, R. Rodriguez, and P. Menendez, "Mesenchymal stem cells and their use as cell replacement therapy and disease modelling tool," *Journal of Cellular and Molecular Medicine*, vol. 12, no. 6B, pp. 2552–2565, 2008.

[5] W. Prasongchean and P. Ferretti, "Autologous stem cells for personalised medicine," *New Biotechnology*, vol. 29, no. 6, pp. 641–650, 2012.

[6] A. F. Steinert, L. Rackwitz, F. Gilbert, U. Noth, and R. S. Tuan, "Concise review: the clinical application of mesenchymal stem cells for musculoskeletal regeneration: current status and perspectives," *Stem Cells Translational Medicine*, vol. 1, no. 3, pp. 237–247, 2012.

[7] L. Wu, X. Cai, S. Zhang, M. Karperien, and Y. Lin, "Regeneration of articular cartilage by adipose tissue derived mesenchymal stem cells: perspectives from stem cell biology and molecular medicine," *Journal of Cellular Physiology*, vol. 228, no. 5, pp. 938–944, 2013.

[8] W. M. Jackson, L. J. Nesti, and R. S. Tuan, "Potential therapeutic applications of muscle-derived mesenchymal stem and progenitor cells," *Expert Opinion on Biological Therapy*, vol. 10, no. 4, pp. 505–517, 2010.

[9] C. W. Chen, J. Huard, and B. Péault, "Mesenchymal stem cells and cardiovascular repair," in *Mesenchymal Stem Sells*, Y. Xiao, Ed., Nova Science Publishers, New York, NY, USA, 2011.

[10] W. M. Jackson, L. J. Nesti, and R. S. Tuan, "Concise review: clinical translation of wound healing therapies based on mesenchymal stem cells," *Stem Cells Translational Medicine*, vol. 1, no. 1, pp. 44–50, 2012.

[11] C. Pontikoglou, F. Deschaseaux, L. Sensebé, and H. A. Papadaki, "Bone marrow mesenchymal stem cells: biological properties and their role in hematopoiesis and hematopoietic stem cell transplantation," *Stem Cell Reviews and Reports*, vol. 7, no. 3, pp. 569–589, 2011.

[12] M. E. J. Reinders, T. J. Rabelink, and J. W. de Fijter, "The role of mesenchymal stromal cells in chronic transplant rejection after solid organ transplantation," *Current Opinion in Organ Transplantation*, vol. 18, no. 1, pp. 44–50, 2013.

[13] L. Wang, Y. Zhao, and S. Shi, "Interplay between mesenchymal stem cells and lymphocytes: implications for immunotherapy and tissue regeneration," *Journal of Dental Research*, vol. 91, no. 11, pp. 1003–1010, 2012.

[14] M. E. Bernardo and W. E. Fibbe, "Safety and efficacy of mesenchymal stromal cell therapy in autoimmune disorders,"

Annals of the New York Academy of Sciences, vol. 1266, no. 1, pp. 107–117, 2012.

[15] L. D. S. Meirelles, A. I. Caplan, and N. B. Nardi, "In search of the in vivo identity of mesenchymal stem cells," *Stem Cells*, vol. 26, no. 9, pp. 2287–2299, 2008.

[16] M. Pevsner-Fischer, S. Levin, and D. Zipori, "The origins of mesenchymal stromal cell heterogeneity," *Stem Cell Reviews and Reports*, vol. 7, no. 3, pp. 560–568, 2011.

[17] C.-W. Chen, M. Corselli, B. Péault, and J. Huard, "Human blood-vessel-derived stem cells for tissue repair and regeneration," *Journal of Biomedicine and Biotechnology*, vol. 2012, Article ID 597439, 9 pages, 2012.

[18] B. Sacchetti, A. Funari, S. Michienzi et al., "Self-renewing osteoprogenitors in bone marrow sinusoids can organize a hematopoietic microenvironment," *Cell*, vol. 131, no. 2, pp. 324–336, 2007.

[19] M. Tavazoie, L. van der Veken, V. Silva-Vargas et al., "A specialized vascular niche for adult neural stem cells," *Cell Stem Cell*, vol. 3, no. 3, pp. 279–288, 2008.

[20] S. Shi and S. Gronthos, "Perivascular niche of postnatal mesenchymal stem cells in human bone marrow and dental pulp," *Journal of Bone and Mineral Research*, vol. 18, no. 4, pp. 696–704, 2003.

[21] W. Tang, D. Zeve, J. M. Suh et al., "White fat progenitor cells reside in the adipose vasculature," *Science*, vol. 322, no. 5901, pp. 583–586, 2008.

[22] M. Tavian, B. Zheng, E. Oberlin et al., "The vascular wall as a source of stem cells," *Annals of the New York Academy of Sciences*, vol. 1044, pp. 41–50, 2005.

[23] M. Crisan, S. Yap, L. Casteilla et al., "A perivascular origin for mesenchymal stem cells in multiple human organs," *Cell Stem Cell*, vol. 3, no. 3, pp. 301–313, 2008.

[24] M. Corselli, C. W. Chen, B. Sun, S. Yap, J. P. Rubin, and B. Péault, "The tunica adventitia of human arteries and veins as a source of mesenchymal stem cells," *Stem Cells and Development*, vol. 21, no. 8, pp. 1299–1308, 2012.

[25] B. Zheng, B. Cao, M. Crisan et al., "Prospective identification of myogenic endothelial cells in human skeletal muscle," *Nature Biotechnology*, vol. 25, no. 9, pp. 1025–1034, 2007.

[26] C. B. Ballas, S. P. Zielske, and S. L. Gerson, "Adult bone marrow stem cells for cell and gene therapies: implications for greater use," *Journal of Cellular Biochemistry*, vol. 38, pp. 20–28, 2002.

[27] H. Chao and K. K. Hirschi, "Hemato-vascular origins of endothelial progenitor cells?" *Microvascular Research*, vol. 79, no. 3, pp. 169–173, 2010.

[28] Y.-H. Choi, A. Kurtz, and C. Stamm, "Mesenchymal stem cells for cardiac cell therapy," *Human Gene Therapy*, vol. 22, no. 1, pp. 3–17, 2011.

[29] K. C. Russell, D. G. Phinney, M. R. Lacey, B. L. Barrilleaux, K. E. Meyertholen, and K. C. O'Connor, "In vitro high-capacity assay to quantify the clonal heterogeneity in trilineage potential of mesenchymal stem cells reveals a complex hierarchy of lineage commitment," *Stem Cells*, vol. 28, no. 4, pp. 788–798, 2010.

[30] R. L. R. Van, C. E. Bayliss, and D. A. K. Roncari, "Cytological and enzymological characterization of adult human adipocyte precursors in culture," *Journal of Clinical Investigation*, vol. 58, no. 3, pp. 699–704, 1976.

[31] I. Dardick, W. J. Poznanski, I. Waheed, and G. Setterfield, "Ultrastructural observations on differentiating human preadipocytes cultured in vitro," *Tissue and Cell*, vol. 8, no. 3, pp. 561–571, 1976.

[32] P. A. Zuk, M. Zhu, P. Ashjian et al., "Human adipose tissue is a source of multipotent stem cells," *Molecular Biology of the Cell*, vol. 13, no. 12, pp. 4279–4295, 2002.

[33] S. R. Daher, B. H. Johnstone, D. G. Phinney, and K. L. March, "Adipose stromal/stem cells: basic and translational advances: the IFATS collection," *Stem Cells*, vol. 26, no. 10, pp. 2664–2665, 2008.

[34] M. Dominici, K. Le Blanc, I. Mueller et al., "Minimal criteria for defining multipotent mesenchymal stromal cells. The International Society for Cellular Therapy position statement," *Cytotherapy*, vol. 8, no. 4, pp. 315–317, 2006.

[35] J. B. Mitchell, K. McIntosh, S. Zvonic et al., "Immunophenotype of human adipose-derived cells: temporal changes in stromal-associated and stem cell-associated markers," *Stem Cells*, vol. 24, no. 2, pp. 376–385, 2006.

[36] C. I. Civin, L. C. Strauss, and C. Brovall, "Antigenic analysis of hematopoiesis. III. A hematopoietic progenitor cell surface antigen defined by a monoclonal antibody raised against KG-1a cells," *Journal of Immunology*, vol. 133, no. 1, pp. 157–165, 1984.

[37] T. Asahara, T. Murohara, A. Sullivan et al., "Isolation of putative progenitor endothelial cells for angiogenesis," *Science*, vol. 275, no. 5302, pp. 964–967, 1997.

[38] C. Sengenès, K. Lolmède, A. Zakaroff-Girard, R. Busse, and A. Bouloumié, "Preadipocytes in the human subcutaneous adipose tissue display distinct features from the adult mesenchymal and hematopoietic stem cells," *Journal of Cellular Physiology*, vol. 205, no. 1, pp. 114–122, 2005.

[39] L. Zimmerlin, V. S. Donnenberg, M. E. Pfeifer et al., "Stromal vascular progenitors in adult human adipose tissue," *Cytometry A*, vol. 77, no. 1, pp. 22–30, 2010.

[40] H. Suga, D. Matsumoto, H. Eto et al., "Functional implications of CD34 expression in human adipose-derived stem/progenitor cells," *Stem Cells and Development*, vol. 18, no. 8, pp. 1201–1209, 2009.

[41] C.-S. Lin, Z.-C. Xin, C.-H. Deng, H. Ning, G. Lin, and T. F. Lue, "Defining adipose tissue-derived stem cells in tissue and in culture," *Histology and Histopathology*, vol. 25, no. 6, pp. 807–815, 2010.

[42] G. Lin, M. Garcia, H. Ning et al., "Defining stem and progenitor cells within adipose tissue," *Stem Cells and Development*, vol. 17, no. 6, pp. 1053–1063, 2008.

[43] H. Li, L. Zimmerlin, K. G. Marra, V. S. Donnenberg, A. D. Donnenberg, and J. P. Rubin, "Adipogenic potential of adipose stem cell subpopulations," *Plastic and Reconstructive Surgery*, vol. 128, no. 3, pp. 663–672, 2011.

[44] K. L. Spalding, E. Arner, P. O. Westermark et al., "Dynamics of fat cell turnover in humans," *Nature*, vol. 453, no. 7196, pp. 783–787, 2008.

[45] M. Witkowska-Zimny and E. Wrobel, "Perinatal sources of mesenchymal stem cells: wharton's jelly, amnion and chorion," *Cellular and Molecular Biology Letters*, vol. 16, no. 3, pp. 493–514, 2011.

[46] R. R. Taghizadeh, K. J. Cetrulo, and C. L. Cetrulo, "Wharton's Jelly stem cells: future clinical applications," *Placenta*, vol. 32, no. 4, pp. S311–S315, 2011.

[47] D. L. Troyer and M. L. Weiss, "Concise review: wharton's Jelly-derived cells are a primitive stromal cell population," *Stem Cells*, vol. 26, no. 3, pp. 591–599, 2008.

[48] V. Kumar, N. Fausto, and A. Abbas, "Robbins and cotran pathologic basis of disease," in *Blood Vessels*, chapter 11, Saunders, Philadelphia, Pa, USA, 7th edition, 2004.

[49] G. Cossu and P. Bianco, "Mesoangioblasts: vascular progenitors for extravascular mesodermal tissues," *Current Opinion in Genetics and Development*, vol. 13, no. 5, pp. 537–542, 2003.

[50] D. Galli, A. Innocenzi, L. Staszewsky et al., "Mesoangioblasts, vessel-associated multipotent stem cells, repair the infarcted heart by multiple cellular mechanisms: a comparison with bone marrow progenitors, fibroblasts, and endothelial cells," *Arteriosclerosis, Thrombosis, and Vascular Biology*, vol. 25, no. 4, pp. 692–697, 2005.

[51] A. Armulik, A. Abramsson, and C. Betsholtz, "Endothelial/pericyte interactions," *Circulation Research*, vol. 97, no. 6, pp. 512–523, 2005.

[52] D. von Tell, A. Armulik, and C. Betsholtz, "Pericytes and vascular stability," *Experimental Cell Research*, vol. 312, no. 5, pp. 623–629, 2006.

[53] H. K. Rucker, H. J. Wynder, and W. E. Thomas, "Cellular mechanisms of CNS pericytes," *Brain Research Bulletin*, vol. 51, no. 5, pp. 363–369, 2000.

[54] P. Dore-Duffy and J. C. LaManna, "Physiologic angiodynamics in the brain," *Antioxidants and Redox Signaling*, vol. 9, no. 9, pp. 1363–1371, 2007.

[55] F. Kuhnert, B. Y. Y. Tam, B. Sennino et al., "Soluble receptor-mediated selective inhibition of VEGFR and PDGFRβ signaling during physiologic and tumor angiogenesis," *Proceedings of the National Academy of Sciences of the United States of America*, vol. 105, no. 29, pp. 10185–10190, 2008.

[56] P. Lindahl, B. R. Johansson, P. Levéen, and C. Betsholtz, "Pericyte loss and microaneurysm formation in PDGF-B-deficient mice," *Science*, vol. 277, no. 5323, pp. 242–245, 1997.

[57] M. W. Majesky, X. R. Dong, V. Hoglund, W. M. Mahoney Jr., and G. Daum, "The adventitia: a dynamic interface containing resident progenitor cells," *Arteriosclerosis, Thrombosis, and Vascular Biology*, vol. 31, no. 7, pp. 1530–1539, 2011.

[58] Y. Hu and Q. Xu, "Adventitial biology: differentiation and function," *Arteriosclerosis, Thrombosis, and Vascular Biology*, vol. 31, no. 7, pp. 1523–1529, 2011.

[59] Z. Tang, A. Wang, F. Yuan et al., "Differentiation of multipotent vascular stem cells contributes to vascular diseases," *Nature Communications*, vol. 3, article 875, 2012.

[60] Y. Hu, Z. Zhang, E. Torsney et al., "Abundant progenitor cells in the adventitia contribute to atherosclerosis of vein grafts in ApoE-deficient mice," *Journal of Clinical Investigation*, vol. 113, no. 9, pp. 1258–1265, 2004.

[61] Y. Shi, J. E. O'Brien Jr., A. Fard, J. D. Mannion, D. Wang, and A. Zalewski, "Adventitial myofibroblasts contribute to neointimal formation in injured porcine coronary arteries," *Circulation*, vol. 94, no. 7, pp. 1655–1664, 1996.

[62] S. Oparil, S.-J. Chen, Y.-F. Chen, J. N. Durand, L. Allen, and J. A. Thompson, "Estrogen attenuates the adventitial contribution to neointima formation in injured rat carotid arteries," *Cardiovascular Research*, vol. 44, no. 3, pp. 608–614, 1999.

[63] M. Crisan, J. Huard, B. Zheng et al., "Purification and culture of human blood vessel-associated progenitor cells," in *Current Protocols in Stem Cell Biology*, John Wiley and Sons, 2007.

[64] A. Dellavalle, M. Sampaolesi, R. Tonlorenzi et al., "Pericytes of human skeletal muscle are myogenic precursors distinct from satellite cells," *Nature Cell Biology*, vol. 9, no. 3, pp. 255–267, 2007.

[65] P. Campagnolo, D. Cesselli, A. Al Haj Zen et al., "Human adult vena saphena contains perivascular progenitor cells endowed with clonogenic and proangiogenic potential," *Circulation*, vol. 121, no. 15, pp. 1735–1745, 2010.

[66] D. Tilki, H.-P. Hohn, B. Ergün, S. Rafii, and S. Ergün, "Emerging biology of vascular wall progenitor cells in health and disease," *Trends in Molecular Medicine*, vol. 15, no. 11, pp. 501–509, 2009.

[67] E. Zengin, F. Chalajour, U. M. Gehling et al., "Vascular wall resident progenitor cells: a source for postnatal vasculogenesis," *Development*, vol. 133, no. 8, pp. 1543–1551, 2006.

[68] M. Okada, T. R. Payne, B. Zheng et al., "Myogenic endothelial cells purified from human skeletal muscle improve cardiac function after transplantation into infarcted myocardium," *Journal of the American College of Cardiology*, vol. 52, no. 23, pp. 1869–1880, 2008.

[69] B. Zheng, C. W. Chen, G. Li et al., "Isolation of myogenic stem cells from cultures of cryopreserved human skeletal muscle," *Cell transplantation*, vol. 21, no. 6, pp. 1087–1093, 2012.

[70] T. S. Park, M. Gavina, C.-W. Chen et al., "Placental perivascular cells for human muscle regeneration," *Stem Cells and Development*, vol. 20, no. 3, pp. 451–463, 2011.

[71] T. Montemurro, G. Andriolo, E. Montelatici et al., "Differentiation and migration properties of human foetal umbilical cord perivascular cells: potential for lung repair," *Journal of Cellular and Molecular Medicine*, vol. 15, no. 4, pp. 796–808, 2011.

[72] N. Zebardast, D. Lickorish, and J. E. Davies, "Human umbilical cord perivascular cells (HUCPVC): a mesenchymal cell source for dermal wound healing," *Organogenesis*, vol. 6, no. 4, pp. 197–203, 2010.

[73] M. M. Carvalho, F. G. Teixeira, R. L. Reis, N. Sousa, and A. J. Salgado, "Mesenchymal stem cells in the umbilical cord: phenotypic characterization, secretome and applications in central nervous system regenerative medicine," *Current Stem Cell Research and Therapy*, vol. 6, no. 3, pp. 221–228, 2011.

[74] E. Jauniaux, G. J. Burton, G. J. Moscoso, and J. Hustin, "Development of the early human placenta: a morphometric study," *Placenta*, vol. 12, no. 3, pp. 269–276, 1991.

[75] A. Bárcena, M. Kapidzic, M. O. Muench et al., "The human placenta is a hematopoietic organ during the embryonic and fetal periods of development," *Developmental Biology*, vol. 327, no. 1, pp. 24–33, 2009.

[76] R. Demir, P. Kaufmann, M. Castellucci, T. Erbengi, and A. Kotowski, "Fetal vasculogenesis and angiogenesis in human placental villi1," *Acta Anatomica*, vol. 136, no. 3, pp. 190–203, 1989.

[77] M. Wareing, "Effects of oxygenation and luminal flow on human placenta chorionic plate blood vessel function," *Journal of Obstetrics and Gynaecology Research*, vol. 38, no. 1, pp. 185–191, 2012.

[78] C. J. P. Jones and G. Desoye, "A new possible function for placental pericytes," *Cells Tissues Organs*, vol. 194, no. 1, pp. 76–84, 2011.

[79] N. M. Castrechini, P. Murthi, N. M. Gude et al., "Mesenchymal stem cells in human placental chorionic villi reside in a vascular Niche," *Placenta*, vol. 31, no. 3, pp. 203–212, 2010.

[80] C. L. Maier, B. R. Shepherd, T. Yi, and J. S. Pober, "Explant outgrowth, propagation and characterization of human pericytes," *Microcirculation*, vol. 17, no. 5, pp. 367–380, 2010.

[81] B. Péault, M. Rudnicki, Y. Torrente et al., "Stem and progenitor cells in skeletal muscle development, maintenance, and therapy," *Molecular Therapy*, vol. 15, no. 5, pp. 867–877, 2007.

[82] B. M. Deasy, Y. Li, and J. Huard, "Tissue engineering with muscle-derived stem cells," *Current Opinion in Biotechnology*, vol. 15, no. 5, pp. 419–423, 2004.

[83] M. Sampaolesi, S. Blot, G. D'Antona et al., "Mesoangioblast stem cells ameliorate muscle function in dystrophic dogs," *Nature*, vol. 444, no. 7119, pp. 574–579, 2006.

[84] B. Cao, B. Zheng, R. J. Jankowski et al., "Muscle stem cells differentiate into haematopoietic lineages but retain myogenic potential," *Nature Cell Biology*, vol. 5, no. 7, pp. 640–646, 2003.

[85] H. Oshima, T. R. Payne, K. L. Urish et al., "Differential myocardial infarct repair with muscle stem cells compared to myoblasts," *Molecular Therapy*, vol. 12, no. 6, pp. 1130–1141, 2005.

[86] A. Uezumi, S.-I. Fukada, N. Yamamoto, S. Takeda, and K. Tsuchida, "Mesenchymal progenitors distinct from satellite cells contribute to ectopic fat cell formation in skeletal muscle," *Nature Cell Biology*, vol. 12, no. 2, pp. 143–152, 2010.

[87] M. P. Pusztaszeri, W. Seelentag, and F. T. Bosman, "Immunohistochemical expression of endothelial markers CD31, CD34, von Willebrand factor, and Fli-1 in normal human tissues," *Journal of Histochemistry and Cytochemistry*, vol. 54, no. 4, pp. 385–395, 2006.

[88] A. W. James, J. N. Zara, M. Corselli et al., "An abundant perivascular source of stem cells for bone tissue engineering," *Stem Cells Translational Medicine*, vol. 1, no. 9, pp. 673–684, 2012.

[89] A. W. James, J. N. Zara, X. Zhang et al., "Perivascular stem cells: a prospectively purified mesenchymal stem cell population for bone tissue engineering," *Stem Cells Translational Medicine*, vol. 1, no. 6, pp. 510–519, 2012.

[90] E. K. Waller, J. Olweus, F. Lund-Johansen et al., "The "common stem cell" hypothesis reevaluated: human fetal bone marrow contains separate populations of hematopoietic and stromal progenitors," *Blood*, vol. 85, no. 9, pp. 2422–2435, 1995.

[91] E. K. Waller, S. Huang, and L. Terstappen, "Changes in the growth properties of CD34+, CD38– bone marrow progenitors during human fetal development," *Blood*, vol. 86, no. 2, pp. 710–718, 1995.

[92] D. J. Simmons, P. Seitz, L. Kidder et al., "Partial characterization of rat marrow stromal cells," *Calcified Tissue International*, vol. 48, no. 5, pp. 326–334, 1991.

[93] S. Kaiser, B. Hackanson, M. Follo et al., "BM cells giving rise to MSC in culture have a heterogeneous CD34 and CD45 phenotype," *Cytotherapy*, vol. 9, no. 5, pp. 439–450, 2007.

[94] R. A. Kopher, V. R. Penchev, M. S. Islam, K. L. Hill, S. Khosla, and D. S. Kaufman, "Human embryonic stem cell-derived CD34+ cells function as MSC progenitor cells," *Bone*, vol. 47, no. 4, pp. 718–728, 2010.

[95] R. Barbet, I. Peiffer, A. Hatzfeld, P. Charbord, and J. A. Hatzfeld, "Comparison of gene expression in human embryonic stem cells, hESC-derived mesenchymal stem cells and human mesenchymal stem cells," *Stem Cells International*, vol. 2011, Article ID 368192, 9 pages, 2011.

[96] M. A. Vodyanik, J. Yu, X. Zhang et al., "A mesoderm-derived precursor for mesenchymal stem and endothelial cells," *Cell Stem Cell*, vol. 7, no. 6, pp. 718–729, 2010.

[97] A. Dar, H. Domev, O. Ben-Yosef et al., "Multipotent vasculogenic pericytes from human pluripotent stem cells promote recovery of murine ischemic limb," *Circulation*, vol. 125, no. 1, pp. 87–99, 2012.

[98] D. O. Traktuev, S. Merfeld-Clauss, J. Li et al., "A population of multipotent CD34-positive adipose stromal cells share pericyte and mesenchymal surface markers, reside in a periendothelial location, and stabilize endothelial networks," *Circulation Research*, vol. 102, no. 1, pp. 77–85, 2008.

[99] H. Yamanishi, S. Fujiwara, and T. Soma, "Perivascular localization of dermal stem cells in human scalp," *Experimental Dermatology*, vol. 21, no. 1, pp. 78–80, 2012.

[100] L. Zimmerlin, V. S. Donnenberg, and A. D. Donnenberg, "Rare event detection and analysis in flow cytometry: bone marrow mesenchymal stem cells, breast cancer stem/progenitor cells in malignant effusions, and pericytes in disaggregated adipose tissue," *Methods in Molecular Biology*, vol. 699, pp. 251–273, 2011.

[101] L. Zimmerlin, V. S. Donnenberg, J. P. Rubin, and A. D. Donnenberg, "Mesenchymal markers on human adipose stem/progenitor cells," *Cytometry A*, vol. 83, no. 1, pp. 134–140, 2012.

[102] L. Zimmerlin, V. S. Donnenberg, and A. D. Donnenberg, "Pericytes: a universal adult tissue stem cell?" *Cytometry A*, vol. 81, no. 1, pp. 12–14, 2012.

[103] K. Yoshimura, T. Shigeura, D. Matsumoto et al., "Characterization of freshly isolated and cultured cells derived from the fatty and fluid portions of liposuction aspirates," *Journal of Cellular Physiology*, vol. 208, no. 1, pp. 64–76, 2006.

[104] D. T. Covas, R. A. Panepucci, A. M. Fontes et al., "Multipotent mesenchymal stromal cells obtained from diverse human tissues share functional properties and gene-expression profile with CD146+ perivascular cells and fibroblasts," *Experimental Hematology*, vol. 36, no. 5, pp. 642–654, 2008.

[105] A. C. W. Zannettino, S. Paton, A. Arthur et al., "Multipotential human adipose-derived stromal stem cells exhibit a perivascular phenotype in vitro and in vivo," *Journal of Cellular Physiology*, vol. 214, no. 2, pp. 413–421, 2008.

[106] M. Maumus, J.-A. Peyrafitte, R. D'Angelo et al., "Native human adipose stromal cells: localization, morphology and phenotype," *International Journal of Obesity*, vol. 35, no. 9, pp. 1141–1153, 2011.

[107] G. Astori, F. Vignati, S. Bardelli et al., "'In vitro' and multicolor phenotypic characterization of cell subpopulations identified in fresh human adipose tissue stromal vascular fraction and in the derived mesenchymal stem cells," *Journal of Translational Medicine*, vol. 5, article 55, 2007.

[108] A. O. Sahin and M. Buitenhuis, "Molecular mechanisms underlying adhesion and migration of hematopoietic stem cells," *Cell Adhesion and Migration*, vol. 6, no. 1, pp. 39–48, 2012.

[109] A. Augello, T. B. Kurth, and C. de Bari, "Mesenchymal stem cells: a perspective from in vitro cultures to in vivo migration and niches," *European Cells and Materials*, vol. 20, pp. 121–133, 2010.

[110] S. K. Kang, I. S. Shin, M. S. Ko, J. Y. Jo, and J. C. Ra, "Journey of mesenchymal stem cells for homing: atrategies to enhance efficacy and safety of stem cell therapy," *Stem Cells International*, vol. 2012, Article ID 342968, 11 pages, 2012.

[111] A. Armulik, G. Genové, and C. Betsholtz, "Pericytes: developmental, physiological, and pathological perspectives, problems, and promises," *Developmental Cell*, vol. 21, no. 2, pp. 193–215, 2011.

[112] A. Arthur, A. Zannettino, R. Panagopoulos et al., "EphB/ephrin-B interactions mediate human MSC attachment, migration and osteochondral differentiation," *Bone*, vol. 48, no. 3, pp. 533–542, 2011.

[113] S. S. Foo, C. J. Turner, S. Adams et al., "Ephrin-B2 controls cell motility and adhesion during blood-vessel-wall assembly," *Cell*, vol. 124, no. 1, pp. 161–173, 2006.

[114] K. Stark, A. Eckart, S. Haidari et al., "Capillary and arteriolar pericytes attract innate leukocytes exiting through venules and "instruct" them with pattern-recognition and motility programs," *Nature Immunology*, vol. 14, no. 1, pp. 41–51, 2013.

[115] Y. Bordon, "Cell migration: pericytes: route planners," *Nature Reviews Immunology*, vol. 13, no. 1, p. 5, 2013.

[116] M. Hellström, M. Kalén, P. Lindahl, A. Abramsson, and C. Betsholtz, "Role of PDGF-B and PDGFR-β in recruitment of vascular smooth muscle cells and pericytes during embryonic blood vessel formation in the mouse," *Development*, vol. 126, no. 14, pp. 3047–3055, 1999.

[117] M. Enge, M. Bjarnegård, H. Gerhardt et al., "Endothelium-specific platelet-derived growth factor-B ablation mimics diabetic retinopathy," *EMBO Journal*, vol. 21, no. 16, pp. 4307–4316, 2002.

[118] A. Abramsson, P. Lindblom, and C. Betsholtz, "Endothelial and nonendothelial sources of PDGF-B regulate pericyte recruitment and influence vascular pattern formation in tumors," *Journal of Clinical Investigation*, vol. 112, no. 8, pp. 1142–1151, 2003.

[119] S. Ejaz, "Importance of pericytes and mechanisms of pericyte loss during diabetes retinopathy," *Diabetes, Obesity and Metabolism*, vol. 10, no. 1, pp. 53–63, 2008.

[120] K. le Blanc, "Immunomodulatory effects of fetal and adult mesenchymal stem cells," *Cytotherapy*, vol. 5, no. 6, pp. 485–489, 2003.

[121] L. B. Ware and M. A. Matthay, "Keratinocyte and hepatocyte growth factors in the lung: roles in lung development, inflammation, and repair," *The American Journal of Physiology*, vol. 282, no. 5, pp. L924–L940, 2002.

[122] G. F. Curley, M. Hayes, B. Ansari et al., "Mesenchymal stem cells enhance recovery and repair following ventilator-induced lung injury in the rat," *Thorax*, vol. 67, no. 6, pp. 496–501, 2012.

[123] C.-W. Chen, E. Montelatici, M. Crisan et al., "Perivascular multi-lineage progenitor cells in human organs: regenerative units, cytokine sources or both?" *Cytokine and Growth Factor Reviews*, vol. 20, no. 5-6, pp. 429–434, 2009.

[124] M. Takeoka, W. F. Ward, H. Pollack, D. W. Kamp, and R. J. Panos, "KGF facilitates repair of radiation-induced DNA damage in alveolar epithelial cells," *The American Journal of Physiology*, vol. 272, no. 6, pp. L1174–L1180, 1997.

[125] B. M. Strem, K. C. Hicok, M. Zhu et al., "Multipotential differentiation of adipose tissue-derived stem cells," *Keio Journal of Medicine*, vol. 54, no. 3, pp. 132–141, 2005.

[126] D. Matsumoto, K. Sato, K. Gonda et al., "Cell-assisted lipotransfer: supportive use of human adipose-derived cells for soft tissue augmentation with lipoinjection," *Tissue Engineering*, vol. 12, no. 12, pp. 3375–3382, 2006.

[127] P. van Pham, K. H.-T. Bui, D. Q. Ngo, L. T. Khuat, and N. K. Phan, "Transplantation of nonexpanded adipose stromal vascular fraction and platelet-rich plasma for articular cartilage injury treatment in mice model," *Journal of Medical Engineering*, vol. 2013, Article ID 832396, 7 pages, 2013.

[128] L. Cai, B. H. Johnstone, T. G. Cook et al., "IFATS collection: human adipose tissue-derived stem cells induce angiogenesis and nerve sprouting following myocardial infarction, in conjunction with potent preservation of cardiac function," *Stem Cells*, vol. 27, no. 1, pp. 230–237, 2009.

[129] U. Kim, D.-G. Shin, J.-S. Park et al., "Homing of adipose-derived stem cells to radiofrequency catheter ablated canine atrium and differentiation into cardiomyocyte-like cells," *International Journal of Cardiology*, vol. 146, no. 3, pp. 371–378, 2011.

[130] A. Banas, T. Teratani, Y. Yamamoto et al., "IFATS collection: in vivo therapeutic potential of human adipose tissue mesenchymal stem cells after transplantation into mice with liver injury," *Stem Cells*, vol. 26, no. 10, pp. 2705–2712, 2008.

[131] D. H. Kim, C. M. Je, J. Y. Sin, and J. S. Jung, "Effect of partial hepatectomy on in vivo engraftment after intravenous administration of human adipose tissue stromal cells in mouse," *Microsurgery*, vol. 23, no. 5, pp. 424–431, 2003.

[132] Y. M. Kim, Y. S. Choi, J. W. Choi et al., "Effects of systemic transplantation of adipose tissue-derived stem cells on olfactory epithelium regeneration," *Laryngoscope*, vol. 119, no. 5, pp. 993–999, 2009.

[133] W. Xing, D. Zhimei, Z. Liming et al., "IFATS collection: the conditioned media of adipose stromal cells protect against hypoxia-ischemia-induced brain damage in neonatal rats," *Stem Cells*, vol. 27, no. 2, pp. 478–488, 2009.

[134] K.-S. Cho, H.-K. Park, H.-Y. Park et al., "IFATS collection: immunomodulatory effects of adipose tissue-derived stem cells in an allergic rhinitis mouse model," *Stem Cells*, vol. 27, no. 1, pp. 259–265, 2009.

[135] P. Sacerdote, S. Niada, S. Franchi et al., "Systemic administration of human adipose-derived stem cells reverts nociceptive hypersensitivity in an experimental model of neuropathy," *Stem Cells and Development*, vol. 22, no. 8, pp. 1252–1263, 2013.

[136] S. Marconi, G. Castiglione, E. Turano et al., "Human adipose-derived mesenchymal stem cells systemically injected promote peripheral nerve regeneration in the mouse model of sciatic crush," *Tissue Engineering A*, vol. 18, no. 11-12, pp. 1264–1272, 2012.

[137] B. Levi, A. W. James, E. R. Nelson et al., "Studies in adipose-derived stromal cells: migration and participation in repair of cranial injury after systemic injection," *Plastic and Reconstructive Surgery*, vol. 127, no. 3, pp. 1130–1140, 2011.

[138] N. M. Vieira, M. Valadares, E. Zucconi et al., "Human adipose-derived mesenchymal stromal cells injected systemically into GRMD dogs without immunosuppression are able to reach the host muscle and express human dystrophin," *Cell Transplantation*, vol. 21, no. 7, pp. 1407–1417, 2012.

[139] N. M. Vieira, C. R. Bueno Jr., V. Brandalise et al., "SJL dystrophic mice express a significant amount of human muscle proteins following systemic delivery of human adipose-derived stromal cells without immunosuppression," *Stem Cells*, vol. 26, no. 9, pp. 2391–2398, 2008.

[140] S. J. Baek, S. K. Kang, and J. C. Ra, "In vitro migration capacity of human adipose tissue-derived mesenchymal stem cells reflects their expression of receptors for chemokines and growth factors," *Experimental and Molecular Medicine*, vol. 43, no. 10, pp. 596–603, 2011.

[141] C. Garrovo, N. Bergamin, D. Bates et al., "In vivo tracking of murine adipose tissue-derived multipotent adult stem cells and ex vivo cross-validation," *International Journal of Molecular Imaging*, vol. 2013, Article ID 426961, 13 pages, 2013.

[142] N. Kakudo, S. Kushida, K. Suzuki et al., "Effects of transforming growth factor-beta1 on cell motility, collagen gel contraction, myofibroblastic differentiation, and extracellular matrix expression of human adipose-derived stem cell," *Human Cell*, vol. 25, no. 4, pp. 87–95, 2012.

[143] P. R. Baraniak and T. C. McDevitt, "Stem cell paracrine actions and tissue regeneration," *Regenerative Medicine*, vol. 5, no. 1, pp. 121–143, 2010.

[144] L. Casteilla, V. Planat-Benard, P. Laharrague, and B. Cousin, "Adipose-derived stromal cells: their identity and uses in clinical trials, an update," *World Journal of Stem Cells*, vol. 3, no. 4, pp. 25–33, 2011.

[145] S. H. Lee, S. Y. Jin, J. S. Song, K. K. Seo, and K. H. Cho, "Paracrine effects of adipose-derived stem cells on keratinocytes and

dermal fibroblasts," *Annals of Dermatology*, vol. 24, no. 2, pp. 136–143, 2012.

[146] L. Hu, J. Zhao, J. Liu, N. Gong, and L. Chen, "Effects of adipose stem cell-conditioned medium on the migration of vascular endothelial cells, fibroblasts and keratinocytes," *Experimental and Therapeutic Medicine*, vol. 5, no. 3, pp. 701–706, 2013.

[147] S. S. Collawn, N. Sanjib Banerjee, J. de la Torre, L. Vasconez, and L. T. Chow, "Adipose-derived stromal cells accelerate wound healing in an organotypic raft culture model," *Annals of Plastic Surgery*, vol. 68, no. 5, pp. 501–504, 2012.

[148] K. M. Moon, Y. H. Park, J. S. Lee et al., "The effect of secretory factors of adipose-derived stem cells on human keratinocytes," *International Journal of Molecular Sciences*, vol. 13, no. 1, pp. 1239–1257, 2012.

[149] X. Fu, L. Fang, H. Li, X. Li, B. Cheng, and Z. Sheng, "Adipose tissue extract enhances skin wound healing," *Wound Repair and Regeneration*, vol. 15, no. 4, pp. 540–548, 2007.

[150] A. E. Karnoub, A. B. Dash, A. P. Vo et al., "Mesenchymal stem cells within tumour stroma promote breast cancer metastasis," *Nature*, vol. 449, no. 7162, pp. 557–563, 2007.

[151] A. Nakamizo, F. Marini, T. Amano et al., "Human bone marrow-derived mesenchymal stem cells in the treatment of gliomas," *Cancer Research*, vol. 65, pp. 3307–3318, 2005.

[152] C. Pendleton, Q. Li, D. A. Chesler, K. Yuan, H. Guerrero-Cazares, and A. Quinones-Hinojosa, "Mesenchymal stem cells derived from adipose tissue vs bone marrow: in vitro comparison of their tropism towards gliomas," *PLoS ONE*, vol. 8, no. 3, Article ID e58198, 2013.

[153] M. Lamfers, S. Idema, F. van Milligen et al., "Homing properties of adipose-derived stem cells to intracerebral glioma and the effects of adenovirus infection," *Cancer Letters*, vol. 274, no. 1, pp. 78–87, 2009.

[154] L. Kucerova, V. Altanerova, M. Matuskova, S. Tyciakova, and C. Altaner, "Adipose tissue-derived human mesenchymal stem cells mediated prodrug cancer gene therapy," *Cancer Research*, vol. 67, no. 13, pp. 6304–6313, 2007.

[155] I. T. Cavarretta, V. Altanerova, M. Matuskova, L. Kucerova, Z. Culig, and C. Altaner, "Adipose tissue-derived mesenchymal stem cells expressing prodrug-converting enzyme inhibit human prostate tumor growth," *Molecular Therapy*, vol. 18, no. 1, pp. 223–231, 2010.

[156] F. L. Muehlberg, Y.-H. Song, A. Krohn et al., "Tissue-resident stem cells promote breast cancer growth and metastasis," *Carcinogenesis*, vol. 30, no. 4, pp. 589–597, 2009.

[157] S. Pinilla, E. Alt, F. J. Abdul Khalek et al., "Tissue resident stem cells produce CCL5 under the influence of cancer cells and thereby promote breast cancer cell invasion," *Cancer Letters*, vol. 284, no. 1, pp. 80–85, 2009.

[158] B. Sun, K.-H. Roh, J.-R. Park et al., "Therapeutic potential of mesenchymal stromal cells in a mouse breast cancer metastasis model," *Cytotherapy*, vol. 11, no. 3, pp. 289–298, 2009.

[159] B. Cousin, E. Ravet, S. Poglio et al., "Adult stromal cells derived from human adipose tissue provoke pancreatic cancer cell death both in vitro and in vivo," *PLoS ONE*, vol. 4, no. 7, Article ID e6278, 2009.

[160] S. Tottey, M. Corselli, E. M. Jeffries, R. Londono, B. Peault, and S. F. Badylak, "Extracellular matrix degradation products and low-oxygen conditions enhance the regenerative potential of perivascular stem cells," *Tissue Engineering A*, vol. 17, no. 1-2, pp. 37–44, 2011.

[161] B. Annabi, Y.-T. Lee, S. Turcotte et al., "Hypoxia promotes murine bone-marrow-derived stromal cell migration and tube formation," *Stem Cells*, vol. 21, no. 3, pp. 337–347, 2003.

[162] R. K. Assoian and M. A. Schwartz, "Coordinate signaling by integrins and receptor tyrosine kinases in the regulation of G1 phase cell-cycle progression," *Current Opinion in Genetics and Development*, vol. 11, no. 1, pp. 48–53, 2001.

[163] I. Hunger-Glaser, R. S. Fan, E. Perez-Salazar, and E. Rozengurt, "PDGF and FGF induce focal adhesion kinase (FAK) phosphorylation at Ser-910: dissociation from Tyr-397 phosphorylation and requirement for ERK activation," *Journal of Cellular Physiology*, vol. 200, no. 2, pp. 213–222, 2004.

[164] C. Huang, K. Jacobson, and M. D. Schaller, "MAP kinases and cell migration," *Journal of Cell Science*, vol. 117, no. 20, pp. 4619–4628, 2004.

[165] I. Rosová, M. Dao, B. Capoccia, D. Link, and J. A. Nolta, "Hypoxic preconditioning results in increased motility and improved therapeutic potential of human mesenchymal stem cells," *Stem Cells*, vol. 26, no. 8, pp. 2173–2182, 2008.

[166] S. Neuss, E. Becher, M. Wöltje, L. Tietze, and W. Jahnen-Dechent, "Functional expression of HGF and HGF receptor/c-met in adult human mesenchymal stem cells suggests a role in cell mobilization, tissue repair, and wound healing," *Stem Cells*, vol. 22, no. 3, pp. 405–414, 2004.

[167] H. Liu, W. Xue, G. Ge et al., "Hypoxic preconditioning advances CXCR4 and CXCR7 expression by activating HIF-1α in MSCs," *Biochemical and Biophysical Research Communications*, vol. 401, no. 4, pp. 509–515, 2010.

[168] C. W. Chen, M. Okada, J. D. Proto, X. Gao et al., "Human pericytes for ischemic heart repair," *Stem Cells*, vol. 31, no. 2, pp. 305–316, 2013.

[169] R. Katare, F. Riu, K. Mitchell et al., "Transplantation of human pericyte progenitor cells improves the repair of infarcted heart through activation of an angiogenic program involving micro-RNA-132," *Circulation Research*, vol. 109, no. 8, pp. 894–906, 2011.

[170] A. Dellavalle, G. Maroli, D. Covarello et al., "Pericytes resident in postnatal skeletal muscle differentiate into muscle fibres and generate satellite cells," *Nature Communications*, vol. 2, no. 1, article 499, 2011.

[171] M. Pierro, L. Ionescu, T. Montemurro, A. Vadivel et al., "Short-term, long-term and paracrine effect of human umbilical cord-derived stem cells in lung injury prevention and repair in experimental bronchopulmonary dysplasia," *Thorax*, vol. 68, no. 5, pp. 475–484, 2013.

[172] M. Corselli, C. J. Chin, C. Parekh, A. Sahaghian et al., "Perivascular support of human hematopoietic stem/progenitor cells," *Blood*, vol. 121, no. 15, pp. 2891–2901, 2013.

[173] X. Zhang, B. Péault, W. Chen et al., "The nell-1 growth factor stimulates bone formation by purified human perivascular cells," *Tissue Engineering A*, vol. 17, no. 19-20, pp. 2497–2509, 2011.

[174] E. Chavakis, C. Urbich, and S. Dimmeler, "Homing and engraftment of progenitor cells: a prerequisite for cell therapy," *Journal of Molecular and Cellular Cardiology*, vol. 45, no. 4, pp. 514–522, 2008.

[175] R. H. Lee, A. A. Pulin, M. J. Seo et al., "Intravenous hMSCs improve myocardial infarction in mice because cells embolized in lung are activated to secrete the anti-inflammatory protein TSG-6," *Cell Stem Cell*, vol. 5, no. 1, pp. 54–63, 2009.

[176] A. Askarinam, A. W. James, J. N. Zara et al., "Human perivascular stem cells show enhanced osteogenesis and vasculogenesis

with nel-like molecule I protein," *Tissue Engineering A*, vol. 19, no. 11-12, pp. 1386–1397, 2013.

[177] X. Zhang, K. Ting, C. M. Bessette et al., "Nell-1, a key functional mediator of Runx2, partially rescues calvarial defects in Runx2+/– mice," *Journal of Bone and Mineral Research*, vol. 26, no. 4, pp. 777–791, 2011.

[178] T. Kitaori, H. Ito, E. M. Schwarz et al., "Stromal cell-derived factor 1/CXCR4 signaling is critical for the recruitment of mesenchymal stem cells to the fracture site during skeletal repair in a mouse model," *Arthritis and Rheumatism*, vol. 60, no. 3, pp. 813–823, 2009.

[179] N. Song, Y. Huang, H. Shi et al., "Overexpression of platelet-derived growth factor-BB increases tumor pericyte content via stromal-derived factor-1α/CXCR4 axis," *Cancer Research*, vol. 69, no. 15, pp. 6057–6064, 2009.

[180] E. Chavakis, M. Koyanagi, and S. Dimmeler, "Enhancing the outcome of cell therapy for cardiac repair: progress from bench to bedside and back," *Circulation*, vol. 121, no. 2, pp. 325–335, 2010.

[181] A. N. Stratman, A. E. Schwindt, K. M. Malotte, and G. E. Davis, "Endothelial-derived PDGF-BB and HB-EGF coordinately regulate pericyte recruitment during vasculogenic tube assembly and stabilization," *Blood*, vol. 116, no. 22, pp. 4720–4730, 2010.

[182] A. N. Stratman, K. M. Malotte, R. D. Mahan, M. J. Davis, and G. E. Davis, "Pericyte recruitment during vasculogenic tube assembly stimulates endothelial basement membrane matrix formation," *Blood*, vol. 114, no. 24, pp. 5091–5101, 2009.

[183] H. Gerhardt and C. Betsholtz, "Endothelial-pericyte interactions in angiogenesis," *Cell and Tissue Research*, vol. 314, no. 1, pp. 15–23, 2003.

[184] L. Díaz-Flores, R. Gutiérrez, J. F. Madrid et al., "Pericytes. Morphofunction, interactions and pathology in a quiescent and activated mesenchymal cell niche," *Histology and Histopathology*, vol. 24, no. 7, pp. 909–969, 2009.

[185] D. E. Sims, "The pericyte-A review," *Tissue and Cell*, vol. 18, no. 2, pp. 153–174, 1986.

[186] K. Gaengel, G. Genové, A. Armulik, and C. Betsholtz, "Endothelial-mural cell signaling in vascular development and angiogenesis," *Arteriosclerosis, Thrombosis, and Vascular Biology*, vol. 29, no. 5, pp. 630–638, 2009.

[187] G. Rajashekhar, D. O. Traktuev, W. C. Roell, B. H. Johnstone, S. Merfeld-Clauss, B. van Natta et al., "IFATS collection: adipose stromal cell differentiation is reduced by endothelial cell contact and paracrine communication: role of canonical Wnt signaling," *Stem Cells*, vol. 26, no. 10, pp. 2674–2681, 2008.

[188] F. A. Saleh, M. Whyte, P. Ashton, and P. G. Genever, "Regulation of mesenchymal stem cell activity by endothelial cells," *Stem Cells and Development*, vol. 20, no. 3, pp. 391–403, 2011.

[189] F. A. Saleh, M. Whyte, and P. G. Genever, "Effects of endothelial cells on human mesenchymal stem cell activity in a three-dimensional in vitro model," *Journal of European Cells and Materials*, vol. 22, pp. 242–257, 2011.

[190] Y. Xue, Z. Xing, S. Hellem, K. Arvidson, and K. Mustafa, "Endothelial cells influence the osteogenic potential of bone marrow stromal cells," *BioMedical Engineering Online*, vol. 8, article 34, 2009.

[191] D. Kaigler, P. H. Krebsbach, E. R. West, K. Horger, Y. C. Huang, and D. J. Mooney, "Endothelial cell modulation of bone marrow stromal cell osteogenic potential," *FASEB Journal*, vol. 19, no. 6, pp. 665–667, 2005.

[192] H. Li, R. Daculsi, M. Grellier, R. Bareille, C. Bourget, and J. Amedee, "Role of neural-cadherin in early osteoblastic differentiation of human bone marrow stromal cells cocultured with human umbilical vein endothelial cells," *The American Journal of Physiology*, vol. 299, no. 2, pp. 422–430, 2010.

[193] M. Grellier, N. Ferreira-Tojais, C. Bourget, R. Bareille, F. Guillemot, and J. Amedee, "Role of vascular endothelial growth factor in the communication between human osteoprogenitors and endothelial cells," *Journal of Cellular Biochemistry*, vol. 106, no. 3, pp. 390–398, 2009.

[194] T. Meury, S. Verrier, and M. Alini, "Human endothelial cells inhibit BMSC differentiation into mature osteoblasts in vitro by interfering with osterix expression," *Journal of Cellular Biochemistry*, vol. 98, no. 4, pp. 992–1006, 2006.

[195] F. Villars, B. Guillotin, T. Amedee, S. Dutoya, L. Bordenave, R. Bareille et al., "Effect of HUVEC on human osteoprogenitor cell differentiation needs heterotypic gap junction communication," *The American Journal of Physiology*, vol. 282, no. 4, pp. 775–785, 2002.

[196] F. Villars, L. Bordenave, R. Bareille, and J. Amedee, "Effect of human endothelial cells on human bone marrow stromal cell phenotype: role of VEGF?" *Journal of Cellular Biochemistry*, vol. 79, no. 4, pp. 672–685, 2000.

[197] B. Guillotin, C. Bourget, M. Remy-Zolgadri, R. Bareille, P. Fernandez, V. Conrad et al., "Human primary endothelial cells stimulate human osteoprogenitor cell differentiation," *Cellular Physiology and Biochemistry*, vol. 14, no. 4–6, pp. 325–332, 2004.

[198] U. Ozerdem and W. B. Stallcup, "Early contribution of pericytes to angiogenic sprouting and tube formation," *Angiogenesis*, vol. 6, no. 3, pp. 241–249, 2003.

[199] U. Ozerdem, K. A. Grako, K. Dahlin-Huppe, E. Monosov, and W. B. Stallcup, "NG2 proteoglycan is expressed exclusively by mural cells during vascular morphogenesis," *Developmental Dynamics*, vol. 222, no. 2, pp. 218–227, 2001.

[200] L. P. Reynolds, A. T. Grazul-Bilska, and D. A. Redmer, "Angiogenesis in the corpus luteum," *Endocrine*, vol. 12, no. 1, pp. 1–9, 2000.

[201] M. Enge, M. Bjarnegård, H. Gerhardt et al., "Endothelium-specific platelet-derived growth factor-B ablation mimics diabetic retinopathy," *EMBO Journal*, vol. 21, no. 16, pp. 4307–4316, 2002.

[202] K. K. Hirschi, S. A. Rohovsky, L. H. Beck, S. R. Smith, and P. A. D'Amore, "Endothelial cells modulate the proliferation of mural cell precursors via platelet-derived growth factor-BB and heterotypic cell contact," *Circulation Research*, vol. 84, no. 3, pp. 298–305, 1999.

[203] A. Blocki, Y. Wang, M. Koch et al., "Not all MSCs can act as pericytes: functional in vitro assays to distinguish pericytes from other mesenchymal stem cells in angiogenesis," *Stem Cells and Development*, vol. 22, no. 17, 2013.

[204] M. Corselli, C.-W. Chen, M. Crisan, L. Lazzari, and B. Péault, "Perivascular ancestors of adult multipotent stem cells," *Arteriosclerosis, Thrombosis, and Vascular Biology*, vol. 30, no. 6, pp. 1104–1109, 2010.

[205] A. Ehninger and A. Trumpp, "The bone marrow stem cell niche grows up: mesenchymal stem cells and macrophages move in," *Journal of Experimental Medicine*, vol. 208, no. 3, pp. 421–428, 2011.

[206] S. Ergün, D. Tilki, and D. Klein, "Vascular wall as a reservoir for different types of stem and progenitor cells," *Antioxidants and Redox Signaling*, vol. 15, no. 4, pp. 981–995, 2011.

[207] A. I. Caplan, "All MSCs are pericytes?" *Cell Stem Cell*, vol. 3, no. 3, pp. 229–230, 2008.

[208] A. M. Müller, A. Mehrkens, D. J. Schäfer et al., "Towards an intraoperative engineering of osteogenic and vasculogenic grafts from the stromal vascular fraction of human adipose tissue," *European Cells and Materials*, vol. 19, pp. 127–135, 2010.

[209] V. Marthiens, I. Kazanis, L. Moss, K. Long, and C. Ffrench-Constant, "Adhesion molecules in the stem cell niche: more than just staying in shape?" *Journal of Cell Science*, vol. 123, no. 10, pp. 1613–1622, 2010.

[210] J. P. Kirton, F. L. Wilkinson, A. E. Canfield, and M. Y. Alexander, "Dexamethasone downregulates calcification-inhibitor molecules and accelerates osteogenic differentiation of vascular pericytes: implications for vascular calcification," *Circulation Research*, vol. 98, no. 10, pp. 1264–1272, 2006.

[211] S. Mathews, R. Bhonde, P. K. Gupta, and S. Totey, "Extracellular matrix protein mediated regulation of the osteoblast differentiation of bone marrow derived human mesenchymal stem cells," *Differentiation*, vol. 84, no. 2, pp. 185–192, 2012.

[212] S. H. Ranganath, O. Levy, M. S. Inamdar, and J. M. Karp, "Harnessing the mesenchymal stem cell secretome for the treatment of cardiovascular disease," *Cell Stem Cell*, vol. 10, no. 3, pp. 244–258, 2012.

[213] I. Takada, A. P. Kouzmenko, and S. Kato, "PPAR-γ signaling crosstalk in mesenchymal stem cells," *PPAR Research*, vol. 2010, Article ID 341671, 6 pages, 2010.

Hindawi Publishing Corporation
Stem Cells International
Volume 2013, Article ID 732742, 13 pages
http://dx.doi.org/10.1155/2013/732742

Review Article

MSCs: Delivery Routes and Engraftment, Cell-Targeting Strategies, and Immune Modulation

Thomas J. Kean,[1] Paul Lin,[2] Arnold I. Caplan,[2] and James E. Dennis[1]

[1] *Benaroya Research Institute, Seattle, WA 98101, USA*
[2] *Skeletal Research Center, Department of Biology, Case Western Reserve University, Cleveland, OH 44106, USA*

Correspondence should be addressed to Thomas J. Kean; tkean@benaroyaresearch.org

Received 30 April 2013; Revised 27 June 2013; Accepted 1 July 2013

Academic Editor: Donald G. Phinney

Mesenchymal stem cells (MSCs) are currently being widely investigated both in the lab and in clinical trials for multiple disease states. The differentiation, trophic, and immunomodulatory characteristics of MSCs contribute to their therapeutic effects. Another often overlooked factor related to efficacy is the degree of engraftment. When reported, engraftment is generally low and transient in nature. MSC delivery methods should be tailored to the lesion being treated, which may be local or systemic, and customized to the mechanism of action of the MSCs, which can also be local or systemic. Engraftment efficiency is enhanced by using intra-arterial delivery instead of intravenous delivery, thus avoiding the "first-pass" accumulation of MSCs in the lung. Several methodologies to target MSCs to specific organs are being developed. These cell targeting methodologies focus on the modification of cell surface molecules through chemical, genetic, and coating techniques to promote selective adherence to particular organs or tissues. Future improvements in targeting and delivery methodologies to improve engraftment are expected to improve therapeutic results, extend the duration of efficacy, and reduce the effective (MSC) therapeutic dose.

1. Introduction

Mesenchymal stem cells (MSCs) are multipotential adult progenitor cells that have the capacity to differentiate along several mesenchymal lineages, including cartilage, adipose, marrow stroma, and bone tissue [1–3]. Studies have been conducted on the use of MSCs as a therapeutic based on this capacity to differentiate directly into these end-stage phenotypes, including the use of MSCs to promote or augment bone repair [4] and for the repair of cartilage defects [4, 5]. In addition to direct differentiation into end-stage phenotypes, MSCs have also been shown to have a positive therapeutic effect in many repair situations because of their capacity to secrete trophic factors (reviewed in [6]) that contribute to repair via the promotion of vascularization and the inhibition of cell death as well as through the modulation of the immune response. Currently, there are over 160 open studies and 116 closed clinical trials (results retrieved (3rd June 2013) in a search of www.clinicaltrials.gov on the search term "mesenchymal stem cells" and excluding trials with an unknown status and those that were conducted *in vitro*) that use MSCs to treat a variety of conditions that range from direct formation of bone tissue to treatments for graft versus host disease (GvHD) [7–9], myocardial infarction, brain trauma, and multiple sclerosis [10, 11] (reviewed by Millard and Fisk [12]). Indeed, MSCs have been well characterized with respect to their ability to produce a range of growth factors and cytokines, which inspired the designation of these cells as a kind of "*injury drugstore*" [13]. An interesting subset of this factory of cytokines is the factors that have been shown to have a profound effect on modulating the immune system. These immune modulatory factors are being tested for their effect on immune disorders such as GvHD, rheumatoid arthritis [14, 15], multiple sclerosis [16, 17], type I diabetes [18, 19], inflammatory bowel disease (IBD) [20–23], and transplant tolerance [24].

Of particular relevance to the therapeutic application of MSCs is their fate post-implantation. Ambiguity seen in the efficacy of MSCs, in both animal studies and clinical trials, with therapies being ineffective or only temporarily

effective could be due to suboptimal application of MSCs. Whether systemically injected or injected directly into a tissue or organ, there is the issue of where the cells go and whether the cells can bind, engraft, and, in many instances, survive. Very few studies have quantified the efficiency of MSC transplantation, and those that have quantified MSC engraftment have shown poor engraftment efficiency. Complicating this determination, as noted in Karp and Leng Teo [25], are the details of the quantification methodology. The techniques for assessing biodistribution of MSCs can be categorized into *in vivo* and *ex vivo* methods. Examples of *in vivo* methods include bioluminescence, whereby cells are transduced to express luciferase and can then be imaged through their metabolism of luciferin resulting in light emission [26]; fluorescence, whereby cells are either loaded with a fluorescent dye or transduced to express a fluorescent reporter which can then be imaged; radionuclide labeling, where cells are loaded with radionuclides and localized with scintigraphy [27], positron emission tomography (PET) or single photon emission computed tomography (SPECT); and magnetic resonance imaging (MRI), wherein cells loaded with paramagnetic compounds (e.g., iron oxide nanoparticles) are traced with an MRI scanner. For further review of these imaging modalities and their clinical application see Srinivas et al. [28] and Reagan and Kaplan [29]. *Ex vivo* methods to assess biodistribution include quantitative PCR, flow cytometry, and histological methods. Histological methods include tracking fluorescently labeled cells; *in situ* hybridization, for example, for Y-chromosomes and for human-specific ALU sequences; and histochemical staining for species-specific or genetically introduced proteins such as bacterial β-galactosidase. These immunohistochemical methods are useful for discerning engraftment location but necessitate the excision of tissue. They are, however, prone to errors for quantification due to sampling, the possibility of false positives, and the loss of signal in studies where MSCs are tagged with fluorescent probes that lose signal with each cell division. With the use of genetic markers, such as luciferase or green fluorescent protein (GFP), the fate of MSCs in whole animals can be tracked without losing signal after cell division. However, luciferase and GFP-like optical probes suffer from limited penetration and 3D localization issues due to tissue shielding; thus, they are most applicable in small animal models, while combinational tracking approaches make it feasible to more accurately track cell fate systemically and over extended periods of time. Additionally, care must be taken in how the cells are labeled, as certain methods of labeling MSCs with reporter genes can affect their proliferation [26] or their differentiation potential [30]. With the use of these newer tracking methods, researchers now have the ability to address the long-term fate of transplanted MSCs, although there is still a paucity of data related to this issue. This review will analyze factors that may influence the therapeutic efficacy of MSCs, including an overview of the immune status of MSCs, "intrinsic" MSC activity, optimal MSC delivery methods, and targeting methods to improve cell engraftment and survival.

2. MSC Immune Modulation

Several characteristics of MSCs are purported to impart immune privilege, thereby allowing MSCs to avoid immune rejection in certain situations, which may facilitate the clinical use of allogenic MSCs. MSCs do not express class II Major Histocompatibility Complex (MHC) or costimulator molecules and express low levels of class I MHC [31]. One of the first indicators of the role of MSCs in modulating immune reactions was in studies showing that activated MSCs inhibit T-cell expansion in mixed lymphocyte reactions [32–34]. MSCs have been shown to influence the immune system through the secretion of a variety of soluble factors including indoleamine 2,3-dioxygenase [35], nitric oxide [9], transforming growth factor beta (TGFβ), prostaglandin E2 (PGE2) [36, 37], and tumor necrosis factor stimulated gene-6 protein (TSG-6) [38]. Di Nicola et al. [39] showed that MSCs could impede T-cell expansion in transwell cultures and that this inhibitory effect was abolished by the addition of antibodies to TGFβ and hepatocyte growth factor (HGF), while Tse et al. [33] showed a similar inhibitory effect that was a soluble factor but not due to TGFβ, PGE2, or interleukin-10. In still another study, this time using adipose-derived MSCs, it was shown that the inhibition of T-cell expansion in mixed lymphocyte reactions was abrogated by the addition of indomethacin, a PGE2 inhibitor, but was not affected by antibodies to TGFβ or HGF [40]. It has also been demonstrated that proinflammatory factors, such as interferon-γ or tumor necrosis factor alpha (TNFα), upregulate the expression of these important regulatory factors [9, 35, 41]. This MSC anti-inflammatory response to proinflammatory stimulation is referred to as "licensing" [35]. For a detailed review on the mechanism of action of each of these factors, see English (2013) [42].

While many studies have shown that soluble factors play a significant role in the immunomodulatory characteristics of MSCs, several other studies indicate that cell-to-cell contact may also be important. In one study, MSCs were shown to inhibit proliferation of memory T-cells but, in this case, direct cell contact was required as the MSCs were ineffective in transwell experiments [35]. Another study showed that MSCs interact with T-cells via Notch signaling and that inactivation of Toll-3 and Toll-4 receptors downregulated Jagged-1 expression in MSCs, thus impeding interaction with Notch on T-cells and resulting in the loss of MSC inhibition of T-cell proliferation [43]. Indeed, several more recent studies indicate that cell-to-cell contact between MSCs and immune cells may be very important in specific situations. For example, it was shown that tissue-resident MSCs are able to promote epithelial cell repair through the secretion of PGE2 after the MSCs had been exposed to microbes of the GI-tract, while mice deficient in Toll-like receptor signaling (myeloid differentiation primary response gene 88 knockouts; Myd88$^{-/-}$) were ineffective at epithelial repair [44]. Additional studies have shown that MSCs may also regulate dendritic cells via Notch signaling [45, 46].

The mechanism of the immunomodulation characteristics of MSCs is critical when considering the potential therapeutic effects of MSC transplantation. If MSCs need

cell-to-cell contact or need to secrete factors at a high local concentration to impart their regulatory role, then MSCs will need to be delivered in close proximity to the target tissue or organ. Alternatively, MSCs may act distally through the secretion of sufficient amounts of soluble factors with an adequate half-life to reach the target lesion. For example, TSG-6 was shown to play a key role in MSC-mediated inflammatory regulation in postmyocardial infarction. In this study, MSCs or TSG-6 alone, but not MSCs treated with TSG-6 siRNA, were able to decrease postmyocardial infarction inflammation and improve cardiac function [38]. A similar anti-inflammatory effect of MSC-produced TSG-6 was shown in a cornea transplant model [47], and another study in a peritonitis model showed that MSCs stimulated by macrophage-produced TNFα produced TSG-6 which acted as a negative feedback loop on macrophage inflammatory signaling [48].

These immunomodulatory characteristics are likely the underlying mechanism(s) of the anti-inflammatory role MSCs play in many of the aforementioned clinical trials. However, this purported ability to avoid rejection remains controversial, with some studies showing rejection in allogenic settings and others showing tolerance, and a selection showing rejection when MSCs begin to differentiate (see review by Griffin et al. [49]). In one study, it was shown that when allogeneic rat MSCs were combined with ceramics and implanted subcutaneously to promote osteoblast differentiation, the MSCs elicited an immune response and were rejected [50], but the MSCs were able to form bone in the ceramic if the host rats were administered an immunosuppressive drug (FK-506). In a rat cardiac study, it was also shown that transplanted MSCs expressing a cardiac phenotype were responsible for the induction of a host immune response and subsequent rejection [51]. In another study, it was also shown that MSCs are unable to avoid detection by the innate immune system and that cell culture conditions alone may impart a change in MSCs that allows innate recognition of autotransplanted MSCs [52]. This rejection issue is an important aspect of developing effective therapies because if most or all of the MSCs are rejected, then the treatment may not be as effective or long lasting. However, if allogeneic MSCs are well tolerated, it would be easier and less expensive to use banked allogeneic MSCs than it would be to use autologous MSCs. If MSCs are rejected after they express class II MHC markers, it does not preclude the use of allogeneic MSCs in cases where MSCs are not expected to differentiate. In fact, many studies have shown that allogeneic MSCs are well tolerated in people, and many of the positive results observed in various clinical trials have come from patients transplanted with allogeneic MSCs (reviewed by Millard and Fisk [12]). However, it may be that, in many studies, the observed therapeutic effects do not require long-term engraftment. In a study examining the long-term engraftment of allotransplanted MSCs in deceased patients having received MSC infusions, it was shown that only small numbers, if any, of the infused MSCs were detectable [53]. This observation has led to the proposal that some MSC therapeutic effects are essentially "hit and run" phenomena. The fact that MSCs often do not engraft seems a likely explanation for why many MSC therapies are marginally or only transiently effective. Indeed, it could be speculated that the initial improvement in cardiac function seen at a 6-month time point in the BOOST clinical trial, that had disappeared by the 18-month time point, could have been extended with improved engraftment [54]. Clinically, if MSCs were to be used in conditions where they might need to differentiate in order to achieve a therapeutic effect or need to be engrafted, the use of autologous MSCs is a preferred option. Whether MSCs are immunomodulatory or used as an autograft, there is the critical issue of effectively delivering them to the site of action and, ideally, enabling engraftment.

3. MSCs, Pericytes, and Tissue Repair

At sites of injury, it has been established that most, if not all, MSCs are derived from perivascular mesenchymal cells, pericytes, that are on the tissue side of blood vessels and sinusoids [55, 56]. This location has been identified in MSCs derived from bone marrow and dental pulp [57], brain [58], umbilical cord [59], adipose tissue [60, 61], and liver [62]. Whether all pericytes are MSCs or whether MSCs are the bone marrow-derived subset of pericytes is debatable since "pericytes" or "MSCs" isolated from different organs of the body can display markedly different differentiation potentials, such as pulp-derived pericytes/MSCs displaying odontoblastic potential [63], while marrow-derived pericyte/MSCs have not shown an odontoblastic phenotype. The argument is that if all pericytes were MSCs, then all pericytes should have equivalent differentiation potentials. Alternatively, it has been proposed that pericytes constitute a reservoir of tissue-specific progenitor cells [64], of which classically defined MSCs may only be a subset.

Regardless of their designation as either pericytes or MSCs, it has been proposed that, during injury, blood vessels break or become inflamed and the pericytes are liberated from their perivascular tethers [65]. These released pericytes become activated and function to modulate the local immune environment and establish a zone of tissue regeneration. It is apparent, in some cases, that this release is a local effect and there is little cell recruitment from uninjured tissue [66]. There are, however, a number of publications that provide evidence that MSCs home to sites of inflammation or tissue injury when infused into living organisms. Thus, it can be inferred that in some injured tissues, MSCs may have an intrinsic affinity for the sites of tissue injury. Several studies have shown that MSCs respond to chemokines, such as SDF-1 [67], MCP-3 [68], CXCL9, CXCL16, CCL20, CCL25 [69], and HGF [70], which can either act locally or recruit MSCs from the bloodstream (the issue of systemic MSC mobilization will not be discussed further here).

The injected or naturally released MSCs are activated by the local microenvironment and respond to these cues by secreting a site-specific array of bioactive molecules. These molecules act to immunomodulate the MSC microenvironment, reduce inflammation, and establish a regenerative milieu. We would further assert that these MSCs are geared to function in the repair of these compromised vessels. Indeed, MSCs are capable not only of stimulating angiogenesis

in injured muscle by secreting large amounts of vascular endothelial growth factor that attracts vascular progenitors and is cytoprotective [71], but also of stabilizing newly formed capillaries [72] by assuming perivascular positions embedded in the basement membranes of newly forming blood vessels.

4. MSC Delivery and Biodistribution

There are two principal methods to introduce cells into the body: local delivery into the tissue and systemic delivery. Local delivery can be further defined by the specific type of delivery, either cells embedded in a scaffold (for review see Arthur et al. [73]) or local injection, for example intraperitoneal (IP), intramuscular, or intracardiac injection. Systemic delivery can be further defined by the vascular route, venous (IV) or arterial (IA). The optimal method of delivery will depend on which mechanism of action of the MSC is being utilized. This review will concentrate on the distribution of injected cells.

Having defined some of the characteristics and functions of MSCs, the question then becomes whether or not MSCs perform best when present at the site of injury/inflammation. If MSCs can exert their effect distally, for example, by secreting cytokines into the circulation [6, 13, 38], then it may not be necessary for the cells to be located at the specific injury site and systemic effects could be achieved using a cell reservoir. For example, when MSCs were injected IP, they were able to prevent the damage caused by collagen-induced arthritis, despite the lack of a detectable presence in the arthritic joints [74]. If, however, MSCs need to be present at the site of injury, for example, by differentiating into replacement cells, as in the treatment of osteogenesis imperfecta (OI) [75] or by the local production of antiapoptotic or angiogenic factors [6], then the delivery system must place cells at, or allow MSCs to migrate to, the site of injury.

Arguments for local injection include not only delivering MSCs to the site of the lesion, but also the possibility that the MSCs have the capacity to migrate toward injured tissue. For example, when MSCs were injected IP, they were found to migrate toward an inflamed colon [76]. While IP injection is a common systemic delivery route for small molecules, IP injected MSCs [76] and neuroprogenitor cells [77] were not found to migrate to other tissues. However, it is possible that lymphoid access could be achieved through this route, leading to widespread distribution of a subset of the injected cells detected by endpoint PCR [78]. In another example, MSCs were found to migrate toward an ischemic lesion of the brain when injected near the location of the ischemia and appeared, morphologically, to differentiate into microglia [79]. MSCs have also been found to migrate toward tumors *in vivo*; it is hypothesized that tumors mimic a chronic wound [80]. When MSCs were directly injected into the brain, they were found to migrate to glioma cells located on the contralateral hemisphere [81]. The disadvantage of local injection is that it can lead to further tissue damage from the injection bolus [69]. It has also been shown with bone marrow mononuclear cells that, although direct injection increased localization, it did not increase engraftment or survival [82]. Furthermore, there has been little evidence that MSCs can migrate out of local tissues and into the circulatory system, which is problematic if MSCs need to be present in multiple body compartments, or if the injury is systemic.

The alternative method is to deliver the cells intravascularly. With this systemic injection methodology, there remain several hurdles to overcome in order to deliver cells to the target tissue and have them engraft. Intravascular injection has the advantage of being minimally invasive, and it allows for wide distribution of cells throughout the body. The most common method for accessing the circulatory system is IV and is historically the most common method for delivering MSCs. However, cells delivered IV have to first pass through the lungs before they can distribute throughout the body. This presents a major problem with what has been termed the pulmonary "first-pass" effect, which results in significant entrapment of cells [83]. This problem arises because MSCs have an estimated diameter of 20–30 μm [27, 83, 84] and experiments with microspheres have demonstrated that most particles of this size are filtered out by the lungs [83, 85]. While this may be an overestimation of the amount of entrapment, as microspheres are rigid and MSCs can deform, experimental data supports that a large proportion of MSCs are entrapped in the lung following IV administration [27] (Figure 1). Furthermore, it was observed that the number of trapped cells decreased with the administration of a vasodilator [27], lending support to the hypothesis that MSC size is a major contributor to the first-pass effect. In addition to size, it is possible that endothelial cell adhesion molecules contribute to lung entrapment. This hypothesis is supported by evidence showing that when the CD49d receptor was blocked, there was a small, but significant, decrease in the number of cells trapped in the lungs [83]. In a comparison between umbilical cord blood-derived MSCs (UCB-MSCs) and bone marrow-derived MSCs (BM-MSCs), a significant difference was found in the cell surface expression of adhesion molecules (significantly higher CD49f, CD49d, and cMET in UCB-MSCs) and glycolipid carbohydrate epitopes (significantly lower GD2 and SSEA4 in UCB-MSCs), and this cell surface profile correlated with lung clearance rates, with UCB-MSCs exiting the lungs faster than BM-MSCs [86].

While the previous examples were from animal models, it is likely that lung entrapment is also a hindrance to MSCs administered to humans. For example, when MSCs were administered IV into OI patients, less than 1% of the cells were detected in the target organ by PCR [87, 88]. Similarly low MSC engraftment levels were found with IV administration of MSCs to treat GvHD [53], or when co-infused with hematopoietic stem cells (HSCs) to promote HSC engraftment [89]. However, it is difficult to ascertain from these two studies whether lung entrapment, or some other mechanism such as cell death, was the cause of the low engraftment efficiency since the injected cells were not tracked in real time.

There has been some suggestion that MSC entrapment in the lungs itself can potentially be therapeutic. In experiments by Lee et al. [38], MSCs trapped in the lungs were still able to improve cardiac function after a myocardial infarction through the release of the anti-inflammatory protein TSG-6. However, experiments with OI patients were not 100%

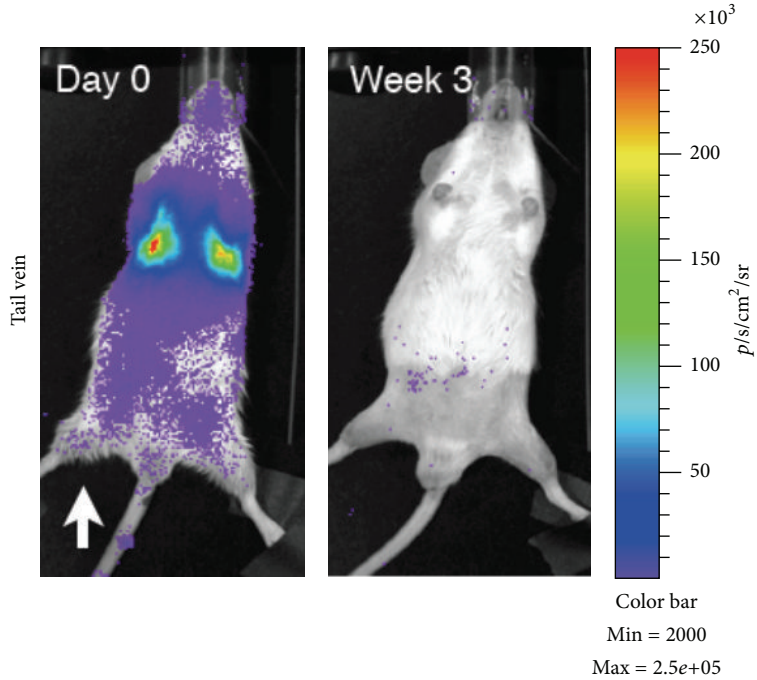

(a)

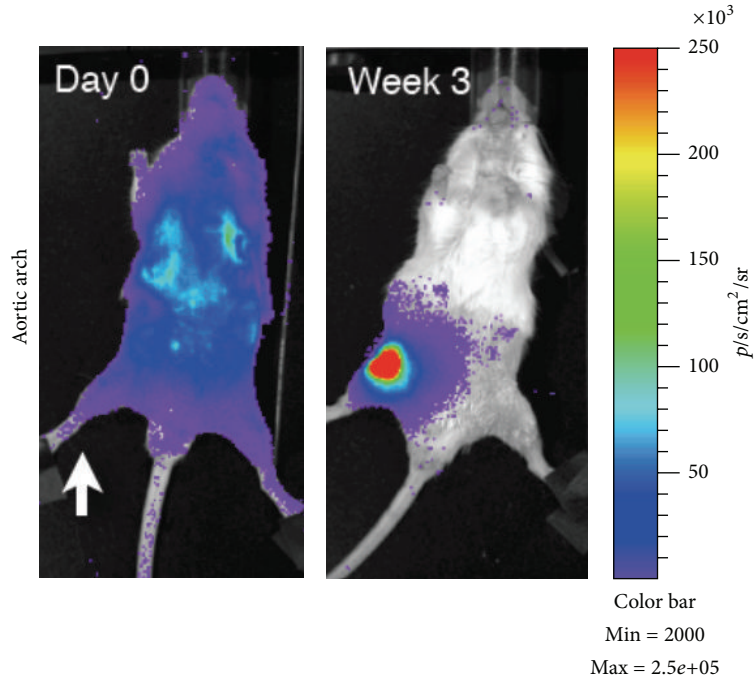

(b)

Figure 1: Comparison of intravenous and intra-arterial cell delivery. Mice were irradiated unilaterally (white arrow) before injection IV (tail vein; a) or IA (aortic arch; b) with 1×10^6 BMC9 MSCs expressing a luciferase reporter.

successful [87], and experiments with IV-delivered MSCs in a mouse model require the use of at least 1×10^6 cells and, more frequently, a dose as high as 5×10^6 cells/mouse to observe any effect. This suggests that in certain circumstances, higher absolute numbers of cells are needed to ensure that a minimum number of cells reach the injury site distal to the lungs. This cell dosing issue has important clinical significance [90], as the vast majority of human clinical trials have been for safety, with efficacy as a secondary endpoint. Little efficacy data has been shown [91] and none reported as yet on clinicaltrials.gov. Across all indications, there is a broad range in the number of cells administered. Of the 276

clinical trials mentioned in our introduction, 59 give a dose per injection per person with a mean of 2.16×10^8 cells/person (1×10^6, 5×10^7, 5×10^9; minimum, median, and maximum, resp.) and 75 give a dose/kg with a mean of 7.24×10^6 cells/kg (1×10^5, 2×10^6, 2×10^8; minimum, median, and maximum, resp.). For instance, Horwitz et al. used a cell dose of 1–5 $\times$ 10^6/kg in treating OI pediatric patients [87], and Le Blanc et al. used a cell dose of 1-2 $\times 10^6$/kg in treating patients with GvHD [92]. Similar to pharmacological studies, in which there is an effective dose (ED) for drug treatment, there is an effective cell dose (ECD) equivalent for cell therapy, which is defined as the minimum cell dose required to discern a significant therapeutic effect. To put this in perspective, a commonly used cell dose of 1×10^6/30 g mouse would be equivalent to 33 $\times$ 10^6/kg or approximately 2.3 billion cells for a 70 kg human. This number is technically and operationally challenging, and most MSC therapies, as part of ongoing clinical trials in humans, use significantly lower cell doses.

Arterial delivery has the potential to alleviate some of these dosing limitations. In theory, arterial delivery allows the cells to bypass the lungs at least once and thus avoid the pulmonary first-pass effect. This venous versus arterial effect has long been recognized in other model systems. For example, to obtain bone engraftment of melanoma cells, tumor cells were injected into the arterial system [93]. If delivered IV, tumor engraftment was primarily seen only in the lungs. Other groups have attempted a similar tactic to deliver MSCs with similar results. For example, Tögel et al. [94, 95] found increased numbers of IA-infused MSCs in kidneys in an acute kidney injury model after 24 h. This was also true in another study: when MSCs were infused IA in a model of acute stroke, it resulted in enhanced cerebral MSC engraftment [96].

Our experiments with delivering MSCs into the arterial system by injection into the aortic arch or tail vein support this "first-pass" cell delivery hypothesis. In this study designed to test for homing to injured tissue, mice were injured prior to injection by irradiating only one leg and were then injected with MSCs transduced with a luciferase reporter gene and the signal tracked over time. As expected, MSCs showed significant entrapment in the lungs when delivered IV into the tail vein. However, when delivered IA through the aortic arch, the cells were more evenly distributed throughout the entire animal (Figure 1). Over time, there was evidence of engraftment of the MSCs at the injury site and not at the contralateral, noninjured leg in the arterial-delivered groups. In the tail vein-injected group, the cells dissipated from the animal after a few days and were undetectable one week after injection.

In a separate set of studies, we were able to decrease the ECD to 2.5×10^5 cells/200 μL/mouse (fourfold $\leq$ original dose), by simply switching from IV to IA delivery (unpublished results). This has important consequences. First, there is concern with cell therapies of creating a cell embolus, even with IA delivery, that could potentially lead to increased mortality [96–98]. These concerns depend on both the concentration and rate of cell delivery [97]. We, and others [99], have found pulmonary emboli and increased mortality in IV-delivered animals at higher cell dose/flow rate. In particular, concentrations above 1.0×10^7 cells/mL by IV administration in mice lead to insufficient dilution of the cells in the blood, resulting in occlusion in the first capillary bed that is encountered (i.e., pulmonary embolism) and a significant increase in mortality. IA delivery is capable of decreasing the dose necessary, administers into a higher flow rate causing greater dilution, and thus decreases the potential risk of cellular embolism. Furthermore, for clinical applications, this reduction in cell dosage translates into a cell dose of ~8×10^6/kg for an average human which is much more feasible than the 33×10^6/kg ECD calculated previously. It should be noted that, while this dose is within the realm of possibility for pediatric patients, this still equates to ~560×10^6 MSCs/70 kg adult, which remains a challenge clinically. As a consequence, further improvements to MSC engraftment are needed.

5. Cell Targeting Strategies

Although there are numerous reports of stem cells homing to injured tissue, the mechanisms have yet to be elucidated and could be heavily reliant on the leaky vasculature found in injured [100, 101] or tumor tissue [102] resulting in passive entrapment in the interstitial space. It is also evident that any endogenous homing is insufficient, with less than 1% of delivered cells being found in target tissues [103]. With this in mind, we now review various methods that have been employed to enhance site-specific delivery using cell surface ligands.

5.1. Targeting Approaches. As with the application of ligand-directed techniques to drug therapies [104], there are a variety of mechanisms which are being investigated to enhance endogenous cell homing. In contrast to synthetic molecules, the cell represents a much more complex and dynamic environment, conferring both advantages and disadvantages. On the positive side, cells are a self-contained manufacturing plant capable of synthesizing therapeutic molecules, sensing the environment, and responding to signals orchestrating regeneration or repair. On the negative side, cells are a difficult product to characterize; more expensive to produce; have nonspecific or unwanted cell-cell interactions; and can internalize targeting ligands applied to the cell surface. The targeting approaches described in the following section are categorized as antibody-, genetically-, selectin-, and peptide-directed cell therapies. For further review of cell surface modification strategies see Stephan and Irvine [105].

5.2. Antibody-Directed Cell Therapy. Antibodies are highly specific ligands with excellent affinity for their antigen. Antibodies have, therefore, found application in producing the first approved ligand-targeted therapeutic, gemtuzumab ozogamicin, an anti-CD33 monoclonal drug conjugate for the treatment of myeloid leukemia [106, 107]. It should be noted that the FDA withdrew approval due to safety concerns in 2010, but clinical trials continue, and the European Medicines Agency has given it an orphan designation (EU/3/00/005).

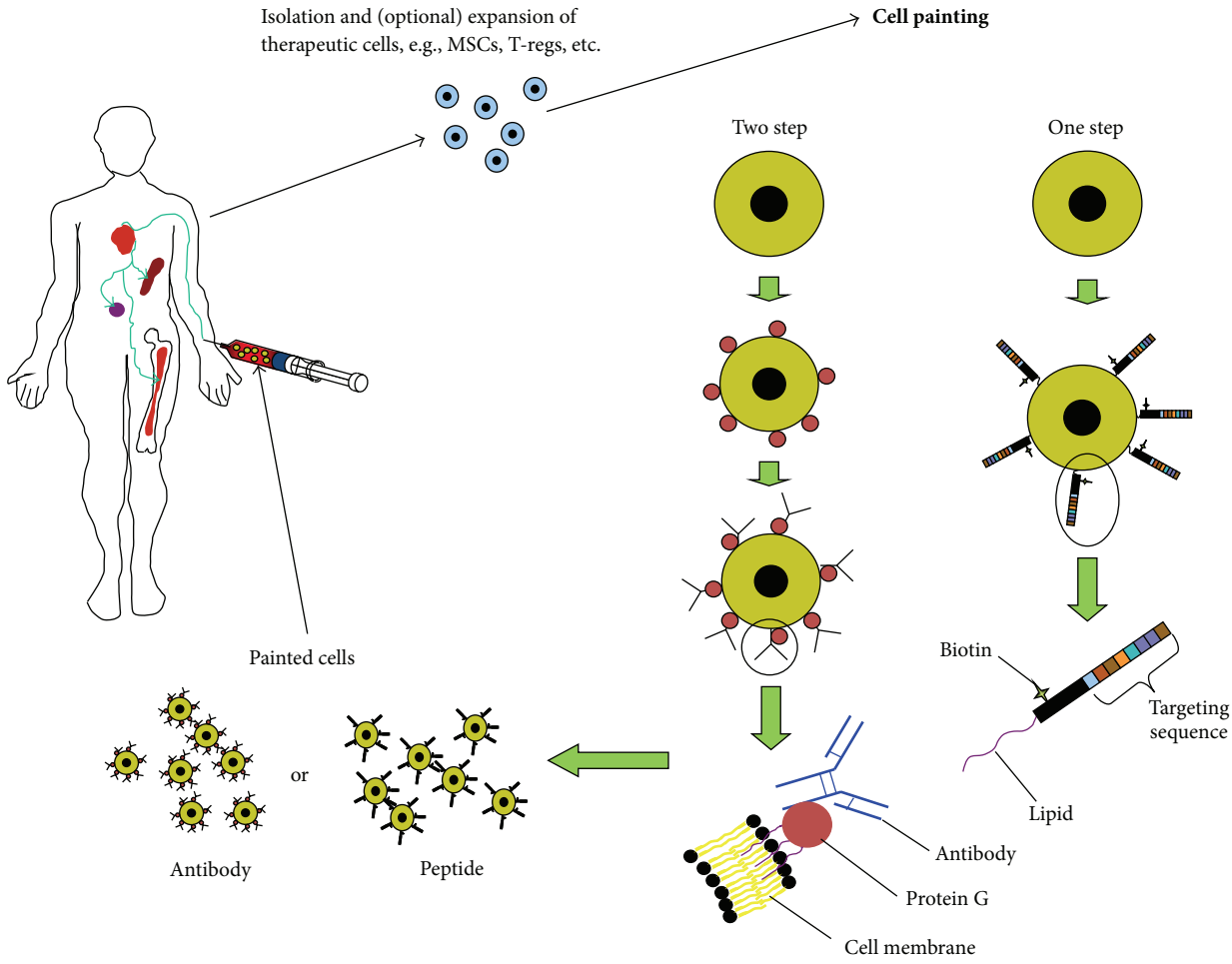

Figure 2: Antibody- and peptide-based cell painting. Therapeutic cells are harvested and "painted" either by a two-step process where the cells are first coated with lipidated protein A (or G) and then incubated with targeting antibody, or a one-step process where the cells are coated with a peptide-targeting molecule that contains a lipid moiety. The coated cells are then reintroduced into the patient where the cells are directed towards specific tissues or organs.

Other antibody-drug conjugates have progressed through phase III clinical trials with positive results, for example, trastuzumab emtansine, an anti-human epidermal growth factor receptor 2-targeted taxane to treat breast cancer [108], which has recently gained FDA approval (Feb. 2013). This same antibody targeting rationale has been applied to the delivery of stem cells. Two methods of antibody attachment to the cell surface have been investigated: the use of lipidated protein-G followed by antibody incubation [109–111] and bispecific antibodies [112–114].

Lipidation has been investigated using palmitated protein A [115] and palmitated protein-G (PPG) [109–111], both of which bind to the Fc domain of antibodies with high affinity, but with differing selectivity based on the immunoglobulin subtypes and species in which the immunoglobulin was raised. This process has been termed "cell painting" [116] and is outlined in Figure 2 [111]. In these studies, we achieved increased cartilage progenitor cell numbers in a cartilage defect with PPG antibody-painted cells over unpainted controls [111]. In more recent work, we have shown that anti-intercellular adhesion molecule-1 (ICAM-1) and anti-vascular cell adhesion molecule-1 (VCAM-1) antibodies can be used to increase cell adherence in antigen-coated plates and in human vascular endothelial cell monolayers stimulated to express ICAM-1 with TNFα. This increase in attached cells is even more apparent when cells are subjected to shear at physiological levels [109]. Cells, in these examples, MSCs, are first coated with PPG by incubating with a physiological buffer containing PPG which intercalates into the phospholipid bilayer of the cell. They are then rinsed and incubated with antibody, rinsed, and injected. This work was then translated to an *in vivo* application where MSCs were targeted to mucosal vascular addressin cell adhesion molecule (MAdCAM) and VCAM in a dextran sodium sulfate-induced inflammatory bowel model, resulting in a significant improvement in survival [110].

An alternative strategy is the use of bispecific antibodies, whereby an antibody targeting the region of interest is conjugated to an antibody against a ligand expressed on the surface of the cell being delivered. This bispecific antibody approach

has been used to target HSCs to damaged vasculature in the heart, using either anti-VCAM-1 conjugated to anti-c-kit [113] or anti-CD45-anti-myosin light chain kinase [112]. This method has also been used in the field of cancer therapy to direct activated T-cells to human epidermal growth factor receptor-2^+ tumor cells *in vitro* [117]. This cancer treatment was tested *in vivo,* yielding reduced tumor size and a significantly increased rate of survival [118]. *In vitro,* a recent report describes the use of an anti-CD90/anti-myosin light chain kinase to bind MSCs and increase their resistance to shear in a parallel plate assay [119].

Of the two antibody-directed cell therapy methods, lipidated protein-G followed by antibody incubation offers the more versatile approach and has been used successfully with MSCs. The same coating technique could, in theory, be applied to any cell type. It is also possible to use multiple antibodies at once [111] and at a higher cell coating density than that achievable with bispecific antibodies because of the limited number of cell surface ligands. Lipidated proteins can also be used to bind other Fc-conjugated ligands; Chen et al. [116] conjugated B7-1 to the Fc portion of human IgG and used it as a co-stimulator. To our knowledge, bispecific antibodies have not been used with an *in vivo* MSC therapy, perhaps because MSCs do not have a cell-specific antibody marker, although any surface-expressed antigen could be utilized. Bispecific antibodies would also have a high cost factor due to difficulties in manufacture and poor stability [120].

5.3. Genetically-Directed Cell Therapy. Genetically-directed cell therapy is defined as the introduction of genetic material into a cell, either DNA- or RNA-based, to express a ligand on the cell surface that will increase its localization in the target tissue. Genetically overexpressing receptor ligands has great potential, but has the additional hurdles of cell transfection (efficiency, timing, stability, immunogenicity, deleterious effects on cell viability, oncogenic integration sites, and consistent activity), and the regulatory problems associated with delivering both a gene- and cell-therapy. If these issues are overcome, it could be a powerful tool to achieve higher efficacy in cell therapies. Within the MSC targeting field, there have been positive results in cardiac-targeted cells directed using the CXCR4 ligand to induce MSCs to home toward the chemokine SDF1 [121, 122]. Both Cheng et al. [121] and Zhang et al. [122] found increased homing of CXCR4-transduced MSCs to infarcted hearts and improved cardiac output, with Zhang et al. also reporting increased angiogenesis within the infarcted area. Cho et al. found that increasing the expression of CXCR4 also aided in the prevention of bone loss in an ovariectomized mouse model, potentiating the effect of an increased expression of RANK ligand [123]. Another study showed increased homing of CXCR4-transduced C3H10T1/2 cells toward bone marrow along with an increased bone mass in steroid-induced osteoporotic mice, along with complete restoration of bone mass in CXCR4- Cbfa1(RUNX2)-cotransduced cells [124]. Outside of MSC therapy, T-cells have been targeted for anticancer therapy using CD19 [125]. Genetically-modified T-cells have progressed to the clinic with mixed results (for review see [126]).

5.4. Selectin-Directed Cell Therapy. Selectin-directed cell targeting was pioneered by Xia et al. [127] who, using α-1,3-fucosyltransferase, modified the surface of $CD34^+$ cord blood cells and found increased engraftment in NOD/SCID mice. Sackstein et al. [128] applied this technique to modify the cell surface of MSCs, to form HCELL, an E-selectin and L-selectin binding ligand. The use of selectins mimics the natural process of endogenous lymphocyte extravasation. In this process, activated endothelial cells express ligands for selectins, which are endogenously present on lymphocytes, causing them to bind to the endothelium and roll, followed by firm adherence and extravasation [129]. When CD44 on human MSCs was modified to produce the HCELL moiety and injected into immunocompromised mice, the MSCs were observed by intravital microscopy in the calvaria of mice where they extravasated [128]. Sarkar et al. avoided enzymatic modification of the cell surface through two methods: one, biotinylation of cell surface proteins followed by incubation with streptavidin and biotin-conjugated sialyl lewis x (slex), a P-selectin ligand [130, 131], and two, liposome surface modification with biotin-conjugated lipids then incubation with streptavidin and biotin-conjugated slex [132]. It is unclear what benefit Sarkar et al. gained from the more recent liposome method, but it is unlikely that either method would have the same intracellular signaling cascade [133] as that achieved with the enzymatic modification method of Sackstein et al. [128]. Although *in vivo* imaging of selectin-targeted MSCs has been demonstrated by both groups, neither has demonstrated efficacy in a disease model.

5.5. Peptide-Directed Cell Therapy. To our knowledge, we are the only group, to date, that has investigated peptide-directed cell therapy. There has, however, been considerable interest in peptide-targeted drugs for some time, especially in the field of anticancer therapies [134]. Targeting peptides can be derived from endogenous binding proteins, or novel ligands can be identified by combinatorial chemistry libraries or using phage display [134]. Phage display is a powerful method where *in vivo* biopanning experiments can be performed to isolate tissue-specific peptides [135, 136]. This phage display method was utilized by our group with a limited phage "play-off" screen, where several previously identified binding phage peptides were analyzed for their ability to bind to infarcted myocardial tissue [137]. The most successful of these peptides were then synthesized as lipidated derivatives and used to coat MSCs, these were then systemically injected via the left ventricle of MI/reperfusion mice and achieved greater MSC numbers in all peptide-targeted groups than with uncoated MSCs (Figure 3) [137]. However, this increased binding to cardiac tissue was not seen in a permanent ligation model (unpublished results). Peptide-based delivery has several advantages over antibody-, gene-, or selectin-directed techniques: peptide manufacture is scalable, and the products have high purity and are relatively inexpensive to produce. Ligands can be highly specific for tissues or

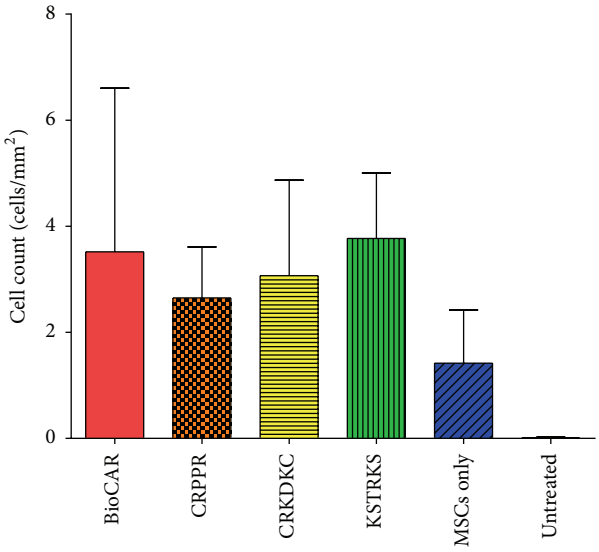

Figure 3: Cell localization in myocardial tissue. Increased cell numbers were found in peptide-targeted (BioCAR, CRPPR, CRKDKC, and KSTRKS) MSCs than in untargeted MSCs (MSCs only). Means of $n \geq 3 \pm$ S.D. Total targeted versus untargeted means are 3.1 versus 1.4, $P < 0.05$ one tailed Student's t-test.

cells of interest and multiple ligands can be attached to the cell surface or drug delivery vehicle. However, in contrast to antibody-based therapies, no peptide-targeted therapeutic has yet made it to market [138].

6. Summary

MSCs are currently being used in clinical trials for the treatment of a range of diseases, with varying degrees of efficacy. At this point, there is no study that we know of that has demonstrated efficient long-term engraftment of MSCs, whether locally or systemically injected, and it is hypothesized that the therapeutic efficacy of delivered MSCs will increase dramatically if MSCs can be made to engraft more efficiently by directing them to the site(s) of the lesion(s) to be treated. The loss of locally injected cells can be attributed to wash out, cell death, and, perhaps, rejection via the innate immune system or, if the MSCs begin to differentiate, they may become targets of the adaptive immune system. For systemic delivery, IV delivery is the most common mode of introduction. At the same time, IV infusion has been shown to result in the entrapment of MSCs in the lung, if only temporarily, which negatively impacts engraftment, and several studies have shown that IA injection is a more effective means of delivering MSCs. Methods to more effectively target MSCs to tissues and organs are being developed, including the coating of cells with antibodies or peptides, modifying native cell surface molecules into endothelium-binding molecules, genetic modification, or biotinylating cell surface molecules and then coating the cells with streptavidin and biotinylated antibodies. Future improvements in the targeting methodologies combined with IA injection have the potential to increase engraftment and improve therapeutic efficacy while, at the same time, reducing the ECD needed.

References

[1] A. I. Caplan, "Mesenchymal stem cells," *Journal of Orthopaedic Research*, vol. 9, no. 5, pp. 641–650, 1991.

[2] A. J. Friedenstein, "Precursor cells of mechanocytes," *International Review of Cytology*, vol. 47, pp. 327–359, 1976.

[3] J. E. Dennis, A. Merriam, A. Awadallah, J. U. Yoo, B. Johnstone, and A. I. Caplan, "A quadripotential mesenchymal progenitor cell isolated from the marrow of an adult mouse," *Journal of Bone and Mineral Research*, vol. 14, no. 5, pp. 700–709, 1999.

[4] J.-T. Vilquin and P. Rosset, "Mesenchymal stem cells in bone and cartilage repair: current status," *Regenerative Medicine*, vol. 1, no. 4, pp. 589–604, 2006.

[5] F. Veronesi, G. Giavaresi, M. Tschon, V. Borsari, N. Nicoli Aldini, and M. Fini, "Clinical use of bone marrow, bone marrow concentrate, and expanded bone marrow mesenchymal stem cells in cartilage disease," *Stem Cells and Development*, vol. 22, pp. 181–192, 2013.

[6] A. I. Caplan and J. E. Dennis, "Mesenchymal stem cells as trophic mediators," *Journal of Cellular Biochemistry*, vol. 98, no. 5, pp. 1076–1084, 2006.

[7] A. E. Aksu, E. Horibe, J. Sacks et al., "Co-infusion of donor bone marrow with host mesenchymal stem cells treats GVHD and promotes vascularized skin allograft survival in rats," *Clinical Immunology*, vol. 127, no. 3, pp. 348–358, 2008.

[8] K. Le Blanc, F. Frassoni, L. Ball et al., "Mesenchymal stem cells for treatment of steroid-resistant, severe, acute graft-versus-host disease: a phase II study," *The Lancet*, vol. 371, no. 9624, pp. 1579–1586, 2008.

[9] G. Ren, L. Zhang, X. Zhao et al., "Mesenchymal stem cell-mediated immunosuppression occurs via concerted action of chemokines and nitric oxide," *Cell Stem Cell*, vol. 2, no. 2, pp. 141–150, 2008.

[10] L. Bai, D. P. Lennon, V. Eaton et al., "Human bone marrow-derived mesenchymal stem cells induce Th2-polarized immune response and promote endogenous repair in animal models of multiple sclerosis," *GLIA*, vol. 57, no. 11, pp. 1192–1203, 2009.

[11] P. Connick, M. Kolappan, C. Crawley et al., "Autologous mesenchymal stem cells for the treatment of secondary progressive multiple sclerosis: an open-label phase 2a proof-of-concept study," *The Lancet Neurology*, vol. 11, no. 2, pp. 150–156, 2012.

[12] S. M. Millard and N. M. Fisk, "Mesenchymal stem cells for systemic therapy: shotgun approach or magic bullets?" *Bioessays*, vol. 35, pp. 173–182, 2013.

[13] A. I. Caplan and D. Correa, "The MSC: an injury drugstore," *Cell Stem Cell*, vol. 9, no. 1, pp. 11–15, 2011.

[14] E. Gonzalez-Rey, M. A. Gonzalez, N. Varela et al., "Human adipose-derived mesenchymal stem cells reduce inflammatory and T cell responses and induce regulatory T cells in vitro in rheumatoid arthritis," *Annals of the Rheumatic Diseases*, vol. 69, no. 1, pp. 241–248, 2010.

[15] M. B. Mueller and R. S. Tuan, "Functional characterization of hypertrophy in chondrogenesis of human mesenchymal stem cells," *Arthritis and Rheumatism*, vol. 58, no. 5, pp. 1377–1388, 2008.

[16] E. Gerdoni, B. Gallo, S. Casazza et al., "Mesenchymal stem cells effectively modulate pathogenic immune response in experimental autoimmune encephalomyelitis," *Annals of Neurology*, vol. 61, no. 3, pp. 219–227, 2007.

[17] E. Zappia, S. Casazza, E. Pedemonte et al., "Mesenchymal stem cells ameliorate experimental autoimmune encephalomyelitis inducing T-cell anergy," *Blood*, vol. 106, no. 5, pp. 1755–1761, 2005.

[18] R. Abdi, P. Fiorina, C. N. Adra, M. Atkinson, and M. H. Sayegh, "Immunomodulation by mesenchymal stem cells: a potential therapeutic strategy for type 1 diabetes," *Diabetes*, vol. 57, no. 7, pp. 1759–1767, 2008.

[19] V. S. Urbán, J. Kiss, J. Kovács et al., "Mesenchymal stem cells cooperate with bone marrow cells in therapy of diabetes," *Stem Cells*, vol. 26, no. 1, pp. 244–253, 2008.

[20] D. García-Olmo, M. García-Arranz, L. Gómez García et al., "Autologous stem cell transplantation for treatment of recto-vaginal fistula in perinatal Crohn's disease: a new cell-based therapy," *International Journal of Colorectal Disease*, vol. 18, no. 5, pp. 451–454, 2003.

[21] E. Gonzalez-Rey, P. Anderson, M. A. González, L. Rico, D. Büscher, and M. Delgado, "Human adult stem cells derived from adipose tissue protect against experimental colitis and sepsis," *Gut*, vol. 58, no. 7, pp. 929–939, 2009.

[22] Y. Hayashi, S. Tsuji, M. Tsujii et al., "Topical implantation of mesenchymal stem cells has beneficial effects on healing of experimental colitis in rats," *Journal of Pharmacology and Experimental Therapeutics*, vol. 326, no. 2, pp. 523–531, 2008.

[23] T. Yabana, Y. Arimura, H. Tanaka et al., "Enhancing epithelial engraftment of rat mesenchymal stem cells restores epithelial barrier integrity," *Journal of Pathology*, vol. 218, no. 3, pp. 350–359, 2009.

[24] X. Zhang, C. Jiao, and S. Zhao, "Role of mesenchymal stem cells in immunological rejection of organ transplantation," *Stem Cell Reviews and Reports*, vol. 5, no. 4, pp. 402–409, 2010.

[25] J. M. Karp and G. S. Leng Teo, "Mesenchymal stem cell homing: the devil is in the details," *Cell Stem Cell*, vol. 4, no. 3, pp. 206–216, 2009.

[26] P. Lin, Y. Lin, D. P. Lennon, D. Correa, M. Schluchter, and A. I. Caplan, "Efficient lentiviral transduction of human mesenchymal stem cells that preserves proliferation and differentiation capabilities," *Stem Cells Translational Medicine*, vol. 1, pp. 886–897, 2012.

[27] J. Gao, J. E. Dennis, R. F. Muzic, M. Lundberg, and A. I. Caplan, "The dynamic in vivo distribution of bone marrow-derived mesenchymal stem cells after infusion," *Cells Tissues Organs*, vol. 169, no. 1, pp. 12–20, 2001.

[28] M. Srinivas, E. H. J. G. Aarntzen, J. W. M. Bulte et al., "Imaging of cellular therapies," *Advanced Drug Delivery Reviews*, vol. 62, no. 11, pp. 1080–1093, 2010.

[29] M. R. Reagan and D. L. Kaplan, "Concise review: mesenchymal stem cell tumor-homing: detection methods in disease model systems," *Stem Cells*, vol. 29, no. 6, pp. 920–927, 2011.

[30] L. Kostura, D. L. Kraitchman, A. M. Mackay, M. F. Pittenger, and J. M. W. Bulte, "Feridex labeling of mesenchymal stem cells inhibits chondrogenesis but not adipogenesis or osteogenesis," *NMR in Biomedicine*, vol. 17, no. 7, pp. 513–517, 2004.

[31] K. Le Blanc, C. Tammik, K. Rosendahl, E. Zetterberg, and O. Ringdén, "HLA expression and immunologic properties of differentiated and undifferentiated mesenchymal stem cells," *Experimental Hematology*, vol. 31, no. 10, pp. 890–896, 2003.

[32] B. Maitra, E. Szekely, K. Gjini et al., "Human mesenchymal stem cells support unrelated donor hematopoietic stem cells and suppress T-cell activation," *Bone Marrow Transplantation*, vol. 33, no. 6, pp. 597–604, 2004.

[33] W. T. Tse, J. D. Pendleton, W. M. Beyer, M. C. Egalka, and E. C. Guinan, "Suppression of allogeneic T-cell proliferation by human marrow stromal cells: implications in transplantation," *Transplantation*, vol. 75, no. 3, pp. 389–397, 2003.

[34] A. Bartholomew, C. Sturgeon, M. Siatskas et al., "Mesenchymal stem cells suppress lymphocyte proliferation in vitro and prolong skin graft survival in vivo," *Experimental Hematology*, vol. 30, no. 1, pp. 42–48, 2002.

[35] M. Krampera, L. Cosmi, R. Angeli et al., "Role for interferon-γ in the immunomodulatory activity of human bone marrow mesenchymal stem cells," *Stem Cells*, vol. 24, no. 2, pp. 386–398, 2006.

[36] K. English, F. P. Barry, C. P. Field-Corbett, and B. P. Mahon, "IFN-γ and TNF-α differentially regulate immunomodulation by murine mesenchymal stem cells," *Immunology Letters*, vol. 110, no. 2, pp. 91–100, 2007.

[37] J. M. Ryan, F. Barry, J. M. Murphy, and B. P. Mahon, "Interferon-γ does not break, but promotes the immunosuppressive capacity of adult human mesenchymal stem cells," *Clinical and Experimental Immunology*, vol. 149, no. 2, pp. 353–363, 2007.

[38] R. H. Lee, A. A. Pulin, M. J. Seo et al., "Intravenous hMSCs improve myocardial infarction in mice because cells embolized in lung are activated to secrete the anti-inflammatory protein TSG-6," *Cell Stem Cell*, vol. 5, no. 1, pp. 54–63, 2009.

[39] M. Di Nicola, C. Carlo-Stella, M. Magni et al., "Human bone marrow stromal cells suppress T-lymphocyte proliferation induced by cellular or nonspecific mitogenic stimuli," *Blood*, vol. 99, no. 10, pp. 3838–3843, 2002.

[40] L. Cui, Y. Shuo, W. Liu, N. Li, W. Zhang, and Y. Cao, "Expanded adipose-derived stem cells suppress mixed lymphocyte reaction by secretion of prostaglandin E2," *Tissue Engineering*, vol. 13, no. 6, pp. 1185–1195, 2007.

[41] G. Ren, J. Su, L. Zhang et al., "Species variation in the mechanisms of mesenchymal stem cell-mediated immunosuppression," *Stem Cells*, vol. 27, no. 8, pp. 1954–1962, 2009.

[42] K. English, "Mechanisms of mesenchymal stromal cell immunomodulation," *Immunology and Cell Biology*, vol. 91, pp. 19–26, 2013.

[43] F. Liotta, R. Angeli, L. Cosmi et al., "Toll-like receptors 3 and 4 are expressed by human bone marrow-derived mesenchymal stem cells and can inhibit their T-cell modulatory activity by impairing notch signaling," *Stem Cells*, vol. 26, no. 1, pp. 279–289, 2008.

[44] S. L. Brown, T. E. Riehl, M. R. Walker et al., "Myd88-dependent positioning of Ptgs2-expressing stromal cells maintains colonic epithelial proliferation during injury," *Journal of Clinical Investigation*, vol. 117, no. 1, pp. 258–269, 2007.

[45] Y.-P. Li, S. Paczesny, E. Lauret et al., "Human mesenchymal stem cells license adult CD34+ hemopoietic progenitor cells to differentiate into regulatory dendritic cells through activation of the notch pathway," *Journal of Immunology*, vol. 180, no. 3, pp. 1598–1608, 2008.

[46] B. Zhang, R. Liu, D. Shi et al., "Mesenchymal stem cells induce mature dendritic cells into a novel Jagged-2 dependent regulatory dendritic cell population," *Blood*, vol. 113, no. 1, pp. 46–57, 2009.

[47] G. W. Roddy, J. Y. Oh, R. H. Lee et al., "Action at a distance: systemically administered adult stem/progenitor cells (MSCs) reduce inflammatory damage to the cornea without engraftment and primarily by secretion of TNF-α stimulated gene/protein 6," *Stem Cells*, vol. 29, no. 10, pp. 1572–1579, 2011.

[48] H. Choi, R. H. Lee, N. Bazhanov, J. Y. Oh, and D. J. Prockop, "Anti-inflammatory protein TSG-6 secreted by activated MSCs attenuates zymosan-induced mouse peritonitis by decreasing TLR2/NF-κB signaling in resident macrophages," *Blood*, vol. 118, no. 2, pp. 330–338, 2011.

[49] M. D. Griffin, A. E. Ryan, S. Alagesan, P. Lohan, O. Treacy, and T. Ritter, "Anti-donor immune responses elicited by allogeneic mesenchymal stem cells: what have we learned so far?" *Immunology and Cell Biology*, vol. 91, pp. 40–51, 2013.

[50] N. Kotobuki, Y. Katsube, Y. Katou, M. Tadokoro, M. Hirose, and H. Ohgushi, "In vivo survival and osteogenic differentiation of allogeneic rat bone marrow mesenchymal stem cells (MSCs)," *Cell Transplantation*, vol. 17, no. 6, pp. 705–712, 2008.

[51] X.-P. Huang, Z. Sun, Y. Miyagi et al., "Differentiation of allogeneic mesenchymal stem cells induces immunogenicity and limits their long-term benefits for myocardial repair," *Circulation*, vol. 122, no. 23, pp. 2419–2429, 2010.

[52] Y. Li and F. Lin, "Mesenchymal stem cells are injured by complement after their contact with serum," *Blood*, vol. 120, pp. 3436–3443, 2012.

[53] L. von Bahr, I. Batsis, G. Moll et al., "Analysis of tissues following mesenchymal stromal cell therapy in humans indicates limited long-term engraftment and no ectopic tissue formation," *Stem Cells*, vol. 30, pp. 1575–1578, 2012.

[54] G. P. Meyer, K. C. Wollert, J. Lotz et al., "Intracoronary bone marrow cell transfer after myocardial infarction: 5-year follow-up from the randomized-controlled BOOST trial," *European Heart Journal*, vol. 30, no. 24, pp. 2978–2984, 2009.

[55] M. Abedin, Y. Tintut, and L. L. Demer, "Mesenchymal stem cells and the artery wall," *Circulation Research*, vol. 95, no. 7, pp. 671–676, 2004.

[56] M. Crisan, S. Yap, L. Casteilla et al., "A perivascular origin for mesenchymal stem cells in multiple human organs," *Cell Stem Cell*, vol. 3, no. 3, pp. 301–313, 2008.

[57] S. Shi and S. Gronthos, "Perivascular niche of postnatal mesenchymal stem cells in human bone marrow and dental pulp," *Journal of Bone and Mineral Research*, vol. 18, no. 4, pp. 696–704, 2003.

[58] S.-G. Kang, N. Shinojima, A. Hossain et al., "Isolation and perivascular localization of mesenchymal stem cells from mouse brain," *Neurosurgery*, vol. 67, no. 3, pp. 711–720, 2010.

[59] N. Zebardast, D. Lickorish, and J. E. Davies, "Human umbilical cord perivascular cells (HUCPVC): a mesenchymal cell source for dermal wound healing," *Organogenesis*, vol. 6, no. 4, pp. 197–203, 2010.

[60] X. Cai, Y. Lin, P. V. Hauschka, and B. E. Grottkau, "Adipose stem cells originate from perivascular cells," *Biology of the Cell*, vol. 103, no. 9, pp. 435–447, 2011.

[61] A. W. James, J. N. Zara, M. Corselli et al., "An abundant perivascular source of stem cells for bone tissue engineering," *Stem Cells Translational Medicine*, vol. 1, pp. 673–684, 2012.

[62] J. C. Gerlach, P. Over, M. E. Turner et al., "Perivascular mesenchymal progenitors in human fetal and adult liver," *Stem Cells and Development*, vol. 21, pp. 3258–3269, 2012.

[63] S. Gronthos, J. Brahim, W. Li et al., "Stem cell properties of human dental pulp stem cells," *Journal of Dental Research*, vol. 81, no. 8, pp. 531–535, 2002.

[64] P. Bianco, P. G. Robey, and P. J. Simmons, "Mesenchymal stem cells: revisiting history, concepts, and assays," *Cell Stem Cell*, vol. 2, no. 4, pp. 313–319, 2008.

[65] P. Dore-Duffy, C. Owen, R. Balabanov, S. Murphy, T. Beaumont, and J. A. Rafols, "Pericyte migration from the vascular wall in response to traumatic brain injury," *Microvascular Research*, vol. 60, no. 1, pp. 55–69, 2000.

[66] M. A. Maloney, R. A. Lamela, and H. M. Patt, "The question of bone marrow stromal fibroblast traffic," *Annals of the New York Academy of Sciences*, vol. 459, pp. 190–197, 1985.

[67] T. Kitaori, H. Ito, E. M. Schwarz et al., "Stromal cell-derived factor 1/CXCR4 signaling is critical for the recruitment of mesenchymal stem cells to the fracture site during skeletal repair in a mouse model," *Arthritis and Rheumatism*, vol. 60, no. 3, pp. 813–823, 2009.

[68] S. Schenk, N. Mal, A. Finan et al., "Monocyte chemotactic protein-3 is a myocardial mesenchymal stem cell homing factor," *Stem Cells*, vol. 25, no. 1, pp. 245–251, 2007.

[69] G. Chamberlain, H. Smith, G. E. Rainger, and J. Middleton, "Mesenchymal stem cells exhibit firm adhesion, crawling, spreading and transmigration across aortic endothelial cells: effects of chemokines and shear," *PLoS ONE*, vol. 6, no. 9, Article ID e25663, 2011.

[70] M. Iwasaki, M. Koyanagi, H. Kossmann et al., "Hepatocyte growth factor mobilizes non-bone marrow-derived circulating mesoangioblasts," *European Heart Journal*, vol. 32, no. 5, pp. 627–636, 2011.

[71] T. Kinnaird, E. S. Burnett, M. Shou et al., "Local delivery of marrow-derived stromal cells augments collateral perfusion through paracrine mechanisms," *Circulation*, vol. 109, no. 12, pp. 1543–1549, 2004.

[72] M. T. Valarmathi, J. M. Davis, M. J. Yost, R. L. Goodwin, and J. D. Potts, "A three-dimensional model of vasculogenesis," *Biomaterials*, vol. 30, no. 6, pp. 1098–1112, 2009.

[73] A. Arthur, A. Zannettino, and S. Gronthos, "The therapeutic applications of multipotential mesenchymal/stromal stem cells in skeletal tissue repair," *Journal of Cellular Physiology*, vol. 218, no. 2, pp. 237–245, 2009.

[74] A. Augello, R. Tasso, S. M. Negrini, R. Cancedda, and G. Pennesi, "Cell therapy using allogeneic bone marrow mesenchymal stem cells prevents tissue damage in collagen-induced arthritis," *Arthritis and Rheumatism*, vol. 56, no. 4, pp. 1175–1186, 2007.

[75] A. I. Caplan, "Osteogenesis imperfecta, rehabilitation medicine, fundamental research and mesenchymal stem cells," *Connective Tissue Research*, vol. 31, no. 4, pp. S9–S14, 1995.

[76] M. T. L. Castelo-Branco, I. D. P. Soares, D. V. Lopes et al., "Intraperitoneal but not intravenous cryopreserved mesenchymal stromal cells home to the inflamed colon and ameliorate experimental colitis," *PLoS ONE*, vol. 7, no. 3, Article ID e33360, 2012.

[77] Y. Tang, K. Shah, S. M. Messerli, E. Snyder, X. Breakefield, and R. Weissleder, "In vivo tracking of neural progenitor cell migration to glioblastomas," *Human Gene Therapy*, vol. 14, no. 13, pp. 1247–1254, 2003.

[78] T. Wilson, C. Stark, J. Holmbom et al., "Fate of bone marrow-derived stromal cells after intraperitoneal infusion or implantation into femoral bone defects in the host animal," *Journal of Tissue Engineering*, vol. 2010, Article ID 345806, 2010.

[79] A. T. Dinh, N. Kubis, Y. Tomita et al., "In vivo imaging with cellular resolution of bone marrow cells transplanted into the ischemic brain of a mouse," *NeuroImage*, vol. 31, no. 3, pp. 958–967, 2006.

[80] H. F. Dvorak, "Tumors: wounds that do not heal: similarities between tumor stroma generation and wound healing," *New*

England Journal of Medicine, vol. 315, no. 26, pp. 1650–1659, 1986.

[81] K. Nakamura, Y. Ito, Y. Kawano et al., "Antitumor effect of genetically engineered mesenchymal stem cells in a rat glioma model," *Gene Therapy*, vol. 11, no. 14, pp. 1155–1164, 2004.

[82] K. T. Chabner, G. B. Adams, J. Qiu et al., "Direct vascular delivery of primitive hematopoietic cells to bone marrow improves localization but not engraftment," *Blood*, vol. 103, no. 12, pp. 4685–4686, 2004.

[83] U. M. Fischer, M. T. Harting, F. Jimenez et al., "Pulmonary passage is a major obstacle for intravenous stem cell delivery: the pulmonary first-pass effect," *Stem Cells and Development*, vol. 18, no. 5, pp. 683–691, 2009.

[84] I. Sekiya, B. L. Larson, J. R. Smith, R. Pochampally, J.-G. Cui, and D. J. Prockop, "Expansion of human adult stem cells from bone marrow stroma: conditions that maximize the yields of early progenitors and evaluate their quality," *Stem Cells*, vol. 20, no. 6, pp. 530–541, 2002.

[85] S. Schrepfer, T. Deuse, H. Reichenspurner, M. P. Fischbein, R. C. Robbins, and M. P. Pelletier, "Stem cell transplantation: the lung barrier," *Transplantation Proceedings*, vol. 39, no. 2, pp. 573–576, 2007.

[86] J. Nystedt, H. Anderson, J. Tikkanen et al., "Cell surface structures influence lung clearance rate of systemically infused mesenchymal stromal cells," *Stem Cells*, vol. 31, pp. 317–326, 2013.

[87] E. M. Horwitz, P. L. Gordon, W. K. K. Koo et al., "Isolated allogeneic bone marrow-derived mesenchymal cells engraft and stimulate growth in children with osteogenesis imperfecta: implications for cell therapy of bone," *Proceedings of the National Academy of Sciences of the United States of America*, vol. 99, no. 13, pp. 8932–8937, 2002.

[88] E. M. Horwitz, D. J. Prockop, L. A. Fitzpatrick et al., "Transplantability and therapeutic effects of bone marrow-derived mesenchymal cells in children with osteogenesis imperfecta," *Nature Medicine*, vol. 5, no. 3, pp. 309–313, 1999.

[89] L. Fouillard, A. Chapel, D. Bories et al., "Infusion of allogeneic-related HLA mismatched mesenchymal stem cells for the treatment of incomplete engraftment following autologous haematopoietic stem cell transplantation," *Leukemia*, vol. 21, no. 3, pp. 568–570, 2007.

[90] J. Muller-Ehmsen, "The problem is obvious, the solution is not: numbers do matter in cardiac cell therapy!," *Cardiovascular Research*, vol. 96, pp. 208–209, 2012.

[91] J. Ankrum and J. M. Karp, "Mesenchymal stem cell therapy: two steps forward, one step back," *Trends in Molecular Medicine*, vol. 16, no. 5, pp. 203–209, 2010.

[92] K. Le Blanc, I. Rasmusson, B. Sundberg et al., "Treatment of severe acute graft-versus-host disease with third party haploidentical mesenchymal stem cells," *The Lancet*, vol. 363, no. 9419, pp. 1439–1441, 2004.

[93] F. Arguello, R. B. Baggs, and C. N. Frantz, "A murine model of experimental metastasis to bone and bone marrow," *Cancer Research*, vol. 48, no. 23, pp. 6876–6881, 1988.

[94] F. Tögel, Y. Yang, P. Zhang, Z. Hu, and C. Westenfelder, "Bioluminescence imaging to monitor the in vivo distribution of administered mesenchymal stem cells in acute kidney injury," *American Journal of Physiology*, vol. 295, no. 1, pp. F315–F321, 2008.

[95] F. Tögel, Z. Hu, K. Weiss, J. Isaac, C. Lange, and C. Westenfelder, "Administered mesenchymal stem cells protect against ischemic acute renal failure through differentiation-independent mechanisms," *American Journal of Physiology*, vol. 289, no. 1, pp. F31–F42, 2005.

[96] P. Walczak, J. Zhang, A. A. Gilad et al., "Dual-modality monitoring of targeted intraarterial delivery of mesenchymal stem cells after transient ischemia," *Stroke*, vol. 39, no. 5, pp. 1569–1574, 2008.

[97] M. Janowski, A. Lyczek, C. Engels et al., "Cell size and velocity of injection are major determinants of the safety of intracarotid stem cell transplantation," *Journal of Cerebral Blood Flow and Metabolism*, vol. 33, pp. 921–927, 2013.

[98] L. Li, Q. Jiang, G. Ding et al., "Effects of administration route on migration and distribution of neural progenitor cells transplanted into rats with focal cerebral ischemia, an MRI study," *Journal of Cerebral Blood Flow and Metabolism*, vol. 30, no. 3, pp. 653–662, 2010.

[99] C. Kyriakou, N. Rabin, A. Pizzey, A. Nathwani, and K. Yong, "Factors that influence short-term homing of human bone marrow-derived mesenchymal stem cells in a xenogeneic animal model," *Haematologica*, vol. 93, no. 10, pp. 1457–1465, 2008.

[100] A. Fleck, G. Raines, F. Hawker et al., "Increased vascular permeability: a major cause of hypoalbuminaemia in disease and injury," *The Lancet*, vol. 1, no. 8432, pp. 781–784, 1985.

[101] L. F. Brown, K.-T. Yeo, B. Berse et al., "Expression of vascular permeability factor (vascular endothelial growth factor) by epidermal keratinocytes during wound healing," *Journal of Experimental Medicine*, vol. 176, no. 5, pp. 1375–1379, 1992.

[102] H. Maeda, J. Wu, T. Sawa, Y. Matsumura, and K. Hori, "Tumor vascular permeability and the EPR effect in macromolecular therapeutics: a review," *Journal of Controlled Release*, vol. 65, no. 1-2, pp. 271–284, 2000.

[103] D. J. Prockop, "Repair of tissues by adult stem/progenitor cells (MSCs): controversies, myths, and changing paradigms," *Molecular Therapy*, vol. 17, no. 6, pp. 939–946, 2009.

[104] V. P. Torchilin, "Multifunctional nanocarriers," *Advanced Drug Delivery Reviews*, vol. 58, no. 14, pp. 1532–1555, 2006.

[105] M. T. Stephan and D. J. Irvine, "Enhancing cell therapies from the outside in: cell surface engineering using synthetic nanomaterials," *Nano Today*, vol. 6, no. 3, pp. 309–325, 2011.

[106] A. K. Burnett, "Treatment of acute myeloid leukemia: are we making progress?" *Hematology/The Education Program of the American Society of Hematology*, vol. 2012, pp. 1–6, 2012.

[107] R. A. Larson, M. Boogaerts, E. Estey et al., "Antibody-targeted chemotherapy of older patients with acute myeloid leukemia in first relapse using Mylotarg (gemtuzumab ozogamicin)," *Leukemia*, vol. 16, no. 9, pp. 1627–1636, 2002.

[108] S. Verma, D. Miles, L. Gianni et al., "Trastuzumab emtansine for HER2-positive advanced breast cancer," *New England Journal of Medicine*, vol. 367, pp. 1783–1791, 2012.

[109] I. K. Ko, T. J. Kean, and J. E. Dennis, "Targeting mesenchymal stem cells to activated endothelial cells," *Biomaterials*, vol. 30, no. 22, pp. 3702–3710, 2009.

[110] I. K. Ko, B.-G. Kim, A. Awadallah et al., "Targeting improves MSC treatment of inflammatory bowel disease," *Molecular Therapy*, vol. 18, no. 7, pp. 1365–1372, 2010.

[111] J. E. Dennis, N. Cohen, V. M. Goldberg, and A. I. Caplan, "Targeted delivery of progenitor cells for cartilage repair," *Journal of Orthopaedic Research*, vol. 22, no. 4, pp. 735–741, 2004.

[112] R. J. Lee, Q. Fang, P. A. Davol et al., "Antibody targeting of stem cells to infarcted myocardium," *Stem Cells*, vol. 25, no. 3, pp. 712–717, 2007.

[113] L. G. Lum, H. Fok, R. Sievers, M. Abedi, P. J. Quesenberry, and R. J. Lee, "Targeting of Lin-Sca+ hematopoietic stem cells with bispecific antibodies to injured myocardium," *Blood Cells, Molecules, and Diseases*, vol. 32, no. 1, pp. 82–87, 2004.

[114] T. C. Zhao, A. Tseng, N. Yano et al., "Targeting human CD34+ hematopoietic stem cells with anti-CD45 X anti-myosin light-chain bispecific antibody preserves cardiac function in myocardial infarction," *Journal of Applied Physiology*, vol. 104, no. 6, pp. 1793–1800, 2008.

[115] S. A. Kim and J. S. Peacock, "The use of palmitate-conjugated protein A for coating cells with artificial receptors which facilitate intercellular interactions," *Journal of Immunological Methods*, vol. 158, no. 1, pp. 57–65, 1993.

[116] A. Chen, G. Zheng, and M. L. Tykocinski, "Hierarchical costimulator thresholds for distinct immune responses: application of a novel two-step Fc fusion protein transfer method," *Journal of Immunology*, vol. 164, no. 2, pp. 705–711, 2000.

[117] M. Sen, D. M. Wankowski, N. K. Garlie et al., "Use of anti-CD3 × anti-HER2/neu bispecific antibody for redirecting cytotoxicity of activated T cells toward HER2/neu+ tumors," *Journal of Hematotherapy and Stem Cell Research*, vol. 10, no. 2, pp. 247–260, 2001.

[118] J. K. Chan, C. A. Hamilton, M. K. Cheung et al., "Enhanced killing of primary ovarian cancer by retargeting autologous cytokine-induced killer cells with bispecific antibodies: a preclinical study," *Clinical Cancer Research*, vol. 12, no. 6, pp. 1859–1867, 2006.

[119] C. W. Gundlach IV, A. Caivano, M. Da Graca Cabreira-Hansen et al., "Synthesis and evaluation of an anti-MLC1 × anti-CD90 bispecific antibody for targeting and retaining bone-marrow-derived multipotent stromal cells in infarcted myocardium," *Bioconjugate Chemistry*, vol. 22, no. 8, pp. 1706–1714, 2011.

[120] V. R. Doppalapudi, J. Huang, D. Liu et al., "Chemical generation of bispecific antibodies," *Proceedings of the National Academy of Sciences of the United States of America*, vol. 107, no. 52, pp. 22611–22616, 2010.

[121] Z. Cheng, L. Ou, X. Zhou et al., "Targeted migration of mesenchymal stem cells modified with CXCR4 gene to infarcted myocardium improves cardiac performance," *Molecular Therapy*, vol. 16, no. 3, pp. 571–579, 2008.

[122] D. Zhang, G.-C. Fan, X. Zhou et al., "Over-expression of CXCR4 on mesenchymal stem cells augments myoangiogenesis in the infarcted myocardium," *Journal of Molecular and Cellular Cardiology*, vol. 44, no. 2, pp. 281–292, 2008.

[123] S. W. Cho, H. J. Sun, J.-Y. Yang et al., "Transplantation of mesenchymal stem cells overexpressing RANK-Fc or CXCR4 prevents bone loss in ovariectomized mice," *Molecular Therapy*, vol. 17, no. 11, pp. 1979–1987, 2009.

[124] C.-Y. Lien, K. C.-Y. Ho, O. K. Lee, G. W. Blunn, and Y. Su, "Restoration of bone mass and strength in glucocorticoid-treated mice by systemic transplantation of CXCR4 and Cbfa-1 co-expressing mesenchymal stem cells," *Journal of Bone and Mineral Research*, vol. 24, no. 5, pp. 837–848, 2009.

[125] J. N. Kochenderfer, W. H. Wilson, J. E. Janik et al., "Eradication of B-lineage cells and regression of lymphoma in a patient treated with autologous T cells genetically engineered to recognize CD19," *Blood*, vol. 116, no. 20, pp. 4099–4102, 2010.

[126] T. S. Park, S. A. Rosenberg, and R. A. Morgan, "Treating cancer with genetically engineered T cells," *Trends in Biotechnology*, vol. 29, no. 11, pp. 550–557, 2011.

[127] L. Xia, J. M. McDaniel, T. Yago, A. Doeden, and R. P. McEver, "Surface fucosylation of human cord blood cells augments binding to P-selectin and E-selectin and enhances engraftment in bone marrow," *Blood*, vol. 104, no. 10, pp. 3091–3096, 2004.

[128] R. Sackstein, J. S. Merzaban, D. W. Cain et al., "Ex vivo glycan engineering of CD44 programs human multipotent mesenchymal stromal cell trafficking to bone," *Nature Medicine*, vol. 14, no. 2, pp. 181–187, 2008.

[129] A. E. Aplin, A. Howe, S. K. Alahari, and R. L. Juliano, "Signal transduction and signal modulation by cell adhesion receptors: the role of integrins, cadherins, immunoglobulin-cell adhesion molecules, and selectins," *Pharmacological Reviews*, vol. 50, no. 2, pp. 197–263, 1998.

[130] D. Sarkar, P. K. Vemula, G. S. L. Teo et al., "Chemical engineering of mesenchymal stem cells to induce a cell rolling response," *Bioconjugate Chemistry*, vol. 19, no. 11, pp. 2105–2109, 2008.

[131] D. Sarkar, J. A. Spencer, J. A. Phillips et al., "Engineered cell homing," *Blood*, vol. 118, no. 25, pp. e184–e191, 2011.

[132] D. Sarkar, P. K. Vemula, W. Zhao, A. Gupta, R. Karnik, and J. M. Karp, "Engineered mesenchymal stem cells with self-assembled vesicles for systemic cell targeting," *Biomaterials*, vol. 31, no. 19, pp. 5266–5274, 2010.

[133] E. Crockett-Torabi, "Selectins and mechanisms of signal transduction," *Journal of Leukocyte Biology*, vol. 63, no. 1, pp. 1–14, 1998.

[134] M. Shadidi and M. Sioud, "Selective targeting of cancer cells using synthetic peptides," *Drug Resistance Updates*, vol. 6, no. 6, pp. 363–371, 2003.

[135] E. Ruoslahti, "Vascular zip codes in angiogenesis and metastasis," *Biochemical Society Transactions*, vol. 32, no. 3, pp. 397–402, 2004.

[136] E. Ruoslahti, S. N. Bhatia, and M. J. Sailor, "Targeting of drugs and nanoparticles to tumors," *Journal of Cell Biology*, vol. 188, no. 6, pp. 759–768, 2010.

[137] T. J. Kean, L. Duesler, R. G. Young et al., "Development of a peptide-targeted, myocardial ischemia-homing, mesenchymal stem cell," *Journal of Drug Targeting*, vol. 20, no. 1, pp. 23–32, 2012.

[138] S. Majumdar and T. J. Siahaan, "Peptide-mediated targeted drug delivery," *Medicinal Research Reviews*, vol. 32, no. 3, pp. 637–658, 2012.

Hindawi Publishing Corporation
Stem Cells International
Volume 2013, Article ID 435093, 7 pages
http://dx.doi.org/10.1155/2013/435093

Review Article

From Blood to the Brain: Can Systemically Transplanted Mesenchymal Stem Cells Cross the Blood-Brain Barrier?

Linan Liu,[1,2] Mark A. Eckert,[1,2] Hamidreza Riazifar,[1,2] Dong-Ku Kang,[1,2] Dritan Agalliu,[3] and Weian Zhao[1,2]

[1] *Department of Pharmaceutical Sciences, Sue and Bill Gross Stem Cell Research Center and Chao Family Comprehensive Cancer Center, University of California, Irvine, 845 Health Sciences Road, Irvine, CA 92697, USA*
[2] *Department of Biomedical Engineering and Edwards Lifesciences Center for Advanced Cardiovascular Technology, University of California, Irvine, 845 Health Sciences Road, Irvine, CA 92697, USA*
[3] *Department of Developmental & Cell Biology, University of California, Irvine, 4236 McGaugh Hall, Irvine, CA 92697, USA*

Correspondence should be addressed to Weian Zhao; weianz@uci.edu

Received 30 April 2013; Accepted 13 July 2013

Academic Editor: Donald G. Phinney

Systemically infused mesenchymal stem cells (MSCs) are emerging therapeutics for treating stroke, acute injuries, and inflammatory diseases of the central nervous system (CNS), as well as brain tumors due to their regenerative capacity and ability to secrete trophic, immune modulatory, or other engineered therapeutic factors. It is hypothesized that transplanted MSCs home to and engraft at ischemic and injured sites in the brain in order to exert their therapeutic effects. However, whether MSCs possess the ability to migrate across the blood-brain barrier (BBB) that separates the blood from the brain remains unresolved. This review analyzes recent advances in this area in an attempt to elucidate whether systemically infused MSCs are able to actively transmigrate across the CNS endothelium, particularly under conditions of injury or stroke. Understanding the fate of transplanted MSCs and their CNS trafficking mechanisms will facilitate the development of more effective stem-cell-based therapeutics and drug delivery systems to treat neurological diseases and brain tumors.

1. Introduction

Despite enormous advances in our understanding of the molecular and cellular basis of neurological diseases, therapies that lead to sustained improvement or resolution of symptoms have remained elusive. Regenerative therapeutics, that encompass embryonic, neural, and adult stem cell therapies, possess great potential to reverse neuronal damage associated with CNS diseases such as stroke, multiple sclerosis (MS), Parkinson's disease (PD), and Alzheimer's disease (AD) [1]. Mesenchymal stem cells (MSCs) are an especially attractive therapeutic agent due to their ease of isolation, established safety, and potential to target multiple pathways involved in neuronal regeneration. MSCs are connective tissue progenitors that can be readily isolated from multiple tissues including bone marrow and adipose tissue [2–4]. While being initially used for treatment of connective tissue disorders due to their potential to differentiate into bone, cartilage, and fat cells, the discovery that MSCs can secrete cytokines and growth factors with antiapoptotic, proangiogenic, neuroprotective, and immunemodulatory properties has sparked broad clinical interest [2–4]. In fact, MSCs are the world's first manufactured stem cell product (i.e., Osiris's Prochymal) approved in Canada to treat graft-versus-host disease (GvHD) [5]. MSCs are currently being tested for treating some neurological diseases in multiple ongoing clinical trials, although their exact therapeutic mechanisms *in vivo* remain largely unknown (i.e., immunomodulation versus secretion of trophic factors that promote tissue regeneration and vascularization) [1, 6, 7]. Furthermore, there is great interest in using MSCs as vehicles to deliver antitumor therapeutics (e.g., tumor necrosis factor-related apoptosis-inducing ligand (TRAIL), interferon-β, and oncolytic viruses) for brain tumor treatment [8–10].

Given the large number of ongoing clinical trials that use systemic infusion (i.e., intravenously (IV) and intra-arterially (IA)) of MSCs expanded *in vitro* [2, 3], a procedure that is minimally invasive and convenient, it is critical to understand if transplanted MSCs can home to and engraft at ischemic and injured sites in the brain to exert their therapeutic effects. Currently, it is unclear whether systemically infused MSCs can actively migrate across the blood-brain barrier (BBB) that separates the blood and brain. This review attempts to synthesize the recent literature on MSC brain tropism, MSC/BBB interactions, and the underlying molecular mechanisms. We will first briefly introduce how leukocytes and tumor cells transmigrate across the BBB, especially under pathological conditions, to provide a mechanistic framework for the subsequent discussion on MSC homing. We will then concentrate on *in vivo* and *in vitro* studies that address whether MSCs actively interact with and transmigrate across the BBB, molecular mechanisms involved in the tropism of MSCs to the injured brain, interactions with the BBB, and biological/therapeutic implications to using MSCs as trophic vehicles for CNS drug delivery. Finally, we will present key challenges and novel approaches that we can utilize in the future in order to effectively study MSC/BBB interactions *in vivo* and develop MSC-based therapeutics to treat neurological diseases. The study of exogenous MSC homing and distribution into the CNS will not only shed light on how transplanted MSCs exert their therapeutic functions but also will allow us to gain insight into how endogenous MSCs migrate, traffic, and function in response to either CNS injury or other diseases. Additionally, studying MSC trafficking across the BBB may also contribute to the development of methods to monitor the fate of endogenous and exogenous stem cells *in vivo*.

2. Leukocyte Transmigration across the Blood-Brain Barrier (BBB)

The BBB is formed by cellular interactions between brain microvascular endothelial cells (BMECs), astrocytes, pericytes, and neurons [11, 12]. CNS endothelial cells (ECs) exhibit three characteristics that establish their BBB properties. (a) ECs have TJs that restrict diffusion of ions and polar molecules, resulting in high electrical resistance (TEER) [13, 14]. Endothelial TJs in the CNS are composed of transmembrane proteins Claudins (-5, -12), Occludin, and junctional adhesion molecules (JAMs), as well as cytoplasmic anchoring proteins such as Zonula Occludens proteins (ZO-1, ZO-2). These proteins regulate the paracellular (i.e., between ECs) permeability of endothelial cells [13, 15]. (b) CNS but not peripheral ECs contain a small number of endocytotic caveolae that serve as intermediates in the receptor-dependent and -independent transcytosis [16]. Caveolae are characterized by expression of Caveolins (Cav-1, -2, and -3), a class of transmembrane proteins (21–24 kDa) that are essential for caveolae formation [17, 18]. Notably, expression of Cav-1 is upregulated prior to BBB breakdown following CNS injury or stroke, concurrent with the increased rate of transcytosis [19, 20]. (c) Finally, CNS endothelium expresses a large number of specific active or passive transporters that regulate passage of nutrients (e.g., glucose or amino acids) from the blood to the brain and prevent drug delivery [15, 21].

The BBB plays a vital role in brain homeostasis by restricting the passage of molecules and leukocytes into and out of the brain [22]. However, during brain inflammation and injury, the BBB becomes compromised and cellular trafficking through the BBB is significantly upregulated [23]. Leukocyte trafficking to sites of CNS inflammation has been well studied and extensively reviewed [22, 24]. We will only provide a brief overview in order to contrast leukocyte and MSC transmigration across the BBB. Circulating leukocyte transmigration (also called extravasation or diapedesis) through the BBB occurs primarily at postcapillary venules and is characterized by a multistep adhesion/migration cascade (Figure 1) [25, 26]. During inflammation, BMECs upregulate cell surface adhesion molecules (e.g., P- and E-selectins, vascular cell adhesion molecule-1 (VCAM-1) and Intercellular Adhesion Molecule-1 (ICAM-1)), and chemoattractants (e.g., stromal cell-derived factor-1 (SDF-1) (or CXCL12) and CCL19). Leukocytes initiate transient selectin-mediated tethering and rolling on the endothelium that triggers activation of leukocyte integrins such as leukocyte function-associated molecule-1 (LFA-1, ligand for ICAM-1), macrophage-1 antigen (Mac-1, ligand for ICAM-1), and very late antigen-4 (VLA-4, ligand for VCAM-1) and leads to leukocyte arrest on ECs. Leukocytes then undergo actin-dependent polarization and Mac-1/ICAM-1-mediated lateral "crawling" over the luminal surface. Eventually, leukocytes migrate across the endothelial barrier through both paracellular (i.e., between endothelial cells (ECs)) and transcellular (i.e., directly through individual ECs) pathways, although the transcellular route is preferred [27, 28]. Adhesion of leukocytes on the EC layer induces clustering of endothelial cell surface adhesion molecules (i.e., ICAM-1 and VCAM-1) and triggers downstream signaling pathways that disrupt junctions and promote paracellular migration. Conversely, during transcellular migration, interactions between ICAM-1 and VCAM-1 on the EC surface induce formation of vertical microvilli-like projections (called "transmigratory cups") [27] that provide directional guidance for leukocyte extravasation. Transcellular migration seems to play a major role in leukocyte trafficking in the CNS system where ECs have strong tight junctions [29]. Actin-containing protrusive structures (e.g., podosomes, filopodia, lamellipodia, and pseudopodia) are often formed in leukocytes to enable them to "probe" into, and subsequently penetrate, ECs [27]. In contrast, in some types of CNS injury, activation of ECs and astrocytes can lead to reduced TJ integrity and formation of paracellular gaps, thereby facilitating the migration of leukocytes through a paracellular route. After passing through the endothelial barrier, leukocytes can then penetrate the endothelial basement membrane (BM) and pericytes through gaps within the ECM facilitated by matrix metalloproteinase-(MMP-)mediated ECM degradation.

3. Tropism of MSCs towards Brain

MSCs delivered systemically have been shown to preferentially localize to sites of inflammation, injury, ischemic

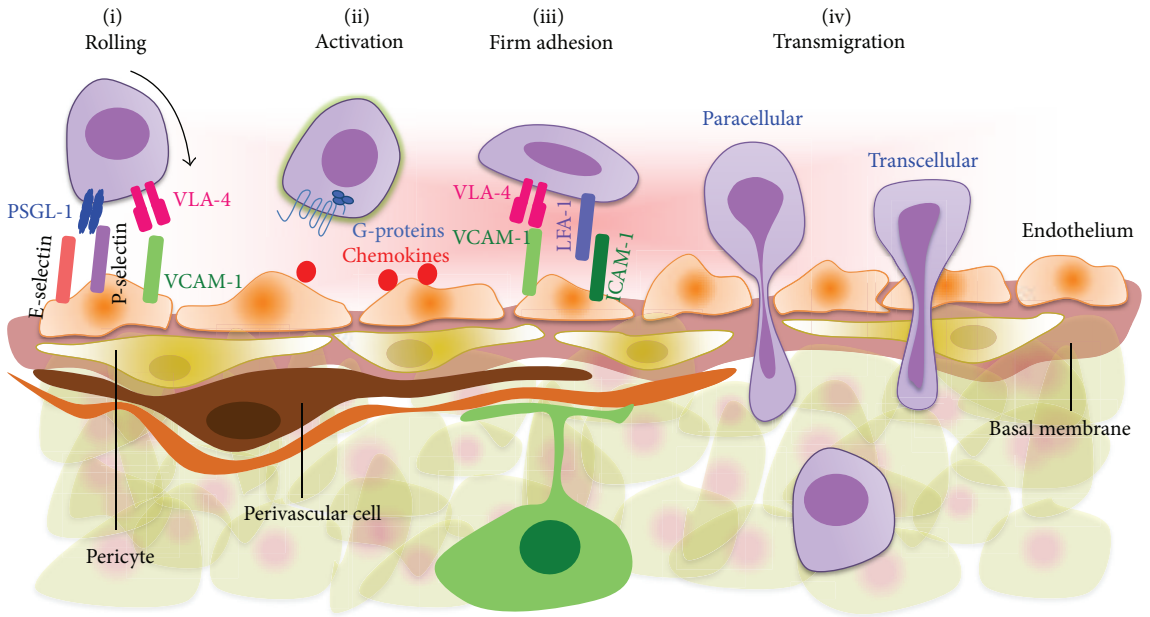

Figure 1: Leukocyte extravasation cascade. Leukocytes initially engage with the endothelium via selectin and VCAM-1 mediating interactions during rolling (i), followed by G-protein-mediated activation (ii) and subsequent integrin-mediated firm adhesion (iii). Transmigration across the BBB may occur via paracellular or transcellular routes (iv). It remains to be determined whether systemically infused MSCs possess similar or distinct features and mechanisms enabling them to transmigrate across the BBB and home to the CNS system *in vivo*.

lesions, and tumors including those in the brain despite their predominant entrapment in the lung vasculature [3, 30, 31]. For instance, Yilmaz et al. found that intravenously (IV) injected mouse bone-marrow-derived MSCs home to the infarct site in the transient middle cerebral artery occlusion (t-MCAO) model for stroke [31]. The brain tropism for MSCs was confirmed by whole body imaging of radiolabeled MSC given to rats with and without t-MCAO. During the first two hours after stroke, MSCs are transiently trapped in the lungs but migrate over time within the region of brain ischemia [32]. Kim et al. also found that human adipose-derived MSCs (hAMSCs) transplanted through an i.v. route crossed the BBB and migrated into the brain in a mouse model for AD [32, 33]. Systemically infused MSCs can also selectively accumulate into certain brain tumors (e.g., gliomas) [8, 10, 34–36]. These studies suggest that MSCs may possess leukocyte-like, active homing mechanisms that enable them to interact with and migrate across the BBB under injury or inflammation. However, the integrity of the cerebral vasculature is likely compromised following injury or inflammation, which can lead to passive MSC accumulation in the brain via entrapment [37]. Therefore, the extent and mechanisms of how MSCs actively cross the BBB remain to be determined.

4. Molecular Mechanisms of MSC/BBB Interaction and Transmigration

Several studies have shown that MSCs can utilize a leukocyte-like, multistep homing cascade (i.e., rolling, adhesion, and transmigration) to engage with ECs. However, a major caveat of the studies that we will discuss below is the use of cultured EC monolayers including non-BMECs such as human umbilical vein ECs (HUVECs) that do not fully acquire BBB properties typical of the *in vivo* situation.

MSCs express a variety of leukocyte homing molecules such as chemokine receptors (e.g., CXCR4, CCR2) and cell adhesion molecules (e.g., CD44, integrins $\alpha 4$ and $\beta 1$, and CD99), while they lack some key homing markers including P-selectin glycoprotein ligand 1 (PSGL-1), LFA-1, and Mac-1 [38]. However, studies of MSC-EC interactions and subsequent transmigration have produced conflicting results. Rüster et al. reported that MSCs interact with activated ECs under flow conditions via P-selectin during the initial tethering and rolling steps, although MSCs do not express common P-selectin ligands such as PSGL-1 and CD24 [39]. However, they found that the rolling velocity of MSCs on HUVEC is 100–600 μm/s under shear stress of 0.1–1 dyn/cm^2, a value that is significantly higher than that of leukocytes (~2–100 μm/sec under physiologically relevant shear stress of 1–4 dyn/cm^2) [39]. On the contrary, several studies reported that MSCs are not able to interact with ECs under flow conditions [40, 41]. Sackstein et al. showed that native MSCs do not express either PSGL-1 or major functional moieties involved in cell rolling such as sialyl Lewis X (SLeX) and therefore do not bind to P- and E-selectins. MSCs therefore have minimal binding interactions with ECs and they only modestly infiltrate the bone marrow [40]. Similar results were also obtained by Brooke and coworkers [42]. Furthermore, the role of VCAM-1/VLA-4, a receptor/ligand pair that mediates both cell rolling and adhesion, in MSC homing is unclear; few reports [43–45] including that of Rüster et al.'s [39] stated that VCAM-1/VLA-4 interactions are involved in MSC firm adhesion on ECs and transmigration while others found that MSCs do not bind to VCAM-1 [46].

Several studies also investigated MSC transmigration through *in vitro* endothelial monolayers [40, 45, 47]. In a coculture system of MSC with an endothelial cell monolayer, Steingen and coworkers found that MSCs transmigrated through the endothelial barrier using adhesion molecules including VCAM-1/VLA-4 and β1 integrin [45]. When MSCs were perfused into an isolated heart and investigated using electron microscopy, the authors observed that the tight junctions between endothelial cells became abolished and MSCs interacted with the endothelial cell layer in association with tight cell-cell contacts. In a recent work published by Teo and coworkers, high-resolution confocal and dynamic live-cell imaging has supported an active mode of MSC transmigration across various EC monolayers from lung microvascular endothelial cells (LMVECs) to rat brain ECs (GPNT, a cell line previously used to model the BBB *in vitro*) [48]. MSCs preferentially transmigrate on TNFα-activated endothelium, rather than naïve endothelium, using VCAM-1 and G-protein-coupled receptor signaling- (GPCR-) dependent pathways. MSCs migrate either by paracellular or transcellular diapedesis through discrete gaps or pores in the endothelial monolayer that are enriched for VCAM-1 (transmigratory cups). In contrast to leukocytes, MSC transmigration does not involve significant lateral crawling, presumably due to the lack of Mac-1 expression. Interestingly, MSC exhibited nonapoptotic membrane blebbing activity in the early stages of endothelial transmigration rather than formation of lamellipodia and invadosomes that are normally found in leukocytes, to potentially breach endothelial cells. Finally, MSC transmigration occurred on the time scale of hours. Although the mechanism of MSC transmigration is comparable to leukocyte transmigration across the BBB in some studies, the time is much longer than leukocyte transmigration in other endothelial systems (usually within minutes) [48]. Yilmaz et al. have studied trafficking of IV-injected mouse bone-marrow-derived MSCs to the brain in the t-MCAO model *in vivo* and found that interactions between the CD44 on MSCs and P- and E-selectins on ECs mediate MSC recruitment to the CNS [31]. Matsushita et al. have also found that rat MSCs could migrate through a monolayer of rat BMECs *in vitro* via a paracellular pathway [47] although the underlying mechanism was not reported. Furthermore, Lin et al. recently reported that MSCs trigger tight junction disassembly in human BMEC monolayers through PI3K and ROCK signaling pathways [49].

Similar to immune cells, chemokine receptors and their chemokine ligands are also found to be involved in MSC migration and endothelial transmigration [50–53]. For instance, Chamberlain et al. demonstrated functional expression of various chemokine receptors on murine MSCs using standard Boyden-type chamber assays [50]. More recently, they found that CXCL9, CXCL16, CCL20, and CCL25 were specifically involved in MSC transendothelial migration across murine aortic endothelial cells (MAECs) [41]. In Bloch's studies, they found that cocultivation of MSCs in the presence of bFGF, VEGF, EPO, and IL-6 resulted in a significant increase of MSC integration with the EC monolayer. They also found that VEGF, EPO, and IL-6 enhanced transmigration, although to different extents, whereas bFGF significantly decreased the transmigration of MSCs [45]. Furthermore, Feng et al. demonstrated that interactions of chemokines and chemokine receptors, specifically through fractalkine-CX3CR1 and SDF-1-CXCR4, partly mediated the migration of rat MSCs to the impaired site in the brain after hypoglossal nerve injury [54].

Finally, the activation of MMPs is also found to be associated with MSC transendothelial migration via degradation of the endothelial BM *in vitro*, providing a potential mechanism for MSC homing and extravasation into injured tissues *in vivo* [55]. MSCs constitutively express MMP-2 and membrane type 1 MMP (MT1-MMP) that may play a role in MSC invasion in reconstituted BM matrigel. In particular, Becker et al. [55] found that MSC transmigration across *in vitro* bone marrow endothelium is at least partially regulated by MMP-2. Interestingly, they also demonstrated that high culture confluence of MSCs was found to increase production of the endogenous MMP-inhibitor TIMP-3 and decrease transendothelial migration of MSCs. The involvement of MMPs in MSC transmigration is also supported by Bloch's study where MSCs-derived MMP-2 but not MMP-9 is found at sites of BM invasion and degradation [45]. Interestingly, TIMP3 expressed by IV administered MSCs is a key player in ameliorating BBB permeability in rodent models after traumatic brain injury (TBI) by blocking vascular endothelial growth factor-A-induced breakdown of endothelial cell adherens junctions [56]. These findings elucidate a potential molecular mechanism for the beneficial effects of MSCs in treating neurological diseases through regulation of BBB integrity.

5. MSC as a Delivery Vehicle for Brain Tumors

The fact that the BBB restricts the passage of molecules of molecular weight >400 Dalton presents a great challenge in delivering therapeutics to treat brain tumors and certain CNS diseases. Besides their endogenous therapeutic effects, the tropic properties of MSCs provide unique opportunities to use them as vehicles for gene and drug delivery to treat brain tumors. For instance, Nakamizo and coworkers have demonstrated that MSCs were capable of migrating into glioma xenografts *in vivo* after intravascular or local delivery [35]. They also found that MSCs engineered to produce IFN-β significantly increased animal survival compared with controls in a U87 intracranial glioma xenograft mouse model [35]. Recently, Kim et al. have tested combination therapy for malignant glioma with TRAIL-secreting MSCs and the lipoxygenase inhibitor MK886 that can increase sensitivity to TRAIL-induced apoptosis [8]. They found that MSC-based TRAIL gene delivery combined with MK886 had greater therapeutic efficacy than single-agent treatment in an orthotopic glioma xenografted mouse model [8]. Interestingly, MSCs can also be used as target-delivery vehicle for anticancer drug-loaded biodegradable nanoparticles [57]. This approach may be advantageous over genetic modification with respect to safety and controlled drug release. Roger et al. have found that coumarin-6 containing polylactic acid nanoparticles and lipid nanocapsules can be efficiently internalized into MSCs without affecting cell viability

or differentiation [36]. Furthermore, they reported that nanoparticle-loaded cells were able to migrate toward an experimental human glioma model, suggesting that MSCs can serve as cellular carriers for drug-loaded nanoparticles to treat brain tumors.

6. Conclusion and Perspectives

MSC transplantation via systemic administration holds enormous potential to treat numerous neurological and brain diseases. However, the *in vivo* efficacy of MSC therapy has not been well established, and some recent clinical trials have produced mixed results [2, 3]. The lack of efficacy is attributed largely to an incomplete understanding of MSC biology and their fate following transplantation *in vivo* [2, 3]. In particular, crossing the BBB may be a prerequisite for MSCs to exert their therapeutic effects in treating neurological diseases or CNS injury [3, 30, 31] and is necessary for their use as vehicles for drug delivery to treat brain tumors [58]. It seems clear that, at least *in vitro*, MSCs possess leukocyte-like, although inefficient, molecular mechanisms involving adhesion molecules, chemokines, and proteases which enable MSC/EC interactions and transmigration. The large discrepancies between studies may be due to the inherent heterogeneity of MSCs combined with variations in experimental techniques and models. A major caveat of *in vitro* studies is the use of EC monolayers that do not fully recapitulate the *in vivo* BBB properties. It will be important to incorporate other BBB cell types, such as primary astrocytes, pericytes, reconstituted basement membrane, and relevant dynamic flow conditions in order to develop more robust *in vitro* systems for studying MSC/EC interactions. Despite the *in vitro* evidence, it remains elusive whether systemically infused MSCs are able to use leukocyte-like homing cascades to actively interact with and transmigrate across the BBB *in vivo* under both normal and pathological conditions. Indeed, it is not clear if MSCs are actually able to actively home or rather are passively "captured" at sites of inflamed and disrupted vessels. Physical factors may act in concert with active homing mechanisms to stop or slow down cells before adhesion interactions subsequently arrest MSCs on ECs.

In order to fully understand the dynamic behavior of transplanted MSCs, imaging of transplanted cells in both the brain and other tissues is required. Both short- and long-term monitoring of cell fate *in vivo* have benefited from improved molecular imaging techniques to visualize cell survival, biodistribution, and behavior [59–62]. Magnetic resonance-based tracking of transplanted cells has confirmed that MSCs rapidly localize to infracted regions of the brain [63–65]. Alternatively, a powerful approach for understanding transplanted cell behavior at the single-cell level is to utilize intravital imaging techniques to study MSC/BBB interactions. In particular, novel transgenic models where TJs between endothelial cells of the BBB or endothelial caveolae are fluorescently tagged may illuminate the mode and dynamics of MSC transmigration in the brain and elsewhere [59]. The study of exogenous MSC homing mechanisms *in vivo* will not only shed light on how transplanted MSCs exert their therapeutic functions in treating neurological diseases but also will allow us to gain insight into how endogenous MSCs migrate, traffic, and function in response to injury. The mechanistic study of MSC tropism to the brain will also facilitate development of MSCs that are engineered with key homing molecules through genetic or chemical modifications in order to improve MSC targeting and drug delivery in case their basal homing process is inefficient [40, 60]. Finally, the elucidation of stem cell fate following transplantation that is believed to be a major bottleneck in stem cell therapy will have broad implications in understanding stem cell functions and developing more effective stem-cell-based therapeutics [2, 3].

Acknowledgments

This work is supported by the start-up fund from the Department of Pharmaceutical Sciences, Sue and Bill Gross Stem Cell Research Center and the Chao Family Comprehensive Cancer Center at UC Irvine, and NCI Cancer Center Support Grant 5P30CA062203-18. M. A. Eckert is supported by a California Institute for Regenerative Medicine (CIRM) Training Grant (TG2-01152).

References

[1] A. Trounson, "New perspectives in human stem cell therapeutic research," *BMC Medicine*, vol. 7, article 29, 2009.

[2] J. Ankrum and J. M. Karp, "Mesenchymal stem cell therapy: two steps forward, one step back," *Trends in Molecular Medicine*, vol. 16, no. 5, pp. 203–209, 2010.

[3] J. M. Karp and G. S. L. Teo, "Mesenchymal stem cell homing: the devil is in the details," *Cell Stem Cell*, vol. 4, no. 3, pp. 206–216, 2009.

[4] A. I. Caplan and D. Correa, "The MSC: an injury drugstore," *Cell Stem Cell*, vol. 9, no. 1, pp. 11–15, 2011.

[5] D. Cyranoski, "Canada approves stem cell product," *Nature Biotechnology*, vol. 30, no. 7, p. 571, 2012.

[6] G. Brooke, M. Cook, C. Blair et al., "Therapeutic applications of mesenchymal stromal cells," *Seminars in Cell and Developmental Biology*, vol. 18, no. 6, pp. 846–858, 2007.

[7] P. Dharmasaroja, "Bone marrow-derived mesenchymal stem cells for the treatment of ischemic stroke," *Journal of Clinical Neuroscience*, vol. 16, no. 1, pp. 12–20, 2009.

[8] S. M. Kim, J. S. Woo, C. H. Jeong, C. H. Ryu, J. Y. Lim, and S. S. Jeun, "Effective combination therapy for malignant glioma with TRAIL-secreting mesenchymal stem cells and lipoxygenase inhibitor MK886," *Cancer Research*, vol. 72, no. 18, pp. 4807–4817, 2012.

[9] M. Studeny, F. C. Marini, J. L. Dembinski et al., "Mesenchymal stem cells: potential precursors for tumor stroma and targeted-delivery vehicles for anticancer agents," *Journal of the National Cancer Institute*, vol. 96, no. 21, pp. 1593–1603, 2004.

[10] A. U. Ahmed, M. A. Tyler, B. Thaci et al., "A comparative study of neural and mesenchymal stem cell-based carriers for oncolytic adenovirus in a model of malignant glioma," *Molecular Pharmaceutics*, vol. 8, no. 5, pp. 1559–1572, 2011.

[11] N. J. Abbott, A. A. K. Patabendige, D. E. M. Dolman, S. R. Yusof, and D. J. Begley, "Structure and function of the blood-brain barrier," *Neurobiology of Disease*, vol. 37, no. 1, pp. 13–25, 2010.

[12] B. V. Zlokovic, "The blood-brain barrier in health and chronic neurodegenerative disorders," *Neuron*, vol. 57, no. 2, pp. 178–201, 2008.

[13] J. M. Anderson and C. M. van Itallie, "Physiology and function of the tight junction," *Cold Spring Harbor Perspectives in Biology*, vol. 1, no. 2, Article ID a002584, 2009.

[14] L. L. Rubin and J. M. Staddon, "The cell biology of the blood-brain barrier," *Annual Review of Neuroscience*, vol. 22, pp. 11–28, 1999.

[15] R. Daneman, L. Zhou, D. Agalliu, J. D. Cahoy, A. Kaushal, and B. A. Barres, "The mouse blood-brain barrier transcriptome: a new resource for understanding the development and function of brain endothelial cells," *PLoS ONE*, vol. 5, no. 10, Article ID e13741, 2010.

[16] S. A. Predescu, D. N. Predescu, and A. B. Malik, "Molecular determinants of endothelial transcytosis and their role in endothelial permeability," *The American Journal of Physiology—Lung Cellular and Molecular Physiology*, vol. 293, no. 4, pp. L823–L842, 2007.

[17] M. Drab, P. Verkade, M. Elger et al., "Loss of caveolae, vascular dysfunction, and pulmonary defects in caveolin-1 gene-disrupted mice," *Science*, vol. 293, no. 5539, pp. 2449–2452, 2001.

[18] M. P. Lisanti, Z. Tang, and M. Sargiacomo, "Caveolin forms a hetero-oligomeric protein complex that interacts with an apical GPI-linked protein: Implications for the biogenesis of caveolae," *Journal of Cell Biology*, vol. 123, no. 3, pp. 595–604, 1993.

[19] C. Kaur and E. A. Ling, "Blood brain barrier in hypoxic-ischemic conditions," *Current Neurovascular Research*, vol. 5, no. 1, pp. 71–81, 2008.

[20] S. Nag, J. L. Manias, and D. J. Stewart, "Expression of endothelial phosphorylated caveolin-1 is increased in brain injury," *Neuropathology and Applied Neurobiology*, vol. 35, no. 4, pp. 417–426, 2009.

[21] J. A. Nicolazzo and K. Katneni, "Drug transport across the blood-brain barrier and the impact of breast cancer resistance protein (ABCG2)," *Current Topics in Medicinal Chemistry*, vol. 9, no. 2, pp. 130–147, 2009.

[22] R. M. Ransohoff and B. Engelhardt, "The anatomical and cellular basis of immune surveillance in the central nervous system," *Nature Reviews Immunology*, vol. 12, no. 9, pp. 623–635, 2012.

[23] C. Uboldi, A. Döring, C. Alt, P. Estess, M. Siegelman, and B. Engelhardt, "L-Selectin-deficient SJL and C57BL/6 mice are not resistant to experimental autoimmune encephalomyelitis," *European Journal of Immunology*, vol. 38, no. 8, pp. 2156–2167, 2008.

[24] B. Engelhardt, "Immune cell entry into the central nervous system: involvement of adhesion molecules and chemokines," *Journal of the Neurological Sciences*, vol. 274, no. 1-2, pp. 23–26, 2008.

[25] E. H. Wilson, W. Weninger, and C. A. Hunter, "Trafficking of immune cells in the central nervous system," *Journal of Clinical Investigation*, vol. 120, no. 5, pp. 1368–1379, 2010.

[26] B. Engelhardt and R. M. Ransohoff, "The ins and outs of T-lymphocyte trafficking to the CNS: anatomical sites and molecular mechanisms," *Trends in Immunology*, vol. 26, no. 9, pp. 485–495, 2005.

[27] C. V. Carman, "Mechanisms for transcellular diapedesis: probing and pathfinding by 'invadosome-like protrusions'," *Journal of Cell Science*, vol. 122, part 17, pp. 3025–3035, 2009.

[28] K. Ley, C. Laudanna, M. I. Cybulsky, and S. Nourshargh, "Getting to the site of inflammation: the leukocyte adhesion cascade updated," *Nature Reviews Immunology*, vol. 7, no. 9, pp. 678–689, 2007.

[29] M. von Wedel-Parlow, S. Schrot, J. Lemmen, L. Treeratanapiboon, J. Wegener, and H. Galla, "Neutrophils cross the BBB primarily on transcellular pathways: an in vitro study," *Brain Research*, vol. 1367, pp. 62–76, 2011.

[30] A. R. Simard and S. Rivest, "Bone marrow stem cells have the ability to populate the entire central nervous system into fully differentiated parenchymal microglia," *FASEB Journal*, vol. 18, no. 9, pp. 998–1000, 2004.

[31] G. Yilmaz, S. Vital, C. E. Yilmaz, K. Y. Stokes, J. S. Alexander, and D. N. Granger, "Selectin-mediated recruitment of bone marrow stromal cells in the postischemic cerebral microvasculature," *Stroke*, vol. 42, no. 3, pp. 806–811, 2011.

[32] S. Kim, K. A. Chang, J. Kim et al., "The preventive and therapeutic effects of intravenous human adipose-derived stem cells in Alzheimer's disease mice," *PLoS ONE*, vol. 7, no. 9, Article ID e45757, 2012.

[33] D. Jeon, K. Chu, S. Lee et al., "A cell-free extract from human adipose stem cells protects mice against epilepsy," *Epilepsia*, vol. 52, no. 9, pp. 1617–1626, 2011.

[34] C. Pendleton, Q. Li, D. A. Chesler, K. Yuan, H. Guerrero-Cazares, and A. Quinones-Hinojosa, "Mesenchymal stem cells derived from adipose tissue versus bone marrow: in vitro comparison of their tropism towards gliomas," *PLoS ONE*, vol. 8, no. 3, Article ID e58198, 2013.

[35] A. Nakamizo, F. Marini, T. Amano et al., "Human bone marrow-derived mesenchymal stem cells in the treatment of gliomas," *Cancer Research*, vol. 65, no. 8, pp. 3307–3318, 2005.

[36] M. Roger, A. Clavreul, M. Venier-Julienne et al., "Mesenchymal stem cells as cellular vehicles for delivery of nanoparticles to brain tumors," *Biomaterials*, vol. 31, no. 32, pp. 8393–8401, 2010.

[37] R. H. Lee, A. A. Pulin, M. J. Seo et al., "Intravenous hMSCs improve myocardial infarction in mice because cells embolized in lung are activated to secrete the anti-inflammatory protein TSG-6," *Cell Stem Cell*, vol. 5, no. 1, pp. 54–63, 2009.

[38] L. D. S. Meirelles, A. I. Caplan, and N. B. Nardi, "In search of the in vivo identity of mesenchymal stem cells," *Stem Cells*, vol. 26, no. 9, pp. 2287–2299, 2008.

[39] B. Rüster, S. Göttig, R. J. Ludwig et al., "Mesenchymal stem cells display coordinated rolling and adhesion behavior on endothelial cells," *Blood*, vol. 108, no. 12, pp. 3938–3944, 2006.

[40] R. Sackstein, J. S. Merzaban, D. W. Cain et al., "Ex vivo glycan engineering of CD44 programs human multipotent mesenchymal stromal cell trafficking to bone," *Nature Medicine*, vol. 14, no. 2, pp. 181–187, 2008.

[41] G. Chamberlain, H. Smith, G. E. Rainger, and J. Middleton, "Mesenchymal stem cells exhibit firm adhesion, crawling, spreading and transmigration across aortic endothelial cells: effects of chemokines and shear," *PLoS ONE*, vol. 6, no. 9, Article ID e25663, 2011.

[42] G. Brooke, H. Tong, J. Levesque, and K. Atkinson, "Molecular trafficking mechanisms of multipotent mesenchymal stem cells derived from human bone marrow and placenta," *Stem Cells and Development*, vol. 17, no. 5, pp. 929–940, 2008.

[43] J. E. Ip, Y. Wu, J. Huang, L. Zhang, R. E. Pratt, and V. J. Dzau, "Mesenchymal stem cells use integrin β1 not CXC chemokine receptor 4 for myocardial migration and engraftment," *Molecular Biology of the Cell*, vol. 18, no. 8, pp. 2873–2882, 2007.

[44] V. F. M. Segers, I. van Riet, L. J. Andries et al., "Mesenchymal stem cell adhesion to cardiac microvascular endothelium: activators and mechanisms," *American Journal of Physiology—Heart and Circulatory Physiology*, vol. 290, no. 4, pp. H1370–H1377, 2006.

[45] C. Steingen, F. Brenig, L. Baumgartner, J. Schmidt, A. Schmidt, and W. Bloch, "Characterization of key mechanisms in transmigration and invasion of mesenchymal stem cells," *Journal of Molecular and Cellular Cardiology*, vol. 44, no. 6, pp. 1072–1084, 2008.

[46] A. Heiskanen, T. Hirvonen, H. Salo et al., "Glycomics of bone marrow-derived mesenchymal stem cells can be used to evaluate their cellular differentiation stage," *Glycoconjugate Journal*, vol. 26, no. 3, pp. 367–384, 2009.

[47] T. Matsushita, T. Kibayashi, T. Katayama et al., "Mesenchymal stem cells transmigrate across brain microvascular endothelial cell monolayers through transiently formed inter-endothelial gaps," *Neuroscience Letters*, vol. 502, no. 1, pp. 41–45, 2011.

[48] G. S. Teo, J. A. Ankrum, R. Martinelli et al., "Mesenchymal stem cells transmigrate between and directly through tumor necrosis factor-α-activated endothelial cells via both leukocyte-like and novel mechanisms," *Stem Cells*, vol. 30, no. 11, pp. 2472–2486, 2012.

[49] M. N. Lin, D. S. Shang, W. Sun et al., "Involvement of PI3K and ROCK signaling pathways in migration of bone marrow-derived mesenchymal stem cells through human brain microvascular endothelial cell monolayers," *Brain Research*, vol. 1513, pp. 1–8, 2013.

[50] G. Chamberlain, K. Wright, A. Rot, B. Ashton, and J. Middleton, "Murine mesenchymal stem cells exhibit a restricted repertoire of functional chemokine receptors: comparison with human," *PLoS ONE*, vol. 3, no. 8, Article ID e2934, 2008.

[51] V. Sordi, M. L. Malosio, F. Marchesi et al., "Bone marrow mesenchymal stem cells express a restricted set of functionally active chemokine receptors capable of promoting migration to pancreatic islets," *Blood*, vol. 106, no. 2, pp. 419–427, 2005.

[52] M. Honczarenko, Y. Le, M. Swierkowski, I. Ghiran, A. M. Glodek, and L. E. Silberstein, "Human bone marrow stromal cells express a distinct set of biologically functional chemokine receptors," *Stem Cells*, vol. 24, no. 4, pp. 1030–1041, 2006.

[53] A. L. Ponte, E. Marais, N. Gallay et al., "The in vitro migration capacity of human bone marrow mesenchymal stem cells: comparison of chemokine and growth factor chemotactic activities," *Stem Cells*, vol. 25, no. 7, pp. 1737–1745, 2007.

[54] J. Feng, J. B. P. He, S. T. Dheen, and S. S. W. Tay, "Interactions of chemokines and chemokine receptors mediate the migration of mesenchymal stem cells to the impaired site in the brain after hypoglossal nerve injury," *Stem Cells*, vol. 22, no. 3, pp. 415–427, 2004.

[55] A. de Becker, P. van Hummelen, M. Bakkus et al., "Migration of culture-expanded human mesenchymal stem cells through bone marrow endothelium is regulated by matrix metalloproteinase-2 and tissue inhibitor of metalloproteinase-3," *Haematologica*, vol. 92, no. 4, pp. 440–449, 2007.

[56] T. Menge, Y. Zhao, J. Zhao et al., "Mesenchymal stem cells regulate blood-brain barrier integrity through TIMP3 release after traumatic brain injury," *Science Translational Medicine*, vol. 4, no. 161, Article ID 161ra150, 2012.

[57] Z. Gao, L. Zhang, J. Hu, and Y. Sun, "Mesenchymal stem cells: a potential targeted-delivery vehicle for anti-cancer drug, loaded nanoparticles," *Nanomedicine*, vol. 9, no. 2, pp. 174–184, 2013.

[58] A. H. Klopp, A. Gupta, E. Spaeth, M. Andreeff, and F. Marini III, "Concise review: dissecting a discrepancy in the literature: do mesenchymal stem cells support or suppress tumor growth?" *Stem Cells*, vol. 29, no. 1, pp. 11–19, 2011.

[59] D. Agalliu and I. Schieren, "Heterogeneity in the developmental potential of motor neuron progenitors revealed by clonal analysis of single cells in vitro," *Neural Development*, vol. 4, no. 1, article 2, 2009.

[60] D. Sarkar, J. A. Spencer, J. A. Phillips et al., "Engineered cell homing," *Blood*, vol. 118, no. 25, pp. e184–e191, 2011.

[61] B. J. Schaller, J. F. Cornelius, N. Sandu, and M. Buchfelder, "Molecular imaging of brain tumors personal experience and review of the literature," *Current Molecular Medicine*, vol. 8, no. 8, pp. 711–726, 2008.

[62] N. Sandu, T. Spiriev, and B. Schaller, "Stem cell transplantation in neuroscience: the role of molecular imaging," *Stem Cell Reviews*, vol. 8, no. 4, pp. 1265–1266, 2012.

[63] W. C. Shyu, C. P. Chen, S. Z. Lin, Y. J. Lee, and H. Li, "Efficient tracking of non-iron-labeled mesenchymal stem cells with serial MRI in chronic stroke rats," *Stroke*, vol. 38, no. 2, pp. 367–374, 2007.

[64] O. Detante, S. Valable, F. de Fraipont et al., "Magnetic resonance imaging and fluorescence labeling of clinical-grade mesenchymal stem cells without impacting their phenotype: study in a rat model of stroke," *Stem Cells Translational Medicine*, vol. 1, no. 4, pp. 333–340, 2012.

[65] S. S. Lu, S. Liu, Q. Q. Zu et al., "In vivo MR imaging of intraarterially delivered magnetically labeled mesenchymal stem cells in a canine stroke model," *PLoS ONE*, vol. 8, no. 2, Article ID e54963, 2013.

Hindawi Publishing Corporation
Stem Cells International
Volume 2013, Article ID 582527, 9 pages
http://dx.doi.org/10.1155/2013/582527

Clinical Study

Intracoronary Infusion of Autologous CD133$^+$ Cells in Myocardial Infarction and Tracing by Tc99m MIBI Scintigraphy of the Heart Areas Involved in Cell Homing

Ubaidullo Kurbonov,[1] Abdusamad Dustov,[2] Alisher Barotov,[3] Murtazokul Khidirov,[1] Giesidin Mirojov,[2] Zikrie Rahimov,[3] Navjuvon Navjuvonov,[3] Eraj Rizoev,[3] Nasim Olimov,[3] Alijon Goibov,[1] Bakhtovar Karim-Zade,[1] Mukim Rakhmatov,[3] Suhayli Muminjonov,[1] Azadeh Didari,[1] Jamila Irgasheva,[1] Oktam Bobokhojaev,[3] Tashpulat Gulmuradov,[3] Amu Therwath,[4] Sohibnazar Rakhmonov,[3] and Massoud Mirshahi[1,4]

[1] *Avicenna Tajik State Medical University, Dushanbe, Tajikistan*
[2] *Institute of Gastroenterology, 734003 Dushanbe, Tajikistan*
[3] *Tajikistan Ministry of Health, 734003 Dushanbe, Tajikistan*
[4] *UMRS 872, CRC-INSERM, Université Pierre et Marie Curie, Paris-VI, Université Paris Descartes, Paris-V, 15 rue de l'Ecole de Médecine, 75006 Paris, France*

Correspondence should be addressed to Massoud Mirshahi; massoud.mirshahi@upmc.fr

Received 11 January 2013; Revised 11 March 2013; Accepted 14 March 2013

Academic Editor: Weian Zhao

CD133 mesenchymal cells were enriched using magnetic microbead anti-CD133 antibody from bone marrow mononuclear cells (BMMNCs). Flow cytometry and immunocytochemistry analysis using specific antibodies revealed that these cells were essentially 89 ± 4% CD133$^+$ and 8 ± 5% CD34$^+$. CD133$^+$/CD34$^+$ BMMNCs secrete important bioactive proteins such as cardiotrophin-1, angiogenic and neurogenic factors, morphogenetic proteins, and proinflammatory and remodeling factors in vitro. Single intracoronary infusions of autologous CD133$^+$/CD34$^+$ BMMNCs are effective and reduce infarct size in patients as analyzed by Tc99m MIBI myocardial scintigraphy. The majority of patients were treated via left coronary artery. Nine months after cell therapy, 5 out of 8 patients showed a net positive response to therapy in different regions of the heart. Uptake of Tc99 isotope and revitalization of the heart area in inferoseptal region are more pronounced ($P = 0.016$) as compared to apex and anterosptal regions after intracoronary injection of the stem cells. The cells chosen here have the properties essential for their potential use in cell therapy and their homing can be followed without major difficulty by the scintigraphy. The cell therapy proposed here is safe and should be practiced, as we found, in conjunction with scintigraphic observation of areas of heart which respond optimally to the infusion of autologous CD133$^+$/CD34$^+$ BMMNCs.

1. Introduction

Heart failure is the leading cause of death worldwide, and current therapies only delay progression of the disease. Cardiomyocytes are a stable cell population with only limited potential for renewal after injury [1, 2]. Tissue regeneration may be due to infiltration of stem cells, which differentiate into cardiomyocytes [3]. Laboratory experiments and recent clinical trials suggest that cell-based therapies can improve cardiac function [4, 5], and the implications of this for cardiac regeneration are causing great excitement. These new findings have stimulated optimism that the progression of heart failure can be prevented or even reversed with cell-based therapy [6].

Numerous studies have documented that transplantation of bone marrow derived cells following acute myocardial infarction and ischemic cardiomyopathy can lead to a reduction in infarct scar size and improvements in left

ventricular function and perfusion. Furthermore, the impact of successes may be affected by quality (progenitor source) and quantity of the cells, timing [7], route (intramuscular, intracoronary) [8], and type of cardiomyopathy [4].

Bone marrow stem cells (BMSCs) can differentiate into multiple cell types present in the heart [9]. Following a sex-mismatched transplantation constellation heart muscle tissue analyzed after autopsy, it was revealed that mesenchymal stem cells of the BM play a pivotal role in the development of mixed chimerism of cardiomyocytes and endothelial cells following transplantation [10].

In several randomized studies in which BMSCs were administered by intracoronary injection, the left ventricular ejection fraction (LVEF) was measured 3–6 months following the myocardial infarction [4]; it was observed that there was a 3–12% increase (average 6%) in cardiac function [5] that has been recently in published a very informative review on ongoing clinical trials of stem cell therapy for heart diseases in USA, which stands as a good source of information.

Source of stem cell therapy for heart disease may come from progenitors from hematopoietic (BM, peripheral blood, umbilical cord blood), mesenchymal (BM, adipose tissues), skeletal (muscle), endothelial (BM, peripheral blood), and cardiac (infarct border, epicardium) cells [5]. These cells are characterized by a high potential of pluripotent activity and can participate in tissues remodeling by secretion of growth factors in an autocrine or paracrine manner. In an animal model (rat), two cell types, namely, skeletal myoblasts or $CD133^+$ progenitors, led to improvement of cardiac function [11, 12].

Current tests such as ECG, LVEF (left ventricle ejection fraction), LVESV (left ventricle end systolic volume) and LVEDV (left ventricle end diastolic volume), are the major indicators for evaluation of efficacy of stem cell therapy. However, the efficacy of cell therapy at the *in situ* level needs to be ascertained and then alone it can be taken into account in any treatment protocol. Imaging by magnetic resonance imaging and scintigraphy allows for *in vivo* tracking of cells and can provide a better understanding and evaluation of functional impact of cardiac stem cell therapy. Among these the direct labeling of cells with isotopes and the tracking is an attractive proposal [13, 14].

Here, we report that $CD133^+$ cells isolated from bone marrow mononuclear cells secrete a large array of regulatory proteins including several growth factors. When these cells are infused immediately in patients with coronary heart disease and postinfarction cardiosclerosis, they are able to modify revitalization of infarct scar as explored by scintigraphy.

2. Material and Methods

2.1. Bone Marrow Specimens. Bone marrow samples were obtained from 5 healthy individuals and 15 patients with different cardiac pathologies. All samples were obtained after informed consent of individual patients and in accordance with the rules of the revised Helsinki protocol. All participants provide their written consent to participate in this study. The ethics committees of Tajikistan Health Ministry gave their approval of the procedures fallowed and for undertaking this study.

2.2. Cell Preparation. Bone marrow mononuclear cells (BMMNCs) were isolated ($n = 5$) by density-gradient centrifugation over Ficoll-400 (PAA Laboratories, Les Mureaux, France). The BMMNCs layer was collected and the monocyte/macrophage cells were eliminated by incubation of the cells with polystyrene surface. $CD133^+$ was separated from BMMNCs by a magnetic bead separation method following the manufacturer's instructions (MACS; Miltenyi Biotec, France). Purity of isolated $CD133^+$ was analyzed using fluorochrome-conjugated anti-CD133 monoclonal antibodies. These cell preparations contained $CD34^+$ cells and their amount was quantified by immunocytochemistry using anti-CD34 monoclonal antibody (mAbs, Miltenyi Biotec, Paris, France). BMMNC-derived $CD133^+/CD34^+$ were employed in the treatment regimen described in this work.

2.3. Cell Culture. BMMNCs or isolated $CD133^+$ cells were plated on 0.2% gelatin-coated wells (Sigma, Saint-Quentin Fallavier, France) and maintained in endothelial cell basal medium MV2 (ECBM MV2, Promocell, Heidelberg, Germany) supplemented with ECBM-MV2 complemented (PromoCell). At 6 days of culture, nonadherent cells were removed, new media was applied, and the culture was further maintained through days 3, 10, or 21.

2.4. Cytokine Array. In order to analyze the *in vitro* secretion of bioactive proteins by bone marrow stem cells, the supernatant of $BMCD133^+$ cells ($n = 3$) were analyzed using a protein cytokine array (RayBio Human Cytokine Antibody). This technique is based on the principle of "sandwich immunoassay." It comprises essentially of screening, in duplicate, 174 different membrane coupled anticytokines along with appropriate controls (experiments repeated 3 times). $BMCD133^+$ cells (10^6 cells per mL) were incubated in RPMI-1640 without fetal calf serum at 37°C in a humidified atmosphere of 5% CO_2 for 24 hours. Supernatants containing cytokines were retrieved and the cytokines were allowed to couple with their specific antibodies previously immobilized on membranes. Membranes were saturated for 2 hours at room temperature with bovine serum albumin (BSA). Incubation of array membranes with supernatants (along with controls) was carried out overnight at 4°C using corresponding antibodies. After several successive washes, membranes were incubated in the presence of a mixture of antibodies and anticytokines biotinylated at 4°C overnight. Streptavidin, coupled with HRP, was added on the membranes for 2 hours at room temperature. The presence of antibody-coupled proteins was revealed by applying ECL (enhanced chemoluminescence) to the membranes, according to the recommendations of the manufacturer. Membranes were then exposed to a photosensitive film (Kodak, X-Omat AR USA). The intensity of chemiluminescence captured on the photosensitive film was measured and recorded. After subtracting the background noise, the results were expressed

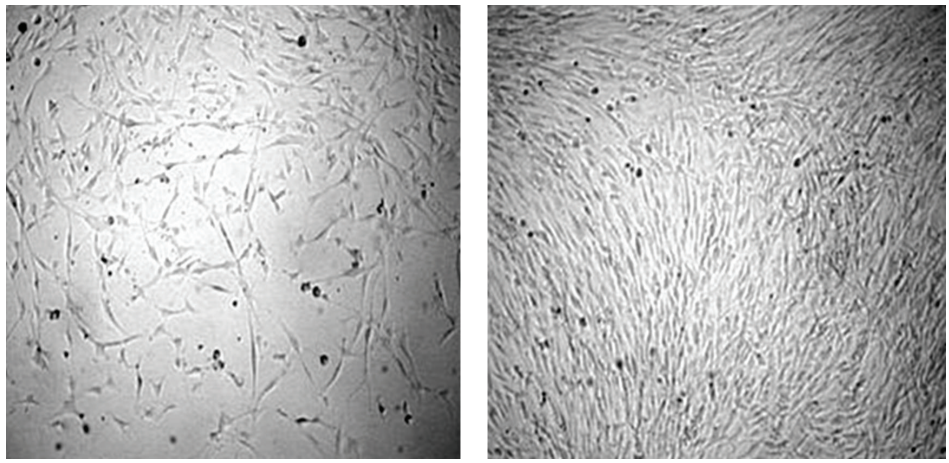

(a) (b)

Figure 1: $CD133^+/CD34^+$ BMMNCs in culture after 3 days (a) and 6 days (b).

as a ratio of chemoluminescence intensity of experimental versus control spots. The positive control was considered as 1. Less than −2 ratio values indicated a reduction of the cytokine and a value greater than +2 indicated an increase in cytokine expression. The proteins detected by protein array from the three independent cell preparations were considered as bioactive proteins.

2.5. Patients. Fifteen patients with a diagnosis of ischemic heart diseases and myocardial infarction (deferred Q-myocardial infarction without significant complications barred from 3 to 6 months) were selected. Immediately prior to implantation of the stem cells, all patients underwent coronary angiography, which was carried out on the angiographic system "Infinix CC" (Toshiba, Japan). Arteriography was performed on left coronary artery at 4–6 projections and the right coronary artery at 3-4 projections. Fluoroscopy time ranged from 2 to 9 minutes. In some of the subjects, coronary angiography revealed severe coronary artery pathology: left coronary artery trunk (4 cases) and 3 vascular lesions (7 cases).

2.6. Treatment of Patients. Bone marrow was taken after standard puncture of the sternum under local anesthesia. CD133 stem cells were isolated from mononuclear cells by density gradient centrifugation using Ficoll, followed by immunomagnetic separation. Isolated cells of patients with coronary artery disease were reinjected intra-arterially into the coronary arteries under angiography with an average dose of 5 mL of suspension containing 0.8–1.5 million cells. Purified $CD133^+$ positive cells were stored at 4°C in 0.9% NaCl until intramyocardial injection. Perfusion of stem cell in the coronary artery was carried out taking into account the angiographic findings and areas of myocardial ischemia: in 12 cases of the stem cells introduced directly into the left coronary artery, and in 3 cases introduced into both the coronary arteries. All the patients, in addition to their classic treatments were treated by estradiol (Estreva 0.75 mg/day for two months).

2.7. Clinical Appreciations. Clinical examination and currently used tests such as ECG, EFLV (ejection fraction of the left ventricle), LVESV (left ventricle end systolic volume), and LVEDV (left ventricle end diastolic volume) were performed in order to evaluate the dynamics of myocardial perfusion in all patients with coronary heart disease and post-infarction cardiosclerosis before and after cell therapy. For 11 out of 15 of the treated patients, we carried out myocardial scintigraphy using Tc99 m with the ligand methoxyisobutylisonitrile (MIBI) after an interval of 1 and 3 months. 8 out of 11 of these patients were further investigated by scintigraphy again after 9 months.

3. Results

3.1. Isolated BMMNCs and BMMNC $CD133^+$ Differentiate into Adherent Cells. BMMNCs were isolated from bone marrow of different normal donors ($n = 5$). $CD133^+$ cells were isolated and their purity was found to be more than 89 ± 4% as assessed by flow cytometry. These cell preparations contained also 8 ± 5% $CD34^+$ BMMNCs.

$CD133^+/CD34^+$ BMMNCs were *in vitro* cultured under specific conditions as described in Section 2. Figure 1 presents the $CD133^+/CD34^+$ BMMNCs after 3 days (a) and 6 days (b) in culture. After 3 weeks in culture, adherent cells displaying totally different morphological aspects were observed. Indeed, certain cells were long and frayed while others were rather small (result not shown).

3.2. The Adherent Cell Population Is Made Up of Various Cell Types. In order to determine the type of cells that compose the culture, immunofluorescent analysis was performed. This revealed that certain cells were positive for a specific marker of smooth muscle cells (αSMactin$^+$), others for the specific marker of endothelial cells (CD31 and vWF^+).

We then quantified, by counting the percentage of each cell type among the adherent cell population the ratio between stained cells/nuclei stained by DAPI (Interchem) in 5 different microscopic visual fields per patient sample, at 40X magnification. These systematic enumerations revealed that the adherent cell population was composed of 23 ± 5% of anti-α-smooth muscle cells and 25 ± 5% of endothelial cells. Interestingly, the remaining adherents' cell population 52 ± 7% was systematically negative for the 2 markers tested.

3.3. The Adherents Cells Secrete Bioactive Proteins. After 3 days of culture, three samples of $CD133^+/CD34^+$ BMMNCs cells from 3 different donors were incubated with conditioned medium at 37°C for 36 h. The supernatants were tested by Ray-Bio protein array. As presented in Table 1, $CD133^+/CD34^+$ BMMNCs secrete *in vitro* important bioactive proteins such as cardiotropin-1, angiogenic factors (angiogenin, angiopoitein-2, basic fibroblast growth factor, placenta growth factor, (VEGF) vascular endothelial growth factor-121, VEGF-165, and VEGF-D), neurogenic factors (agouti-related protein, brain-derived neurotropic factor, human ciliary neurotrophic factor, basic nerve growth factor, amphiregulin, neurotrophin-3, and 4, activin A and prolactin), morphogenetic proteins (bone morphogenetic protein, BMP-4, 5, 6, and 7), and several proinflammatory and remodeling factors. Several cytokines were absent however among the bioactive proteins tested (results not shown).

3.4. Use of $CD133^+/CD34^+$ BMMNCs for Intracoronary Infusions. For cell therapy, isolated $CD133^+/CD34^+$ BMMNCs were injected into the coronary arteries via the femoral artery. Patients were examined after 3, 6, and 9 months.

The results of clinical examinations of patients at these two time intervals showed a net improvement beginning three months and also six and nine months after infusion. Examination indicated that the general physical state of patients improved, such as effort tolerance, physical endurance, and overall autonomy. In addition, the treated patients had a better psychic state "the effect of a perfect action" as compared to the control. One of the patients in the treated group died as also two others in the control group (one of them by accident).

3.5. Infarct Scar Size Was Reduced after Intra coronary Stem Cell Infusion. Myocardial Tc99m MIBI scintigraphy in 11 patients was performed to evaluate the dynamics of myocardial perfusion. Figure 2 presents the kinetics of uptake of Tc99 isotope in cardiac areas before and after stress (after 33 and 190 days of cell therapy). Scintigraphy investigations of heart in Eight out of 11 (Table 2) patients after 1 and 3 months of cell perfusion in left coronary artery ($n = 7$) and right coronary artery ($n = 1$) showed considerable increase in stable perfusion, as monitored by indicators. The continuing progress was again noted after a period of 9 months. In these patients, high inclusion of Tc99 (%) in the region of anteroseptal (Table 3(a)), inferoseptal (Table 3(b)), and apex (Table 3(c)) before cell therapy (rest and stress) and after cell therapy (stress) as determined. Images were assessed by quantitative measurements of activity in the area at risk and expressed as the difference between postoperative perfusion and preoperative perfusion. After a single infusion of stem cells (Figure 3), we noted a difference in Tc99 isotope uptake of myocardium in 5 out of 8 patients for Anteroseptal, 7 out of 8 patients for Inferoseptal and 6 out of 8 patients for

Table 1: Biological classification of the bioactive proteins secreted by the primo culture of $CD133^+/CD34^+$ BMMNCs (87 ± 4%/8 ± 5%) after 36 h in conditioned culture medium.

Growth factors secreted by $CD133^+/CD34^+$ BMMNCs
(a) Proangiogenic factors
Angiogenin
Angiopoitien-2
b-FGF (basic fibroblast growth factor)
PLGF (placenta growth factor)
VEGF-121 (vascular endothelial growth factor-121)
VEGF165 (vascular endothelial growth factor-165)
VEGF-D (vascular endothelial growth factor-D)
(b) Proinflammatory factors
I-309 (CCL-1 (C-C motif) ligand-1)
MCP-1 (CCL-2 (C-C motif) ligand-2)
MIP-1a (CCL-4 (C-C motif) ligand-4)
RANTES (CCL-5 (C-C motif) ligand-5)
IL-1ra (interleukin-1 receptor antagonist)
CXCL-16 (C-X-C motif) ligand-16
MIF (macrophage migration inhibitory factor)
sTNFR-1 (soluble tumor necrosis factor receptor-1)
(c) MMPs-TIMPs
MMP-1 (matrix metalloproteinase-1)
MMP-3 (matrix metalloproteinase-3)
MMP-9 (matrix metalloproteinase-9)
MMP-13 (matrix metalloproteinase-13)
TIMP-1 (tissue inhibitor of metalloproteinases-1)
TIMP-2 (tissue inhibitor of metalloproteinases-2)
TIMP-4 (tissue inhibitor of metalloproteinases-4)
(d) Neurophilic factors
AGRP (agouti-related protein)
BDNF (brain-derived neurotrophic factor)
CTNF (human ciliary neurotrophic factor)
b-NGF (basic nerve growth factor)
AREG (amphiregulin)
NT-3 (neurotrophin-3)
NT-4 (neurotrophin-4)
Activin A (promotes neural cell differentiation)
Prolactin (promotes neurogenesis in maternal and foetal brains)
(e) Morphogenetic proteins
BMP-4 (bone morphogenetic protein-4)
BMP-5 (bone morphogenetic protein-5)
BMP-6 (bone morphogenetic protein-6)
BMP-7 (bone morphogenetic protein-7)

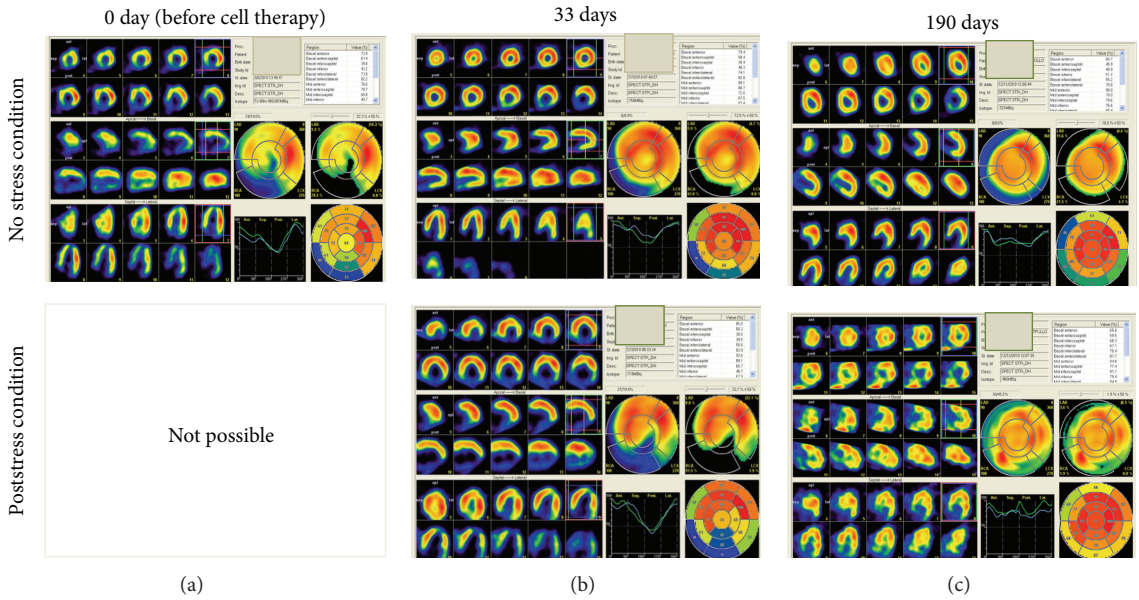

Figure 2: Kinetic of the areas that benefit from myocardial revitalization after cell therapy carried out by myocardial scintigraphy before and after 33 and 190 days. The strong uptake of Tc99 isotope in the inferoseptal region of the heart in poststress condition showed by arrow. (black, no perfusion; blue-green-yellow-red, increasing perfusion).

Table 2: characteristics of patients.

Samples	Patients	B.D	Diseases	Routes	I.C. infused cells $\times 10^4$
1	S.Sh.	1961	MI	LCA	60
2	Sh.I.	1944	MI	LCA	52
3	F.K.	1951	MI	LCA	116
4	A.L.	1950	MI	LCA	72
5	K.A.	1947	MI	LCA	80
6	B.M.	1948	MI	LCA	116
7	M.A.	1953	MI	RCA	76
8	M.Sh.	1966	MI	LCA	68

B.D: birth day, MI: myocardial infarction, LCA: left coronary artery, RCA: right coronary artery, intracoronary (I.C.) infused cells.

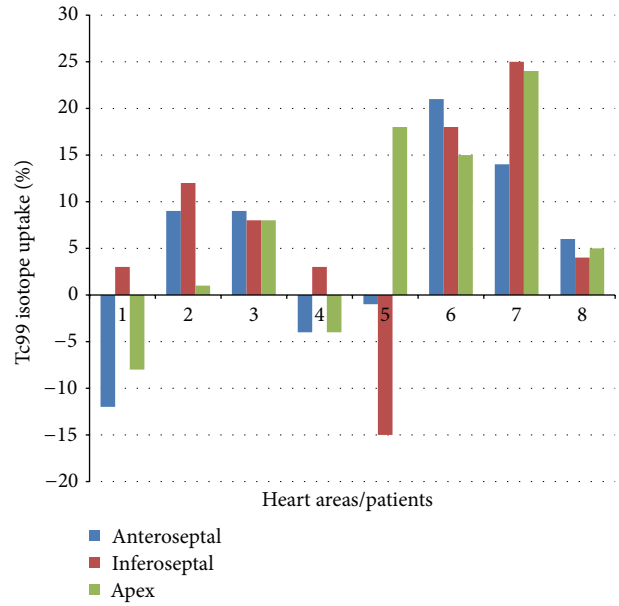

Figure 3: Tc99 isotope uptake in different areas of the heart I poststress condition, quantitative measurements of activity in the area at risk (anteroseptal, inferoseptal, and apex) expressed as the difference between postoperative perfusion and preoperative perfusion.

apex regions. These results show that revitalization of the myocardium is not the same in different anatomic parts of the heart.

As presented in Table 4, the treated patients were divided into two categories: (A) responders and (B) non responders. High inclusion of Tc99, after cell therapy, changed significantly only in inferoseptal region ($P = 0.016$) in responder patients ($n = 5$). In non responders, inclusion of Tc99 in different regions of the heart was not significantly different between preoperative and postoperative perfusion under stress conditions ($n = 3$). These results suggest that the inferoseptal zone is a good target for stem cell therapy. In 7 patients out of 8, uptakes of isotope in all parts of the heart were increased.

The areas that benefit from a myocardial revitalization, 9 months after cell therapy in case of two patients are presented in Figure 4. One of these two (Sh.I., patient no. 2), presented a minimal uptake of Tc99 before treatment in anterior, septal, anteroseptal and inferoseptal regions (Figure 4(a)).

Table 3: Scintigraphy investigations of heart in 8 out of 11 patients after a period of 9 months. High inclusion of Tc99 (%) in the regions of anteroseptal (a), inferoseptal (b), and apex (c) before cell therapy (rest and stress) and after cell therapy (stress). The difference between postoperative perfusion and preoperative perfusion in stress condition presented as evaluation.

(a) Anteroseptal regions of heart

No. of months	Patients	Anteroseptal before		Anteroseptal after treatment 9 months stress %	Evaluation stress %
		Rest %	Stress %		
1	S.Sh	62,0	81,0	69,0	−12
2	Sh.I	47,0	73,0	82,0	9
3	F.K	58,0	57	66,0	9
4	A.L	46,0	60,0	56,0	−4
5	K.A	55,0	73,0	72,0	−1
6	B.M	61,0	63,0	84,0	21
7	M.A	33,0	43,0	57,0	14
8	M.Sh	41,0	47,0	53,0	6

(b) Inferoseptal regions of heart

No. of months	Patients	Inferoseptal before		Inferoseptal after treatment 9 months stress %	Evaluation stress %
		Rest %	Stress %		
1	S.Sh	50,0	63,0	66,0	3
2	Sh.I	51,0	50,0	62,0	12
3	F.K	39,0	58	66,0	8
4	A.L	35,0	35,0	38,0	3
5	K.A	61,0	66,0	51,0	−15
6	B.M	71,0	57,0	75,0	18
7	M.A	45,0	43,0	68,0	25
8	M.Sh	41,0	50,0	54,0	4

(c) Apex regions of heart

No. of months	Patients	Apex before		Apex after treatment 9 months stress %	Evaluation stress %
		Rest %	Stress %		
1	S.Sh	51,0	67,0	59,0	−8
2	Sh.I	61,0	56,0	57,0	1
3	F.K	52,0	41,0	49,0	8
4	A.L	43,0	45,0	41,0	−4
5	K.A	58,0	48,0	66,0	18
6	B.M	70,0	59,0	74,0	15
7	M.A	55,0	44,0	68,0	24
8	M.Sh	56,0	59,0	64,0	5

After treatment, the regions of anterior and septal of the heart were strongly revitalized (Figure 4(b)). This patient was treated by 52×10^4 $CD133^+/CD34^+$ BMMNCs, and the cells were introduced by left coronary artery (LCA). In the second patient (M.A, patient no. 7), the septal, anteroseptal, and inferoseptal regions were damaged (Figure 4(a)). After cell therapy, revitalization was observed in all these regions (see Figure 4(b)). This patient was treated by 68×10^4 $CD133^+/CD34^+$ BMMNCs, and the cells were introduced by right coronary artery (RCA). These results clearly demonstrate a positive effect of cell therapy as ascertained by scintigraphic diagnostics with Tc99 m in patients with CHD and post-infarction cardiosclerosis during 9 months monitoring periods following cell therapy. These patients continue to make progress as of present.

4. Discussion

Bone marrow CD133-positive ($CD133^+$) cells possess strong hematopoietic and angiogenic capacity and can differentiate into several tissue types such as adipocyte, chondrocyte, osteocyte, neurocyte, and myocyte. We tested the feasibility, safety, and functional effects of the use of enriched $CD133^+$ progenitor cells after intracoronary administration in patients with coronary heart disease and post-infarction cardiosclerosis.

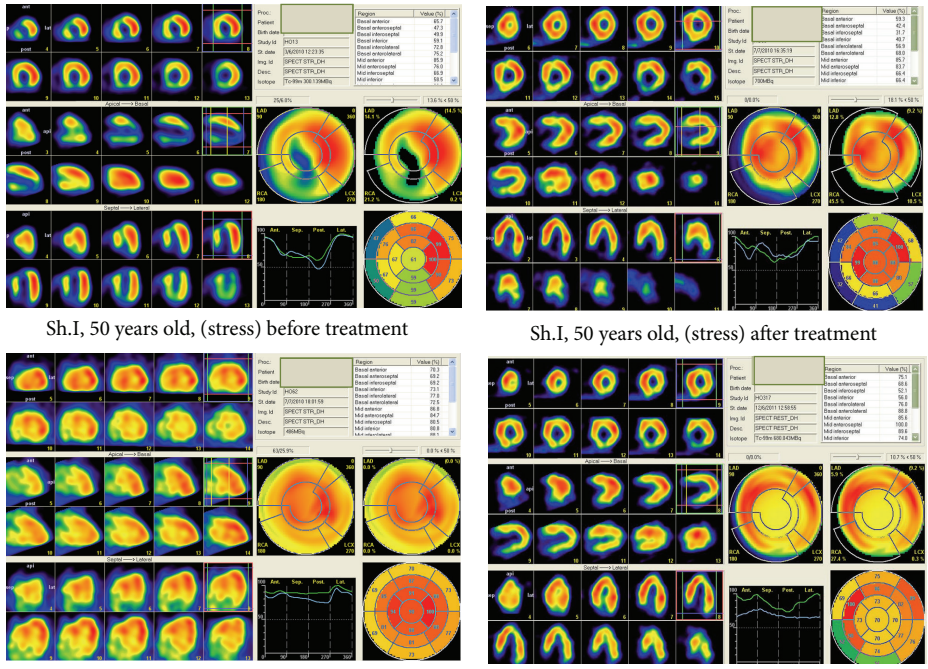

Figure 4: The areas that benefit from myocardial revascularization after single cell therapy in two patients, carried out by myocardial scintigraphy (post stress condition) before treatments and after 9 months (black, no perfusion; blue-green-yellow-red, increasing perfusion).

Table 4: Scintigraphic investigations of heart in (A) in responders (5 out of 8 patients) and (B) in nonresponders (3 out of 8 patients) before treatment and after a period of 9 months. Inclusion of Tc99 in the regions of anteroseptal, inferoseptal, and apex before and after cell therapy (stress condition) increased significantly only in inferoseptal region ($P = 0.016$) in responder patients. In nonresponders, inclusion of Tc99 in different regions of the heart was not significantly different between preoperative and postoperative perfusions under stress conditions.

(A)	Before treatment	After treatment	P value
Anteroseptal	56,60 ± 12,12	68,40 ± 14,55	0,194
Inferoseptal	51,60 ± 6,11	65,00 ± 7,75	0,016
Apex	51,80 ± 8,64	62,10 ± 9,71	0,106
(B)	Before treatment	After treatment	P value
Anteroseptal	71,33 ± 10,60	65,00 ± 6,7	0,510
Inferoseptal	50,33 ± 15,50	50,33 ± 12,0	1,00
Apex	49,67 ± 5,69	54,60 ± 12,6	0,566

We noted that when we use magnetic microbead technique for enrichment of $CD133^+$ cells, the cell preparation also contained $CD34^+$ progenitor cells. $CD133^+/CD34^+$ BMMNCs with specific medium can differentiate into several cells types such as endothelial cells, adipocyte, osteocyte, neurocyte, and myocyte [15] (results not shown). In this study, only differentiation of $CD133^+/CD34^+$ BMMNCs to endothelial and myofibroblasts with αSMactin$^+$ cells was demonstrated. These results confirm the earlier observation concerning the pluripotent nature of $CD133^+/CD34^+$ BMMNCs.

We analyzed the secretion of bioactive proteins of $CD133^+/CD34^+$ BMMNCs *in vitro*. The proteins secreted are angiogenic and neurogenic factors, morphogenetic proteins and several growth factors. One of the interesting bioactive proteins secreted by these cells is cardiotrophin-1 (CT-1) which is a member of the interleukin-6 type cytokine family. These cytokines mediate overlapping pleiotropic actions in a variety of cell types including cardiac myocytes, hepatocytes, megakaryocytes, osteoclasts, and neuronal cells. It is important to note that CT-1 was shown to specifically protect the cardiac myocytes from ischemic damage [16]. The role of CD133 in undertaking repair of heart regions is multistep and the intervention of several factors during the process undeniably reinforces our choice of CD133 for the treatment protocol in heart disease.

$CD133^+/CD34^+$ BMMNCs have also a strong pro-angiogenic capacity (Table 1(a)) as they secrete several factor such as angiogenin, angiopoitein-2, VEGF-121 (vascular endothelial growth factor) and 165, VEGF-D, PLGF (placenta growth factor) and b-FGF (basic fibroblast growth factor). These factors could be involved in angiogenesis/revascularization after cell therapy [17].

We have shown that $CD133^+/CD34^+$ BMMNCs also produce several pro-inflammatory factors including chemokines I-309 (CCL-1), MCP-1 (CCL-2), MIP-1 family (CCL-4), RANTES (CCL-5), interleukin-1 receptor antagonist (IL-1ra), CXCL-16, MIF, and sTNFR-1. These proinflammatory factors

secreted by the stem cells (Table 1(b)) in all probability intervene in tissue remodeling in the infarct zone.

Bone marrow stem cells secrete several interesting matrix metalloproteinase (MMPs) such as MMP1 (collagenase), MMP3 (stromelysin), MMP9 (gelatinase), MMP13 (collagenase), and their inhibitors (TIMPs): TIMP1, TIMP2, and TIMP4. MMPs belong to a larger family of proteases known for their role in remodeling extracellular matrix and affecting cell behaviors such as cell proliferation, migration, differentiation and angiogenesis. The tissue inhibitors of metalloproteinases are naturally occurring proteins that specifically inhibit matrix metalloproteinases and contribute towards maintaining a balance between matrix destruction and matrix formation (Table 1(c)). The presence of these specialized family proteins, secreted by stem cells, goes in favor of their importance in matrix guided remodeling of tissue substrates.

As presented in Tables 1(d) and 1(e), $CD133^+/CD34^+$ BMMNCs secrete neurophilic and bone morphogenetic bioactive proteins. The neurophilic factors essentially AGRP (agouti-related protein), BNDF (brain-derived neurotrophic factor), CNTF (human ciliary neurotrophic factor), AREG (schwannoma-derived growth factor, Amphiregulin) is a growth factor as well as a mitogen for astrocytes, Schwann cells, and fibroblasts [18], b-NGF (basic nerve growth factor), NT-3 (neurotrophin-3), NT-4 (neurotrophin-3), activin A, and prolactin (Table 1(d)). These factors promote neurogenesis and neural cell differentiation [19]. These factors are of importance in establishing/reestablishing axis of control between the myocardium and the nerve innervations.

The morphogenetic proteins produced by $CD133^+/CD34^+$ BMMNCs are BMP-4, BMP-5, BMP-6, and BMP-7 (Table 1(e)). These proteins constitute a group of important morphogenetic signals, needed in orchestering tissue architecture throughout the body [20]. They are the major actors during embryonic development, particularly in embryonic patterning and early skeletal formation [21]. They also participate in vasculature-guided neuronal migration under both normal and pathological conditions [22]. Once again, the coordinated action of angiogenic, neurogenics and morphogenic provided by $CD133^+/CD34^+$ BMMNCs seems necessary in the cellular mechanism leading to recovery of damage in the heart.

For regeneration of myocardium in heart disease, several strategies with different progenitor cells were proposed (see Section 1). Among these, use of $CD133^+/CD34^+$ BMMNCs seemed an attractive candidate. The fact is that the stem cells provide the molecular and cellular properties towards altering the microenvironment with which they come in contact seems unquestionable. They seem to have an inherent capacity for reprogramming of microenvironment at cellular and molecular levels. The cell-cell-matrix interaction is a necessary phase leading to tissues repair of injury/scar. It is thus obvious that $CD133^+/CD34^+$ BMMNCs stem cell therapy in heart disease is the one of choice that can be proposed to patients with minimal risk.

In this work, we therefore used $CD133^+/CD34^+$ BMMNCs in cardiac tissue remodeling in patients with coronary heart diseases and postinfarction cardiosclerosis. In 12 patient stem cells were introduced directly into the left coronary artery and in 3 cases: into both the left and the right coronary arteries. However in practice there were fewer injections of stem cells into the right coronary artery on account of frequent occurrence of occlusion of this blood vessel. In such cases, the introduction of the total dose of stem cells via the left coronary artery contributed to the passage of these cells in the ischemic zone of the right coronary artery through the collateral interconnections.

In 7 out of 8 patients, the cells were injected in left anterior descending coronary artery and only in one patient the cells were infused in right coronary artery. The patients were monitored during 1 to 9 months. We attempted using scintigraphy to follow up the effect of introduction of stem cells in the different areas of the heart. This study therefore confines to an *in situ* observation of heart condition after cell infusion.

Intracoronary stem cell infusion yielded a reduction of Infarct scar size. This revitalization that was observed in 11 of 15 patients (results not shown) may be due to an angiogenesis process after $CD133^+/CD34^+$ BMMNCs therapy or cardiomyogenesis, or both. $CD133^+$ cells can differentiate into both myocytes and endothelial cells, but $CD34^+$ cells may be differentiate to give only endothelial cells via angioblast maturation.

Nine months after cell therapy, 5 out of 8 patients showed a net positive response to therapy in different regions of the heart evaluated by scintigraphy. Uptake of Tc99 isotope and revitalization of the heart area in inferoseptal region are more pronounced as compared to the apex and anterospetal regions after intracoronary injection of the stem cells. In addition, we noted that uptakes of TC99 isotope in 2 patients before and after cell therapy 9 months after treatment. They showed that cell therapy by 2 different routes (LCA or RCA) was able to revitalize different areas of the heart and suggesting that stem cell therapy can generate the collateral vasculature for irrigation of heart areas. After 9 months, a better psychic state was also noted in all treated patients.

In conclusion, in this nonrandomized study, we indicate that CD133 BMMNCs secrete important bioactive proteins and can be an excellent choice for cell therapy. Intracoronary infusion of autologous $CD133^+/CD34^+$ BMMNCs reduces infarct size in patient with coronary heart disease and post infarction cardiosclerosis. The cell therapy approach proposed here should be practiced in conjunction with scintigraphy observation of areas of heart which respond optimally to the infusion of autologous $CD133^+/CD34^+$ BMMNCs.

Conflict of Interests

The authors have no financial conflict of interests.

Acknowledgments

The authors thank Mr. J. Almajid from Dubai, Prrofessor H. Sadeghi from Cardiovascular Surgery, University of Lausanne, and Dr. K. Farid from Hôtel Dieu Hospital, Paris, for their precious help. This study was funded by the Tajikistan

Ministry of Health, Clinical Trials, Government number, 01011TD053.

References

[1] A. J. Wagers and I. M. Conboy, "Cellular and molecular signatures of muscle regeneration: current concepts and controversies in adult myogenesis," *Cell*, vol. 122, no. 5, pp. 659–667, 2005.

[2] X. Shi and D. J. Garry, "Muscle stem cells in development, regeneration, and disease," *Genes and Development*, vol. 20, no. 13, pp. 1692–1708, 2006.

[3] A. Leri, J. Kajstura, and P. Anversa, "Role of cardiac stem cells in cardiac pathophysiology: a paradigm shift in human myocardial biology," *Circulation Research*, vol. 109, no. 8, pp. 941–961, 2011.

[4] A. Abdel-Latif, R. Bolli, I. M. Tleyjeh et al., "Adult bone marrow-derived cells for cardiac repair: a systematic review and meta-analysis," *Archives of Internal Medicine*, vol. 167, no. 10, pp. 989–997, 2007.

[5] J. Hoover-Plow and Y. Gong, "Challenges for heart disease stem cell therapy," *Journal of Vascular Health and Risk Management*, vol. 8, pp. 99–113, 2012.

[6] V. F. Segers and R. T. Lee, "Stem-cell therapy for cardiac disease," *Nature*, vol. 451, no. 7181, pp. 937–942, 2008.

[7] A. Aicher, C. Heeschen, K. I. Sasaki, C. Urbich, A. M. Zeiher, and S. Dimmeler, "Low-energy shock wave for enhancing recruitment of endothelial progenitor cells: a new modality to increase efficacy of cell therapy in chronic hind limb ischemia," *Circulation*, vol. 114, no. 25, pp. 2823–2830, 2006.

[8] M. Hofmann, K. C. Wollert, G. P. Meyer et al., "Monitoring of bone marrow cell homing into the infarcted human myocardium," *Circulation*, vol. 111, no. 17, pp. 2198–2202, 2005.

[9] R. Liao, O. Pfister, M. Jain, and F. Mouquet, "The bone marrow—cardiac axis of myocardial regeneration," *Progress in Cardiovascular Diseases*, vol. 50, no. 1, pp. 18–30, 2007.

[10] J. Thiele, E. Varus, C. Wickenhauser et al., "Mixed chimerism of cardiomyocytes and vessels after allogeneic bone marrow and stem-cell transplantation in comparison with cardiac allografts," *Transplantation*, vol. 77, no. 12, pp. 1902–1905, 2004.

[11] O. Agbulut, S. Vandervelde, N. Al Attar et al., "Comparison of human skeletal myoblasts and bone marrow-derived CD133+ progenitors for the repair of infarcted myocardium," *Journal of the American College of Cardiology*, vol. 44, no. 2, pp. 458–463, 2004.

[12] D. A. Taylor, B. Z. Atkins, P. Hungspreugs et al., "Regenerating functional myocardium: improved performance after skeletal myoblast transplantation," *Nature Medicine*, vol. 4, no. 8, pp. 929–933, 1998, Erratum in *Nature Medicine*, vol. 4, no. 10, pp. 1200, 1998.

[13] C. Stamm, B. Westphal, H. D. Kleine et al., "Autologous bone-marrow stem-cell transplantation for myocardial regeneration," *The Lancet*, vol. 361, no. 9351, pp. 45–46, 2003.

[14] S. L. M. A. Beeres, F. M. Bengel, J. Bartunek et al., "Role of imaging in cardiac stem cell therapy," *Journal of the American College of Cardiology*, vol. 49, no. 11, pp. 1137–1148, 2007.

[15] T. Tondreau, N. Meuleman, A. Delforge et al., "Mesenchymal stem cells derived from CD133-positive cells in mobilized peripheral blood and cord blood: proliferation, Oct4 expression, and plasticity," *Stem Cells*, vol. 23, no. 8, pp. 1105–1112, 2005.

[16] M. Jougasaki, "Cardiotrophin-1 in cardiovascular regulation," *Advances in Clinical Chemistry*, vol. 52, pp. 41–76, 2010.

[17] M. Lohela, M. Bry, T. Tammela, and K. Alitalo, "VEGFs and receptors involved in angiogenesis versus lymphangiogenesis," *Current Opinion in Cell Biology*, vol. 21, no. 2, pp. 154–165, 2009.

[18] K. J. Wilson, C. Mill, S. Lambert et al., "EGFR ligands exhibit functional differences in models of paracrine and autocrine signaling," *Growth Factors*, vol. 30, no. 2, pp. 107–116, 2012.

[19] H. Park and M. M. Poo, "Neurotrophin regulation of neural circuit development and function," *Nature Reviews Neuroscience*, vol. 14, no. 1, pp. 7–23, 2012.

[20] B. van Wijk, A. F. M. Moorman, and M. J. B. van den Hoff, "Role of bone morphogenetic proteins in cardiac differentiation," *Cardiovascular Research*, vol. 74, no. 2, pp. 244–255, 2007.

[21] M. Wan and X. Cao, "BMP signaling in skeletal development," *Biochemical and Biophysical Research Communications*, vol. 328, no. 3, pp. 651–657, 2005.

[22] Y. Sun, T. Fei, T. Yang et al., "The suppression of CRMP2 expression by Bone Morphogenetic Protein (BMP)-SMAD gradient signaling controls multiple stages of neuronal development," *The Journal of Biological Chemistry*, vol. 285, no. 50, pp. 39039–39050, 2010.

Hindawi Publishing Corporation
Stem Cells International
Volume 2013, Article ID 892065, 9 pages
http://dx.doi.org/10.1155/2013/892065

Research Article

Hepatocyte Growth Factor-Loaded Biomaterials for Mesenchymal Stem Cell Recruitment

Julia van de Kamp,[1] Willi Jahnen-Dechent,[2] Bjoern Rath,[3] Ruth Knuechel,[1] and Sabine Neuss[1,2]

[1] *Institute of Pathology, Aachen University Hospital, RWTH Aachen University, 52074 Aachen, Germany*
[2] *Biointerface Group, Helmholtz Institute of Biomedical Engineering, Biointerface Group, RWTH Aachen University, 52074 Aachen, Germany*
[3] *Department of Orthopaedic Surgery, Aachen University Hospital, RWTH Aachen, 52074 Aachen, Germany*

Correspondence should be addressed to Sabine Neuss; sabine.neuss@post.rwth-aachen.de

Received 14 March 2013; Revised 2 May 2013; Accepted 7 May 2013

Academic Editor: Weian Zhao

Human adult mesenchymal stem cells (MSC) can be readily harvested from bone marrow through aspiration. MSC are involved in tissue regeneration and repair, particularly in wound healing. Due to their high self-renewal capacity and excellent differentiation potential *in vitro*, MSC are ideally suited for regenerative medicine. The complex interactions of MSC with their environment and their influence on the molecular and functional levels are widely studied but not completely understood. MSC secrete, for example, hepatocyte growth factor (HGF), whose concentration is enhanced in wounded areas and which is shown to act as a chemoattractant for MSC. We produced HGF-loaded biomaterials based on collagen and fibrin gels to develop a recruitment system for endogenous MSC to improve wound healing. Here, we report that HGF incorporated into collagen or fibrin gels leads to enhanced and directed MSC migration *in vitro*. HGF-loaded biomaterials might be potentially used as *in vivo* wound dressings to recruit endogenous MSC from tissue-specific niches towards the wounded area. This novel approach may help to reduce costly multistep procedures of cell isolation, *in vitro* culture, and transplantation usually used in tissue engineering.

1. Introduction

Wound healing is involved in all processes of tissue regeneration and repair. Its complex processes depend on the proper interactions between cells of different origin and extracellular matrix (ECM) components. Beside, cells of the immune system and diverse resident cells, mesenchymal stem cells (MSC) play a key role in wound healing [1].

Human MSC can be isolated from various tissues (e.g., bone marrow or adipose tissue) and their stem cell characteristics are described in detail since the pioneering work of Friedenstein and coworkers in 1968 [2, 3]. In addition, MSC possess immunomodulatory and trophic properties, making them a promising cell source for regenerative medicine [4]. Endogenous MSC migrate towards the damaged area, participating strongly in the wound healing response through paracrine communication [5]. Paracrine communication occurs via a concerted action of bioactive factors, such as vascular endothelial growth factor, epidermal growth factor, keratinocyte growth factor, and hepatocyte growth factor (HGF) [6, 7]. HGF is outstanding because of its proangiogenic and chemotactic properties. Its receptor c-met is expressed in MSC, making the cells migrate towards a higher HGF gradient. This gradient is additionally established by macrophages and apoptotic cells [8, 9]. Furthermore, MSC participate in the wound response through the secretion of ECM molecules, thus influencing tissue remodeling and wound contraction [10].

In chronic wounds, healing processes are disordered and delayed requiring medical intervention to improve the healing situation [11]. Biomaterials can serve as wound dressings to provide a structure in case of severe tissue loss. Natural and artificial biomaterials can influence cell behavior in different ways, for example, in viability, proliferation,

and differentiation. Among the wide range of prospective biomaterials, fibrin and collagen are suitable candidates for wound healing [12, 13]. Fibrin, a native component highly involved in blood coagulation, is a key factor in wound healing as shown in one of the first animal studies [14]. Over the years, fibrin has come to use as a tool for cell and drug delivery [15–17] as well as for the expansion of cord blood-derived hematopoietic stem cells [18]. The first use of collagen as a natural matrix has enhanced wound healing in a porcine study [19]. In recent years, collagen has been shown to induce chemotaxis and haptotaxis of rabbit and human MSC [20]. It also exhibits increasing valuable influence on the interaction and differentiation of MSC [21]. Collagen is a potential nonimmunogenic degradable scaffold for the incorporation of MSC in dermal tissue engineering [10].

In the present study, we analyzed the effect of HGF incorporated into fibrin and collagen gels on the recruitment and migration of MSC using standardized *in vitro* assays. We carried out a scratch assay, a simple, time-, and cost-efficient method to evaluate cell migration [22]. In addition, we used a modified Boyden chamber assay to evaluate the chemotactic activity of HGF on cell migration [23].

In summary, the concept of MSC being involved in the process of wound healing and tissue repair is widely accepted. Fibrin, collagen, and HGF are useful components to direct MSC migration *in vitro* and *in vivo*. Our study sheds light on the motility of MSC in the context of two degradable biomaterials in combination with HGF. We describe for the first time a robust and directed MSC migration towards HGF released from fibrin and collagen *in vitro*. These results pave the way for the development of a recruitment system for endogenous MSC to improve wound healing in burns or chronic diseases *in vivo*.

2. Materials and Methods

2.1. Mesenchymal Stem Cell Isolation and Cell Culture. Procedures were approved by the local ethics committee. Human donors gave informed consent. Human mesenchymal stem cells (MSC) were isolated from femoral heads according to the protocols of Haynesworth et al. and Pittenger et al. [3, 24]. Briefly, femoral heads of patients undergoing total hip joint endoprosthesis were rinsed several times with stem cell medium, containing 60% DMEM, 40% MCDB-201, 1x ITS + BSA-linoleic acid, 1 nM dexamethasone, 100 μM ascorbic acid, 10 ng/mL EGF, 40.000 U Penicillin, 40 mg Streptomycin, and 2% FCS (PAN Biotech, Aidenbach, Germany). Cell suspension was transferred to a 50 mL tube and centrifuged at 500 g for 10 minutes. The cell pellet was resuspended in fresh medium and seeded in a T75 tissue culture flask. After 24 hours, nonadherent cells were removed by medium change. At 80–90% confluence, stem cells were trypsinized with stem cell trypsin (Invitrogen, Darmstadt, Germany) and reseeded in a density of 5.000 cells/cm^2 for optimal proliferation. Medium change occurred every 3-4 days. All cells were characterized by flow cytometry and multipotency using standard protocols as required by the International Society for Cellular Therapy [25, 26] and as previously described [8]. Cells were incubated in a 20% O_2 and 5% CO_2 humidified atmosphere at 37°C. Cells in passages between 2 and 5 were used for the experiments.

2.2. Fibrin Gel Preparation. Fibrin gels were prepared by polymerization using thrombin and fibrinogen as described before [27]. A fibrinogen solution was prepared by dissolving 160 mg fibrinogen powder in 8 mL of water (*aqua ad iniectabilia)* in 8 mL GBSH5 buffer incomplete. The mixture was transferred into a dialysis tube and equilibrated with GBSH5 buffer incomplete at 4°C over night. The next day, the fibrinogen solution was placed into an Oak Ridge Centrifuge Tube and centrifuged at 1200 g for 30 min. The clear supernatant was aspirated, sterile filtrated, and frozen at −80°C. Directly before cell seeding, $CaCl_2$ buffer (50 mM in ddH20, sterile filtrated) and GBSH5 buffer complete were added to fibrinogen. For polymerization, 10 μL thrombin (1000 U/mL) and 180 μL fibrinogen solutions were mixed in a 24-well plate. In addition, 75 ng/mL HGF was added before polymerization. The plate was shaken carefully to enhance polymerization and incubated at 37°C for 20 min. After polymerization, medium was added. All results were based on five independent experiments ($n = 5$).

2.3. Collagen Gel Preparation. Collagen gels were generated as previously described [28, 29]. Briefly, eight volumes of acidic collagen G (3 mg/mL collagen I/III in 12 mM HCl) were mixed with one volume 10-fold DMEM (both from Biochrom, Berlin, Germany), following neutralization with 2 M sodium hydroxide. One volume of medium ±75 ng/mL HGF (PromoCell, Heidelberg, Germany) was added to the gel mixture. The gel was placed in the bottom compartment of a 24-well plate and incubated at 37°C for 2 h to polymerize, and medium was added afterwards. All results were based on five independent experiments ($n = 5$).

2.4. HGF ELISA. HGF was incorporated before polymerization of the gels in a 96-well plate. Supernatant was collected after 1, 2, 4, 6, 8, 24, 48, and 168 hours of culture. HGF ELISA (PromoCell GmbH, Heidelberg) was carried out according to the manufacturers' instructions. Briefly, standards and samples were incubated in a 96-well plate at 4°C overnight. The next day, biotin antibody was added to each well and incubated for 1 h at room temperature. Afterwards, streptavidin solution was added and the plate was left to incubate for 45 minutes at room temperature. Next, TMB one-step substrate reagent was added to each well and incubated for 30 minutes at room temperature. Stop solution was added before the plate was read at 450 nm.

2.5. Scratch Assay. Cells were grown until confluence in both compartments of a culture-insert (ibidi GmbH, Martinsried, Germany) inside a 24-well format dish (Figure 1). The inserts were used for creating uniform scratch dimensions throughout the experiments. Inserts were removed carefully and medium ±75 ng/mL HGF was added to each well. Closure of the resulting *in vitro* wound was documented photographically at 0, 8, 16, and 24 h after removal of the insert. Pictures

Figure 1: Culture-insert in a 24-well format dish to produce uniform scratches in parallel samples.

were processed with Adobe Photoshop 7.0 and analyzed with Octave 3.2.4.

2.6. Boyden Chamber Assay. For analysis of directed cell migration, MSC were seeded in a density of 10^5 cells/mL in the top compartment of a transwell system (Corning Costar, Corning, USA) (modified Boyden chamber) in a 24-well plate. The top compartment was separated from the bottom compartment by a polycarbonate membrane with 8 μm pores. To exclude a solely chemokinetic effect of HGF on the migration of MSC, we simultaneously added the same concentration of HGF to the top and the bottom compartment and also only to the top compartment. Collagen or fibrin ±75 ng/mL HGF was deposited in the bottom compartment as described above. This assay was termed "migration assay."

To mimic the *in vivo* situation and to check for possible delayed release of HGF from the biomaterials, collagen and fibrin were both coated with a thin layer of Matrigel (BD biosciences, Franklin Lakes, USA). This assay was termed "invasion assay." To analyze any chemotactic/chemokinetic influence of Matrigel itself on the cells, the bottom of the lower compartment of the transwell (without biomaterials) was covered with a thin layer of Matrigel.

In both assays, basal migration (no HGF, no biomaterial) was used for normalizing values; medium +HGF in lower compartment served as an internal control. Cells were allowed to migrate for 24 hours before analysis and quantification. After removal of the transwell, the top cell layer was wiped off with a lint-free cloth (Wepa, Arnsberg, Germany); membranes were fixated and stained with Hemacolor (Merck, Darmstadt, Germany) and mounted on objective slides with cover slips and Vitro-Clud (Langenbrinck, Emmendingen, Germany). Cells on the bottom side of the membrane were quantified in 5 different high-power fields per membrane at 200-fold magnification. Each analysis was performed in triplicate for five different donors.

2.7. Statistical Analysis. Data were presented as mean values ± standard deviation (SD). One-way ANOVA and Tukey's posttest were used for statistical analysis; significance was defined as $^{*}P < 0.05$, $^{**}P < 0.005$, $^{***}P < 0.001$. The corresponding graphical representations were generated with GraphPad Prism 4.0 (GraphPad Software Inc., San Diego, USA).

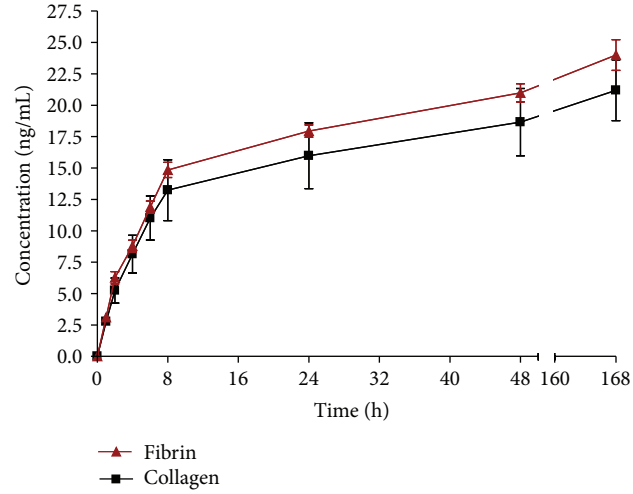

Figure 2: HGF (ng/mL) released from fibrin and collagen gels over time. 75 ng/mL HGF was incorporated into collagen and fibrin gels. Supernatant was used for ELISA and gels without HGF served as control. $n = 2$.

3. Results & Discussion

3.1. HGF ELISA. The release kinetics of HGF from fibrin and collagen gels was analyzed with a human HGF ELISA kit. During the first 8 hours, HGF was released quickly both from collagen and fibrin (17% and 20%, resp.). After this time, HGF was released in a more gradual way. In total, both biomaterials show a comparable release kinetic. However, a higher concentration of HGF was flushed out from fibrin compared to collagen. After a total of 168 hours, the cumulative releases of HGF from collagen and fibrin were about 28% and 32%, respectively (Figure 2). A continued gradual release process of HGF is expected, because over 60% of HGF is still present in the biomaterials. After the initially strong release, the favored slow release of HGF is expected, which is reasonable for *in vivo* applications. Therefore, our system shows promising results *in vitro*. In our ongoing *in vivo* study (mouse), we specifically focus on the inflammatory phase, in which several growth factors, such as platelet-derived growth factor and vascular endothelial growth factor, are released rapidly by macrophages to attract inflammatory cells [30]. Our HGF kinetics can be correlated to the physiological conditions described by Clark and Henson [31] as well as Cohen and colleagues [32].

Xu and colleagues studied the controlled release of HGF from a bovine scaffold for vocal fold reconstruction. They came to similar release kinetics for HGF from acellular scaffolds. They showed a total release of 32.6% HGF after 7 days, which is in accordance with our results [33]. For both of our gels, the HGF release is well acceptable and will be analyzed further in terms of cell migration and degradation properties in our *in vivo* model.

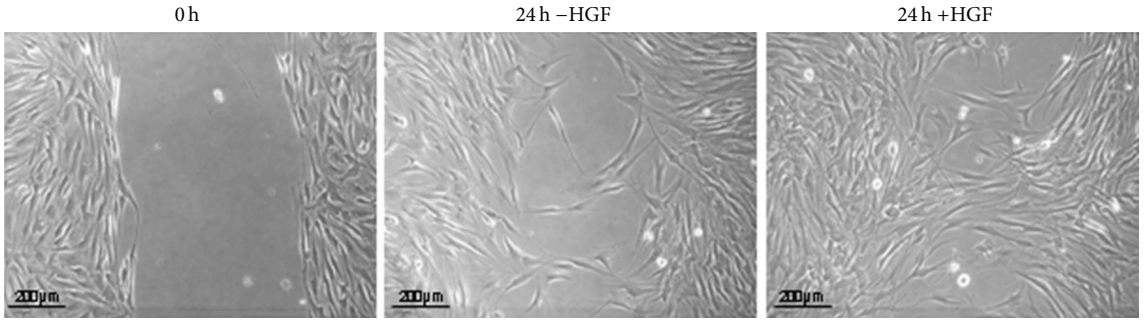

Figure 3: MSC ±HGF after 0 and 24 hours. All assays were carried out with 4 different donors in passages 2 to 5. One representative donor is shown exemplarily. Scale bars: 200 μm.

A study on the potential of collagenous matrices as release carriers of exogenous growth factors was carried out by Kanematsu et al. [34]. They analyzed the *in vivo* release of several growth factors (bFGF, HGF, PDGF-BB, VEGF, and HB-EGF) from a collagen sponge over a period of 28 days. After 7 days of implantation, 70% HGF was released from the matrix and a strong correlation between the release profile and the degradation profile of the matrix was found.

3.2. Scratch Assay. Based on a scratch assay by Neuss et al. [8], a cell migration assay was carried out (Figure 3). Neuss and colleagues determined the HGF concentration which was optimal for cell migration in the range of 50 to 100 ng/mL. We chose 75 ng/mL for all assays. MSC were cultured in culture inserts until confluence; inserts were removed (=0 hours) and stem cell medium ±75 ng/mL HGF was added. No difference in cell migration in the presence or absence of HGF was observed after 8 and 16 hours (data not shown). However, after 24 hours, MSC cultured with HGF showed a higher number of migratory cells (approx. 50% of cell-free area covered) than the counterparts without HGF (approx. 25% of cell-free area covered; Figure 4).

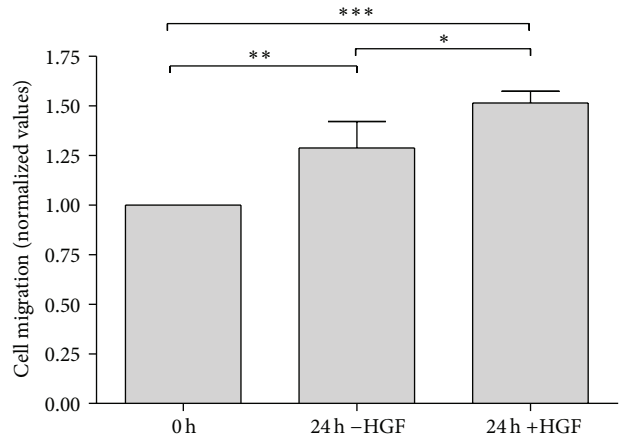

Figure 4: Analysis of HGF-dependent MSC migration after 24 hours in the presence and absence of HGF. Results based on $n = 4$. $^{*}P < 0.05$, $^{**}P < 0.01$, $^{***}P < 0.001$.

A number of *in vitro* studies reported on HGF as a chemoattractant for different cell types, thus underlining our findings. All studies showed an enhanced, if not significantly increased, cell migration in the presence of HGF compared to counterparts cultured with less concentration of HGF or no HGF [35–38]. Interestingly, cotreatment of HGF with transforming growth factor-β1 led to superior cell migration than HGF alone, suggesting a combination of cytokines as beneficial for wound healing, too [39]. Recently, a new quantitative approach for analyzing long-term kinetics of wound healing was introduced. Adenocarcinoma cell lines migrated in a coordinated and collective fashion and expressed a higher cell velocity in the presence of HGF, therefore showing accelerated wound closure [40]. In summary, HGF has a strong chemotactic influence on the cell migration of different cell types.

3.3. Boyden Chamber Assay. To further evaluate the migratory influence of HGF on MSC, we based our first Boyden chamber experiment on the results described by Neuss and coworkers [8]. To check for any chemokinetic influences of HGF, the assay was carried out with the same concentration of HGF but differently localized (no HGF = basal migration, bottom compartment only, top and bottom compartment, Figure 5; and top compartment only, Figure 6). The chemotactic effect of HGF is significantly stronger than the chemokinetic effect. MSC migration is clearly enhanced ($^{*}P < 0.05$; Figure 5) when compared to basal migration and when equal amounts of HGF are present in both compartments simultaneously. This effect has also been described by Zheng et al. [41] and confirms our hypothesis of the chemotactic effect of HGF on the migratory behavior of MSC.

Based on the scratch assays results, we further investigated the effects of HGF incorporated into collagen and fibrin using a modified Boyden chamber assay. For both assays, migration (biomaterials) and invasion (biomaterials plus a thin layer of Matrigel), collagen and fibrin were either free of or loaded with 75 ng/mL HGF (Figure 7).

Migration Assay. HGF in medium alone (no biomaterial) showed a significant increase in cell migration compared to basal migration (without HGF, without biomaterial) as previously described for different cell types [8, 36, 42]. In addition, HGF incorporated into collagen and fibrin showed

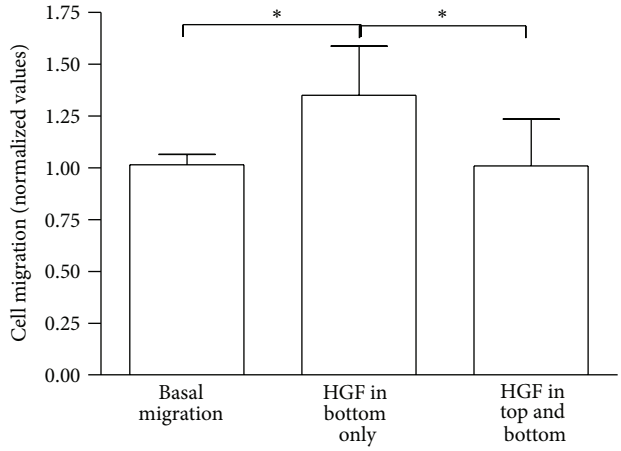

Figure 5: Boyden chamber assay with HGF in top and bottom compartment. All values compared to basal migration and based on $n = 4$. $^{*}P < 0.05$.

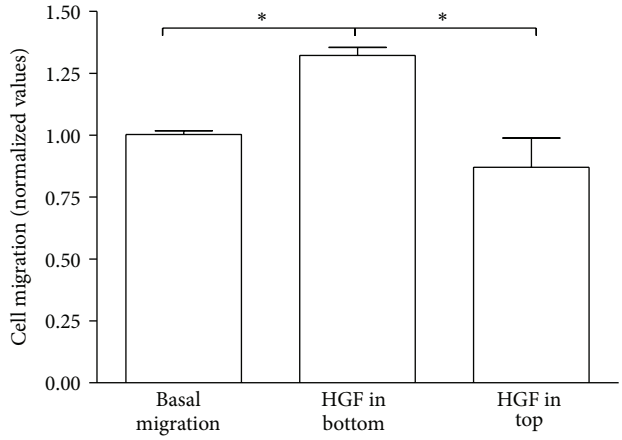

Figure 6: Boyden chamber assay with HGF in top compartment only. Values compared to basal migration and HGF in bottom compartment only. $n = 2$. $^{*}P < 0.05$.

a significantly higher cell migration than basal migration (approx. 56% and 31%, resp.; Figures 8(a) and 8(c)). Since our project aims for a release of HGF with the help of wound dressings for chronic diseases or burns from a natural carrier material, these results are useful for future *in vivo* studies.

A haptotactic effect of fibrin on the migration of vascular smooth muscle cells was described early [43]. Another study on the dose-dependent effect of fibrin on bovine endothelial cells showed the positive influence of fibrin on the migratory activity of the cells [44]. In our study, we did not observe this effect of fibrin without HGF on the MSC, but only in combination with HGF (Figure 8(c)). We think that MSC might not be as susceptible to fibrin and its components as vascular and/or endothelial cells since both of these cell types were shown to play a key role in the regulation of the inflammation site in wound healing (through their interaction with fibrinogen metabolites and other migrating cells) [45]. A study combining HGF into fibrin was carried out by Zhang

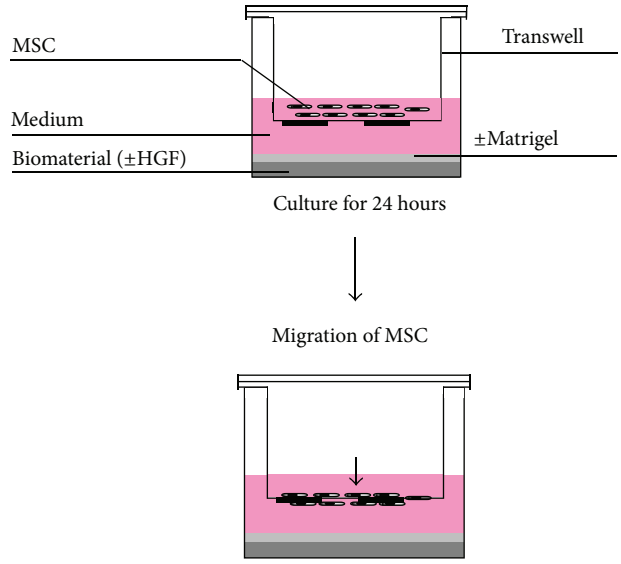

Figure 7: Sketch of modified Boyden chamber assay.

and colleagues, who used fibrin as an injectable biomatrix. They stated the efficacy of a PEGylated fibrin biomatrix regarding stem cell transplantation for the regeneration of myocardium in a murine model [46]. The authors considered HGF loading of biomaterials a platform technology with potential applications in other biomaterial and growth factor combinations as well. Along these lines, fibrin could serve as a potential carrier of HGF in a wound dressing.

As early as 1981, different concentrations of human collagen (type I, III, V) were found to have chemotactic effects on various types of tumor cells [47]. Later on, the chemo- and haptotactic effects of type I collagen were described for rabbit and human MSC [20]. These descriptions are in accordance with our findings. A modified assay (membrane coated with type I collagen) to evaluate the invasion of endometrial adenocarcinoma cell lines stimulated by the addition of HGF in a dose-dependent manner [48] underlines our results. Although the modification was different to ours, type I collagen was found to enhance cell migration. A few years ago, Bhargava and coworkers showed the diffusion of HGF from a collagen gel, enhancing the repair of meniscal injuries in a dog study. Particularly in combination with platelet-derived growth factor, HGF released from collagen exerted a significantly higher effect on the cell migration to the simulated defect than collagen gel alone [49].

In vivo models need to be performed to evaluate to what extend the direct incorporation of HGF into fibrin and collagen influences MSC migration. One study by Kanematsu et al. showed the release profile of HGF, among other growth factors, incorporated into a collagenous matrix which was implanted into mouse subcutis [34]. This group described collagen type I as a suitable carrier for growth factors regarding the *in vivo* release in a mouse model. Their results, based solely on *in vivo* experiments, indicate the functionality of our *in vitro* analyzed system in our upcoming mouse study.

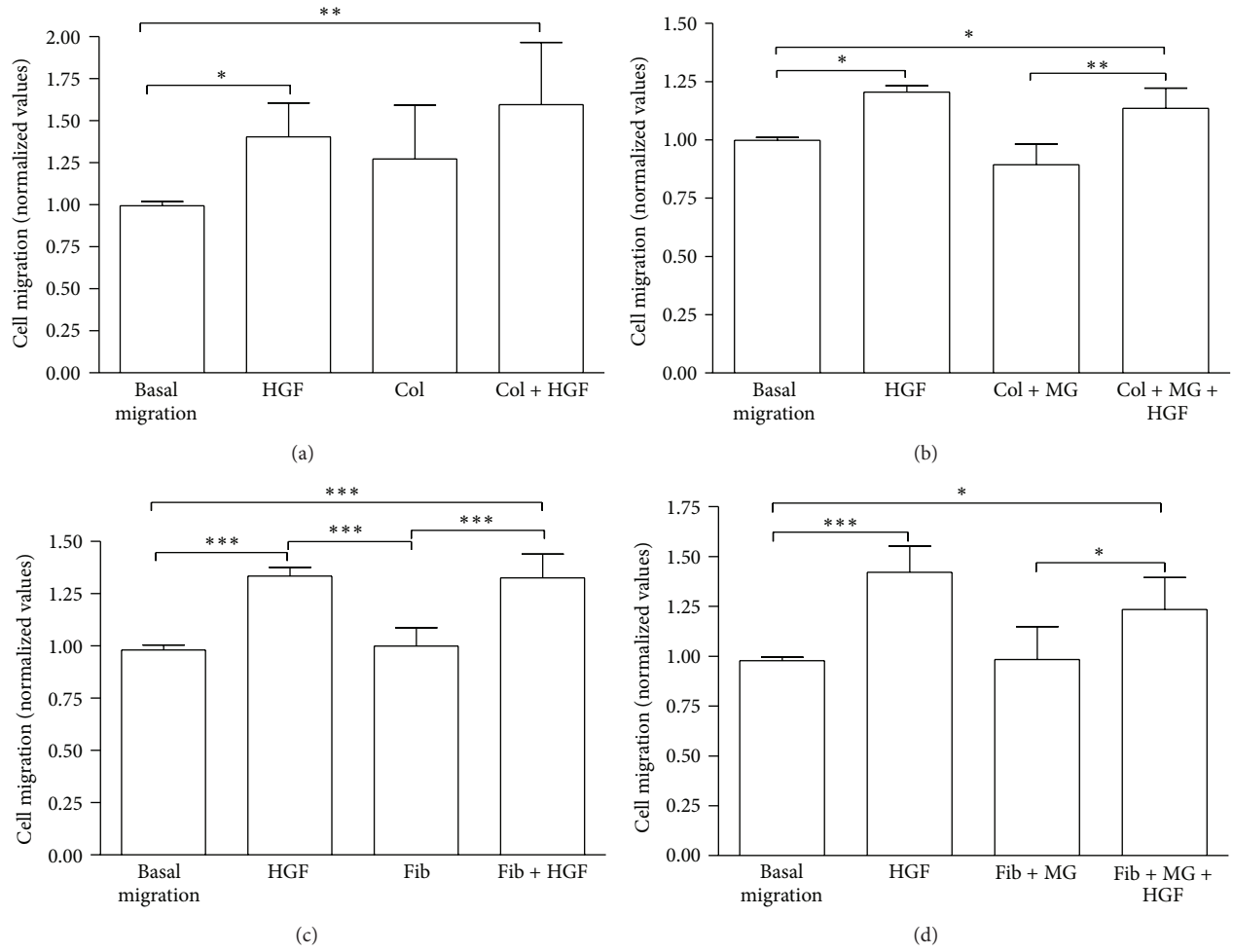

Figure 8: MSC migration towards biomaterials ±75 ng/mL HGF. Migration assay ±HGF in (a) collagen and (c) fibrin. Invasion assay ±HGF + layer of Matrigel on (b) collagen and (d) fibrin. All values normalized to basal migration. $^{*}P < 0.05$, $^{**}P < 0.01$, $^{***}P < 0.001$. All results based on $n = 5$.

Overall, the aforementioned studies are in accordance with our findings, so that HGF alone and in combination with collagen and fibrin acted as a promoter of higher MSC motility and migration.

Invasion Assay. To mimic the *in vivo* situation of foreign body response after implantation of (HGF-loaded) biomaterials, collagen and fibrin were coated with a thin layer of Matrigel. As in the migration assays, HGF in stem cell medium alone showed significantly higher cell migration than basal migration. Collagen with HGF coated with Matrigel showed a significantly higher cell migration (approx. 22%) compared to collagen without HGF but with Matrigel. The same result was found for fibrin (approx. 25%; Figures 8(b) and 8(d)). Here, Matrigel ±HGF served as control to exclude any possible chemotactic effects of Matrigel on MSC (Figure 9). We deliberately chose to coat the biomaterials on the bottom of the well (not the membrane) to check for a possible retarded release of HGF from the biomaterials in this particular experiment, which is a novel adaptation of the Boyden chamber assay, since all previous studies (exclusively in cancer research) described the coating of the membranes.

To exclude any possible chemotactic or chemokinetic effect of Matrigel on the migration of MSC, the modified Boyden chamber assay was carried out without collagen and fibrin gel, but only with Matrigel on the bottom of the plate. There is no difference in the migration of cells when the wells are coated with a thin layer of Matrigel compared to basal migration. However, when HGF is added to the bottom compartment coated with Matrigel, the cell migration is significantly enhanced ($^{***}P < 0.001$, Figure 9). Therefore, we can exclude any effect of Matrigel on the cell migration and further evaluated the effect of the collagen and fibrin gels.

Even though the Boyden chamber is the method of choice for the investigation of cell motility and directed migration, studies regarding the combinatory approach of fibrin and Matrigel are absent. Matrigel-coated membrane assays have been applied in the field of angiogenesis, invasive cell migration, penetration of the basement membrane, and the preclinical development of anti-invasive and antiangiogenic agents [50–53], and they were reviewed recently [54]. However, the Boyden chamber assay has not been previously used to test growth factor-loaded biomaterials with fibrin and

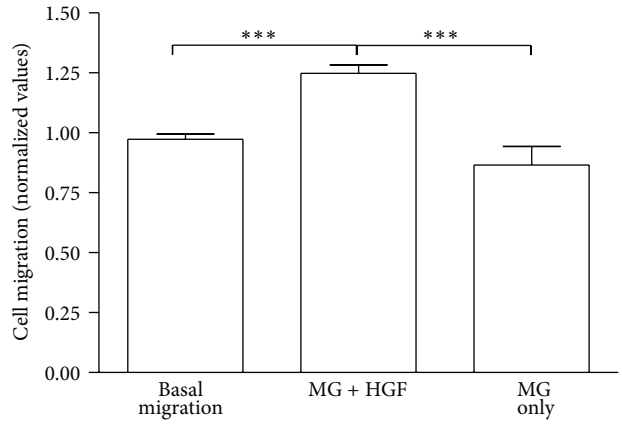

Figure 9: MSC invasion assay with Matrigel ±HGF. MG: Matrigel. All values normalized to basal migration. $^{***}P < 0.001$. Results represent $n = 3$.

MSC. In an early approach with type I collagen as the major structural component of the boundary layer, the coating with type IV collagen and laminin established a selective barrier [55]. These results were similar to our findings using the combination of collagen and MSC.

When coating the Boyden chamber inserts with type IV collagen on both sides and using HGF in various concentrations (10 to 100 ng/mL) for different human lung cancer cell lines, both chemotactic and chemokinetic motilities on tumor cells were induced [56]. Another group coated both sides of the filter with type I collagen because they previously found that this was an appropriate molecule to support adhesion and migration of MSC. In their comprehensive analysis of chemotactic factors for bone marrow MSC and rabbit MSC, they concluded HGF to be an essential concentration-dependent chemoattractant for rabbit and human MSC [57]. Both studies once more emphasized the important influence of HGF on the chemotactic and chemokinetic motility of different cell types. All in all, our approach opens up new insights into the topic of growth factor-induced chemotaxis. In summary, collagen and fibrin are promising candidates as HGF carriers, which we will elucidate in further *in vivo* studies.

4. Conclusion

We were able to show the gradual release of HGF from both collagen and fibrin gels, which is an important prerequisite for our MSC recruitment system. Furthermore, we showed the positive effect of HGF dissolved in medium or released from fibrin or collagen gels (coated with or without Matrigel) on the directed migration and recruitment of human mesenchymal stem cells *in vitro*. Since Matrigel alone did not have any chemotactic or chemokinetic effect on the migration of the cells, we deduce enhanced migration solely from HGF and HGF in combination with fibrin and collagen gels.

In the clinics, HGF-loaded biomaterials could be immediately implanted into chronic wounds or burn areas, thus overcoming the critical issues of time and costs for *in vitro* cell expansion. To further elucidate the direct mechanisms of fibrin and collagen gels with HGF on cell migration and wound healing, we will hereafter start an *in vivo* model.

Conflict of Interests

The authors declare that they have no conflict of interests.

Acknowledgments

The authors thank Norina Labude for excellent technical assistance throughout the study, Julia Falkenstein and Svenja Petersen (all Institute of Pathology, RWTH Aachen University) for performing ELISA assays, and the DFG for funding this project.

References

[1] W. M. Jackson, L. J. Nesti, and R. S. Tuan, "Concise review: clinical translation of wound healing therapies based on mesenchymal stem cells," *Stem Cells Translational Medicine*, vol. 1, no. 1, pp. 44–50, 2012.

[2] A. J. Friedenstein, K. V. Petrakova, A. I. Kurolesova, and G. P. Frolova, "Heterotopic of bone marrow. Analysis of precursor cells for osteogenic and hematopoietic tissues," *Transplantation*, vol. 6, no. 2, pp. 230–247, 1968.

[3] M. F. Pittenger, A. M. Mackay, S. C. Beck et al., "Multilineage potential of adult human mesenchymal stem cells," *Science*, vol. 284, no. 5411, pp. 143–147, 1999.

[4] H. K. Salem and C. Thiemermann, "Mesenchymal stromal cells: current understanding and clinical status," *Stem Cells*, vol. 28, no. 3, pp. 585–596, 2010.

[5] J. M. Sorrell and A. I. Caplan, "Topical delivery of mesenchymal stem cells and their function in wounds," *Stem Cell Research & Therapy*, vol. 1, no. 4, p. 30, 2012.

[6] L. Chen, E. E. Tredget, P. Y. G. Wu, and Y. Wu, "Paracrine factors of mesenchymal stem cells recruit macrophages and endothelial lineage cells and enhance wound healing," *PLoS One*, vol. 3, no. 4, article e1886, 2008.

[7] L. Li, Y. Zhang, Y. Li et al., "Mesenchymal stem cell transplantation attenuates cardiac fibrosis associated with isoproterenol-induced global heart failure," *Transplant International*, vol. 21, no. 12, pp. 1181–1189, 2008.

[8] S. Neuss, E. Becher, M. Wöltje, L. Tietze, and W. Jahnen-Dechent, "Functional expression of HGF and HGF receptor/c-met in adult human mesenchymal stem cells suggests a role in cell mobilization, tissue repair, and wound healing," *Stem Cells*, vol. 22, no. 3, pp. 405–414, 2004.

[9] S. Vogel, T. Trapp, V. Börger et al., "Hepatocyte growth factor-mediated attraction of mesenchymal stem cells for apoptotic neuronal and cardiomyocytic cells," *Cellular and Molecular Life Sciences*, vol. 67, no. 2, pp. 295–303, 2010.

[10] R. K. Schneider, J. Anraths, R. Kramann et al., "The role of biomaterials in the direction of mesenchymal stem cell properties and extracellular matrix remodelling in dermal tissue engineering," *Biomaterials*, vol. 31, no. 31, pp. 7948–7959, 2010.

[11] K. G. Harding, H. L. Morris, and G. K. Patel, "Science, medicine, and the future: healing chronic wounds," *British Medical Journal*, vol. 324, no. 7330, pp. 160–163, 2002.

[12] S. Siedler and S. Schuller-Petrovic, "Allogenic keratinocytes suspended in human fibrin glue used for wound healing support in chronic leg ulcers," *Archives of Dermatology*, vol. 136, no. 5, pp. 676–678, 2000.

[13] H. M. Powell and S. T. Boyce, "EDC cross-linking improves skin substitute strength and stability," *Biomaterials*, vol. 27, no. 34, pp. 5821–5827, 2006.

[14] R. A. Clark, J. M. Lanigan, P. DellaPelle, E. Manseau, H. F. Dvorak, and R. B. Colvin, "Fibronectin and fibrin provide a provisional matrix for epidermal cell migration during wound reepithelialization," *Journal of Investigative Dermatology*, vol. 79, no. 5, pp. 264–269, 1982.

[15] W. Bensaïd, J. T. Triffitt, C. Blanchat, K. Oudina, L. Sedel, and H. Petite, "A biodegradable fibrin scaffold for mesenchymal stem cell transplantation," *Biomaterials*, vol. 24, no. 14, pp. 2497–2502, 2003.

[16] V. Falanga, S. Iwamoto, M. Chartier et al., "Autologous bone marrow-derived cultured mesenchymal stem cells delivered in a fibrin spray accelerate healing in murine and human cutaneous wounds," *Tissue Engineering*, vol. 13, no. 6, pp. 1299–1312, 2007.

[17] P. P. Spicer and A. G. Mikos, "Fibrin glue as a drug delivery system," *Journal of Controlled Release*, vol. 148, no. 1, pp. 49–55, 2010.

[18] M. S. Ferreira, W. Jahnen-Dechent, N. Labude et al., "Cord blood-hematopoietic stem cell expansion in 3D fibrin scaffolds with stromal support," *Biomaterials*, vol. 33, no. 29, pp. 6987–6997, 2012.

[19] G. Ksander and Y. Ogawa, "Collagen wound healing matrices and process for their production," US patent no. 4,950,483, 1990.

[20] M. M. Thibault, C. D. Hoemann, and M. D. Buschmann, "Fibronectin, vitronectin, and collagen I induce chemotaxis and haptotaxis of human and rabbit mesenchymal stem cells in a standardized transmembrane assay," *Stem Cells and Development*, vol. 16, no. 3, pp. 489–502, 2007.

[21] S. Neuss, R. Stainforth, J. Salber et al., "Long-term survival and bipotent terminal differentiation of human mesenchymal stem cells (hMSC) in combination with a commercially available three-dimensional collagen scaffold," *Cell Transplantation*, vol. 17, no. 8, pp. 977–986, 2008.

[22] C. C. Liang, A. Y. Park, and J. L. Guan, "In vitro scratch assay: a convenient and inexpensive method for analysis of cell migration in vitro," *Nature Protocols*, vol. 2, no. 2, pp. 329–333, 2007.

[23] S. Boyden, "The chemotactic effect of mixtures of antibody and antigen on polymorphonuclear leucocytes," *The Journal of Experimental Medicine*, vol. 115, no. 3, pp. 453–466, 1962.

[24] S. E. Haynesworth, J. Goshima, V. M. Goldberg, and A. I. Caplan, "Characterization of cells with osteogenic potential from human marrow," *Bone*, vol. 13, no. 1, pp. 81–88, 1992.

[25] E. M. Horwitz, K. le Blanc, M. Dominici et al., "Clarification of the nomenclature for MSC: the International Society for Cellular Therapy position statement," *Cytotherapy*, vol. 7, no. 5, pp. 393–395, 2005.

[26] M. Dominici, K. le Blanc, I. Mueller et al., "Minimal criteria for defining multipotent mesenchymal stromal cells. The International Society for Cellular Therapy position statement," *Cytotherapy*, vol. 8, no. 4, pp. 315–317, 2006.

[27] S. Neuss, R. K. M. Schneider, L. Tietze, R. Knüchel, and W. Jahnen-Dechent, "Secretion of fibrinolytic enzymes facilitates human mesenchymal stem cell invasion into fibrin clots," *Cells Tissues Organs*, vol. 191, no. 1, pp. 36–46, 2010.

[28] R. K. M. Schneider, S. Neuss, R. Stainforth et al., "Three-dimensional epidermis-like growth of human mesenchymal stem cells on dermal equivalents: contribution to tissue organization by adaptation of myofibroblastic phenotype and function," *Differentiation*, vol. 76, no. 2, pp. 156–167, 2008.

[29] J. van de Kamp, R. Kramann, J. Anraths et al., "Epithelial morphogenesis of germline-derived pluripotent stem cells on organotypic skin equivalents *in vitro*," *Differentiation*, vol. 83, no. 3, pp. 138–147, 2012.

[30] A. J. Singer and R. A. F. Clark, "Cutaneous wound healing," *The New England Journal of Medicine*, vol. 341, no. 10, pp. 738–746, 1999.

[31] R. A. F. Clark and P. M. Henson, *The Molecular and Cellular Biology of Wound Repair*, Plenum Press, New York, NY, USA, 1988.

[32] I. K. Cohen, R. F. Diegelmann, and W. J. Lindblad, *Wound Healing: Biochemical and Clinical Aspects*, W. B. Saunders Company, Philadelphia, Pa, USA, 1992.

[33] C. C. Xu, R. W. Chan, D. G. Weinberger, G. Efune, and K. S. Pawlowski, "Controlled release of hepatocyte growth factor from a bovine acellular scaffold for vocal fold reconstruction," *Journal of Biomedical Materials Research Part A*, vol. 93, no. 4, pp. 1335–1347, 2010.

[34] A. Kanematsu, S. Yamamoto, M. Ozeki et al., "Collagenous matrices as release carriers of exogenous growth factors," *Biomaterials*, vol. 25, no. 18, pp. 4513–4520, 2004.

[35] R. L. H. Bigelow and J. A. Cardelli, "The green tea catechins, (-)-Epigallocatechin-3-gallate (EGCG) and (-)-Epicatechin-3-gallate (ECG), inhibit HGF/Met signaling in immortalized and tumorigenic breast epithelial cells," *Oncogene*, vol. 25, no. 13, pp. 1922–1930, 2006.

[36] K. P. Xu and F. S. X. Yu, "Cross talk between c-met and epidermal growth factor receptor during retinal pigment epithelial wound healing," *Investigative Ophthalmology and Visual Science*, vol. 48, no. 5, pp. 2242–2248, 2007.

[37] J. Chmielowiec, M. Borowiak, M. Morkel et al., "c-Met is essential for wound healing in the skin," *Journal of Cell Biology*, vol. 177, no. 1, pp. 151–162, 2007.

[38] S. Cerny-Reiterer, V. Ghanim, G. Hoemann et al., "Identification of basophils as a major source of hepatocyte growth factor in chronic myeloid leukemia: a novel mechanism of BCR-ABL1-independent disease progression," *Neoplasia*, vol. 14, no. 7, pp. 572–584, 2012.

[39] H. J. Nam, Y. Y. Park, G. Yoon, H. Cho, and J. H. Lee, "Co-treatment with hepatocyte growth factor and TGF-β1 enhances migration of HaCaT cells through NADPH oxidase-dependent ROS generation," *Experimental and Molecular Medicine*, vol. 42, no. 4, pp. 270–279, 2010.

[40] A. Zaritsky, S. Natan, E. Ben-Jacob, and I. Tsarfaty, "Emergence of HGF/SF-induced coordinated cellular motility," *PLoS One*, vol. 7, no. 9, Article ID e44671, 2012.

[41] B. Zheng, C. Wang, L. He et al., "Neural differentiation of mesenchymal stem cells influences chemotactic responses to HGF," *Journal of Cellular Physiology*, vol. 228, no. 1, pp. 149–162, 2013.

[42] G. Forte, M. Minieri, P. Cossa et al., "Hepatocyte growth factor effects on mesenchymal stem cells: proliferation, migration, and differentiation," *Stem Cells*, vol. 24, no. 1, pp. 23–33, 2006.

[43] M. Naito, T. Hayashi, M. Kuzuya, C. Funaki, K. Asai, and F. Kuzuya, "Effects of fibrinogen and fibrin on the migration of vascular smooth muscle cells in vitro," *Atherosclerosis*, vol. 83, no. 1, pp. 9–14, 1990.

[44] J. Qi and D. L. Kreutzer, "Fibrin activation of vascular endothelial cells: induction of IL-8 expression," *Journal of Immunology*, vol. 155, no. 2, pp. 867–876, 1995.

[45] R. A. F. Clark, "Fibrin and wound healing," *Annals of the New York Academy of Sciences*, vol. 936, pp. 355–367, 2001.

[46] G. Zhang, Q. Hu, E. A. Braunlin, L. J. Suggs, and J. Zhang, "Enhancing efficacy of stem cell transplantation to the heart with a PEGylated fibrin biomatrix," *Tissue Engineering. Part A*, vol. 14, no. 6, pp. 1025–1036, 2008.

[47] G. R. Mundy, S. DeMartino, and D. W. Rowe, "Collagen and collagen-derived fragments are chemotactic for tumor cells," *Journal of Clinical Investigation*, vol. 68, no. 4, pp. 1102–1105, 1981.

[48] V. Bae-Jump, E. M. Segreti, D. Vandermolen, and S. Kauma, "Hepatocyte growth factor (HGF) induces invasion of endometrial carcinoma cell lines in vitro," *Gynecologic Oncology*, vol. 73, no. 2, pp. 265–272, 1999.

[49] M. M. Bhargava, C. Hidaka, J. A. Hannafin, S. Doty, and R. F. Warren, "Effects of hepatocyte growth factor and platelet-derived growth factor on the repair of meniscal defects in vitro," *In Vitro Cellular and Developmental Biology. Animal*, vol. 41, no. 8-9, pp. 305–310, 2005.

[50] A. Albini, Y. Iwamoto, H. K. Kleinman et al., "A rapid in vitro assay for quantitating the invasive potential of tumor cells," *Cancer Research*, vol. 47, no. 12, pp. 3239–3245, 1987.

[51] L. A. Repesh, "A new in vitro assay for quantitating tumor cell invasion," *Invasion and Metastasis*, vol. 9, no. 3, pp. 192–208, 1989.

[52] D. Muir, L. Sukhu, J. Johnson, M. A. Lahorra, and B. L. Maria, "Quantitative methods for scoring cell migration and invasion in filter-based assays," *Analytical Biochemistry*, vol. 215, no. 1, pp. 104–109, 1993.

[53] S. Yamakawa, Y. Furuyama, and N. Oku, "Development of a simple cell invasion assay system," *Biological and Pharmaceutical Bulletin*, vol. 23, no. 10, pp. 1264–1266, 2000.

[54] A. Albini and D. M. Noonan, "The 'chemoinvasion' assay, 25 years and still going strong: the use of reconstituted basement membranes to study cell invasion and angiogenesis," *Current Opinion in Cell Biology*, vol. 22, no. 5, pp. 677–689, 2010.

[55] V. P. Terranova, E. S. Hujanen, D. M. Loeb, G. R. Martin, L. Thornburg, and V. Glushko, "Use of a reconstituted basement membrane to measure cell invasiveness and select for highly invasive tumor cells," *Proceedings of the National Academy of Sciences of the United States of America*, vol. 83, no. 2, pp. 465–469, 1986.

[56] C. G. Bredin, Z. Liu, D. Hauzenberger, and J. Klominek, "Growth-factor-dependent migration of human lung-cancer cells," *International Journal of Cancer*, vol. 82, no. 3, pp. 338–345, 1999.

[57] Y. Ozaki, M. Nishimura, K. Sekiya et al., "Comprehensive analysis of chemotactic factors for bone marrow mesenchymal stem cells," *Stem Cells and Development*, vol. 16, no. 1, pp. 119–129, 2007.

Hindawi Publishing Corporation
Stem Cells International
Volume 2013, Article ID 656839, 11 pages
http://dx.doi.org/10.1155/2013/656839

Research Article

Dynamic Imaging of Marrow-Resident Granulocytes Interacting with Human Mesenchymal Stem Cells upon Systemic Lipopolysaccharide Challenge

Jay T. Myers,[1] Deborah S. Barkauskas,[1] and Alex Y. Huang[1,2]

[1] *Department of Pediatrics, Division of Pediatric Hematology/Oncology, Case Western Reserve University School of Medicine, Cleveland, OH 44106-7288, USA*
[2] *Department of Pathology, Case Western Reserve University School of Medicine, Cleveland, OH 44106-7288, USA*

Correspondence should be addressed to Alex Y. Huang; alex.y.huang@case.edu

Received 20 January 2013; Accepted 27 February 2013

Academic Editor: G. Phinney Donald

Human mesenchymal stem cells (hMSCs) have gained intense research interest due to their immune-modulatory, tissue differentiating, and homing properties to sites of inflammation. Despite evidence demonstrating the biodistribution of infused hMSCs in target organs using static fluorescence imaging or whole-body imaging techniques, surprisingly little is known about how hMSCs behave dynamically within host tissues on a single-cell level *in vivo*. Here, we infused fluorescently labeled clinical-grade hMSCs into immune-competent mice in which neutrophils and monocytes express a second fluorescent marker under the lysozyme M (LysM) promoter. Using intravital two-photon microscopy (TPM), we were able for the first time to capture dynamic interactions between hMSCs and $LysM^+$ granulocytes in the calvarium bone marrow of recipient mice during systemic LPS challenge in real time. Interestingly, many of the infused hMSCs remained intact despite repeated cellular contacts with host neutrophils. However, we were able to observe the destruction and subsequent phagocytosis of some hMSCs by surrounding granulocytes. Thus, our imaging platform provides opportunities to gain insight into the biology and therapeutic mechanisms of hMSCs *in vivo* at a single-cell level within live hosts.

1. Introduction

Human mesenchymal stem cells (hMSCs) are self-renewing precursor cells capable of differentiating into bone, adipose tissue, cartilage, and stromal cells of the bone marrow depending on the stimuli [1]. Available data indicate that hMSCs are pericytes whose pleiotropic nature allows them to sense and respond to inflammatory processes in the microenvironment [2]. Although hMSCs are found at low frequency *in vivo* in a variety of adult tissues including bone marrow, muscle, fat, and dermis, they can be expanded to large numbers under appropriate culture conditions. For this reason, hMSCs have been applied therapeutically in rapidly expanding clinical investigations including more than 200 currently active clinical trials worldwide [1, 3–6]. A wide range of diseases including diabetes, atherosclerosis, multiple sclerosis, systemic lupus, Crohn's disease, myocardial infarction, stroke, Parkinson's disease, bone and cartilage repair, wound healing, and graft-versus-host disease [1, 3] have been treated using hMSCs as a cellular therapy. These clinical trials aimed to explore the therapeutic potential of hMSCs with regard to their immune-modulatory properties, tissue regenerative capacity, graft enhancement, tissue protection, and repair capabilities. Similarly, hMSCs have been applied *in vivo* for their efficacy in a variety of human disease models in immune-competent mice including skin and spinal cord repair [7], Huntington's disease, [8], other demyelinating diseases [9], and graft-versus-host disease [10].

Despite intense research interest and active clinical applications of hMSCs, there has been some controversy and little evidence regarding the biodistribution and actual cellular behavior of hMSCs upon infusion *in vivo*. Investigators have

utilized a variety of whole-body imaging and static histological analyses to track the presence and possible local function of hMSCs in diseased and normal anatomical sites [11]. These tracking modalities include magnetic resonance imaging [12, 13], near-infrared whole-body *in vivo* imaging system [14], chromium^{51} (Cr-51) tracking [15], and bioluminescence and static fluorescence microscopy [16–21]. Recently, Eggenhofer et al. traced the fate of Cr-51 labeled syngeneic MSCs that had been infused intravenously into C57BL/6 mice and showed that viable MSCs could only be recovered in the lungs up to 24 hours after infusion [22]. Based on these data, the authors concluded that MSCs are rather short-lived after intravenous infusion, that viable MSCs were trapped within the lung tissue with some cellular debris transported to and cleared in the liver, and that infused MSCs must exert their immune-modulatory and regenerative effects via a third-party cell type.

All of the studies mentioned above were useful in demonstrating that, under inflammatory insults or tissue injury, infused hMSCs accumulate at disease sites, thus supporting the hypothesis of their *in vivo* survival and homing capacity to target organs. However, whole-organ or whole-mouse tracking studies lacked the single-cell resolution within the intact tissue microenvironment to fully explore the behavior of infused hMSCs. On the other hand, high-resolution detection of fixed tissue analyses was devoid of the dynamic information regarding cellular migrations and interactions, which are hallmarks of essential immune cell functions *in vivo*. What would be more informative is the study of individual hMSC interaction dynamics within undisrupted live tissue microenvironment in real time.

In our current study, we utilized intravital TPM to monitor intravenously infused, fluorescently labeled hMSCs in the bone marrow of immune competent mice in which host myeloid cells expressing lysozyme M (LysM)—principally neutrophils and monocytes—can be concurrently tracked at the single-cell level. By observing in high-definition the interaction dynamics between hMSCs and host innate immune cells before and after a systemic LPS challenge, we provide the first glimpse into how hMSCs behave locally with surrounding immune cells in the native murine bone marrow environment, thereby directly refuting the claims of a previous study which argues that since viable MSCs do not go past the lungs, the immune-modulatory and regenerative effects of infused MSC must therefore be mediated via other cell types. Furthermore, we also captured *in vivo* the active process of hMSC destruction by LysM-expressing cells in the bone marrow.

2. Materials and Methods

2.1. Mice. C57BL/6 mice (stock #664) were obtained from Jackson Laboratory (Bar Harbor, ME, USA). C57BL/6 mice containing GFP inserted into the *lysozyme M* locus ($LysM^{+/GFP}$) were obtained from Dr. Thomas Graf [23]. Eight-to-twelve-week-old mice were used for these experiments. Animals were housed, bred, and handled in the Animal Resource Center facilities at Case Western Reserve University according to the approved protocols. Similarly, all animal experiments were executed with strict adherence to active experimental animal protocols approved by Case Western Reserve University Institutional Animal Care and Use Committee.

2.2. Cell Labeling and Injections. Clinical-grade marrow-derived hMSCs were obtained from the Hematopoietic Stem Cell Core Facility in the Case Comprehensive Cancer Center at Case Western Reserve University where they had been expanded and characterized to possess renewal and tri-lineage differentiation potential (osteogenic, chondrogenic, and adipogenic) [24–28]. We refer to these cells as hMSCs rather than hMSPCs (human mesenchymal stem and progenitor cells) (1) since these hMSCs have been demonstrated to enrich stem cell activity as part of the routine protocol in the Hematopoietic Stem Cell Facility at the Case Comprehensive Cancer Center. Briefly, aliquots of frozen hMSCs were thawed and washed in pre-warmed complete media (αMEM supplemented with L-glutamine, pen/strep, Fungizone, and 10% FCS). They were then washed twice with PBS and subsequently labeled with either 5 μM CellTracker Red CMTPX (Invitrogen) or 2.5 μM CellTracker Orange CMTMR (CTO; Invitrogen) at room temperature in PBS for 15 minutes. Two-to-four-fold volumes of PBS with 1% FBS were added to quench the labeling reaction and the cells were washed twice with PBS. Labeled cells were then injected *i.v.* at various concentrations. Where indicated, mice were also injected *i.v.* with 100 ng of *S. enterica* LPS (Sigma).

2.3. Mouse Surgery and Preparation for Intravital Imaging. Intravital TPM of the calvarium was performed as previously described [29]. Briefly, mice were anesthetized with nebulized isoflurane (2% induction, 1.5% maintenance) in 30% O_2/70% air and placed in a stereotactic holder. The hair on top of the skull was clipped and the remaining hair removed with Nair hair remover. The skin was then excised, and dental acrylic was used to create a trough on top of the calvarium to maintain the water column to facilitate imaging. The animal body temperatures were monitored and maintained between 36.5 and 38°C using a combination of a temperature-controlled environmental chamber, heating pads, and a rectal probe throughout the entire mouse preparation and imaging session. Breathing rate and animal responsiveness were used to ensure adequate levels of anesthesia. Respiratory rate was maintained at ~60–100 breaths per minute and animal responsiveness was assessed by foot and tail pinch. Ten to 30 minutes prior to imaging, mice were injected *i.v.* with either 100 μL of 2.5 mg/mL FITC-dextran (Sigma) or 100 μL of 0.2 μM QTracker-655 (Invitrogen) to allow blood vessel visualization as indicated.

2.4. TPM Equipment and Data Acquisition. Upon completion of the tissue preparation for intravital imaging, the entire mouse imaging assembly, including the stereotactic holder, was placed on the microscope stage that was enclosed within a custom-made temperature-controlled environmental chamber. The tissues were imaged using a Leica SP5

fitted with a DM6000 stage, a 20X water immersion lens (N.A. 1.0; Leica HCX-APO-L), and a 16W Ti/Sapphire IR laser (Chameleon, Coherent) tuned to excitation wavelengths between 800 nm and 860 nm. Imaging planes (776 × 776 μm) collected at 5 μm z steps were repeated at 30-second intervals for up to 3 hours to yield *xyzt* datasets collected through a four-channel nondescanned external detector using a filter set separating ≤495 nm, 500–550 nm, 565–605 nm, and 625–675 nm emission spectra. The raw imaging data set was then used for the processing and analysis using Imaris software (BitPlane, Inc.) as described below.

2.5. Immunofluorescence Histology. After completion of intravital bone marrow imaging, hMSC-infused $LysM^{+/GFP}$ mice were sacrificed by CO_2 asphyxiation. Lungs, liver, lymph node, and spleen were harvested and fixed in 2% PFA at 4°C. High-resolution *xyz* imaging stacks of the fixed, unsectioned samples were collected using the Leica SP5/two-photon imaging equipment as described above. Image stacks were analyzed using Imaris software (BitPlane, Inc.) as described below.

2.6. Image Analysis. High-resolution fluorescent 4D imaging data sets collected from intravital TPM experiments were analyzed using the Imaris software (BitPlane, Inc.). A typical imaging volume of 776 × 776 × 150 μm^3 was analyzed. We utilized channel subtraction algorithms available in the Imaris Software in order to determine the localization of hMSC-CTO signal in relation to the LysM-GFP signal in the bone marrow. In short, a new CTO channel was created using the Matlab Channel Arithmatics Function in Imaris in which the CTO signals (channel 3, AKA ch3) which overlap the GFP signal (ch2) were removed by subtraction: ch3-ch2. This step subtracts the fluorescence of the GFP channel from the CTO channel at the pixel level. Cell identification and tracking were performed using the Spots Analysis Function in Imaris with the cell diameter set at 15 μm. The *xyzt* positional data for both the hMSCs and $LysM^+$ cells was exported to Matlab for further analysis of interaction frequency between hMSCs and $LysM^+$ neutrophils. We defined neutrophil interaction with the hMSC by parsing the neutrophils whose center of mass was within a 20 μm radius from that of a hMSC, compared the number of neutrophils that satisfied this positional requirement to the total cell number in the image field, and averaged over 30-minute intervals to derive the time average % of cellular interactions. To determine the directional migration of the neutrophils in relation to the hMSCs, we compared the angular components of individual instantaneous velocity of the neutrophils with 25 μm radius to the hMSC and compared them to the vector angle formed between the centers of the neutrophil and the hMSC. We identified any neutrophils that were either moving towards (<95°) or away (>95° and <180°) from the hMSC and calculated a "cell flux index" defined as: (number of cells migrating towards-number of cells migrating away)/total cells within the 25 μm radius of the hMSC. The cells designated as moving towards the hMSC include those that possess a tangential directional angle (at 90°), with an absolute angular limit value of 95°.

3. Results

To test the biodistribution and tissue homing potential of the hMSCs in immune-competent mice, we fluorescently labeled 4×10^6 hMSCs and administered them intravenously into C57BL/6 recipient mice. One day later, these mice were then subjected to both intravital TPM imaging of the bone marrow through intact calvarium, and static, fixed whole-organ TPM imaging of the lung, liver, lymph node, and spleen (Figure 1(a)). As expected from other published reports, we found a large number of the infused hMSCs in the lungs, liver and spleen, with 1443, 1825, and 4142 cells per mm^3 of imaged tissue, respectively. Interestingly, we were able to easily detect fewer numbers of hMSCs in the lymph node and the bone marrow, with 90 and 337 cells per mm^3 of imaged tissues, respectively (Figure 1(b)).

Even though we could easily visualize individual $CMTPX^+$ signals in various anatomical sites following hMSC infusion, these initial *in vivo* whole-organ tracking experiments of fluorescently labeled hMSCs were against a backdrop of the dark background in the imaging fields which are known to be packed full of a myriad of nonfluorescent host cells. In particular, from the first set of experiments, we could not formally distinguish whether the visualized fluorescent signals were coming from intact hMSCs, or from phagocytes such as neutrophils or monocytes that had phagocytosed dead hMSC debris that arrived at the liver, lymphoid organs, or the bone marrow. Indeed, a recent report indicates that, at least in the murine system, live mouse MSCs that had been administered intravenously could only be found in the lungs, whereas only MSC debris was found in the liver and spleen [22]. In order to rigorously test this, we employed high-resolution dynamic TPM imaging to the bone marrow cavity underneath the calvarium. Furthermore, we chose as recipients the $LysM^{+/GFP}$ mice in which the gene encoding the green fluorescent protein (GFP) replaced the *LysM* locus encoding lysozyme M, an enzyme that is highly expressed in granulocytes such as neutrophils and, to a lesser extent, monocytes [23]. Using this combination of fluorescent probes, we set out to observe the cellular integrity and interactions between labeled hMSCs with bone-marrow-resident neutrophils and monocytes ("granulocytes"). We fluorescently tagged 8×10^6 hMSCs with CTO and injected them *i.v.* into a naive $LysM^{+/GFP}$ mouse, then performed intravital TPM imaging of the bone marrow cavity in the mouse calvarium a day later. As shown in Figure 1, multiple hMSCs could be visualized to colocalize in the same general vicinity of the bone marrow with the $LysM^+$ granulocytes, with most hMSCs in close proximity to the granulocytes while few cells were seen to be devoid of contact with the GFP^+ cells (Figure 2(a)). Most of the visualized hMSC-associated CTO signals occupied the perivascular region of the bone marrow, confirming the previously, published findings [30–32] (Figure 2(b)). However, the CTO-labeled hMSCs do not express GFP (Figure 2(b)). Upon close inspection, some CTO signals could be seen as intracellular inclusions within GFP^+ $LysM^+$ granulocytes, suggesting that cellular debris from infused CTO-labeled hMSCs were

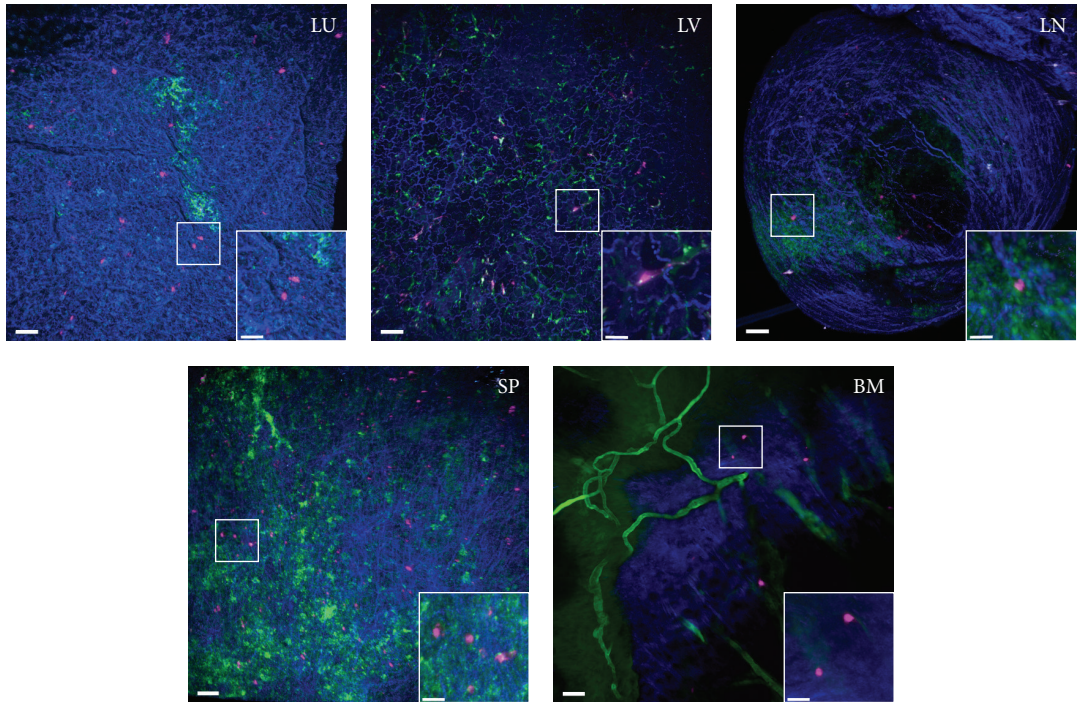

(a)

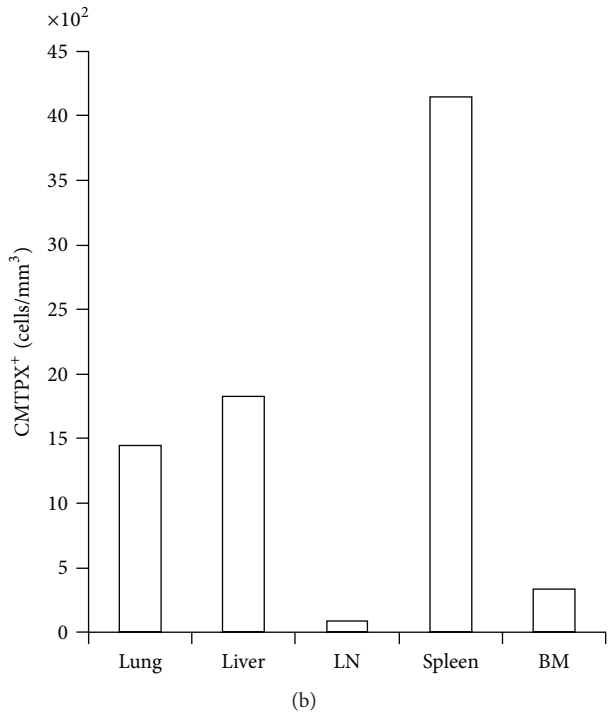

(b)

Figure 1: Distribution of CMTPX-labeled hMSCs 24 hours after i.v. injection into a C57BL/6 mouse.FITC-dextran was injected 15–30 minutes before intravital TPM imaging to highlight the vasculature. The calvarium bone marrow (BM) was imaged immediately and all other tissues were removed and fixed overnight in 2% PFA for whole-organ TPM imaging the next day. (a) Representative high-resolution TPM images of lung (LU), liver (LV), lymph node (LN), spleen (SP), and bone marrow (BM) are shown. Blue: collagen (second-harmonics); Green: FITC-dextran vessel dye; Magenta: infused hMSCs. Outset scale bars = 50 μm; inset scale bars = 20 μm. (b) Numbers of CMTPX$^+$ hMSC cells per mm^3 of imaged tissue were enumerated.

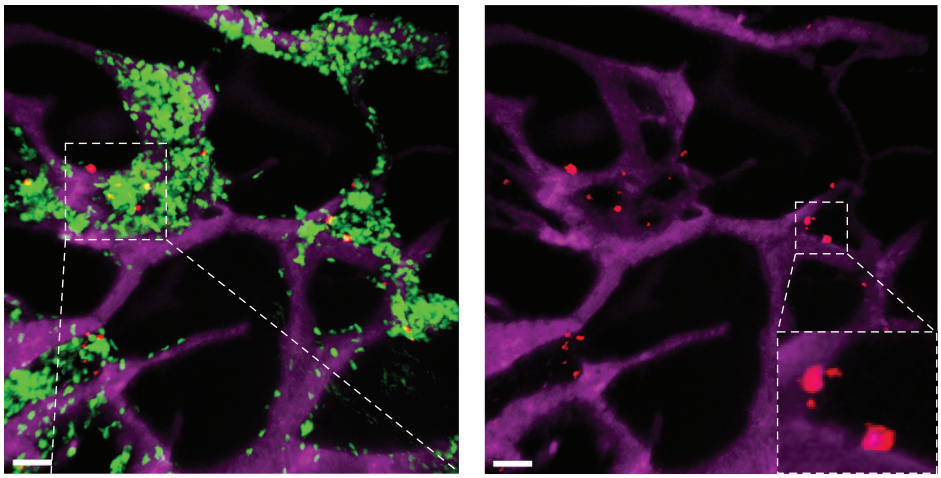

(a) (b)

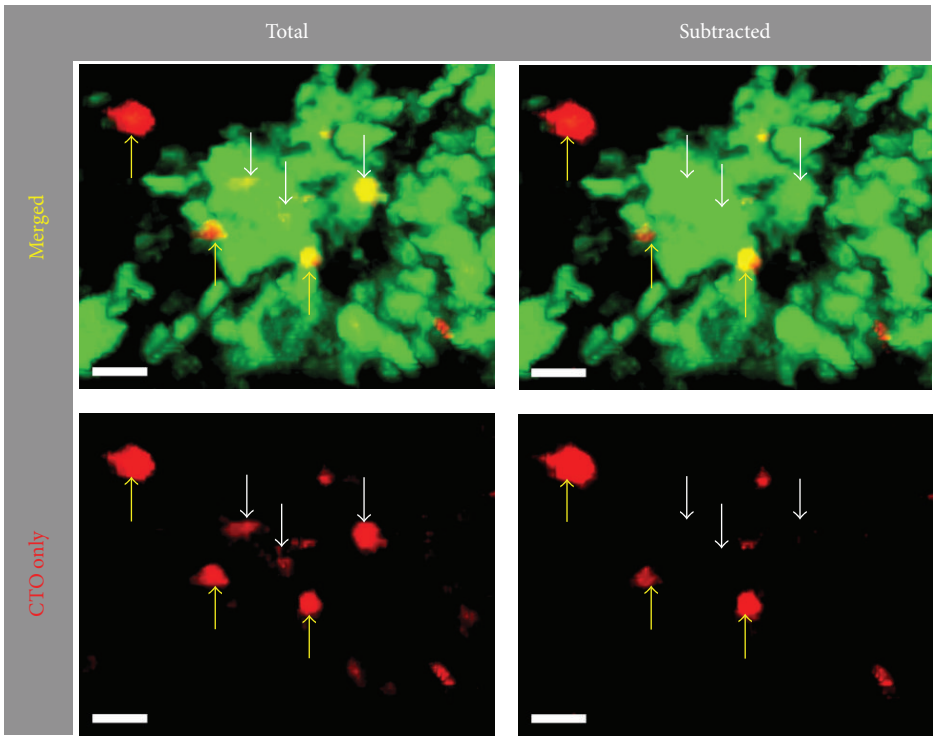

(c)

FIGURE 2: Distribution of CTO-labeled hMSCs in the calvarium of a $LysM^{+/GFP}$ mouse. A total of 8×10^6 CTO-labeled hMSCs (red) were injected *i.v.* into a $LysM^{+/GFP}$ recipient mouse containing $LysM^+$ (green) neutrophils and monocytes. Intravital TPM was performed through intact calvarium of live recipient mice 20 hours after *i.v.* injection of hMSCs. (a) Distribution of labeled hMSCs in the calvarium bone marrow within the general vicinity of bone marrow-resident $LysM^+$ myeloid-lineage cells. Vessels were highlighted with Qtracker-655 (magenta). Scale bar = 50 μm. (b) Same image as in (a) after channel subtraction to remove CTO signal inclusions inside of the $LysM^+$ GFP signals, showing close association of the hMSCs with the vessels (inset). (c) Zoomed-in view of the inset in (a), showing that many hMSCs (red) remain intact in the bone marrow and do not colocalize with the GFP signal (yellow arrows). However, a small number of $LysM^+$ granulocytes can be seen to harbor CTO^+ inclusions inside the cell body (white arrows). Channel subtraction of the micrograph in the left column removed CTO signal that resided within $LysM^+$ cell body, further supporting the presence of CTO signal inside a few $LysM^+$ cells (right column; white arrows). Scale bars = 20 μm.

the source of these intracellular inclusion bodies found in $LysM^+$ cells (Figure 2(c); white arrows). However, in the same imaging field we were also able to detect larger CTO^+ cells that did not coexpress the GFP signal, suggesting that these may be intact, viable hMSCs that were infused a day earlier (Figure 2(c); yellow arrows). Thus, by subtracting the overlapping GFP signal from the CTO signal in the intravital imaging sequence, it was possible to distinguish intact hMSCs from GFP^+ $LysM^+$ granulocytes that had engulfed fluorescent hMSC debris. Our data strongly suggest that, contrary to recent reports, intact hMSCs do indeed survive past the lungs and can migrate to the bone marrow at least a day after *i.v.* administration [22].

Armed with the technical capability to detect individual hMSCs and granulocytes in intact bone marrow of a live mouse, we applied time-resolved intravital TPM to visualize the response and interaction dynamics of granulocytes and hMSCs in the bone marrow of recipient mice undergoing active systemic LPS challenge (Figure 3). With the anesthetized, hMSC-infused $LysM^{+/GFP}$ mouse situated under the TPM imaging objective during a continuous sequential *xyz* imaging data acquisition, we injected 100 ng of *S. enterica* LPS *i.v.* and visualized the behavior of both hMSCs and GFP^+ granulocytes (Supplemental Movie 1, See Supplementary Materials available online at http://dx.doi.org/10.1155/2013/656839). $LysM^+$ cells interacted with the hMSCs only sporadically during both the 1-hour imaging before LPS injection (data not shown) and the first 30 minutes after LPS injection (Figure 3; $t = 0'$–$30'$). Starting around 30 minutes following LPS injection, we observed dramatic changes in granulocyte behavior, including increases in their instantaneous speed and apparent overall activity (Figure 3). By 50 minutes post-LPS administration, the granulocytes began to cluster ("swarm") around some of the hMSCs (Figures 3(a) and 3(d); Supplemental Movie 1). We examined several parameters which together contribute to the observed neutrophil "swarming" behavior, namely: (I) total cellular accumulation (reflected as changes in total GFP fluorescence; Figure 3(b)); (II) frequency of neutrophil-hMSC contact (calculated as time-averaged % cellular interactions; Figure 3(c)); (III) migration speed and trajectory of neutrophils (Figure 3(d)); and (IV) flux of neutrophils coming towards and leaving from the neutrophil-hMSC cluster (enumerated as cell flux index; Figure 3(e)). The total GFP signals (as a reflection of total GFP^+ granulocytes) around the tracked hMSCs were variable, with some decreasing (Figure 3(b), panel 1) or exhibiting transient fluctuation in signal intensity (Figure 3(b), panel 2), while other hMSCs experienced dramatic increases in GFP signal intensity over time following LPS injection (Figure 3(b), panel 3). In order to further demonstrate the dynamic recruitment, clustering, and direct cellular interactions between GFP^+ cells and some hMSCs, we analyzed the time-averaged percentage of GFP^+ cells that traversed to within a 20 μm radius of the hMSCs. Some, but not all, of the hMSCs experienced increasing numbers of interactions with GFP^+ granulocytes starting at 60–90 minutes after LPS treatment (Figures 3(c) and 3(d)). These dynamic data indicate that the observed hMSCs did not all encounter the same granulocyte "swarming" behavior at the same time or to the same extent, as some labeled hMSCs did not appear to participate in the "swarming" behavior during the entire imaging session. Our observation helps to explain the observed behavior of $LysM^+$ cells showing that granulocyte clusters can form in different spots within the bone marrow at various times following LPS administration (Supplemental Movie 1). Some of the "swarming" locations occurred in areas without any observable labeled hMSCs and may presumably be caused by the presence of unlabeled, endogenous stromal cells or MSCs that were stimulated with the TLR4 agonist [33–37].

Understanding the fate of infused hMSCs is of particular clinical relevance as their persistence and elimination *in vivo* may correlate with their clinical efficacy. As shown in Figure 2, $LysM^+$ granulocytes were able to engulf CTO-labeled hMSC fragments that were distinguishable from intact, viable hMSCs. To this end, we were able to use the dynamic intravital TPM to visualize the active process of dying hMSC fragmentation and subsequent distribution and digestion of hMSC cell fragments by multiple $LysM^+$ cells in the bone marrow (Figure 4; Supplemental Movie 2). Over a 40-minute period, we observed an hMSC digested into multiple large fragments (Figure 4(a)). These fragments were taken up by multiple $LysM^+$ cells (Figure 4(b)). At least one of the CTO^+ GFP^+ cells was seen to migrate away from the cluster into the blood vessel (Figure 4(c)). The fluorescence intensity of the CTO-containing GFP^+ cell appeared dimmer compared with surrounding bright neutrophils (Figure 4(b), $t = 80'$ inset), suggesting that the migrating $LysM^+GFP^{dim}$ cell may represent a monocytic cell [38, 39]. It is interesting to note that the observed fragmentation process of hMSC began before any LPS was administered to the animal, indicating that a portion of infused hMSCs were actively being eliminated even before onset of inflammation. Additionally, the intact hMSCs initially observed in the beginning of the imaging session (one hour prior to LPS administration) were still visibly intact during the entire two-hour imaging tracking following LPS injection throughout the neutrophil swarming behavior. Analyzing all available imaging datasets, we observed a total of 151 CTO^+ events during the one-hour imaging session prior to LPS administration, with 18 CTO^+ signals comprised of intact hMSC cells (11.9%). During the two-hour data acquisition following LPS administration, we observed a total of 143 CTO^+ events, with 14 CTO^+ signals generated from intact hMSCs (9.8%). There was no statistically significant difference ($P = 0.36$) between the percentage of intact CTO^+ hMSCs before and after LPS challenge, indicating that, at least within the limits of the 3-hour imaging session, LPS administration did not cause an accelerated destruction of hMSCs in the marrow.

4. Discussion and Conclusion

There has been much debate about how therapeutically administered hMSCs exert their immune-modulatory function *in vivo* (i.e., systemic versus local effect). In rodents, hMSCs have been shown to confer therapeutic effects on

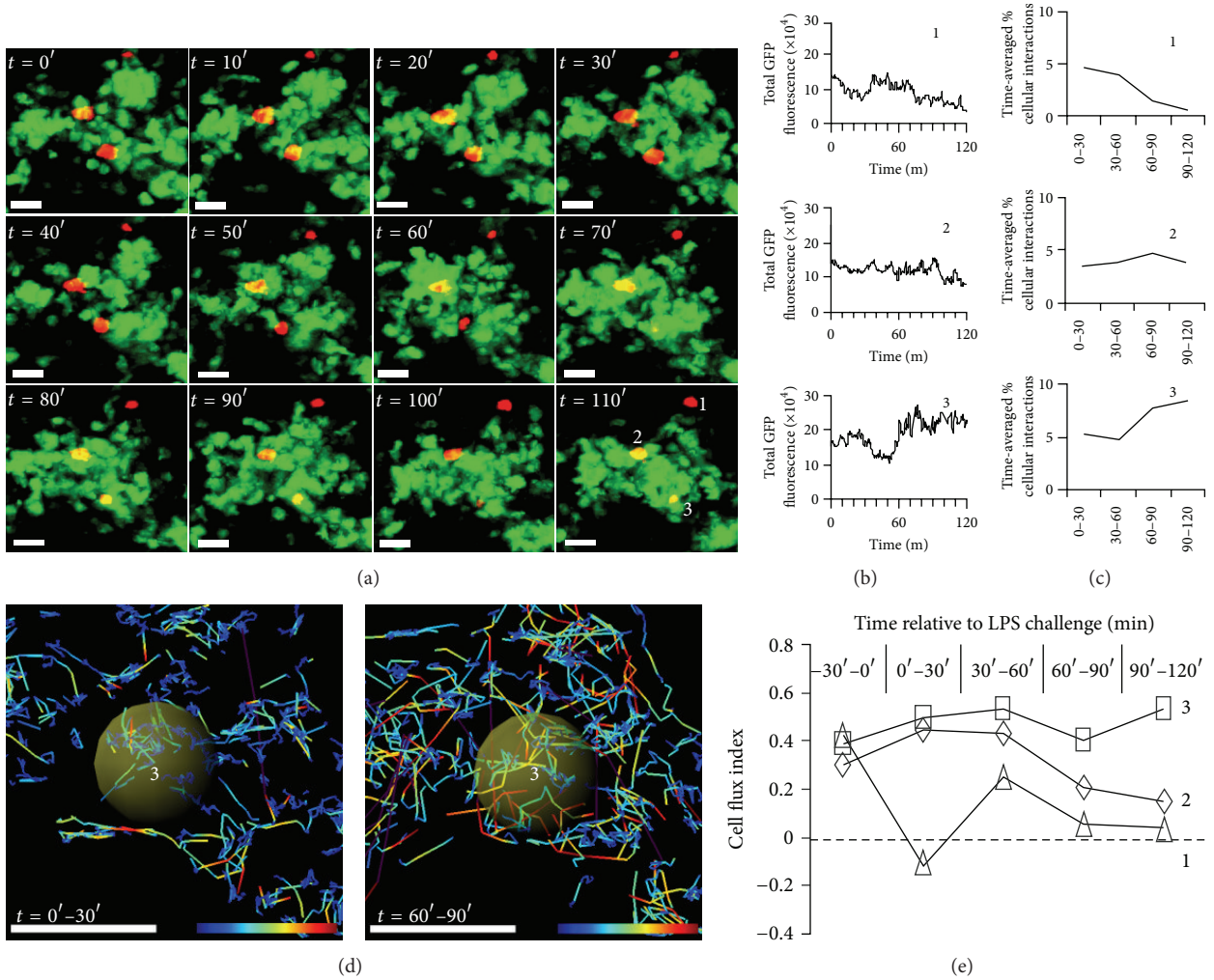

Figure 3: Time-lapse TPM images of LysM$^+$ granulocytes interacting with hMSC after systemic LPS administration. CTO-labeled hMSCs (red) were injected *i.v.* into a *LysM*$^{+/GFP}$ recipient mouse containing LysM$^+$ (green) granulocytes 20 hours prior to performing intravital TPM of the bone marrow through intact calvarium of the live recipient mouse. The recipient mouse received a 100 ng of LPS injection *i.v.* at relative time = 0 min ($t = 0'$). (a) Sequential TPM images from Supplemental Movie 1 (See Supplementary Materials available online at http://dx.doi.org/10.1155/2013/656839) displayed at 10-minute intervals for a total of 110 minutes ($t = 110'$) starting from the time of LPS injection ($t = 0'$), showing the accumulation of LysM$^+$ GFP$^+$ granulocytes surrounding 2 out of 3 hMSCs (red) that are clearly visible within the imaging field. Scale bar = 20 μm. (b) Total fluorescence of GFP signal within a 20 μm radius of each of the three hMSCs identified in (a) at $t = 110'$ over time. (c) Time-averaged percent of LysM$^+$ GFP$^+$ neutrophils within 20 μm radius of the hMSC that formed a cell-cell contact with the said hMSCs after LPS challenge. The percent was normalized to the contact frequency at $t = 0'$. (d) Track analysis of cell number 3 in (a) $t = 110'$. Shown are migration tracks of surrounding LysM$^+$ GFP$^+$ granulocytes during 0 to 30 minutes (left panel) and 60 to 90 minutes (right panel) after LPS administration. Individual migration heat map tracks are color-coded based on the calculated instantaneous speed. Yellow sphere = 20 μm radius around the center of hMSC number 3. Scale bar = 50 μm. (e) Cell flux indices for 3 different hMSCs identified in (a) are shown, where all three hMSCs showed net increased neutrophil flux towards them after LPS administration, although hMSC number 3 exhibited heightened and sustained positive cellular flux. hMSC number 2 had an initial increase in positive flux, which reached homeostasis two hours after LPS injection. hMSC number 1 initially had a negative cellular flux due to local neutrophils being attracted to hMSCs number 2 and number 3. However, neutrophils from regions beyond the imaging field began to migrate towards the hMSC 30 to 60 minutes following LPS injection before the cellular traffic reached a steady-state level (cell flux index of ~ 0).

the outcome of various disease models including systemic lupus erythematosis (SLE) and sepsis [40–42]. An emerging paradigm indicates that hMSCs can exhibit both proinflammatory (type 1) and anti-inflammatory (type 2) responses *in vivo* depending on the specific stimuli encountered by the hMSCs [35]. In particular, this modulation of hMSC function was shown to occur during stimulation with Toll-like receptor (TLR) agonists [33, 35, 37]. In response to stimulation with the TLR4 agonist LPS, bone marrow MSCs upregulate inflammatory cytokines such as MCP-1 [36] and IL-8 [34] and can affect mobilization of granulocytes. All of the information regarding the role(s) of MSCs in

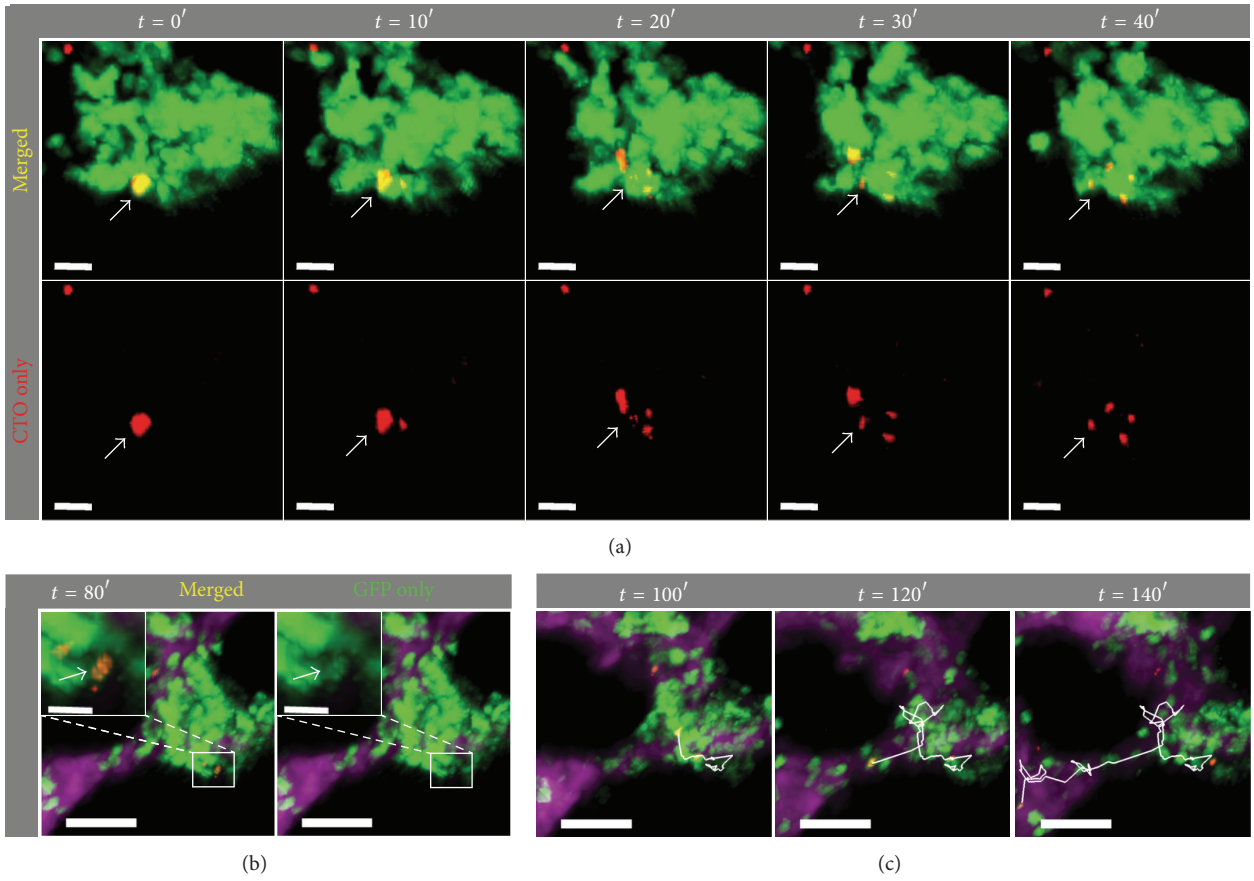

Figure 4: Cellular fragmentation of a dying hMSC followed by phagocytosis of migrating LysM$^+$ GFP$^+$ granulocyte engulfing hMSC debris. (a) Intravital TPM images of a different area of the calvarium bone marrow from Figures 2 and 3, demonstrating the dramatic fragmentation of the CTO-labeled (red) hMSC cell body (white arrow) into at least 4 pieces over a period of 40 minutes ($t = 0'$ corresponds to 20 minutes prior to LPS injection). Scale bar = 20 μm. (b) A LysM$^+$GFP^{dim} cell containing phagocytosed CTO-labeled hMSC debris is shown to demonstrate colocalization of GFP (green) and CTO (red) signals (inset: zoomed view at $t = 80'$ with (left; "merged") and without (right; "GFP only") CTO signal). (c) A LysM$^+$ GFP$^+$ CTO$^+$ cell exhibited a highly motile behavior over a long distance in the bone marrow (white tracks) over a 60-minute imaging period. Scale bar outset = 50 μm; inset scale bar = 10 μm.

inflammation, however, has come from indirect methods involving bulk cell analysis with virtually no information on the cellular interaction dynamics between granulocytes and MSCs during inflammatory responses.

In this study, we tracked the fate of infused hMSCs in the bone marrow of immune competent mice and observed their dynamic interactions with host bone-marrow-resident LysM$^+$ neutrophils and monocytes before and after systemic LPS administration. Our *in situ* single-cell imaging data directly refutes a prior published report claiming that intravenously administered mouse MSCs were unable to reach tissues other than the liver, lung, and the spleen, and that the biological effect of hMSCs *in vivo* is therefore likely due to systemic effects [22]. As observed in our dynamic imaging studies, live hMSCs were able to traffic to the bone marrow, survive in a xenograft environment with an intact host immune system, and interact with surrounding neutrophils following systemic challenge with a TLR agonist. At the same time, we also observed the destruction and subsequent phagocytosis of hMSCs by host immune cells.

Of particular interest is our finding that mouse granulocytes exhibit a highly dynamic "swarming" behavior around hMSCs in response to LPS challenge and that hMSCs remain essentially intact during such an active host innate immune response. The observed granulocyte behavior was similar to that described in peripheral organs such as the liver during infectious processes [38], suggesting that the clustering and dynamic behavior was a general phenomenon of the granulocytes *in vivo*. The hMSCs have been shown to directly respond to TLR stimulation [33–37] and release chemokines MCP-1 and IL-8 for neutrophil recruitment [34, 36]; therefore, it is possible that the bone marrow neutrophils were actively responding to local chemokines released by the hMSCs following LPS stimulation. Alternatively, the neutrophils may respond directly to LPS [43] or signals that are released by other cell types in the bone marrow as a result of TLR stimulation, and that both hMSCs and granulocytes nest in the same niche where the signal source resides or the same anatomical sites where exiting and entering cells colocalize in the bone marrow. Additional experiments are

needed to interrogate the roles of various nonfluorescent stromal and marrow-derived elements that appeared "dark" or were not labeled in our imaging background during this dynamic inflammatory interplay between hMSCs and host cells and the destruction of hMSCs in the xenograft environment as witnessed in the current study. In addition, future investigations are needed to address how *in vivo* interactions with the hMSCs affect functional and behavioral changes in neutrophils and other host immune cells.

A limitation in our current study is the lack of lineage-specific fluorescent markers to differentiate the GFP^+ responding cells that were actively engaging hMSCs. While >95% of GFP^+ cells in our mouse model express $Gr1^+/CD11b^+/GFP^{bright}$ markers consistent with neutrophils [38, 39], we cannot determine with certainty the true identity of the imaged GFP^{dim} cells as belonging to either the monocyte/macrophage or neutrophil lineages (Figure 4(b), inset). Multicolor lineage-specific fluorescent reporters will be required to further distinguish the responses these cell types of hMSCs and LPS challenge. Another limitation of this study is that our description of the hMSC behavior with neutrophils was restricted to the calvarium bone marrow and not other marrow cavities such as that found in the femurs and other long bones. As intravital imaging of the latter would require additional manipulations such as removal of bone and muscles, as well as mechanical thinning of the cortical bone, these procedures may potentially introduce additional trauma to the underlying hMSC-neutrophil biology. For this reason we purposely restricted our observation to the calvarium marrow in order to minimize tissue damage and inflammation.

We were also intrigued by the variable interaction kinetics between neutrophils and different hMSCs in the bone marrow (Figure 3) with some of the infused hMSCs undergoing apoptosis while others remained intact (Figure 4). Interestingly, the rate of hMSC destruction and subsequent phagocytosis by $LysM^+$ cells was not exacerbated by LPS stimulation. The variable interaction kinetics may be due to heterogeneous states of differentiation and maturation within the infused hMSC population incurred either during the *in vitro* culture process or as a result of different local signals received by hMSCs within different microniches in the bone marrow. Another, though less likely, possibility is cellular contaminant in the infused cell cohort that was not MSCs. In the future, a possible way to address this issue will be to construct marker-specific fluorescent reporters in the infused hMSCs rather than employing nonspecific, pan-cell fluorescent dyes. In either scenario, it is important to understand how these cells behave *in vivo* as they represent the actual cellular products that are currently being infused into patients who are enrolled in a variety of active clinical trials. Furthermore, as recent data support the notion that neutrophils are active participants in a variety of adaptive immune responses [44–47], it would be extremely interesting to study the associated functional changes in the hMSC debris-containing neutrophils in a variety of inflammatory or pathological settings, and whether phagocytosis of hMSC cellular components may represent a potential mechanism by which hMSCs exert their immune-modulatory effect *in vivo*. Together, our current study demonstrated the value and utility of intravital TPM approach in furthering our limited understanding of the biology and *in situ* cellular mechanisms by which hMSCs traffic to and exert therapeutic and immune-modulatory effects upon host tissues.

Authors' Contribution

J. T. Myers and A. Y. Huang conceived and planned the experiments. J. T. Myers performed the experiments. J. T. Myers and D. S. Barkauskas analyzed the data. J. T. Myers, D. S. Barkauskas, and A. Y. Huang drafted the paper. All authors concurred with the final paper draft prior to submission.

Conflict of Interests

The authors do not have any conflict of interests to declare.

Acknowledgments

The authors are grateful to Dr. David Wald, M.D., Ph.D., Director of Hematopoietic Stem Cell Core Facility, Case Comprehensive Cancer Center, for helpful comments and suggestions related to hMSC preparation, characterization, and handling. The authors also thank Dr. Thomas Graf for generously providing the $LysM^{+/GFP}$ mice and acknowledge the contribution of Dr. Iuliana Dit Bobanga, M.D., and Josepoh Nthale for helpful review and suggestions during the preparation of this paper. This research was supported by the National Center for Regenerative Medicine Pilot Grant (Tech 09-071), with partial funding support from the National Cancer Institute (CA154656), St. Baldrick's Foundation, Alex's Lemonade Stand Foundation, Gabrielle's Angel Foundation, Hematopoietic Stem Cell Core Facility of the Case Comprehensive Cancer Center (P30 CA43703), and T32 EB7509 (to D. S. Barkauskas). Case Western Reserve University acknowledges the contribution of the State of Ohio, Department of Development, which provided funding in support of Center for Stem Cell and Regenerative Medicine: Commercial and Clinical Application project.

References

[1] P. S. Frenette, S. Pinho, D. Lucas, and C. Scheiermann, "Mesenchymal stem cell: keystone of the hematopoietic stem cell niche and a stepping-stone for regenerative medicine," *Annual Review of Immunology*, 2013.

[2] A. I. Caplan, "Adult mesenchymal stem cells for tissue engineering versus regenerative medicine," *Journal of Cellular Physiology*, vol. 213, no. 2, pp. 341–347, 2007.

[3] N. G. Singer and A. I. Caplan, "Mesenchymal stem cells: mechanisms of inflammation," *Annual Review of Pathology*, vol. 6, pp. 457–478, 2011.

[4] M. J. Hoogduijn, F. C. Popp, A. Grohnert et al., "Advancement of mesenchymal stem cell therapy in solid organ transplantation (MISOT)," *Transplantation*, vol. 90, no. 2, pp. 124–126, 2010.

[5] M. E. J. Reinders, W. E. Fibbe, and T. J. Rabelink, "Multipotent mesenchymal stromal cell therapy in renal disease and kidney transplantation," *Nephrology Dialysis Transplantation*, vol. 25, no. 1, pp. 17–24, 2010.

[6] H. K. Salem and C. Thiemermann, "Mesenchymal stromal cells: Current understanding and clinical status," *Stem Cells*, vol. 28, no. 3, pp. 585–596, 2010.

[7] E. Mansilla, G. H. Marin, F. Sturla et al., "Human mesenchymal stem cells are tolerized by mice and improve skin and spinal cord injuries," *Transplantation Proceedings*, vol. 37, no. 1, pp. 292–294, 2005.

[8] Y. T. Lin, Y. Chern, C. K. J. Shen et al., "Human mesenchymal stem cells prolong survival and ameliorate motor deficit through trophic support in Huntington's disease mouse models," *PLoS ONE*, vol. 6, no. 8, Article ID e22924, 2011.

[9] J. Croitoru-Lamoury, K. R. Williams, F. M. J. Lamoury et al., "Neural transplantation of human MSC and NT2 cells in the twitcher mouse model," *Cytotherapy*, vol. 8, no. 5, pp. 445–458, 2006.

[10] M. J. Jang, H. S. Kim, H. G. Lee et al., "Placenta-derived mesenchymal stem cells have an immunomodulatory effect that can control acute graft-versus-host disease in mice ," *Acta Haematologica*, vol. 129, no. 4, pp. 197–206, 2012.

[11] S. K. Kang, I. S. Shin, M. S. Ko, J. Y. Jo, and J. C. Ra, "Journey of mesenchymal stem cells for homing: strategies to enhance efficacy and safety of stem cell therapy," *Stem Cells International*, vol. 2012, Article ID 342968, 11 pages, 2012.

[12] Y. Qi, G. Feng, Z. Huang, and W. Yan, "The application of super paramagnetic iron oxide-labeled mesenchymal stem cells in cell-based therapy," *Molecular Biology Reports*, vol. 40, no. 3, pp. 2733–2740, 2013.

[13] F. Drey, Y. H. Choi, K. Neef et al., "Noninvasive in vivo tracking of mesenchymal stem cells and evaluation of cell therapeutic effects in a murine model using a clinical 3.0 T MRI," *Cell Transplantation*, 2012.

[14] Jasmin, L. A. Jelicks, W. Koba et al., "Mesenchymal bone marrow cell therapy in a mouse model of chagas disease. Where do the cells go?" *PLoS Neglected Tropical Diseases*, vol. 6, no. 12, article e1971, 2012.

[15] A. Mukherjee, S. Tipnis, H. D. Sarma et al., "Radiolabeling of umbilical cord-derived mesenchymal stem cells for in vivo tracking," *Cancer Biotherapy & Radiopharmaceuticals*, vol. 27, no. 9, pp. 614–619, 2012.

[16] N. L. Payne, G. Sun, C. McDonald et al., "Distinct immunomodulatory and migratory mechanisms underpin the therapeutic potential of human mesenchymal stem cells in autoimmune demyelination," *Cell Transplantation*, 2012.

[17] E. L. Spaeth, S. Kidd, and F. C. Marini, "Tracking inflammation-induced mobilization of mesenchymal stem cells," *Methods in Molecular Biology*, vol. 904, pp. 173–190, 2012.

[18] M. Ozdemir, A. Attar, I. Kuzu et al., "Stem cell therapy in spinal cord injury: in vivo and postmortem tracking of bone marrow mononuclear or mesenchymal stem cells," *Stem Cell Reviews*, vol. 8, no. 3, pp. 953–962, 2012.

[19] K. S. Jang, K. S. Lee, S. H. Yang, and S. S. Jeun, "In vivo tracking of transplanted bone marrow-derived mesenchymal stem cells in a murine model of stroke by bioluminescence imaging," *Journal of Korean Neurosurgical Society*, vol. 48, no. 5, pp. 391–398, 2010.

[20] M. Gyöngyösi, J. Blanco, T. Marian et al., "Serial noninvasive in vivo positron emission tomographic tracking of percutaneously intramyocardially injected autologous porcine mesenchymal stem cells modified for transgene reporter gene expression.," *Circulation*, vol. 1, no. 2, pp. 94–103, 2008.

[21] F. Tögel, Z. Hu, K. Weiss, J. Isaac, C. Lange, and C. Westenfelder, "Administered mesenchymal stem cells protect against ischemic acute renal failure through differentiation-independent mechanisms," *American Journal of Physiology*, vol. 289, no. 1, pp. F31–F42, 2005.

[22] E. Eggenhofer, V. Benseler, A. Kroemer et al., "Mesenchymal stem cells are short-lived and do not migrate beyond the lungs after intravenous infusion," *Frontiers in Immunology*, vol. 3, article 297, 2012.

[23] N. Faust, F. Varas, L. M. Kelly, S. Heck, and T. Graf, "Insertion of enhanced green fluorescent protein into the lysozyme gene creates mice with green fluorescent granulocytes and macrophages," *Blood*, vol. 96, no. 2, pp. 719–726, 2000.

[24] L. A. Solchaga, J. J. Auletta, E. A. Zale, and J. F. Welter, "Fibroblast growth factor-2 enhances expansion of human bone marrow-derived mesenchymal stromal cells without diminishing their immunosuppressive potential," *Stem Cells International*, vol. 2011, Article ID 235176, 10 pages, 2011.

[25] Y. Li and F. Lin, "Mesenchymal stem cells are injured by complement after their contact with serum," *Blood*, vol. 120, no. 17, pp. 3436–3443, 2012.

[26] L. D. Solorio, A. S. Fu, R. Hernández-Irizarry, and E. Alsberg, "Chondrogenic differentiation of human mesenchymal stem cell aggregates via controlled release of TGF-β1 from incorporated polymer microspheres," *Journal of Biomedical Materials Research A*, vol. 92, no. 3, pp. 1139–1144, 2010.

[27] L. D. Solorio, E. L. Vieregge, C. D. Dhami, P. N. Dang, and E. Alsberg, "Engineered cartilage via self-assembled hMSC sheets with incorporated biodegradable gelatin microspheres releasing transforming growth factor-beta1," *Journal of Controlled Release*, vol. 158, no. 2, pp. 224–232, 2012.

[28] L. D. Solorio, C. D. Dhami, P. N. Dang, E. L. Vieregge, and E. Alsberg, "Spatiotemporal regulation of chondrogenic differentiation with controlled delivery of transforming growth factor-beta1 from gelatin microspheres in mesenchymal stem cell aggregates," *Stem Cells Translational Medicine*, vol. 1, no. 8, pp. 632–639, 2012.

[29] C. Lo Celso, H. E. Fleming, J. W. Wu et al., "Live-animal tracking of individual haematopoietic stem/progenitor cells in their niche," *Nature*, vol. 457, no. 7225, pp. 92–96, 2009.

[30] M. Crisan, S. Yap, L. Casteilla et al., "A perivascular origin for mesenchymal stem cells in multiple human organs," *Cell Stem Cell*, vol. 3, no. 3, pp. 301–313, 2008.

[31] M. Crisan, C. W. Chen, M. Corselli, G. Andriolo, L. Lazzari, and B. Péault, "Perivascular multipotent progenitor cells in human organs," *Annals of the New York Academy of Sciences*, vol. 1176, pp. 118–123, 2009.

[32] C. Farrington-Rock, N. J. Crofts, M. J. Doherty, B. A. Ashton, C. Griffin-Jones, and A. E. Canfield, "Chondrogenic and adipogenic potential of microvascular pericytes," *Circulation*, vol. 110, no. 15, pp. 2226–2232, 2004.

[33] J. Lei, Z. Wang, D. Hui et al., "Ligation of TLR2 and TLR4 on murine bone marrow-derived mesenchymal stem cells triggers differential effects on their immunosuppressive activity," *Cellular Immunology*, vol. 271, no. 1, pp. 147–156, 2011.

[34] R. Romieu-Mourez, M. François, M. N. Boivin, M. Bouchentouf, D. E. Spaner, and J. Galipeau, "Cytokine modulation of TLR expression and activation in mesenchymal stromal cells leads to a proinflammatory phenotype," *Journal of Immunology*, vol. 182, no. 12, pp. 7963–7973, 2009.

[35] R. S. Waterman, S. L. Tomchuck, S. L. Henkle, and A. M. Betancourt, "A new mesenchymal stem cell (MSC) paradigm: Polarization into a pro-inflammatory MSC1 or an immunosuppressive MSC2 phenotype," *PLoS ONE*, vol. 5, no. 4, Article ID e10088, 2010.

[36] C. Shi, T. Jia, S. Mendez-Ferrer et al., "Bone marrow mesenchymal stem and progenitor cells induce monocyte emigration in response to circulating toll-like receptor ligands," *Immunity*, vol. 34, no. 4, pp. 590–601, 2011.

[37] O. Delarosa, W. Dalemans, and E. Lombardo, "Toll-like receptors as modulators of mesenchymal stem cells," *Frontiers in Immunology*, vol. 3, article 182, 2012.

[38] N. C. Peters, J. G. Egen, N. Secundino et al., "In vivo imaging reveals an essential role for neutrophils in leishmaniasis transmitted by sand flies," *Science*, vol. 321, no. 5891, pp. 970–974, 2008.

[39] W. Li, R. G. Nava, A. C. Bribriesco et al., "Intravital 2-photon imaging of leukocyte trafficking in beating heart," *The Journal of Clinical Investigation*, vol. 122, no. 7, pp. 2499–2508, 2012.

[40] S. Shin, Y. Kim, S. Jeong et al., "The therapeutic effect of human adult stem cells derived from adipose tissue in endotoxemic rat model," *International Journal of Medical Sciences*, vol. 10, no. 1, pp. 8–18, 2013.

[41] E. W. Choi, I. S. Shin, S. Y. Park et al., "Reversal of serologic, immunologic, and histologic dysfunction in mice with systemic lupus erythematosus by long-term serial adipose tissue-derived mesenchymal stem cell transplantation," *Arthritis & Rheumatism*, vol. 64, no. 1, pp. 243–253, 2012.

[42] A. Krasnodembskaya, G. Samarani, Y. Song et al., "Human mesenchymal stem cells reduce mortality and bacteremia in gram-negative sepsis in mice in part by enhancing the phagocytic activity of blood monocytes," *American Journal of Physiology*, vol. 302, no. 10, pp. L1003–L1013, 2012.

[43] A. Mantovani, M. A. Cassatella, C. Costantini, and S. Jaillon, "Neutrophils in the activation and regulation of innate and adaptive immunity," *Nature Reviews Immunology*, vol. 11, no. 8, pp. 519–531, 2011.

[44] S. M. Krams, "New approaches to inducing the death of alloreactive lymphocytes," *Clinical and Experimental Immunology*, vol. 126, no. 3, pp. 371–373, 2001.

[45] D. Kreisel, S. Sugimoto, J. Zhu et al., "Emergency granulopoiesis promotes neutrophil-dendritic cell encounters that prevent mouse lung allograft acceptance," *Blood*, vol. 118, no. 23, pp. 6172–6182, 2011.

[46] Z. Granot, E. Henke, E. A. Comen, T. A. King, L. Norton, and R. Benezra, "Tumor entrained neutrophils inhibit seeding in the premetastatic lung," *Cancer Cell*, vol. 20, no. 3, pp. 300–314, 2011.

[47] Z. G. Fridlender, J. Sun, S. Kim et al., "Polarization of tumor-associated neutrophil phenotype by TGF-β: "N1"versus "N2" TAN," *Cancer Cell*, vol. 16, no. 3, pp. 183–194, 2009.

Hindawi Publishing Corporation
Stem Cells International
Volume 2013, Article ID 353105, 10 pages
http://dx.doi.org/10.1155/2013/353105

Research Article

Optimal Labeling Dose, Labeling Time, and Magnetic Resonance Imaging Detection Limits of Ultrasmall Superparamagnetic Iron-Oxide Nanoparticle Labeled Mesenchymal Stromal Cells

Anders Bruun Mathiasen,[1] Louise Hansen,[1] Tina Friis,[1] Carsten Thomsen,[2] Kishore Bhakoo,[3] and Jens Kastrup[1]

[1] *Cardiac Stem Cell Laboratory and Catheterization Laboratory, Rigshospitalet, Copenhagen University Hospital, Blegdamsvej 9, 2100 Copenhagen, Denmark*
[2] *Department of Radiology, Rigshospitalet, Copenhagen University Hospital, Copenhagen, Denmark*
[3] *Translational Molecular Imaging Group, Singapore Bioimaging Consortium, Agency for Science, Technology and Research (A*-STAR), Singapore 138667*

Correspondence should be addressed to Anders Bruun Mathiasen; abbe@dadlnet.dk

Received 30 December 2012; Revised 9 February 2013; Accepted 11 February 2013

Academic Editor: Weian Zhao

Background. Regenerative therapy is an emerging treatment modality. To determine migration and retention of implanted cells, it is crucial to develop noninvasive tracking methods. The aim was to determine *ex vivo* magnetic resonance imaging (MRI) detection limits of ultrasmall superparamagnetic iron-oxide (USPIO) labeled mesenchymal stromal cells (MSCs). *Materials and Methods.* 248 gel-phantoms were constructed and scanned on a 1.5T MRI-scanner. Phantoms contained human MSCs preincubated with USPIO nanoparticles for 2, 6, or 21 hours using 5 or 10 μg USPIO/10^5 MSCs. In addition, porcine hearts were scanned after injection of USPIO labeled MSCs. *Results.* Using 21 h incubation time and 10 μg USPIO/10^5 MSCs, labeled cells were clearly separated from unlabeled cells on MRI using 250.000 ($P < 0.001$), 500.000 ($P = 0.007$), and 1.000.000 MSCs ($P = 0.008$). At lower incubation times and doses, neither labeled nor unlabeled cells could be separated. In porcine hearts labeled, but not unlabeled, MSCs were identified on MRI. *Conclusions.* As few as 250.000 MSCs can be detected on MRI using 21 h incubation time and 10 μg USPIO/10^5 MSCs. At lower incubation times and doses, several million cells are needed for MRI detection. USPIO labeled cells can be visualized by MRI in porcine myocardial tissue.

1. Introduction

Stem cell therapy with potential to regenerate damaged myocardium is an emerging treatment modality for ischemic heart disease [1–3]. For future success of cardiac stem cell therapy, it is crucial to develop noninvasive tracking methods for determining the biodistribution and fate of the stem cells after delivery.

Thus far, tracking of cardiovascular delivered stem cells in a clinical setting has been limited to direct cell labeling with radioisotopes and tracking with gamma-cameras, single-photon emission computed tomography, or positron emission tomography [4]. Although providing highly sensitive visualization, these methods are limited by low spatial resolution and short half-lives of radioisotopes from minutes to hours, thus only permitting short-term tracking of the cells. Other drawbacks are exposure to ionizing radiation and nontarget signal leakage.

Tracking of cells labeled with superparamagnetic iron-oxide (SPIO) or ultrasmall superparamagnetic iron-oxide (USPIO) nanoparticles using magnetic resonance imaging (MRI) offers high spatial resolution in combination with high

soft tissue detail, without exposing the patient to ionizing radiation. Furthermore, the cells can be tracked for months. Cellular labeling methods with SPIO or USPIO are relatively simple, fast and inexpensive.

Iron-oxide is nontoxic, since iron is a naturally occurring metal in the human body, and the iron oxide core is coated with biocompatible shell, allowing its eventual assimilation via endogenous metabolic iron cycles. The use of SPIO and USPIO labeling is clinically safe and does not influence cell function [5].

MRI tracking of SPIO and USPIO labeled cells has been utilized *in vivo* in rat, canine, and porcine models of myocardial infarction (MI) using a variety of delivery methods [6–13]. The labeled cells were tracked for up to 8 weeks after delivery. *In vivo* tracking of SPIO and USPIO labeled cells has not yet been utilized in a clinical cardiovascular setting, but both SPIO and USPIO have been used successfully in a number of noncardiovascular clinical studies [14–19].

There has been some concern that MRI signals from SPIO and USPIO labeled cells may originate from macrophages that have engulfed the labeled cells. This was seen in a few rat studies [6, 20], but the majority of animal studies have shown the opposite, that the MRI does in fact originate from the labeled cells and not macrophages [7–9, 11–13, 21, 22]. A general concern for cardiovascular cell therapy has been that the number of cells that remain in the heart after treatment may be limited to only a few percent. However, it has recently been demonstrated that these studies may be severely biased, as there is considerable spontaneous leaking of the radioisotopes used in these studies [23]. Therefore, the number of cells remaining in the heart after treatment may be as high as 60% one week after treatment.

For tracking of nonphagocytic cells, USPIO particles are probably more suitable than SPIO particles, due to higher cellular uptake [24] and longer plasmatic half-life [25]. The USPIO particles used in the present study (IODEX) have an additional cross-linking of the dextran coating compared to traditionally used SPIO and USPIO particles [26]. This stabilizes the iron core of the particles allowing for longer cell tracking periods.

The aim of the present study was to determine *ex vivo* MRI detection limits of IODEX labeled human MSCs with respect to cell numbers and USPIO concentration and incubation period for future clinical application.

2. Materials and Methods

2.1. Isolation and Culture Expansion of MSCs. Bone marrow was obtained from the iliac crest by needle aspiration from healthy donors. The studies were conducted under local ethical approval. Mononuclear cells were then isolated by gradient centrifugation and cultured in complete medium consisting of Dulbecco's modified Eagle medium supplemented with HEPES and L-glutamine, (PAA Laboratories, Austria), 10% fetal bovine serum (PAA Laboratories, Austria), and 1% penicillin/streptomycin (Invitrogen, Austria). Cells were incubated at 37°C in humid air with 5% CO_2. Medium was changed twice a week. The cells were grown to confluence before each passage. After two passages, the cells were washed with PBS (Invitrogen, Austria) and harvested with TrypLE Select (Invitrogen, Austria). Cells from each donor were characterized by flow cytometry for CD90, CD73, CD105, CD13, CD45, and CD34, in accordance with the minimal criteria for defining multipotent mesenchymal stromal cells [27].

2.2. USPIO Preparation. Tat-peptide derivatized USPIO nanoparticles coated with dextran (IODEX-TAT-FITC; 15–20 nm) were prepared in our laboratory using the method described by Josephson et al. [28]. Briefly, the dextran-coated USPIO nanoparticles were synthesized and subsequently conjugated with TAT-fluorescein isothiocyanate (FITC) peptide [GRKKRRQRRR GYK(FITC)C-NH2]. TAT-FITC was synthesized using FMOC-protected amino acid (2-(1-H-benzotriazol-2-yl)-1,1,3,3-tetramethyluronium hexafluorophosphate; HBTU) activation chemistry. The final iron concentration was 2.5 mg/mL, and the solution was sterilized by gamma-irradiation prior to use.

2.3. USPIO Labeling of MSCs. Dose titrating evaluation of iron concentrations added to cells and resulting amounts of iron bound to cells by Josephson et al. [28] revealed that a plateau phase was reached at 100 μg iron per 10^6 cells (10 μg iron per 10^5 cells). In the present study, we wanted to evaluate both this maximum dose of 10 μg iron per 10^5 cells and also the half of this dose, 5 μg iron per 10^5 cells, as this dose reached near optimum iron binding in the original titration study [28]. In the mentioned titrating study, cells were incubated overnight (18–21 hours), whereas animal studies using IODEX-TAT-FITC for labeling MSCs have used only 4–6 hours of incubation [13, 29]. In the present study, we evaluate the mentioned iron doses at 2, 6, and 21 hours of incubation.

MSCs were labeled by incubation with USPIO nanoparticles at a concentration of either 5 μg iron per 10^5 cells (half dose) or 10 μg iron per 10^5 cells (full dose) in complete medium for 2, 6, or 21 hours at 37°C in humid air with 5% CO_2. Then, the cells were washed 3 times in PBS and harvested with TrypLE Select and centrifuged 5 min at 300 g. After centrifugation, the cells were resuspended in PBS, and the number of cells and cell viability was determined by propidium iodide staining using a NucleoCounter NC-100 (Chemometec, Denmark).

2.4. USPIO Iron Concentration. MSCs in a volume corresponding to 1×10^5 cells were transferred to microfuge tubes and centrifuged for 5 min at 500 g. Cell pellet was frozen and stored at −20°C until date of quantification. Then, the cells were resuspended in 50 μL PBS, hydrolysed for 30 min with 100 μL 6 M HCl, and pH neutralized by addition of 60 μL 10 M NaOH. The cells were centrifuged for 2 min at 1300 g, and 100 μL supernatant was used for automatic iron quantitation by use of a Konelab 60i robot (Therma Electron, Finland).

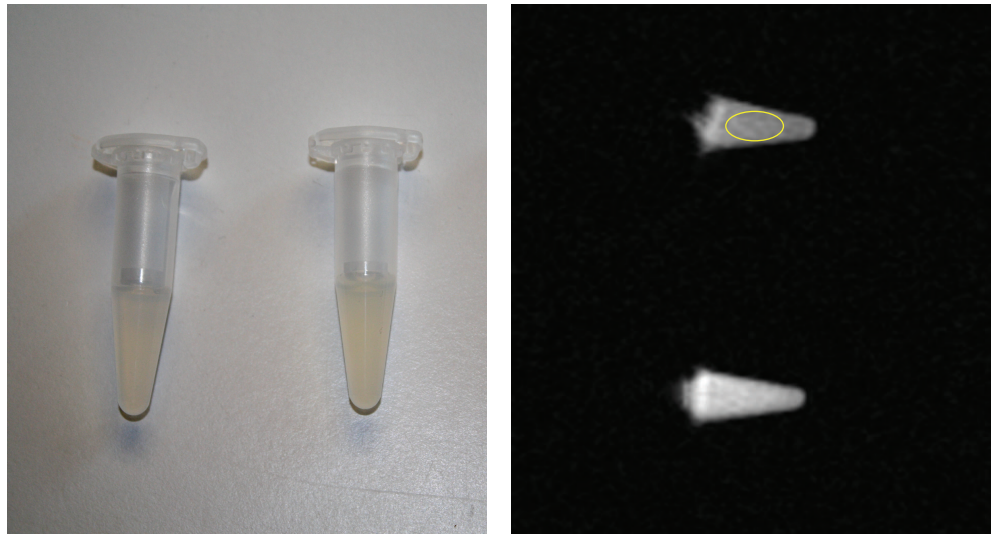

(a) (b)

Figure 1: MRI phantoms. (a) Two phantoms containing USPIO labeled cells. (b) MRI image of 2 phantoms with an ellipsoid region of interest placed in the upper phantom. USPIO: ultrasmall superparamagnetic iron-oxide.

Table 1: Number of MRI phantoms.

Number of MSCs	USPIO dose	USPIO incubation time		
		2 hours	6 hours	21 hours
2.5×10^5	full	13	10	13
5×10^5	full	11	7	9
1×10^6	full	12	7	8
2.5×10^5	half	14	5	9
5×10^5	half	11	5	8
1×10^6	half	11	4	8
2.5×10^5	0	14	5	12
5×10^5	0	10	6	11
1×10^6	0	12	5	8

MSC: mesenchymal stromal cell; USPIO: ultrasmall super-paramagnetic iron-oxide. USPIO dose—full = 10 μg per 10^5 cells; half = 5 μg per 10^5 cells.

2.5. MRI-Phantoms. Labeled and unlabeled MSCs were transferred to microfuge tubes with 2.5×10^5, 5×10^5, or 1×10^6 MSCs per tube. Tubes were centrifuged at 500 g for 5 minutes. The cells were then suspended in 500 μL 1% agarose-gel. In total, 248 phantoms were constructed containing either unlabeled MSCs or MSCs labeled with half or full USPIO dose, incubated for 2, 6, or 21 hours. Two phantoms are shown in Figure 1(a). An overview of all MRI phantoms is provided in Table 1. A number of reference phantoms containing only agarose-gel were constructed as reference controls.

2.6. MRI Phantom Scanning Protocol and Image Analysis. Phantoms were scanned using a 1.5T GE Signa Excite HD MRI scanner with a 4-channel receive-transmit brain coil (GE Healthcare). Two phantoms and one reference phantom with no cells were scanned concurrently. Phantoms were placed in an Eppendorf tube rack, with the reference phantom in the center and a randomly selected MSC phantom on each side with 4 cm distance to the reference phantom. The rack was placed and fixated with tape on top of 4 other racks inside the coil to achieve a central position within the coil. Images were acquired using a brain-hemorrhage $T2^*$-weighted gradient-echo (GRE) sequence with repetition-time (TR) = 620 ms, echo-time (TE) = 15.7 ms, flip-angle = 35°, matrix = 192 × 256, field of view (FOV) = 140 × 140 mm, and slice thickness = 7 mm.

Image analysis was performed using an Advantage Workstation AW4.3-05 (GE Healthcare). An ellipsoid region of interest (ROI) of 20 mm^2 was placed on the images in the center of each phantom, avoiding the edges. The postprocessing tool produces mean intensity values for each ROI. Each pixel in the ROI is given an intensity value between 0 and 4095. The mean intensity value is the mean of these values for all the pixels in the ROI (Operators manual, GE Healthcare). For comparative analysis, the difference in mean intensity values between reference and cell phantom was used. Figure 1(b) shows MRI image of 2 phantoms with an ellipsoid ROI placed in the upper phantom.

Table 2: Cellular iron content.

Group	Iron content per cell	n	Multiple comparisons (Bonferroni corrected)						
			Group A	Group B	Group C	Group D	Group E	Group F	Group G
(A) Unlabeled	0.48 ± 0.17 pg	44	—	ns	$P = 0.02$	$P < 0.001$	$P < 0.001$	$P < 0.001$	$P < 0.001$
(B) Half dose, 2 hours incubation	1.22 ± 0.52 pg	17	—	—	ns	ns	$P = 0.001$	$P < 0.001$	$P < 0.001$
(C) Full dose, 2 hours incubation	1.54 ± 0.83 pg	17	—	—	—	ns	$P = 0.03$	$P < 0.001$	$P < 0.001$
(D) Half dose, 6 hours incubation	2.36 ± 0.65 pg	17	—	—	—	—	ns	$P < 0.001$	$P < 0.001$
(E) Full dose, 6 hours incubation	2.71 ± 0.86 pg	21	—	—	—	—	—	$P < 0.001$	$P < 0.001$
(F) Half dose, 21 hours incubation	4.26 ± 1.59 pg	37	—	—	—	—	—	—	$P = 0.002$
(G) Full dose, 21 hours incubation	5.24 ± 1.50 pg	44	—	—	—	—	—	—	—

Values are shown ± SD.
USPIO: ultrasmall super-paramagnetic iron-oxide. USPIO dose—full = 10 μg per 10^5 cells. half = 5 μg per 10^5 cells, ns: nonsignificant.

2.7. Porcine Hearts. Two hearts from freshly slaughtered pigs were placed and fixated with small wooden sticks in a polystyrene box. The hearts were MRI scanned before and after injection of MSCs. One heart was injected with 4 injections of USPIO labeled MSCs (full dose—21 hours incubation), each injection with approximately 2×10^6 MSCs in 0.4 mL. The other heart received 4 injections with unlabeled cells. Care was taken that the hearts remained in the exact same position before and after injections.

2.8. MRI Scanning of Porcine Hearts. Hearts were scanned using a 1.5T Siemens Magnetom Avanto MRI scanner and a body matrix coil (Siemens AG, Germany). The scanning protocol was a thalassemia T2* weighted GRE sequence with TR = 200 ms, flip angle = 20°, matrix = 96 × 256, FOV = 135 × 180 mm, and slice thickness of 5 mm. The entire left ventricle was scanned with concurrent slice thickness of 5 mm with no gaps. The protocol produces 8 images for each slice, with different TE times (3.05, 5.89, 8.73, 11.57, 14.41, 17.25, 20.09, and 22.93 ms).

2.9. Statistical Analysis. Statistical analysis was carried out using SPSS 20 (SPSS Inc., USA). One-way ANOVA tests were used for comparing cellular iron content and MRI intensity differences between groups. A P value < 0.05 was considered significant. If the ANOVA test of the groups was significant, a multiple group versus group comparison was made within the ANOVA procedure, to determine which of the groups differed. All P values in these tests were adjusted using the Bonferroni method to counteract the issue of multiple comparisons.

Normality was determined for each group with Kolmogorov-Smirnov and Shapiro-Wilk tests. Equal variances were determined with Levene's test for homogeneity of variances.

3. Results

3.1. Iron Content in MSCs. Determination of the cellular iron load showed a positive correlation between iron content per cell and the length of the USPIO incubation period. The results are illustrated in Figure 2, and iron values and statistics are provided in Table 2.

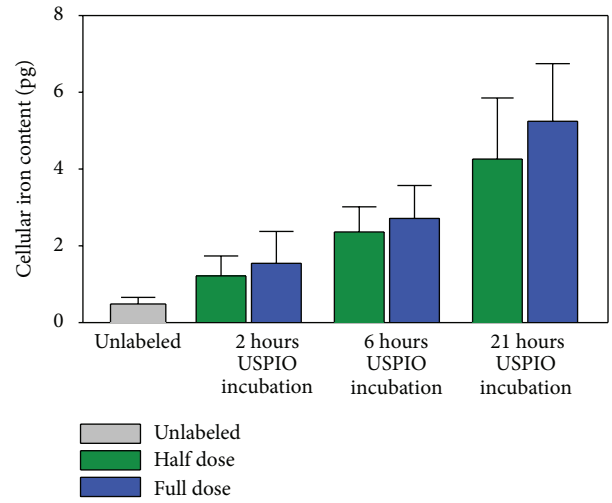

Figure 2: Cellular iron content. The iron content per cell was determined in unlabeled MSC and MSC incubated with half or full dose USPIO for 2, 6, and 21 hours. MSC: mesenchymal stromal cells. USPIO: ultrasmall superparamagnetic iron-oxide. USPIO dose—full: 10 μg per 10^5 cells; half: 5 μg per 10^5 cells.

After 2 hours USPIO incubation time, the cellular iron content was only slightly higher than that of the unlabeled cells. This increase was only significant for the full USPIO dose compared to the unlabeled cells. After 6 hours USPIO incubation time, there was a highly significant increase in cellular iron content compared to unlabeled cells. When comparing to 2-hour incubation times, only the full USPIO dose was significantly higher after 6 hours. After 21 hours, the increase in cellular iron content was highly significant compared to both unlabeled and labeled cells for 2 and 6 hours at both USPIO doses. The cells labeled for 21 hours with the full USPIO dose also had significantly higher iron content than the cells labeled for 21 hours with only half USPIO dose.

3.2. MRI of USPIO Incubated Phantoms. Overall MRI intensity diminished with increasing cell numbers and USPIO dosage. A graphical illustration of the *absolute* MRI intensities of phantoms incubated with USPIO for 21 hours is provided in Figure 3, and an illustration of the numeric

Table 3: MRI intensity differences after 21-hour USPIO incubation.

USPIO dose	1×10^6 cells	5×10^5 cells	2.5×10^5 cells
Full	249 ± 102	135 ± 91	100 ± 64
Half	134 ± 82	91 ± 76	45 ± 92
Unlabeled	46 ± 58	25 ± 47	8 ± 53
Multiple comparisons	$P < 0.001$	$P = 0.007$	$P = 0.008$
Full versus unlabeled	$P < 0.001$	$P = 0.006$	$P = 0.006$
Full versus half	$P = 0.034$	ns	ns
Half versus unlabeled	ns	ns	ns

The MRI intensities are mean pixel intensities (values between 0 and 4095) of a 20 mm^2 region of interest in the center area of each phantom, supplied by the imaging software. Values are shown ± SD.
USPIO: ultrasmall super-paramagnetic iron-oxide. USPIO dose—full = 10 μg per 10^5 cells. half = 5 μg per 10^5 cells, ns: non-significant.

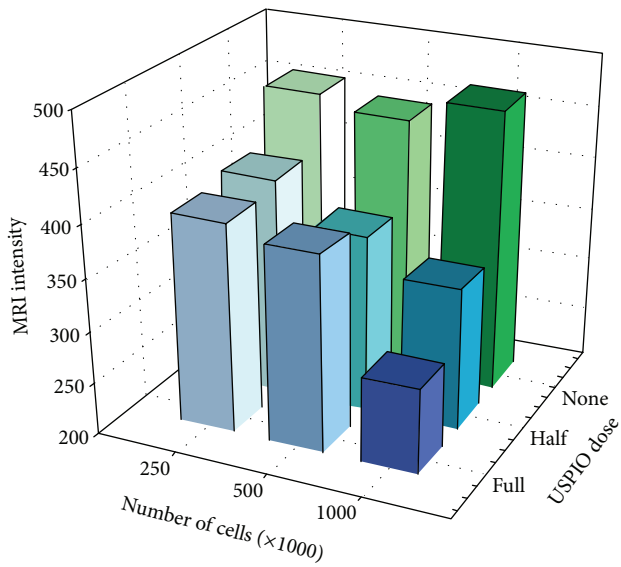

Figure 3: Absolute phantom MRI intensities after 21 hour USPIO incubation. MRI intensities are absolute mean values. USPIO: ultrasmall superparamagnetic iron-oxide. USPIO dose: full = 10 μg per 10^5 cells; half = 5 μg per 10^5 cells.

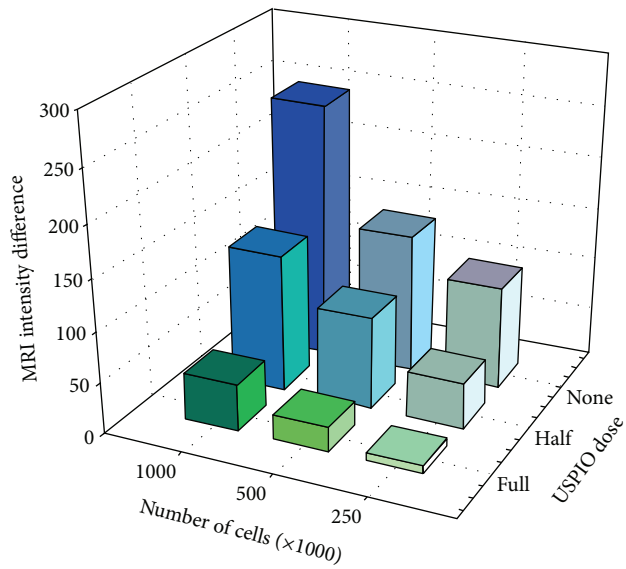

Figure 4: Phantoms intensity differences after 21-hour USPIO incubation. MRI intensity differences are the mean numeric difference between absolute MRI intensities of phantoms and reference gels. USPIO = ultrasmall superparamagnetic iron-oxide. USPIO dose: full = 10 μg per 10^5 cells; half = 5 μg per 10^5 cells.

differences in MRI intensity compared to the reference gels is provided in Figure 4. The differences and statistics are shown in Table 3.

USPIO labeled MSCs in amounts of 250.000, 500.000, and 1.000.000 could all be significantly separated on MRI from the same number of unlabeled cells, when using USPIO incubation time of 21 hours and full USPIO dosage.

MSCs labeled with half USPIO dosage could not be separated from unlabeled MSCs at any concentration on MRI. With 2 and 6 hours of incubation time, it was not possible to differentiate between labeled and unlabeled cells at any dose or concentration on MRI (see Tables 4 and 5).

Therefore, the MRI detection limits are as low as 250.000 cells when using full USPIO dose and 21 hours of incubation time. For cells labeled with lower USPIO dose and lower incubation times, no significant difference was detected on MRI compared to unlabeled cells, and the detection limits for cells labeled using these conditions will therefore be at least several million cells.

3.3. MRI of Porcine Hearts. There are distinct differences in the before and after images when looking at MRI images from porcine hearts receiving USPIO labeled MSCs (Figure 5). Hypointense areas can be identified in the after images which are equivalent to the USPIO labeled MSC injection areas. The figure images are with TE = 22.93 ms, which was the TE that gave the best visualization of the differences.

MRI images from the heart receiving unlabeled cells were without visual differences; thus, unlabeled MSCs are undetectable on MRI (Figure 6).

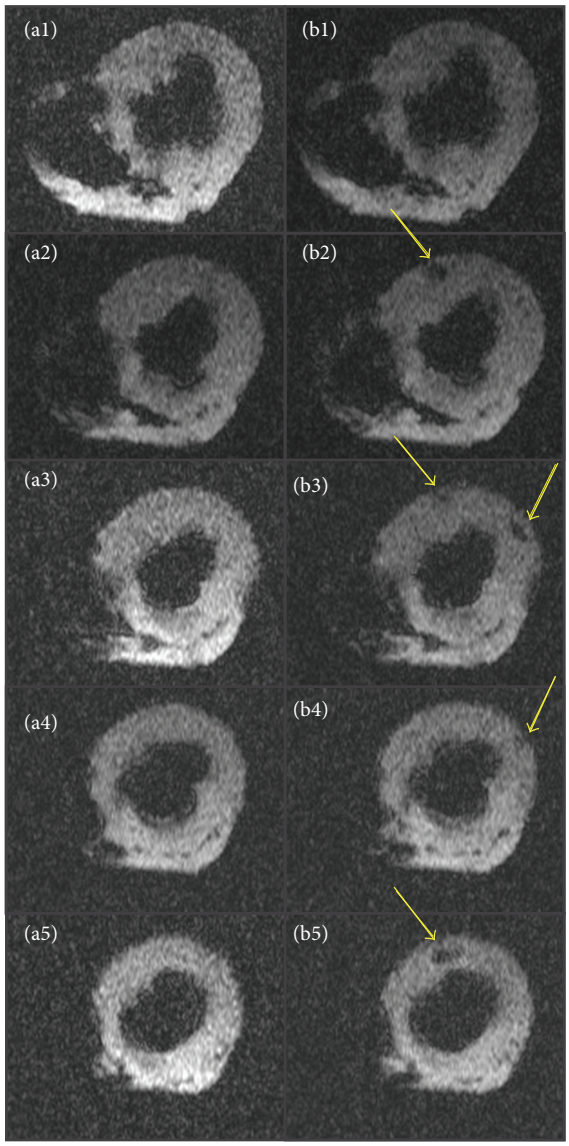

Figure 5: MRI images of porcine myocardium before and after USPIO labeled MSC injection. T2*-images of porcine myocardium before injection (a1–a5) and after injection (b1–b5) of USPIO-labeled MSCs. USPIO labeled MSCs are identified as hypointense areas (arrows). MSCs: mesenchymal stromal cells. USPIO: ultrasmall superparamagnetic iron-oxide.

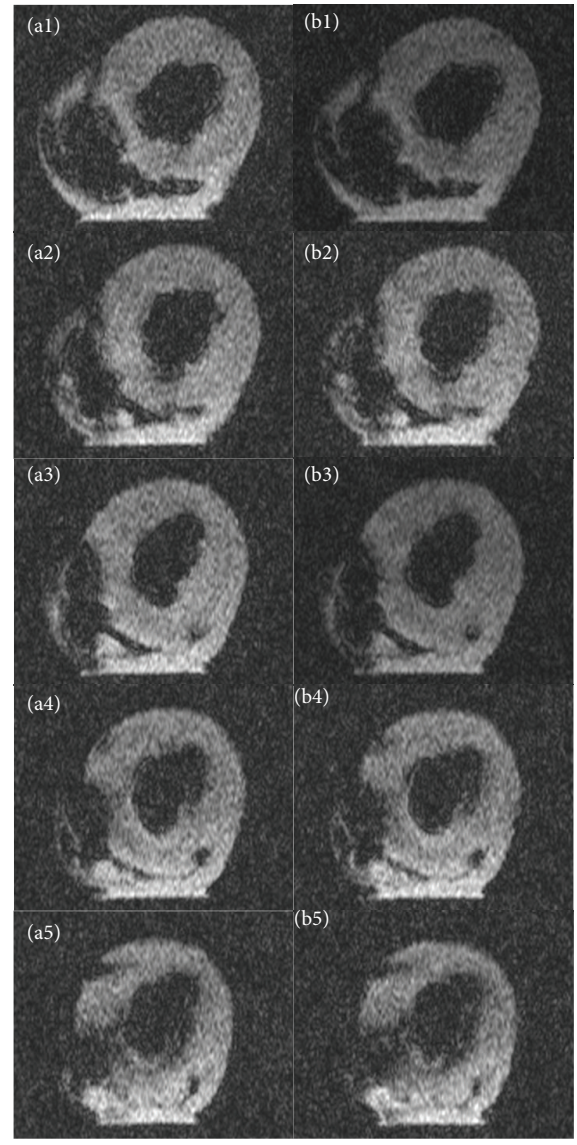

Figure 6: MRI images of porcine myocardium before and after unlabeled MSC injection. T2*-images of porcine myocardium before injection (a1–a5) and after injection (b1–b5) of unlabeled MSCs. Unlabeled cells cannot be identified. MSCs: mesenchymal stromal cells. USPIO: ultrasmall superparamagnetic iron-oxide.

Table 4: MRI intensity differences after 6-hour USPIO incubation.

USPIO dose	1×10^6 cells	5×10^5 cells	2.5×10^5 cells
Full	74 ± 50	30 ± 26	38 ± 30
Half	57 ± 48	36 ± 32	19 ± 36
Unlabeled	47 ± 32	43 ± 20	6 ± 50
	ns	ns	ns

The MRI intensities are mean pixel intensities (values between 0 and 4095) of a 20 mm^2 region of interest in the center area of each phantom, supplied by the imaging software. Values are shown ± SD.
USPIO: ultrasmall super-paramagnetic iron-oxide. USPIO dose—full = 10 μg per 10^5 cells. half = 5 μg per 10^5 cells. ns: non-significant.

Table 5: MRI intensity differences after 2-hour USPIO incubation.

USPIO dose	1×10^6 cells	5×10^5 cells	2.5×10^5 cells
Full	59 ± 65	57 ± 39	60 ± 68
Half	39 ± 38	36 ± 62	41 ± 70
Unlabeled	71 ± 46	101 ± 41	55 ± 39
	ns	ns	ns

The MRI intensities are mean pixel intensities (values between 0 and 4095) of a 20 mm^2 region of interest in the center area of each phantom, supplied by the imaging software. Values are shown ± SD.
USPIO: ultrasmall super-paramagnetic iron-oxide. USPIO dose—full = 10 μg per 10^5 cells; half = 5 μg per 10^5 cells. ns: non-significant.

4. Discussion

In the present study, we have examined MRI detection limits of USPIO labeled MSCs *in vitro* with regard to cell numbers and USPIO incubation dosage and incubation time. The study demonstrated that an incubation period of 21 hours with USPIO is superior to 2 and 6 hours incubation times and that a USPIO incubation dose of 10 μg per 10^5 cells is preferable over 5 μg per 10^5 cells. In addition, USPIO labeled MSCs could be distinguished by MRI when injected into myocardial tissue. The hypointense MRI injection-regions were due to USPIO labeling, as unlabeled cells were not visible on MRI scans.

MRI tracking of cells labeled with iron-oxide based nanoparticles in cardiovascular disease has been utilized in a variety of animal studies. In one study, rats were subjected to MI and intramyocardial injection of SPIO labeled allogeneic MSCs [21]. The MSCs were injected in the border zone of the infarct area. Hypointense regions were visible on MRI in the entire 16-week followup period. In non-MI control rats injected with labeled cells, the hypointense regions were only visible on MRI for 1 week. This was also the case for MI control rats receiving SPIO particles alone. This indicated that cell retention is dependent on the presence of inflammation in the target tissue and also that SPIO particles from dead cells will be cleared from the area, and therefore the hypointense regions on MRI corresponded to SPIO particles within live cells. This was confirmed in histologic analysis done after 1, 16, and 20 weeks. SPIO-containing cells were identified at the injection site. Macrophage specific CD68 staining showed that macrophages were only present after 1 week and not after 16 and 20 weeks. The majority of CD68 positive cells did not contain iron, and most of the iron-containing cells did not express CD68. Thus, the originally labeled cells were present and not within macrophages. In a canine MI model, SPIO labeled MSCs were injected intramyocardially into the border zone of the infarct [7]. Injection sites were visible on MRI as hypointense regions for the entire 8 week followup period. Histology with Prussian Blue (PB) staining showed presence of SPIO containing cells well integrated within the tissue.

Interesting results were found in a study using a rat MI model, where SPIO labeled MSCs were injected intramyocardially directly into the infarct lesion [6]. Hypointense regions were visible on MRI in the entire followup period of 4 weeks. In this study, postmortem tissue staining revealed that the delivery sites for both labeled and nonlabeled cells were infiltrated with inflammatory cells and that most MSCs did not survive. Similar results, where iron particles were engulfed in macrophages, were found in another rat study, where rats received intramyocardial injections of either xenogeneic human cells or allogeneic rat cells [20]. In both studies, the cells were injected directly into infarct lesion, whereas most other studies have injected their cells into the border zone of the infarct area. Perhaps the alternative injection site could explain the diverse results in these studies.

Moreover, five other studies have also histologically evaluated intramyocardial injection [8] and intracoronary infusion of SPIO and USPIO labeled autologous MSCs [9, 12, 22] or endothelial progenitor cells [11] in porcine MI settings. In all these studies, hypointense regions were visible on MRI in the infarct region in the entire followup periods of 3–8 weeks. Interestingly and in strong contrast to the aforementioned rat study, post mortem analysis of sections of the infarct regions showed that SPIO and USPIO particles remained within the originally labeled cells and that these cells corresponded with hypointense MRI signals. Only one of the studies using SPIO labeling detected sparse amounts of macrophages in the tissue, and these were clearly separated from labeled cells [11]. These findings are supported by another study using a rat MI model, where USPIO labeled MSCs were intramyocardially injected. Histology in this study confirmed that the original labeled MSCs remained in the infarcted area up to 6 weeks after implantation using both MRI and histology [13].

A major concern with MRI tracking of SPIO and USPIO labeled cells has been that the obtained MRI signals could originate from macrophages that consumed the SPIO particles after cell death of the original labeled cells. The vast majority of animal studies have found the labeled cells to live at the injection sites with no signs of macrophages or other phagocytic cells. Therefore, concern for phagocytic engulfment of injected cells seems overrated and should not hinder future studies in this area.

Another concern has been that the number of cells that remain in the heart for a prolonged period of time may be limited. A number of animal studies have attempted to assess the number of cells that remain in the heart at different time points after intramyocardial injection. The study by Tran et al. [23] used ^{111}In-oxine labeled culture expanded autologous MSCs from rats injected intramyocardially 4 weeks after MI. In an initial *in vitro* experiment, the spontaneous leaking rate of ^{111}In-oxine from labeled MSCs was 28% per hour during the first 2 hours, and hereafter decreased rapidly. As a consequence of this, only 44% of ^{111}In-oxine was retained within the MSCs at 2 hours, 27% at day 1 and 20% at day 7. Using a gamma-camera, ^{111}In-oxine activity in the hearts after 2 hours was 27.1%, 17.4% at day 1, and 11.5% at day 7. Once these values were corrected for the ^{111}In-oxine leakage measured at the same time-points, a mean constant value of 60% of injected MSCs could be estimated to be retained within the hearts over a period of 7 days. Similar studies in porcine using radioisotope labeled cells to determine long time cell retention have reported low long-term cell numbers similar to the uncorrected observations reported by Tran et al. [23]. These studies did not take into account the spontaneous radioisotope leakage from labeled cells, and long-term cell numbers would probably have been considerably higher if this had been taken into consideration [30, 31]. Long-term cell retention has also been evaluated in an allogeneic rat MI model, where female rats received intramyocardial injections with "male" MSCs [32]. Rats were sacrificed at different time intervals, and samples from the hearts were used to quantify male cell retention. At the initial time point, the cell retention varied from 9% to 80%, and after 6 weeks, the cell retention was down to 2% and 3.5%. However, the study has limitations as cell retention numbers were based on analysis of small myocardial samples that may not represent the whole

myocardium. Moreover, the number of rats (only 2 to 5 in each group) was very small. That cells which may present in the heart for much longer were recently demonstrated using reporter genes in a mouse study where human $CD34^+$ cells were detected up to 52 weeks after intramyocardial injection in the heart after MI [33].

MRI tracking of iron-oxide-based nanoparticles labeled cells has yet to be carried out in a clinical cardiovascular setting, but both SPIO and USPIO have been used successfully in different clinical studies. In one study, 10 patients with spinal cord injury received spinal injections of autologous $CD34^+$ cells labeled with magnetic beads [14]. Treatment was safe and the labeled cells were tracked with MRI as hypointense signals in five patients up to 35 days after injection. In another study, SPIO labeled autologous dendritic cells were injected in lymph nodes in 11 melanoma patients [15]. The treatment was safe and labeled cells could be tracked on MRI. Histology of resected lymph nodes confirmed the presence of the original labeled cells. The SPIO labeled cells were negative for the macrophage marker CD68, indicating that the SPIO positive cells were not macrophages. SPIO labeled cells were also used in 15 patients with multiple sclerosis and 19 patients with amyotrophic lateral sclerosis [16]. Patients received spinal injections of SPIO labeled MSCs. Treatment was safe, and the labeled MSCs were visualized as hypointense signals with MRI. SPIO labeled pancreatic islets were transplanted into the livers of 4 patients with type 1 diabetes [18]. Treatment was safe, and labeled islets were identified as hypointense spots in 3 of 4 patients with MRI. In yet another study, one patient with brain trauma was transplanted with SPIO labeled neural cells [19]. Treatment was safe, and the labeled cells were tracked for 3 weeks. USPIO particles have been used with success in clinical settings as an MRI contrast in patients with stroke [17] and for sentinel node identification in cancer patients [34, 35].

For clinical use, commercial SPIO and USPIO products were available a few years ago, but these products have been taken of the market. The USPIO particles used in the present study (IODEX) were developed for clinical use and can be used as such, when produced under Good Manufacturing Practice (GMP) conditions. The IODEX particles are designed to remain stable for months without releasing the iron core. This is achieved with additional cross-linking of the dextran coating with epichlorohydrin [26]. In addition, the highly cationic HIV-tat peptide was used for internalization of intracellular MRI contrast agents [28]. This has a much higher cellular uptake than traditionally used such as poly-L-lysine or protamine sulfate.

As an intracellular contrast agent for nonphagocytic cells, we find that USPIO particles might be more suitable than SPIO particles for clinical use. In a comparison study, USPIO particles exhibited significantly higher uptake in nonphagocytic cells compared to SPIO particles [24]. These data suggest that smaller particles are internalized more efficiently into nonphagocytic cells. In contrast, another study found that uptake of SPIO was better than USPIO for nonphagocytic cells [36]. In this study, however, cells were only incubated for 4 hours, which may explain the lower USPIO uptake. As demonstrated in the present study, a longer incubation time is needed for optimal labeling with USPIO particles. For labeling of phagocytic cells though, SPIO particles might be more suitable, as SPIO particles are easily recognized and internalized into monocytes and macrophages [37]. Another advantage of USPIO particles is that they have longer plasmatic half-life (>36 hours) and this allows for longer cell tracking observation periods [25].

5. Conclusions

The present study demonstrated that to label MSCs for MRI tracking, the preferable USPIO incubation time and dosage were 21 hours and 10 μg USPIO per 10^5 MSCs, respectively. In porcine myocardial tissue, the USPIO labeled MSC could be visualized on MRI, whereas unlabeled cells could not. Clinical studies should be conducted, with MRI tracking of myocardial injected USPIO labeled MSCs in patients with heart disease to obtain important information on retention, migration, and efficacy of the cells after implantation.

Conflict of Interests

The authors declare that they have no conflict of interests.

Acknowledgment

The authors would like to thank chief physician Niels Fogh-Andersen, Department of Clinical Biochemistry, Herlev Hospital, Denmark for assistance with quantification of cellular iron content and lending of equipment.

References

[1] T. Friis, M. Haack-Sørensen, A. B. Mathiasen et al., "Mesenchymal stromal cell derived endothelial progenitor treatment in patients with refractory angina," *Scandinavian Cardiovascular Journal*, vol. 45, no. 3, pp. 161–168, 2011.

[2] A. B. Mathiasen, M. Haack-Sørensen, and J. Kastrup, "Mesenchymal stromal cells for cardiovascular repair: current status and future challenges," *Future Cardiology*, vol. 5, no. 6, pp. 605–617, 2009.

[3] J. Kastrup, "Stem cells therapy for cardiovascular repair in ischemic heart disease: how to predict and secure optimal outcome?" *EPMA Journal*, vol. 2, no. 1, pp. 107–117, 2011.

[4] W. Y. Zhang, A. D. Ebert, J. Narula, and J. C. Wu, "Imaging cardiac stem cell therapy: translations to human clinical studies," *Journal of Cardiovascular Translational Research*, vol. 4, no. 4, pp. 514–522, 2011.

[5] J. W. M. Bulte, "In vivo MRI cell tracking: clinical studies," *American Journal of Roentgenology*, vol. 193, no. 2, pp. 314–325, 2009.

[6] Y. Amsalem, Y. Mardor, M. S. Feinberg et al., "Iron-oxide labeling and outcome of transplanted mesenchymal stem cells in the infarcted myocardium," *Circulation*, vol. 116, no. 11, pp. I38–I45, 2007.

[7] J. W. M. Bulte, L. Kostura, A. Mackay et al., "Feridex-labeled mesenchymal stem cells: cellular differentiation and MR assessment in a canine myocardial infarction model," *Academic Radiology*, vol. 12, no. 5, pp. S2–S6, 2005.

[8] D. L. Kraitchman, A. W. Heldman, E. Atalar et al., "In vivo magnetic resonance imaging of mesenchymal stem cells in myocardial infarction," *Circulation*, vol. 107, no. 18, pp. 2290–2293, 2003.

[9] G. S. Ma, C. M. Qi, N. F. Liu et al., "Efficiently tracking of stem cells in vivo using different kinds of uperparamagnetic iron oxide in swine with myocardial infarction," *Chinese Medical Journal*, vol. 124, no. 8, pp. 1199–1204, 2011.

[10] C. Y. Yang, J. K. Hsiao, M. F. Tai et al., "Direct labeling of hMSC with SPIO: the long-term influence on toxicity, chondrogenic differentiation capacity, and intracellular distribution," *Molecular Imaging and Biology*, vol. 13, no. 3, pp. 443–451, 2011.

[11] J. J. Graham, W. D. Foltz, A. K. Vaags et al., "Long-term tracking of bone marrow progenitor cells following intracoronary injection post-myocardial infarction in swine using MRI," *American Journal of Physiology*, vol. 299, no. 1, pp. H125–H133, 2010.

[12] C. Peng, K. Yang, P. Xiang et al., "Effect of transplantation with autologous bone marrow stem cells on acute myocardial infarction," *International Journal of Cardiology*, vol. 162, no. 3, pp. 158–165, 2013.

[13] C. Chapon, J. S. Jackson, E. O. Aboagye, A. H. Herlihy, W. A. Jones, and K. K. Bhakoo, "An in vivo multimodal imaging study using MRI and pet of stem cell transplantation after myocardial infarction in rats," *Molecular Imaging and Biology*, vol. 11, no. 1, pp. 31–38, 2009.

[14] F. Callera and C. M. T. P. De Melo, "Magnetic resonance tracking of magnetically labeled autologous bone marrow $CD34^+$ cells transplanted into the spinal cord via lumbar puncture technique in patients with chronic spinal cord injury: $CD34^+$ cells' migration into the injured site," *Stem Cells and Development*, vol. 16, no. 3, pp. 461–466, 2007.

[15] I. J. M. De Vries, W. J. Lesterhuis, J. O. Barentsz et al., "Magnetic resonance tracking of dendritic cells in melanoma patients for monitoring of cellular therapy," *Nature Biotechnology*, vol. 23, no. 11, pp. 1407–1413, 2005.

[16] D. Karussis, C. Karageorgiou, A. Vaknin-Dembinsky et al., "Safety and immunological effects of mesenchymal stem cell transplantation in patients with multiple sclerosis and amyotrophic lateral sclerosis," *Archives of Neurology*, vol. 67, no. 10, pp. 1187–1194, 2010.

[17] N. Nighoghossian, M. Wiart, S. Cakmak et al., "Inflammatory response after ischemic stroke: a USPIO-enhanced MRI study in patients," *Stroke*, vol. 38, no. 2, pp. 303–307, 2007.

[18] C. Toso, J. P. Vallee, P. Morel et al., "Clinical magnetic resonance imaging of pancreatic islet grafts after iron nanoparticle labeling," *American Journal of Transplantation*, vol. 8, no. 3, pp. 701–706, 2008.

[19] J. Zhu, L. Zhou, and F. XingWu, "Tracking neural stem cells in patients with brain trauma," *The New England Journal of Medicine*, vol. 355, no. 22, pp. 2376–2378, 2006.

[20] J. Terrovitis, M. Stuber, A. Youssef et al., "Magnetic resonance imaging overestimates ferumoxide-labeled stem cell survival after transplantation in the heart," *Circulation*, vol. 117, no. 12, pp. 1555–1562, 2008.

[21] D. J. Stuckey, C. A. Carr, E. Martin-Rendon et al., "Iron particles for noninvasive monitoring of bone marrow stromal cell engraftment into, and isolation of viable engrafted donor cells from, the heart," *Stem Cells*, vol. 24, no. 8, pp. 1968–1975, 2006.

[22] K. Yang, P. Xiang, C. Zhang et al., "Magnetic resonance evaluation of transplanted mesenchymal stem cells after myocardial infarction in swine," *Canadian Journal of Cardiology*, vol. 27, no. 6, pp. 818–825, 2011.

[23] N. Tran, Y. Li, F. Maskali et al., "Short-term heart retention and distribution of intramyocardial delivered mesenchymal cells within necrotic or intact myocardium," *Cell Transplantation*, vol. 15, no. 4, pp. 351–358, 2006.

[24] M. Song, K. M. Woo, Y. Kim, D. Lim, I. C. Song, and B. W. Yoon, "Labeling efficacy of superparamagnetic iron oxide nanoparticles to human neural stem cells: comparison of ferumoxides, monocrystalline iron oxide, cross-linked iron oxide (CLIO)-NH_2 and tat-CLIO," *Korean Journal of Radiology*, vol. 8, no. 5, pp. 365–371, 2007.

[25] B. Bonnemain, "Nanoparticles: the industrial viewpoint. Applications in diagnostic imaging," *Annales Pharmaceutiques Francaises*, vol. 66, no. 5-6, pp. 263–267, 2008.

[26] P. Wunderbaldinger, L. Josephson, and R. Weissleder, "Cross-linked iron oxides (CLIO): a new platform for the development of targeted MR contrast agents," *Academic Radiology*, vol. 9, no. 2, pp. S304–S306, 2002.

[27] M. Dominici, K. Le Blanc, I. Mueller et al., "Minimal criteria for defining multipotent mesenchymal stromal cells. The International Society for Cellular Therapy position statement," *Cytotherapy*, vol. 8, no. 4, pp. 315–317, 2006.

[28] L. Josephson, C. H. Tung, A. Moore, and R. Weissleder, "High-efficiency intracellular magnetic labeling with novel superparamagnetic-tat peptide conjugates," *Bioconjugate Chemistry*, vol. 10, no. 2, pp. 186–191, 1999.

[29] J. Jackson, C. Chapon, W. Jones, E. Hirani, A. Qassim, and K. Bhakoo, "In vivo multimodal imaging of stem cell transplantation in a rodent model of Parkinson's disease," *Journal of Neuroscience Methods*, vol. 183, no. 2, pp. 141–148, 2009.

[30] T. Freyman, G. Polin, H. Osman et al., "A quantitative, randomized study evaluating three methods of mesenchymal stem cell delivery following myocardial infarction," *European Heart Journal*, vol. 27, no. 9, pp. 1114–1122, 2006.

[31] D. Hou, E. A. S. Youssef, T. J. Brinton et al., "Radiolabeled cell distribution after intramyocardial, intracoronary, and interstitial retrograde coronary venous delivery: implications for current clinical trials," *Circulation*, vol. 112, no. 9, pp. I150–I156, 2005.

[32] J. Müller-Ehmsen, B. Krausgrill, V. Burst et al., "Effective engraftment but poor mid-term persistence of mononuclear and mesenchymal bone marrow cells in acute and chronic rat myocardial infarction," *Journal of Molecular and Cellular Cardiology*, vol. 41, no. 5, pp. 876–884, 2006.

[33] J. Wang, S. Zhang, B. Rabinovich et al., "Human $CD34^+$ cells in experimental myocardial infarction: long-term survival, sustained functional improvement, and mechanism of action," *Circulation Research*, vol. 106, no. 12, pp. 1904–1911, 2010.

[34] R. Dinniwell, P. Chan, G. Czarnota et al., "Pelvic lymph node topography for radiotherapy treatment planning from ferumoxtran-10 contrast-enhanced magnetic resonance imaging," *International Journal of Radiation Oncology Biology Physics*, vol. 74, no. 3, pp. 844–851, 2009.

[35] J. M. Froehlich, M. Triantafyllou, A. Fleischmann, P. Vermathen, G. N. Thalmann, and H. C. Thoeny, "Does quantification of USPIO uptake-related signal loss allow differentiation of benign and malignant normal-sized pelvic lymph nodes?" *Contrast Media and Molecular Imaging*, vol. 7, no. 3, pp. 346–355, 2012.

[36] D. L. J. Thorek and A. Tsourkas, "Size, charge and concentration dependent uptake of iron oxide particles by non-phagocytic cells," *Biomaterials*, vol. 29, no. 26, pp. 3583–3590, 2008.

[37] R. D. Oude Engberink, S. M. A. Van Der Pol, E. A. Döpp, H. E. De Vries, and E. L. A. Blezer, "Comparison of SPIO and USPIO for in vitro labeling of human monocytes: MR detection and cell function," *Radiology*, vol. 243, no. 2, pp. 467–474, 2007.